Breaking the weakest link: Evolution and ecology of antibiotic tolerance in cross-feeding bacterial communities

A THESIS SUBMITTED TO THE FACULTY OF THE UNIVERSITY OF MINNESOTA BY

ELIZABETH MCKINNON ADAMOWICZ

IN PARTIAL FULFILLMENT OF THE REQUIREMENTS FOR THE DEGREE OF DOCTOR OF PHILOSOPHY

Advisor: Dr. William Harcombe

May 2019

Acknowledgements

First and foremost, I would like to thank my advisor, Dr. Will Harcombe, without whom I would have crashed and burned many times in my PhD. From day one in the lab, Will's message to lab members is 'you're here because you already know a lot, and I want to do whatever I can to help you get where you want to go'. It's rare to find a P.I. who engineers such a collaborative, professional, supportive, creative lab environment, and Will has set the bar high as far as what a truly great training and working space looks like. This thesis is a testament to what happens when P.I.s find the right combination of letting a student blindly chase down a project they're passionate about, and guiding and mentoring that project into a meaningful body of work. I can also honestly say that the only reason I got through the hardest parts of this degree were because of Will's eternal optimism and consistent messaging that I was a competent scientist, and that yes, I should be taking breaks. I spent a lot of time and energy during my PhD on non-research-related topics like advocacy for women in STEM, and Will's continual reinforcement that this was a) important, valuable work and b) not a waste of good research time means more than I could ever describe.

Second, I would like to thank my scientific cohort. My lab-mates are the best group of folks one could ever want to do science with, and I've learned so much from working with people from so many different research backgrounds and expertise. I'm really going to miss our lab happy hours, and our trips up to Itasca in January, when it's always –30°C but we still go skiing/snowshoeing/ hiking anyway. To my MICaB classmates, thanks for being in the trenches with me all the way through this. I'll be watching to see if any of you win a Nobel prize and make our group-signed mugs worth any money.

Thanks also to the EEB and BTI scientists who created such a fantastic work environment, and who also always seem to have beer and doughnuts around somewhere.

The faculty I've worked with during my degree have been pivotal in learning how to be a good scientist. My thesis committee, Drs. Kirsten Nielsen, Daniel Bond, Gary Dunny, Ryan Hunter, and Mike Travisano— your guidance and advice over the years has made this thesis go a lot more smoothly than it would have otherwise. To the faculty of the microbiology journal club, especially Drs. Sandy Armstrong and Tim Brickman— you taught me more about reading papers and thinking critically about science than any class I've ever taken. Special thanks to the other MICaB faculty who took an interest in my work despite it being outside their field, and genuinely made it better by suggesting approaches and experiments I never would have thought of.

Finally, thanks to my wider family— the non-scientists in my life who gave context to my work and made me learn to a) make science accessible, and b) get out of the lab occasionally. The folks at First Congregational Church have given me friendship and community since I first arrived in Minnesota, and being in the choir has given me a place to make music alongside some of the kindest, wisest people I know. My parents, of course— throughout my life, their love, support, and encouragement has made it possible for me to work hard for the work I love. To my sweet cat Callie, who joined me one month into my PhD and passed away two months before it ended— you are missed every day. And finally, none of this would have been possible without Josh, who first reached out during one of the most stressful periods of grad school and who is truly greatest partner a person could ask for.

Dedication

This work is dedicated to the women who made me into the scientist I am today. To Diane Fisher, my high school biology teacher, who showed me what an unapologetically enthusiastic, badass woman in STEM looks like. To Dr. Leluo Guan, my first lab mentor, who was willing to take a chance on a high school student who didn't know anything and who sparked my desire to chase a career in science. To my mother, who teaches me every day that when bad things happen, sometimes the only thing to do is to roll with it. And finally, to my Babcia, whose stubborn refusal to give up in the face of inconceivable adversity is forever inspiring.

Abstract

Microbes frequently rely on metabolites excreted by other bacterial species, but little is known about how this cross-feeding influences the effect of antibiotics. We hypothesized that when species rely on each other for essential metabolites, the minimum inhibitory concentration (MIC) for all species will drop to that of the "weakest link"— the species least resistant in monoculture. We tested this hypothesis in an obligate cross-feeding system that was engineered between *Escherichia coli, Salmonella enterica,* and *Methylobacterium extorquens.* The effect of tetracycline and ampicillin were tested on both liquid and solid media. In all cases, resistant species were inhibited at significantly lower antibiotic concentrations in the cross-feeding community than in monoculture or a competitive community. However, deviation from the "weakest link" hypothesis was also observed in cross-feeding communities apparently as a result of changes in the timing of growth and cross-protection. Comparable results were also observed in a clinically relevant system involving facultative cross-feeding between *Pseudomonas aeruginosa* and an anaerobic consortium found in the lungs of cystic fibrosis patients. *P. aeruginosa* was inhibited by lower concentrations of ampicillin when cross-feeding than when grown in isolation. These results suggest that cross-feeding significantly alters tolerance to antibiotics in a variety of systems.

Table of Contents

List of Tables

List of Figures

Chapter 1. Introduction and literature review

No bacterium is an island

An estimated 10^{12} species of bacteria are predicted to exist worldwide (1, 2), from expected environments such as doorknobs to toilet seats on the international space station (3). Yet, even the very concept of a species in bacteria may be flawed, with the macroscopic species definitions of reproductive isolation and genetic dissimilarity falling apart at the microscopic level (4–6). Bacteria exist in a world defined not by a species concept but by their environment and by their interactions with each other; interspecies interactions have shaped selection for possibly billions of years longer than any anthropomorphic selection pressure. Even antibiotics, one of the great public health advances of the 20th century, likely originally evolved in bacteria as a mechanism of competition and possibly communication, as well as functioning as a carbon source (7–9). The importance of considering the bacterial community around a focal species, therefore, cannot be overstated.

Historically, microbiological research has been performed using a reductionist approach of studying a single species in isolation. Particularly in the study of infectious agents, these monoculture studies have proved both useful and essential in the development of effective treatments for various bacterial diseases. In the context of a human infection, Koch's postulates state that an infection is caused by a single infectious agent which can be transmitted to a healthy person and cause the same disease (10). However, a growing body of evidence suggests that not only do many infectious diseases occur in the context of an existing microbial community, but many infections are polymicrobial in nature (11–15). Nowhere is this more evident than in cystic fibrosis, where communities of commensal and pathogenic bacteria colonize the human lung and cause life-threatening

decreases in lung function (16–18). From dental plaque (19, 20), to *Pseudomonas aeruginosa*– *Staphylococcus aureus* co-infections in ulcers and burn wounds (21, 22), to polymicrobial interactions in urinary tract infections (15), polymicrobial infections are increasingly recognized as significant detriments to human health.

The ways in which microbes interact, and the ecological sign of those interactions, are myriad in their complexity and are likely underappreciated in how they contribute to microbial ecology and evolution. Quorum sensing, which was originally noted as a way for bacteria to sense the population sizes of their own species, is now being identified as a mechanism for interspecies and even interkingdom signaling (23–25). Interspecies quorum signals are known to alter expression of virulence genes, toxins, motility genes, and even metabolic processing (23, 26, 27) — suggesting that community context is an important factor in bacterial behavior and physiology. Horizontal gene transfer, wherein species exchange and acquire genetic material from others, has obvious implications for the transfer of antibiotic resistance (28, 29) but may also impact metabolic flexibility and evolution of novel metabolic pathways (30–32). Interference competition through the production of antibiotics, toxins, and other effectors has been harnessed by humans as a method of biological control in a variety of contexts (33–35). The exclusion of competitors by resource competition for nutrients or space has also been extensively studied; this is thought to be one mechanism behind the success of fecal microbiome transplants, where native flora are thought to more successfully compete for nutrients in the colonic environment than a *C. difficile* invader (36). Similarly, siderophore production as a mechanism of iron competition has been shown to influence *Pseudomonas aeruginosa*– *Streptococcus* competition in the cystic fibrosis lung (37),

downregulation antibiotic production in *Streptomyces* species in competitive environments (38), and prevent swarming of *Vibrio alginolyticus* near the siderophore producer *Shewanella algae* (39).

Despite the focus of much research on competitive interspecies interactions, cooperative interactions among bacteria are also common in natural communities (40–43). Interspecies cooperation is likely to especially manifest in the phenomenon of cross-feeding, wherein one species provides an essential metabolite that another is unable to synthesize or derive from the environment (44, 45). Many cross-fed nutrients have relatively little cost to producer species, and may explain how biodiversity is higher than ecological theory would predict in nutrient-poor environments (46). The prevalence of cross-feeding may explain the difficulty in culturing bacteria from natural environments in the lab— even in supposedly rich growth medium, bacteria may be unable to obtain essential nutrients in the absence of co-evolved partners (40). Cross-feeding has been shown to maintain species diversity in microbial communities (47) and lowers the energetic costs of metabolic processes such as amino acid production (40, 41, 48). This latter phenomenon makes cross-feeding an attractive field of research for biotechnology applications. Indeed, cellulose degradation and biofuel production using a consortium of bacterial species, each with a specific enzymatic role, has proven much more efficient than a single species producing all necessary enzymes (49–51). These lowered energetic costs may explain why cross-feeding is so common in natural communities, and has implications for community stability over time.

Community stability may be measured in terms of (but not limited to) species richness (the number of different species present) or in terms of total biomass (52). Ecological

theory and experimentation have shown that cooperative interactions such as cross-feeding stabilize species richness at the expense of biomass, and that competitive interactions stabilize total biomass (47, 53). The latter phenomenon is often driven by the concept of competitive release, wherein the removal of a competitor species by some environmental pressure frees the focal species and allows it to propagate in the environment (54, 55). This concept is crucial in the development of antibiotic treatment regimens, especially in cases where resistance is thought to be associated with a fitness cost. The duration and intensity of the environmental pressure (in this case, an antibiotic course) must be sufficient to eliminate both sensitive and resistant strains of a pathogen; otherwise, the antibiotic will eliminate only the sensitive strains, thereby removing any competitors of the resistant strain (56). *C. difficile* invasion is also thought to occur via competitive release— the long-term antibiotic exposure that many *C. difficile* patients have undergone decimates natural intestinal communities, allowing *C. difficile* to colonize without competition (36). Given that pathogens are often viewed as invading species, it makes sense that research on the community context of infectious diseases has focused on competition. However, with more and more infections being recognized as polymicrobial and at least somewhat cooperative in nature, more research must be done on the role of cooperation, and its ability to stabilize species richness at the cost of biomass, in pathogenic bacteria.

Antibiotic resistance (or is it tolerance?): definitions and mechanisms

In an interview following his 1945 Nobel Prize win for the discovery of penicillin, Alexander Fleming warned the scientific community of the potential for the rapid evolution of antibiotic resistance (57). Since his discovery, antibiotics have saved

millions of lives globally; however, antibiotic-resistant infections currently kill 700,000 people globally per year and are estimated to kill 10 million people a year by 2050 (58). The baffling speed with which bacteria evolve and spread resistance has stymied the global health community. This, coupled with the relatively slow and ultimately ineffectual development of novel antimicrobials, have resulted in the need for creative solutions to this issue. Much evolutionary theory and experimentation have resulted in a relatively clear understanding of how antibiotic resistance evolves and spreads within, and even between, species— horizontal gene transfer has proved an especially common mechanism by which high-level resistance is exchanged between proximal bacteria. The relative fitness costs to a bacterium of carrying a resistance element, both chromosomally and exogenously encoded, have also been well-studied— resistance is generally costly to a bacterium, and may be lost in non-selective environments (this is particularly true of resistance plasmids). Despite this, the problem remains— bacteria evolve resistance quickly, and the costs of resistance are insufficient to keep resistance from spreading in bacterial populations and communities.

The terminology surrounding antibiotic resistance is often imprecise and terms such as resistance and tolerance are used interchangeably. However, throughout this thesis I will be using the following terminology based on recommendations from Brauner et al. (59). Antibiotic resistance is defined as a genetic mechanism which confers a heritable increased ability to grow and/or survive at increased antibiotic concentrations. Antibiotic tolerance, in contrast, may be considered a phenotypic trait describing the ability of a species to grow transiently at high antibiotic concentrations. A given population of bacteria may, therefore, have high tolerance but low resistance under certain

environmental conditions (or vice versa). Tolerance is also a useful term for describing antibiotic responses at the community level. ‘Community tolerance’ (i.e. the ability of a community to grow in the presence of antibiotic) makes more sense than ‘community resistance’, which may incorrectly assume genetically encoded resistance mechanisms for each community member.

Cellular mechanisms of antibiotic resistance have been described exhaustively elsewhere (60–66); I will provide a brief explanation here for context. Cellular-level resistance may be broken up into four main types: target modification, target bypass, efflux/ uptake, and antibiotic inactivation. The former two may generally be considered ‘private’ resistance mechanisms; that is, they confer resistance only on the cells which contain the requisite mutations. The latter two, however, have the potential to influence antibiotic effects on other cells in the population, with antibiotic inactivation even representing a mechanism of public-goods resistance. Target modification involves modifications to the target site of antibiotics which reduce antibiotic binding and/or inhibition of the target; notable examples include *rpoB* mutations in rifampicin resistance which prevent binding to RNA polymerase (67) and *gyrA* mutations which prevent fluoroquinolone binding and inhibition of gyrase (68). Target bypass involves expression of an alternate cellular pathway which decreases the cell’s dependence on an antibiotic-inhibited pathway. For example, resistance to trimethoprim, a folate biosynthesis inhibitor, often occurs via duplication or increased expression of dihydrofolate reductase, an essential enzyme in folate biosynthesis (69). Resistance-conferring porin mutations (via a change in type, expression, or function) are common but confer low levels of resistance on their own (61). Efflux pump-mediated resistance is a particular concern in clinical microbes as it

tends to confer high-level resistance to a broad spectrum of antibiotics (63). Enzymatic degradation of antibiotics is perhaps most commonly associated with β-lactamases which degrade β-lactam antibiotics such as penicillin; however, degradation enzymes also exist for a variety of other antibiotics (61, 70). These mechanisms are not mutually exclusive to an antibiotic or a species. β-lactam resistance, for example, may arise by any of these mechanisms: mutations in penicillin-binding proteins (PBPs) which decrease its affinity for β-lactam antibiotics; decreased cell wall permeability and/or efflux pump expression; β-lactamase degradation of the antibiotic, or expression of PBPs with low β-lactam binding affinity (71). Generally, resistance mutations which confer increased drug efflux/ decreased drug uptake confer lower levels of resistance than those that modify the drug or its target (72).

In addition to the antibiotic class-specific mechanisms described above, bacteria can also evolve more generalized resistance through a more global modification of cellular functions such as stress response and growth rate. These mutations, which often occur in global stress response regulators such as the *Mar*, *Sox,* and *Rob* regulons in *Enterobacteriaceae*, often play a significant role in increasing broad-spectrum antibiotic resistance by inducing multidrug efflux pump expression, decreasing cell wall permeability, and inducing a protective dormant state (73–75). Modifications to cellular growth rate have long been known to increase phenotypic antibiotic tolerance; the phenomenon of persister cells, which are heterogeneously metabolically inactive but highly antibiotic tolerant (76), has proven challenging in eliminating pathogens such as *Staphylococcus aureus, Mycobacterium tuberculosis,* uropathogenic *E. coli*, and others (77). Increases in mutation rate in antibiotic-exposed populations can also increase the

rate of resistance evolution, as the pool of possible resistance mutations expands (78–80); horizontal gene transfer (HGT) and genomic rearrangements can greatly increase mutation rates (72), as can antibiotics themselves (60, 80).

Changes in cellular metabolism can also induce antibiotic tolerance (81, 82). Particularly for antibiotics which target specific cellular pathways, diversion of metabolic flux away from these pathways may diminish or eliminate the effectiveness of the antibiotic. In *E. coli* grown in rich medium, bleomycin application at low concentrations is lethal and induces a strong SOS response to repair double-stranded breaks induced by the drug. In minimal medium, however, *E. coli* are resistant to bleomycin and show fewer double-stranded breaks; the authors speculate that the change in nutrient environment induced a transcriptomic shift that led to this increased tolerance (83). Increased nutrient availability can also induce tolerance: methionine antagonizes para-aminosalicylic acid killing of *Mycobacterium tuberculosis* (84), and addition of N and P increased *Enterococcus faecalis* resistance to a variety of antibiotics (85). In these cases, nutrient environment can greatly alter the costs and even the possibility of tolerance arising in a population. However, the difficulty in quantifying the specific metabolites available in infection sites, for example, has made this type of work challenging.

One possible solution to the relative ease with which bacteria can induce tolerance is the use of multiple antibiotics to treat an infection. Combination therapy, wherein multiple antibiotics are administered at the same time, has two main goals. First, it may be clinically necessary in cases where a single drug is ineffective at tolerable concentrations (as is the case in tuberculosis) (86), or in cases where the most effective antibiotic is unknown (87). Second, the ideal combination therapy is one wherein the multiple

antibiotics synergize with each other; that is, they are more effective (and can be used in lower dosages) when administered together than when they act alone. Antibiotics may also antagonize each other, becoming less effective when used in combination than when used alone. A well-established example of this is the use of protein synthesis inhibitors such as tetracycline alongside DNA synthesis inhibitors such as ciprofloxacin. Use of a single drug causes a cellular imbalance in the DNA to protein ratio in cells which slows their growth; using both drugs in combination, however, restores the ratio and allows rapid growth to resume (88).

The most widespread use of synergizing compounds in treatment of bacterial infections is the use of antibiotic adjuvants, compounds which alone have no antimicrobial activity but which potentiate the activity of antibiotics (89). For example, β-lactam antibiotics are often administered in conjunction with clavulanic acid or other β-lactamase inhibitors. These compounds covalently bind and inhibit the β-lactamases present in many clinically relevant pathogens such as *Acinetobacter baumanii,* and are currently the focus of much research (90, 91). Beyond adjuvant therapy, however, use of antibiotics in combination therapy in the clinic has had mixed success (92, 93). It also remains unclear how combination therapy affects microbial communities, as few antibiotic interaction studies have been performed using multispecies systems. One study, however, found that synergizing combinations of arginine and fluoride suppressed the growth of caries— inducing oral bacteria. In a mixed community of *Streptococcus mutans, Streptococcus sanguinis,* and *Porphyromonas gingivalis,* the arginine-fluoride combination suppressed the growth of acid-producing *S. mutans* growth and facilitated alkali-producing *S. sanguinis* growth. Growth of the oral anaerobe *P. gingivalis* was also

suppressed in the presence of arginine-fluoride, likely due to increased competition from the streptococci (94). However, in this study, the precise nature of the interspecies interactions was unknown, making such effects difficult to predict in other communities.

Factors impacting antibiotic resistance evolution: a little nudge has a big effect

It is well established that the context in which bacteria acquire resistance can have significant impacts on the type of resistance mechanism they evolve, as well as the fitness costs of resistance. The canonical view of antibiotic resistance evolution, or indeed of evolution in general, is that a selection pressure is required to make one genotype (in this case, a resistant genotype) more fit versus other genotypes. Over time, this genotype will spread in the population to some optimal frequency and remain as such until the environment shifts such that it is no longer the most fit. However, in the case of antibiotic resistance, many additional parameters factor into the biologically– and environmentally– dependent fitness costs of resistance.

Predicting the evolutionary trajectory of antibiotic resistance evolution requires information about mutation rates, the level of resistance conferred by a given mutation, the fitness of the resistant mutant at a given antibiotic concentration, and the strength of the antibiotic selection pressure (60, 72). When mutation supplies are limited (due to small population sizes, low mutation rates, and/or small mutation target sizes), the most likely resistance mutation to be selected is the one which arises first or at all; if mutation supplies are less limited, clonal interference may cause the resistant mutant with the highest competitive fitness to be selected (72, 95). For example, a study of ciprofloxacin resistance found that rare but relatively cost-free resistance was selected first, allowing

the few surviving resistant clones to do so with their competitive fitness relatively intact (68). Another study found that population size alters antibiotic tolerance and some changes in tolerance were associated with changes in extracellular pH during the exponential growth phase (96)— suggesting that population size may modulate environmental parameters affecting antibiotic tolerance. In clinical settings, the appearance and frequency of antibiotic resistance does not appear to be correlated with mutation rates; this is likely because bacterial population sizes in infection contexts are sufficiently high to supply pre-existing resistance mutations into an infected host, rather than relying on a high mutation rate to generate resistant mutants during the course of an infection (60, 72).

Resistance mutations do not always carry fitness costs, particularly in competitive environments and *in vivo* models of infection (60, 97). For example, rifampicin and nalidixic acid resistance mutations in *E. coli* have been shown to increase fitness over non-resistant mutants in nutrient-limited antibiotic–free environments (98). In *Pseudomonas putida* genetically diverse colonies, selection for private mechanisms of resistance (e.g. *rpsL* mutations which modify the target site of streptomycin) occurs quickly and even at low concentrations of antibiotic (99). Even if resistance mutations are initially costly, subsequent rounds of evolution (in the clinic or in the natural environment) decreases these costs through compensatory mutations (97); for example, by making a costly resistance gene inducible only in the presence of an antibiotic (100). Identifying the context in which mutations are costly and where they are not, therefore, becomes critical in predicting where and when they will be selected. This makes it particularly important to begin studying the evolution of resistance in more ecologically

relevant scenarios, such as the polymicrobial nature of many infection contexts (11, 19, 101), or in environmental microbial communities where high, sustained concentrations of antibiotics are unlikely (102). In these contexts, in conjunction with the fact that high-fitness-cost resistance genes are expected to be lost in the absence of antibiotic selection, resistance genes which successfully spread in bacterial populations (including to pathogens) have also likely evolved to lower the fitness cost of carriage and expression (102). This phenomenon of low-cost resistance likely contributes to the difficulty in eliminating resistant pathogens in infection contexts, where antibiotic-sensitive competitors do not have the fitness advantage that they might otherwise have in, for example, an *in vitro* lab scenario where resistance has been newly introduced to a strain on a plasmid. It is therefore critical to identify novel resistance mechanisms as they evolve, and before they spread through a bacterial population alongside compensatory mutations that decrease their fitness costs.

Genetic background and epistasis also impact the fitness costs and benefits of resistance mutations (60, 100). When streptomycin resistance was added to *E. coli* rifampicin-sensitive and resistant genetic backgrounds evolved in the absence of antibiotics, the rifampicin-resistant backgrounds showed less of a fitness cost for streptomycin resistance than the rifampicin-sensitive background (103). This suggests that adaptation to a given environment by a previously resistant strain diminishes the cost of resistance to a new antibiotic. However, a phenomenon known as collateral sensitivity has also demonstrated the opposite effect— that high-level resistance to one antibiotic can result in sensitivity to many others (104–106). In an analysis of co-evolved polymorphisms in *Streptococcus pnerumoniae*, mutations in penicillin-binding proteins (PBPs) were

observed to be strongly epistatic, likely because PBPs are part of a multimeric complex (107). This epistasis is manifested in the observations that mutations in multiple PBPs are required to develop resistance, and in that fitness defects caused by mutations in one PBP are compensated for by mutations in other PBPs (108). Similar epistatic patterns have also been observed in *Neisseria gonorrhoeae* resistance to cephalosporins and penicillin (109). The genetic background and evolutionary history of a given species, therefore, is critical in understanding its present and future resistance profiles.

Rates of resistance evolution are affected by a variety of factors and can have additional effects on the fitness costs of resistance mutations. Generally, high-dosage antibiotics are expected to select for high-cost, high-benefit resistance; however, as described above, there are many factors which might determine the specific costs and benefits of resistance (see (72) for a comprehensive review). Low-dose antibiotics, particularly sublethal antibiotics, are known to select for low-cost but often high-benefit resistance. In these cases, the distribution of mutations which allows for survival is larger, thereby increasing the possibility of acquiring a big-benefit, low cost mutation or a series of compounding low-cost, low benefit mutations (67, 99, 110–112). Modeling experiments have also shown that antibiotic gradients may alter the evolutionary trajectory of resistance, though the extent and precise effects are dependent on the mutational pathway of resistance development and the fitness effects of sequential mutations (113). If sequential mutations increase resistance monotonically, gradients can accelerate resistance evolution by increasing selection on the most resistant sub-population. If, however, there are epistatic interactions between resistance mutations leading to intermediate less fit genotypes along the mutational path to resistance, gradients will

slow resistance evolution due to smaller effective population sizes of most fit/ most resistant mutants (113). In situations where resistance has a longer mutational pathway (i.e. a greater number of independent mutations required for high-level resistance), gradients also increase the rate of resistance evolution (113).

Overall, antibiotic resistance evolution is highly complex and modulated by a variety of genetic and environmental factors. While most of these are beyond the scope of this work, it is important to mention them as it is likely, if not probable, that all of them are playing some role in the experiments described here. Despite the decades of research being done on antibiotic resistance, many questions remain as to how it arises and how best to mitigate its spread in human-impacted settings. My research focuses particularly on antibiotic resistance evolution and ecology in a microbial community, and the role of metabolic interactions on resistance manifestation and mechanisms. However, it is worth noting that this is only a tiny (if often overlooked) aspect of resistance evolution, and many other factors may be at play in my work than the ones that I discuss.

One for all, and all for one: antibiotic resistance and tolerance in microbial communities

The problem with only taking resistance mechanisms into account when studying, and trying to prevent the evolution of, antibiotic resistance, is that resistance mechanisms are often viewed in a single-cell or single-species context; they occur in, and benefit, only one cell at a time. However, antibiotic resistance frequently evolves and occurs in polymicrobial contexts— from periodontal disease to chronic wound infections to catheter-associated infections (12, 114); polymicrobial infections are common and

frequently more serious than mono-species infections (115–117). Polymicrobial infections are a great challenge in antimicrobial treatment— with multiple species present, will a narrow-spectrum antibiotic be an effective treatment? Or should a broad-spectrum antibiotic be used, which increases the rate of resistance acquisition in other bacteria and potentially decimates the natural microbial communities in the host? In these infections, the ecology of the infection and the precise nature of the interactions between the species involved could prove essential in understanding the best treatment protocol.

The concept of shared, or public-good, antimicrobial resistance is especially critical in polymicrobial infection contexts. In a monoculture, the fitness costs of target site modification (e.g. *rpoB* mutations in rifampicin resistance) might be less than that of enzymatic inactivation (e.g. production of a β-lactamase). However, if the resistant species is engaged in a mutualism with another sensitive species, the production of a publicly available resistance mechanism may be evolutionarily favorable. In this context, production of a β-lactamase functions as a public good — something that comes at a cost to the producer but that benefits the whole community. One would predict that public-goods resistance would be more likely to evolve in microbial communities with high levels of interdependence, but few studies have examined this. Conversely, the production of public-goods resistance might complicate the relationship between a pathogen and the native microbial communities with which it ostensibly completes during an infection. The evolutionary dynamics of an invader which competes for space and nutrients with native species but also protects them from antibiotic pressure remains an outstanding question.

Polymicrobial communities are particularly prevalent in biofilm-associated infections (114). Biofilms represent a growth phase of bacteria wherein they adhere to a surface and produce an exopolysaccharide matrix to maintain their position. This matrix serves a variety of functions, but mainly works to protect the bacteria from external environmental disturbances, such as mechanical disturbances, phage predators, and antimicrobials (118). Mixed-species biofilms are significantly more resistant to antibiotics than planktonic cultures or single-species biofilms, sometimes through the acquisition and transfer of resistance elements between species but also by minimizing exposure to antimicrobials though factors such as exopolysaccharide production (119), breakdown of antibiotics by one species which protects other sensitive species (120–122), or induction of stress response genes in neighboring sensitive bacterial species (123–125). Biofilms also create spatially structured environments wherein different bacterial species can engage in beneficial cross-feeding interactions which would be impossible in a planktonic growth/ mass action environment. For example, in a synthetic community of *Acinetobacter* sp. Strain C6 and *Pseudomonas putida* strain R1, planktonic co-cultures competed for benzyl alcohol, their sole carbon and energy source. However, under biofilm conditions, these species grew synergistically, with *Acinetobacter* consuming the benzyl alcohol and excreting a benzoate intermediate where it is preferentially consumed by *P. putida* (126). Therefore, understanding the metabolic interactions between bacterial species is critical for assessing their response to external selection pressures such as antibiotics.

Additionally, growth in a multispecies community has been demonstrated to protect sensitive species through induction of tolerance via small molecule signaling (127). The

signaling molecule indole has received great attention for its ability to modulate gene expression in recipient cells to increase their antibiotic tolerance. In an *E. coli–Pseudomonas putida* mixed-species community, indole production by *E. coli* induced expression of a multidrug efflux pump in *P. putida*, increasing its tolerance to a variety of antibiotics (125). Similarly, *S. enterica* tolerance to carbenicillin and ciprofloxacin increased when indole production from co-cultured *E. coli* resulted in induction of the *S. enterica* SOS response (123). Interspecies quorum sensing, which is widespread in interspecies communities (25), can induce expression of multidrug efflux pumps and subsequent increases in antibiotic tolerance (128, 129). These factors, in addition to those described above, clearly indicate that antibiotic resistance and tolerance can be modulated by interspecies interactions in myriad ways. One avenue of research that has been less explored, however, is how cooperative metabolic exchange might impact resistance ecology and evolution.

The idea that metabolic interactions might modulate antibiotic resistance ecology and evolution has remained an outstanding question in both the microbial ecology and the microbiology fields. However, much research suggests that bacterial metabolism and antibiotic resistance are inexorably linked, raising some testable hypotheses as to the nature of these interactions. For example, mutations in *rpoB* conferring rifampicin resistance can have wide-ranging effects on bacterial growth phenotypes and pleiotropic effects on gene expression throughout the cell, as *rpoB* mutations modify the functionality of RNA polymerase and therefore may have a profound effect on global cellular transcription (130). *rpoB* mutations have also been shown to modify metabolic capabilities of *Bacillus subtilis* (130); these changes could alter the cross-feeding

relationship between species and potentially change the fitness cost of resistance in monocultures vs. multispecies communities. Antibiotic resistance mutations have also been shown to cause metabolic network rearrangement (131), increase expression of secondary metabolism pathways (132), and modify substrate utilization capabilities (130). Generally, resistance mutations depress metabolic capabilities, but some pathways are also expressed only in the presence of resistance mutations (130, 132). This is one possible mechanism by which resistance evolution might differ between monocultures and multispecies systems.

The research being performed on how competition impacts resistance evolution and ecology has yielded some interesting insights. Generally, competition increases resistance evolution— likely partially because competition may involve nutrient limitation, which can induce antibiotic tolerance as described above. One mathematical model suggests that resistance evolution is only prevented by high dosages of antibiotics if competition between resistant and sensitive species is minimal, or if the resistant species is a poor competitor. If the resistant strain is more fit, however, a moderate antibiotic dose is more effective as it allows the sensitive strain to better compete with the resistant strain (133). In a study of two species of *Candida* competing for a shared carbon source (glucose), changes in both antifungal concentration and nutrient availability were shown to drive different species of different resistance phenotypes to dominate the community. This effectively allowed resistant phenotypes to increase in frequency even if the antifungal was withdrawn (134). In a co-culture of *Burkholdaria thailandensis* and *Chromobacterium violaceum*, nutrient competition is mediated through quorum sensing – controlled antimicrobial production by each species.

Additionally, *C. violaceum* quorum sensing allows it to upregulate an efflux pump to increase its resistance to *B. thailandensis* produced antimicrobials (129). Interspecies competition also drives *Bacillus subtilis* efflux pump expression as a response to antibiotics produced by a *Streptomyces* co-cultured competitor (135). This phenomenon may happen in the clinic as well as in laboratory co-cultures — competition between co-evolving *Staphylococcus aureus* strains has been shown to facilitate the evolution of clinically relevant vancomycin resistance (136). While nutrient competition can increase resistance evolution, or at least modulate the resistance evolution trajectory, few studies have yet specifically tested the impact of cooperative metabolic interactions on resistance.

How does metabolic cross-feeding modulate bacterial responses to antibiotics?

Antibiotic resistance is a broad field, and as such a myriad of approaches have been taken to attempt to mitigate resistance evolution and spread. Significant work has been done especially on the cellular and global mechanisms of resistance, as well as their associated fitness costs. Additionally, polymicrobial communities are known to facilitate tolerance induction and resistance evolution through a variety of interspecies interactions including horizontal gene transfer, small molecule signaling, and public-goods resistance. When looking specifically at metabolic interactions between bacteria, however, only competitive interactions have hitherto been explored as potentially impacting resistance evolution. To date, only one study - aside from the ones described here - has looked specifically at how resistance in microbial communities is impacted by metabolic cross-feeding (55). However, given the ubiquity of cross-feeding in microbial

communities, including those containing pathogens, it is an important area of research to investigate.

The goal of my thesis work is to draw together hypotheses from many fields described above (clinical microbiology, microbial ecology, evolutionary biology, bacterial genetics, etc.) to develop a more cohesive understanding of how obligate metabolic exchange between bacterial species impacts antibiotic resistance. The main system I used to conduct this research is an engineered two– or three– species synthetic consortium of *Escherichia coli, Salmonella enterica* serovar Typhimurium, and *Methylobacterium extorquens*. This system was previously engineered such that any species (or combination thereof) can be grown independently, competitively, or in obligate cooperation depending on the nutrient sources supplied in minimal medium. The *E. coli* strain is an engineered MG1655 strain containing a clean deletion of *metB,* a cystathionine gamma-synthase required for methionine biosynthesis (137). The *S. enterica* strain was evolved and selected in a two-step process to create a strain which excretes methionine at sufficient concentrations to sustain the *E. coli* auxotroph in methionine-free medium. First, *S. enterica* LT2 was grown on ethionine, a toxic methionine analog that represses methionine biosynthesis. Ethionine resistance arose through mutations in *metJ,* a transcriptional repressor of several methionine biosynthesis genes (138). The *metJ* mutants were then plated on lactose minimal medium with *E. coli* methionine auxotrophs. In this environment, *S. enterica* is unable to grow unless *E. coli* metabolizes lactose to acetate, and *E. coli* is unable to grow unless *S. enterica* secretes methionine; thus, consortium growth only occurred if a *S. enterica* methionine-excreting mutant arose (137). Successful methionine-excreting mutants contained a *metA*

(homoserine trans-succinylase) mutation which stabilized enzyme homodimer formation (139). This two-species system could then grow independently (*E. coli* on lactose and methionine, *S. enterica* on acetate or glucose) or in obligate co-culture (in lactose medium only). Later, a third species, *Methylobacterium extorquens*, was added to the system. *M. extorquens* is a model organism for C1 metabolism and produces NH_3 from single-carbon compounds such as methylamine. To allow for obligate growth in the consortium, the hydroxypyruvate reductase gene *hprA* was deleted; this allowed *M. extorquens* to assimilate nitrogen but not carbon from C1 compounds, forcing it to rely on *E. coli* for carbon in the form of acetate. In return, *M. extorquens* could provide NH_3 to *E. coli* and *S. enterica* (140). This system is unique in that the interactions between species can be precisely calibrated by manipulating nutrient availability and serves as a useful tool in investigating the impact of interspecies interactions on antibiotic tolerance.

My thesis focuses on three main questions relating to how microbial communities respond to antibiotic pressure. The null hypothesis underlying much of this work is that metabolic dependencies determine community survival; that is, the loss of any one metabolite producing community member will cause the death of the others. I call this the "weakest link" hypothesis— the community is only tolerant of a given selection pressure to the point that its weakest member is tolerant. Though there are many factors influencing antibiotic tolerance as described above, the weakest link hypothesis is a useful entry point into these investigations as it is easily tested in our system. The first question I sought to answer is this: can community antibiotic tolerance be predicted by weakest link dynamics? Using the above three–species system, I found that this is generally true, with some notable exceptions (see chapter 2). In chapter 3, I extend this

hypothesis to evolutionary timescales to see how weakest link dynamics might impact the rate and mechanisms of antibiotic resistance evolution. Again, I found that metabolic dependencies slow resistance acquisition, though their impact on mechanism was mixed. In chapter 4, I added an additional layer of complexity by asking how drug interactions might be modulated by cross-feeding and weakest link dynamics. Here, I found that weakest link–based predictions of antibiotic interactions in co-cultures were generally correct, and that weakest link dynamics can largely nullify antagonistic or synergistic antibiotic interactions which may be present in monoculture. Overall, my work demonstrates that metabolic interactions are both an important factor in determining community response to antibiotics and represent a potentially untapped tool in research efforts to mitigate the evolution and spread of antibiotic resistance.

Chapter 2. Cross-feeding modulates antibiotic tolerance in bacterial communities[1]

Summary

Microbes frequently rely on metabolites excreted by other bacterial species, but little is known about how this cross-feeding influences the effect of antibiotics. We hypothesized that when species rely on each other for essential metabolites, the minimum inhibitory concentration (MIC) for all species will drop to that of the "weakest link" — the species least resistant in monoculture. We tested this hypothesis in an obligate cross-feeding system that was engineered between *Escherichia coli, Salmonella enterica,* and *Methylobacterium extorquens.* The effect of tetracycline and ampicillin were tested on both liquid and solid media. In all cases, resistant species were inhibited at significantly lower antibiotic concentrations in the cross-feeding community than in monoculture or a competitive community. However, deviation from the "weakest link" hypothesis was also observed in cross-feeding communities apparently as result of changes in the timing of growth and cross-protection. Comparable results were also observed in a clinically relevant system involving facultative cross-feeding between *Pseudomonas aeruginosa* and an anaerobic consortium found in the lungs of cystic fibrosis patients. *P. aeruginosa* was inhibited by lower concentrations of ampicillin when cross-feeding than when grown in isolation. These results suggest that cross-feeding significantly alters tolerance to antibiotics in a variety of systems.

Introduction

Antibiotic resistant bacteria pose a considerable public health threat worldwide; the World Health Organization reports that 25-50% of hospital-acquired pathogens are now multiple-drug-resistant (141). Despite extensive research on cellular mechanisms of resistance in many bacterial species (142, 143), a growing body of research suggests that a single-species view of pathogen response to an antibiotic may be incomplete. Many infections are known to involve multiple pathogens (15, 101) or interactions between pathogens and commensals, (11, 17, 19). As well, we still have little understanding of how interspecies ecological interactions influence the impact of antibiotics on microbial communities.

Growth in a microbial consortium can influence a species' antibiotic tolerance by multiple mechanisms (124, 144, 145). Resistant species can protect more sensitive species by degrading antibiotics; for example, production of antibiotic-degrading enzymes by one species causes detoxification of shared growth medium (122, 124, 146). Additionally, secretions from one species can induce resistance mechanisms in others; for example, by activating stress-response pathways (123) or efflux pump expression (125). Spatial structure may also play a role in protective interactions; a synthetic community of *Pseudomonas aeruginosa, Pseudomonas protegens,* and *Klebsiella pneumoniae* was found to have greater tobramycin resistance when grown as a multispecies biofilm versus single species biofilm or multispecies planktonic culture (147). Less directly, community growth may alter antibiotic resistance by inducing physiological changes in bacteria that increase drug uptake or slow their metabolic rate

(148–151). In many cases, however, mechanisms underlying communities' effects on resistance remain unclear (15).

Few studies have investigated how exchange of essential nutrients in a bacterial community modulates the impact of antibiotics (55, 152). When metabolites produced by one organism are used as a nutrient or energy source by another it is known as cross-feeding (42, 153). This phenomenon is nearly ubiquitous in microbial communities (41, 43, 154) and is thought to contribute to our inability to cultivate most bacterial species in isolation (155, 156). Cross-feeding has also been shown to play a critical role in the human microbiome (20, 157, 158). Given the ubiquity and importance of cross-feeding in human-associated microbial communities, greater investigation into how cross-feeding influences population and community responses to antibiotics is needed.

Here, we test how cross-feeding changes the effect of antibiotics on bacterial communities. We define tolerance as the ability of species to grow in a given antibiotic concentration. Tolerance as we define it can change as a function of physiological state or environmental conditions, while changes in resistance would require a change in DNA sequence (59). We hypothesize that when species depend on one another the community tolerance (i.e. the level of antibiotic required to inhibit detectable community growth) will be set by the tolerance of the ‘weakest link’ (the least tolerant community member). Alternatively, community tolerance may be higher than that of the weakest species in monoculture (‘community protection’ hypothesis), or lower (‘community sensitivity’ hypothesis). Higher than expected tolerance may occur if one or more species in a community excretes a compound which either actively degrades antibiotics in the medium (121, 124), or which activates tolerance mechanisms such as efflux pump

expression in neighboring species (125, 127). Lower than expected tolerance could result if sublethal concentrations of antibiotic, while not sufficient to arrest or kill any one species, sufficiently disrupt cross-feeding to inhibit community growth.

We tested the impact of cross-feeding using an engineered obligate mutualism involving *Escherichia coli*, *Salmonella enterica* serovar Typhimurium, and *Methylobacterium extorquens* (159). In one minimal medium, these species rely on each other for essential metabolites in a cooperative community (**Figure 2.1A**). However, if essential metabolites are provided in the medium, the species can be grown as monocultures, or in a competitive community (**Figure 2.1B**). We compared the tolerance of each species grown in monoculture to tolerance in the mutualism, both overall in the community and at the species level. Our system is ideal to test our 'weakest link' hypothesis because the mechanism of dependency between species is known, and the identity of the weakest link can be changed by altering the antibiotic used. This system allows us to rigorously connect observed changes in tolerance to ecological interactions between species.

To test the generality of our hypotheses, and to determine conditions under which deviation from them might occur, we employed multiple experimental setups. We tested two antibiotics with different mechanisms of action— ampicillin is a bactericidal inhibitor of cell wall synthesis (124), whereas tetracycline is a bacteriostatic protein synthesis inhibitor (61). Additionally, ampicillin resistance commonly arises as a function of enzymatic degradation by β-lactamases (61), allowing the potential for cross-protection of less tolerant species (124). Conversely, tetracycline resistance often involves mutations that would only protect the species that possesses them, such as efflux pump upregulation or target site modification (160). Tetracycline degradation

enzymes do exist, but are far less common than β-lactamases (160, 161). The impact of these antibiotics was tested in both liquid media and on agar plates to test the influence of spatial structure. Finally, we investigated the effect of cross-feeding on tolerance in a model relevant for cystic fibrosis. This second system involves two components: the pathogen *Pseudomonas aeruginosa*, which grows poorly on mucin, a major carbon source in the cystic fibrosis lung; and a previously defined consortium of anaerobic bacteria that break down mucin into usable metabolites for *P. aeruginosa* (18). Changing antibiotics, environmental structure, and model systems makes it possible to identify both system-specific and general impacts of cross-feeding on antibiotic tolerance.

Across all treatments and both model systems, resistant bacteria were inhibited by lower concentrations of antibiotic when cross-feeding than when growing independently. However, we found that cross-feeding can conditionally provide protection to less tolerant bacteria. For both ampicillin and tetracycline, cases arose in which tolerance was higher than predicted based on measurements of tolerance in monoculture. Our results demonstrate that metabolic interactions impact antibiotic tolerance in a community and suggest that antibiotic-resistant pathogens may be inhibited by targeting their less tolerant metabolic partners.

Methods

Bacterial strains and media

The three-species community contained strains of *Escherichia coli*, *Salmonella enterica* and *Methylobacterium extorquens* described previously (53, 159). The *E. coli* str. K12 contains a Δ*metB* mutation. The *S. enterica* strain excretes methionine as a result of mutations in *metA* and *metJ* (137–139). The *M. extorquens* AM1 Δ*hprA* mutant is unable to assimilate carbon from C1 compounds (162). In lactose minimal medium, the species rely on each other for essential metabolites. *E. coli* secretes acetate byproducts which the other species rely on for a carbon source. *M. extorquens* releases ammonia byproducts which provide a source of nitrogen for other species. *S. enterica* secretes methionine, which is essential because our *E. coli* strain is auxotrophic for this amino acid (**Figure 2.1**). Each species has a fluorescent label integrated into its genome: cyan fluorescent protein (CFP) for *E. coli*, yellow fluorescent protein (YFP) for *S. enterica*, and red fluorescent protein (RFP) for *M. extorquens*. Bacteria were grown in minimal Hypho media (159) containing varying amounts and types of carbon and nitrogen, depending on medium type (see **Supplementary table S2.1**).

The cross-feeding system of *Pseudomonas aeruginosa* strain PA14 and a four-species consortium of anaerobic mucin-degrading species has also been previously described. Briefly, *P. aeruginosa* monoculture yield on mucin is relatively low due to its inability to break down mucin into a usable growth substrate. However, when *P. aeruginosa* is co-cultured on mucin with the anaerobic consortium, the latter degrades mucin into usable metabolic by-products and *P aeruginosa* yield increases tenfold (18).

Pseudomonas aeruginosa strain PA14 (163) was obtained from D.K. Newman (Caltech). The anaerobic consortium (composed primarily of *Prevotella sp., Veillonella sp., Fusobacterium sp., and Streptococcus sp.*) was derived from human saliva using porcine gastric mucin enrichment as previously described (18).

Liquid media experiments

Bacteria were inoculated along an antibiotic gradient to measure the minimum inhibitory concentration (MIC) for monocultures and co-cultures. Each species was grown from freezer stocks at 30°C in species-specific monoculture Hypho medium; monocultures and communities were inoculated from these same monoculture growth conditions (see **Supplementary table S2.1**). Once cultures reached mid-log phase (OD~0.2-0.3), they were diluted 1/200. Cells were inoculated into a 96-well plate, with fresh Hypho and varying concentrations of an antibiotic. The inoculate size for a species was kept constant at ~10^4 cells per well in monoculture and community (i.e. community treatments started with 3x more total cells than monocultures). Ampicillin was used at 0, 0.2, 0.5, 1, 2, and 5µg/mL for *E. coli*, *S. enterica*, and the communities, and at 0, 2, 5, 10, 20, and 50µg/mL for *M. extorquens*; these concentrations provided the best range of sublethal to lethal ampicillin concentrations. Tetracycline was used at 0, 1, 2, 3, 5, and 10µg/mL for *E. coli*, *M. extorquens*, and the community, and 0, 10, 20, 30, 50, and 100µg/mL were used for *S. enterica*. 96-well plates were placed into a Tecan InfinitePro 200 at 30°C for 120 hours. Measurements of OD600 were taken every 15 minutes to track overall bacterial growth, and fluorescence measurements were taken to track growth of individual species. Correlations between colony-forming units (CFU) and OD600 as well as fluorescence can be found in **Supplementary figure S2.1.** Minimum

inhibitory concentration (MIC) was defined as the lowest antibiotic concentration at which no growth (as measured by fluorescence) was seen by 3x the time to detectable growth of the antibiotic–free control.

Solid media antibiotic susceptibility experiments

Resistance on plates was determined by measuring the zone of inhibition diameter around an antibiotic containing disk. For monocultures, 150µL of log-phase culture (OD= 0.5) was spread on Hypho plates (1% agar) in a lawn; for communities, 150µL of culture from each species was mixed, spun down, and re-suspended in 150µL of the appropriate community medium before plating onto Hypho plates. Discs of filter paper 6mm in diameter were inoculated with 25µg antibiotic and left to dry for 10 minutes. Discs were applied to the center of plates with bacteria and incubated at 30°C for 48 hours (*E. coli*, *S. enterica*, competitive community) or 72 hours (*M. extorquens*, cooperative community), depending on how long it took for cells outside the zone of inhibition to become confluent. Three technical replicates for the zone of clearing were measured for each plate and averaged to provide a single plate diameter; at least eight biological replicate plates were measured for each condition (see **Supplementary tables S2.2-S2.3** for summary statistics).

Fluorescence microscopy

Fluorescent images were obtained using a Nikon AZ100 Multizoom macroscope with a C1si Spectral confocal attachment, 4x objective lens at 3.40x magnification at the University of Minnesota Imaging Center. 457nm, 514nm and 561nm argon lasers were used to visualize CFP, YFP and RFP, respectively. Emission maxima are 480nm for

CFP, 550nm for YFP, and 590nm for RFP. Disc diffusion Petri plates were placed on the stage and images from 2x12 fields of view were obtained and stitched together using Nikon NIS Elements software. Images for each fluorophore were quantified for fluorescence location and overlaid using Fiji image analysis software (164) (see **Supplementary tables S2.4-S2.5** for summary statistics).

Testing β-lactamase production

Nitrocefin discs (Sigma-Aldrich, 49862) were used to determine if *M. extorquens* was producing a β-lactamase. For solid medium, cells were scraped off agar and suspended in the appropriate liquid medium; the OD600 of the suspension was then diluted to ~0.5, to match the OD600 of liquid cultures. Discs were placed on a microscope slide and 15µL of liquid culture or diluted solid medium suspension was added to the disc. After 60 minutes, a color change from yellow to purple/ pink indicated the production of a β-lactamase that hydrolyzed the nitrocefin in the disc (165). As a positive control, an *E. coli* strain carrying a pBR322 plasmid, which contains a *bla* β-lactamase gene was also tested. Plasmid-free *E. coli* were used as a negative control.

***Pseudomonas aeruginosa* cross-feeding model[2]**

Antibiotic tolerance assays were performed in minimal medium containing 1 mM magnesium sulfate, 60 mM potassium phosphate (pH 7.4), 90 mM sodium chloride, trace minerals (166) and supplemented with autoclaved and dialyzed pig gastric mucin (30g/L, Sigma-Aldrich) for co-cultures; mucin or glucose (12 mM) was used for *P. aeruginosa* monoculture as indicated. Ampicillin was added at indicated concentrations. For mucin fermenting community assays, cultures were inoculated from freezer stock

characterized previously (18) and allowed to grow under anaerobic conditions containing carbon dioxide, hydrogen and nitrogen (5:5:90) at 37°C for 48 hrs. For *P. aeruginosa* assays, cultures were inoculated from overnight cultures grown in LB and grown aerobically while shaking at 37°C for 16 hrs. Optical densities were determined using a Biotek Synergy H1 plate reader and are given as mean and standard deviation of three replicates.

Cross-feeding assays were performed as described previously (18). Briefly, a mucin fermenting community from freezer stock was inoculated into the minimal mucin medium and allowed to grow for 48 hours anaerobically at 37°C. This culture (OD= 0.03) was used to inoculate the lower phase (1:100 dilution) which contained 2 mL of minimal mucin medium, 1% agar, and supplemented with ampicillin as indicated. After solidification of the mucin fermenting agar cultures in 16mm glass culture tubes, *P. aeruginosa* PA14 was added to buffered media containing no mucin and 0.7% agar to 1/1000 from an LB overnight culture (inoculum CFU/mL approximately $5x10^7$). This mixture was then added to the top of the mucin fermenting community and allowed to solidify. This allowed oxygen to diffuse to *P. aeruginosa* from the top of the tube and mucin degradation products to diffuse from the anaerobic community below. After 60 hours at 37^OC, the top agar section (containing PA14) was removed, homogenized by pipette in sterile saline, serially diluted, and plated on LB agar to enumerate PA14.

Statistical analyses

For liquid and solid media assays, at least eight biological replicates of each treatment were obtained for each antibiotic. Pairwise comparisons between monocultures and co-

cultures were conducted using a Mann-Whitney U test with an applied Bonferroni correction for ten multiple comparisons. For *P. aeruginosa* cross-feeding assays, triplicate experiments were performed for each antibiotic concentration and community type. Normalized CFU values were calculated by dividing CFU at each antibiotic concentration by the CFU at 0µg/mL ampicillin. Comparisons of normalized values at each concentration were performed using a Mann-Whitney U test. Raw data for these experiments is found in **Supplementary figure S2.8**.

Results

Obligate cross-feeding in the cooperative community reduces the amount of antibiotic necessary to inhibit resistant bacteria in liquid media.

The minimum inhibitory concentration (MIC) of each species was tested in monoculture, cooperative community (cross-feeding), and competitive community. MIC was defined as the lowest concentration of antibiotic at which no growth (as measured by species-specific fluorescent markers) was detected after 3x the time to detection of growth in the relevant antibiotic–free control. This metric was used to take into account different growth rates of each of our species, and each growth condition. Media compositions and carbon sources for each growth condition can be found in **Supplementary table S2.1**.

In monoculture experiments, species' MICs varied widely in the different antibiotics tested. When grown in the presence of ampicillin, *M. extorquens* had a median MIC of 100µg/ml, which was significantly higher than the 2µg/ml and 1µg/ml necessary to inhibit *E. coli* and *S. enterica*, respectively (**Figure 2.2A**, $P<0.0001$ for each). In tetracycline, *S. enterica* had a median MIC of 50µg/ml (**Figure 2.2B)**. This was significantly higher than the median MIC of 5µg/ml in *M. extorquens* ($P<0.0001$) and 2µg/ml in *E. coli* ($P<0.0001$). We note that the spread in MIC for the most tolerant species is in part due to increasing step-size between antibiotic concentrations along the gradient; for example, growth at 50 vs. 100µg/ml represents a single step, as does 5 vs. 10µg/ml.

Consistent with the weakest link hypothesis, antibiotic concentrations needed to inhibit resistant species decreased substantially when bacteria were grown in an obligate mutualism rather than in monocultures. Fifty-fold less ampicillin was needed to inhibit the cooperative community (1μg/mL) than to inhibit *M. extorquens* in monoculture (**Figure 2.2A,** $P < 0.0001$). Similarly, the median MIC of tetracycline for *S. enterica* decreased significantly from 50μg/ml in monoculture to 4μg/ml in the cooperative community (**Figure 2.2B**, $P < 0.0001$).

We next distinguished the effect of species interactions from community complexity by measuring the MIC of the bacterial community when species were competing for common resources (**Figure 2.1B, Figure 2.2**). The median MIC for resistant bacteria was not significantly different in the competitive community than it was in monoculture (for *M. extorquens* in ampicillin **Figure 2.3C**, $P > 0.90$; for *S. enterica* in tetracycline, **Figure 2.3E**, $P = 0.80$). Therefore, decreased tolerance of resistant species to these antibiotics was a result of metabolic interdependence, rather than simply the presence of other species.

As an additional control, we examined the monoculture and competitive co-culture MIC of the three species using carbon sources that matched those that they consume in cooperative community (**Supplementary figure S2.2**). We found that the same qualitative patterns were observed, with *M. extorquens* showing high tolerance to ampicillin and *S. enterica* demonstrating high tolerance to tetracycline in both monoculture and competitive community.

Tolerance to tetracycline was higher than expected in community

Unexpectedly, we saw a small but significant trend towards protection of *E. coli* in cooperative community in tetracycline. *E. coli* median monoculture MIC was 2μg/mL while median MIC in the cooperative community was 4μg/mL (P= 0.0111, **Figure 2.3D**); we expected these MICs to match, as *E. coli* was the weakest link in tetracycline. This effect was not due to higher starting cell density in community, which can increase antibiotic tolerance (167) (**Supplementary figure S2.3A)**. As tetracycline is known to rapidly photolyse (168), we predicted that its increased time to detectable growth in the cooperative community might be protecting *E. coli* by allowing time for tetracycline to break down. Several lines of evidence indicate that tetracycline breakdown is occurring as *E. coli* experiences a delay in nutrient access when obtaining metabolites from cross-feeding partners instead of growth medium. First, *E. coli* monoculture MIC increases if tetracycline-containing media sits for 20 hours before cells are added (**Supplementary figure S2.3A).** Second, the time to detectable *E. coli* growth is significantly longer in cooperative community than in monoculture (**Supplementary figure S2.3B**, $P < 0.001$). Third, the MIC of *E. coli* in monoculture increased if cells sat in tetracycline for 20 hours before nitrogen and methionine were added to the media (P= 0.001, **Supplementary figure S2.3A**).

Interspecies competition sets *M. extorquens* tolerance in tetracycline

M. extorquens growth in tetracycline also did not follow the hypothesized weakest link pattern, though for different reasons than *E. coli.* In monoculture, tetracycline MIC for *M. extorquens* was 5μg/ml, while in the competitive community *M. extorquens* growth

was not observed even in the absence of antibiotic (**Figure 2.3F)**. *M. extorquens* was able to grow in the ampicillin experiments because it can grow at high ampicillin concentrations where its better competitors are antibiotic-inhibited (**Supplementary figure S2.4**). This suggests that growth patterns of *M. extorquens* in tetracycline are governed by competitive ability rather than resistance, while in ampicillin *M. extorquens* experiences competitive release (where removal of a stronger competitor species, in this case by antibiotic, allows a weaker competitor to grow).

Resistant bacteria are also constrained by sensitive partners in structured environments

We next tested whether growth on agar (rather than growth in liquid media) altered the impact of species interactions on antibiotic resistance. We hypothesized that spatial structure might enhance the ability of resistant bacteria to protect metabolic partners from degradable antibiotics like ampicillin, and thereby eliminate reduction of tolerance in the cross-feeding system.

Tolerance patterns on agar largely mirrored results from liquid media. Less antibiotic was needed to inhibit resistant bacteria in cooperative community than was needed in monoculture (**Figure 2.4-2.6**). Note that small clearing diameters signify high resistance, so relative rankings in **Figures 2.4-2.6** are the inverse of **Figure 2.2** and 2.**3**. Ampicillin cleared growth of *M. extorquens* out to a median diameter of 37.2 mm in cooperative community, but only 26.55 mm in monoculture (**Figure 2.5H**, $P = 0.0006$). Similarly, on tetracycline, *S. enterica* had a median clearing diameter of 8.67mm in monoculture and 41.2 mm in the cooperative community (**Figure 2.6G**, $P = 0.0012$). In the competitive

community, zones of clearing matched those of the most resistant monoculture (**Figure 2.4A**, *M. extorquens* vs. competitive community *P*= 0.999; **Figure 2.4B**, *S. enterica* vs. competitive community *P*= 0.4242). As in liquid, *M. extorquens* is only observed in ampicillin competitive community at diameters where it has higher tolerance than *E. coli* and *S. enterica* (**Figure 2.5E**), and not at all in in tetracycline competitive community (**Figure 2.6E, H**). Finally, using acetate as the carbon source for *S. enterica* and *M. extorquens* in monocultures and competitive community again showed qualitatively similar results (**Supplementary figure S2.5**).

Though *M. extorquens* had lower tolerance for ampicillin in cooperative community, we did observe cross-protection of more sensitive species. The cooperative community overall had a significantly smaller zone of inhibition than either *S. enterica* or *E. coli* monocultures (**Figure 2.4A,** *P* <0.0001 for *S. enterica* and *P*= 0.01 for *E. coli*). Quantification of fluorescence on these plates indicates that inhibition of both sensitive species was reduced in cooperative community (**Figure 2.5F,** *E. coli* monoculture vs. cooperative community diameter *P*= 0.0057, and **Figure 2.5G,** *S. enterica* monoculture vs. cooperative community diameter *P*= 0.02). This can also be observed qualitatively (**Figure 2.5,** panels **A** and **B** vs. **D**). We found that protection was not due to an increase in initial cell density on community versus monoculture plates (**Supplementary figure S2.6A**), and that *M. extorquens* was responsible for providing protection (**Supplementary figure S2.6B**). Consistent with the observed cross-protection, genes encoding ampicillin degrading β-lactamases were found in the genome of *M. extorquens*. Nitrocefin disks were used to demonstrate β-lactamase activity when *M. extorquens* was grown on agar in the presence of ampicillin (**Supplementary Figure S2.7**).

Metabolic dependency reduces antibiotic tolerance of a pathogen

To test whether our findings extend to a medically relevant system, we investigated how co-culturing influences the effective tolerance of *Pseudomonas aeruginosa* to ampicillin. *P. aeruginosa* is a leading cause of morbidity and mortality in people with cystic fibrosis (169). It was recently demonstrated that *P. aeruginosa* can cross-feed on carbon generated by mucin-degrading anaerobes that are also associated with CF lung disease (18). In addition to its medical relevance, this system is distinct from our previous system in that cross-feeding is not obligate (*P. aeruginosa* growth on mucin decreases but is not abolished by the absence of anaerobes). We tested how ampicillin influenced the growth of *P. aeruginosa*, when grown alone on mucin versus in a facultative cross-feeding co-culture.

Consistent with previous findings (170), *P. aeruginosa* was highly resistant to ampicillin in monoculture (**Figure 2.7, Supplementary figure S2.8A**). No observable decrease in final CFU count was observed across any concentration out to 25μg/mL of the drug. In contrast, ampicillin inhibited the final density of mucin-degrading anaerobes (as measured by OD600), starting at 5μg/mL (P= 0.0216) (**Figure 2.7, Supplementary figure S2.8B**). Consistent with expectations, ampicillin also reduced the final CFU of *P. aeruginosa* grown in co-cultures on mucin, starting at 5μg/mL ampicillin (P= 0.0173). These data suggest that applying antibiotic to inhibit the growth of cross-feeding partners can inhibit resistant species even in a non-obligate cross-feeding system of clinical significance.

Discussion

Our results demonstrate that metabolic dependency between microbial community members plays a critical role in mediating the effect of antibiotics. In both mass-action (liquid) and structured (solid) environments we observed that bacterial species that show high levels of tolerance to a given antibiotic in monoculture are inhibited at much lower concentrations in an obligate mutualism. The constraint of cross-feeding on bacterial tolerance was consistent across drugs and microbial systems; this was true for two antibiotics with different modes of action and extended to a medically relevant system with facultative cross-feeding. *P. aeruginosa* growth was reduced by substantially lower concentrations of ampicillin when the pathogen was cross-feeding off of mucin-degrading anaerobes that were sensitive to the drug.

We have shown that the ability of a given bacterial species to grow in the presence of an antibiotic is a combination of its intrinsic tolerance and the tolerance of species on which it relies for metabolites. Dependence on other bacteria reduced the MIC of bacteria with high resistance in monoculture, regardless of the antibiotic and mechanism of action. This change in MIC was driven by inhibition of a beneficial partner rather than a change in the resistance of the focal species. The effective tolerance of a cross-feeding network, therefore, is generally set by the 'weakest link' species; that is, the species with the lowest resistance to the antibiotic, whose tolerance in community usually matches its monoculture tolerance. This suggests that antibiotics will often be more effective at controlling microbial communities where there is extensive metabolic interdependence, and that tolerance in cross-feeding communities can be approximated from monoculture studies.

Unexpectedly, we did see deviations from our weakest link hypothesis. *E. coli* had a higher tetracycline MIC in the cross-feeding community than in monoculture, suggesting some protective effect of cooperative community growth. This slight, but significant, increase was likely driven by an increase in time to detectable *E. coli* growth when cross-feeding. Tetracycline breaks down rapidly, so this delay likely allowed *E. coli* to experience reduced antibiotic concentrations. Similar antibiotic dynamics may often occur in clinical or environmental settings (168, 171), where metabolically inactive "persisters" commonly survive antibiotic treatment by delaying growth (59), particularly in the case of bacteriostatic drugs such as tetracycline. Although we have evidence that a delay in growth in cooperative community coupled with tetracycline breakdown can explain the increased *E. coli* tolerance to tetracycline, it is important to note that other factors may also contribute.

Community context further altered tolerance by enabling cross-protection of less tolerant species by more tolerant partners. On agar with ampicillin, both *E. coli* and *S. enterica* grew closer to the antibiotic disc in the presence of *M. extorquens.* This protection was likely caused by degradation of the antibiotic due to β-lactamase activity in *M. extorquens.* Our results are consistent with previous observations that spatial structure can allow bacteria to lower local antibiotic gradients sufficiently to permit growth of sensitive isolates (124). There were limits on the extent of cross-protection in our community, however. The cross-feeding community increased tolerance of *E. coli* and *S. enterica* but, tolerance of *M. extorquens* was still lower in the cooperative community than it was in monoculture. Cross-protection may reduce the magnitude of the constraints placed on resistant species by their more sensitive metabolic partners, but it

does not eliminate this constraint. As well, degradative enzymes are not available for all antibiotics nor for all bacterial species, limiting the ubiquity of this mechanism. Further research is needed on the interaction of cross-protection and cross-feeding, particularly in polymicrobial infection contexts, as these studies may help direct antibiotic choice.

This study also demonstrates some issues which can arise when measuring the effect of antibiotics in microbial communities. It has previously been shown that MIC is a problematic metric that can be influenced by factors such as changes in initial microbial density, or metabolic state (59, 167). In our study, it was not possible to measure the tolerance of *M. extorquens* to tetracycline in the competitive community, as *M. extorquens* was always outcompeted. The competitive release of *M. extorquens* in ampicillin treated competitive communities again deviates from standard patterns for MIC. This may also impact antibiotic choice in polymicrobial infections. If, for example, a pathogen grown in monoculture is highly antibiotic-resistant but limited *in vivo* by less tolerant competitors, application of high levels of antibiotic might only serve to remove competitor species that would have otherwise kept the pathogen at bay; this has been observed in *C. difficile* infections, which are often precipitated by antibiotic-mediated depletion of healthy intestinal microbiome species (36, 172, 173). Our results highlight that the community context further complicates challenges associated with interpreting MIC measurements.

The constraint of cross-feeding on antibiotic tolerance also extended to a microbial community relevant to cystic fibrosis. It should be noted that this system involved facultative cross-feeding, so inhibiting anaerobes only reduced the yield of *P. aeruginosa* by two-fold. While this reduction is substantially smaller than the complete

elimination of growth in the obligate system, two-fold changes may be medically relevant (174–178). More broadly, the constraint in this treatment speaks to the generality of our findings. Even in scenarios with less extreme metabolic dependency, the impact of antibiotics can be magnified when highly resistant species are cross-feeding from less resistant species. Given that metabolic interactions are common in infection contexts (11, 19), this work suggests that even narrow-spectrum antibiotics, designed to target a single species, may have widespread effects throughout a metabolically interconnected community.

Our results highlight that mutualistic networks are highly susceptible to environmental change. This result is consistent with work in other ecological systems from plant-pollinator to insect-symbiont (179–181). Integrating these ecological concepts into a microbial perspective may allow greater precision in our medical practices. Broad-spectrum reductions of bacteria in the gut can cause long-lasting negative health outcomes such as facilitating infections by *Clostridium difficile* (172). To develop precision treatments, predicting the impact of a drug on a focal population, and how a drug will affect off-target members of a microbial community, is essential. Our work highlights that precision microbiome management will require not only improved pharmacology but also a more comprehensive understanding of ecological interactions in microbial systems.

Footnotes

[1] This work has been previously published: Adamowicz EM, Flynn J, Hunter RC, Harcombe WR. 2018. Cross-feeding modulates antibiotic tolerance in bacterial communities. The ISME Journal 12:2723–2735. © 2018

[2] These experiments were performed by Dr. Jeffry Flynn.

Chapter 2 Figures and Tables

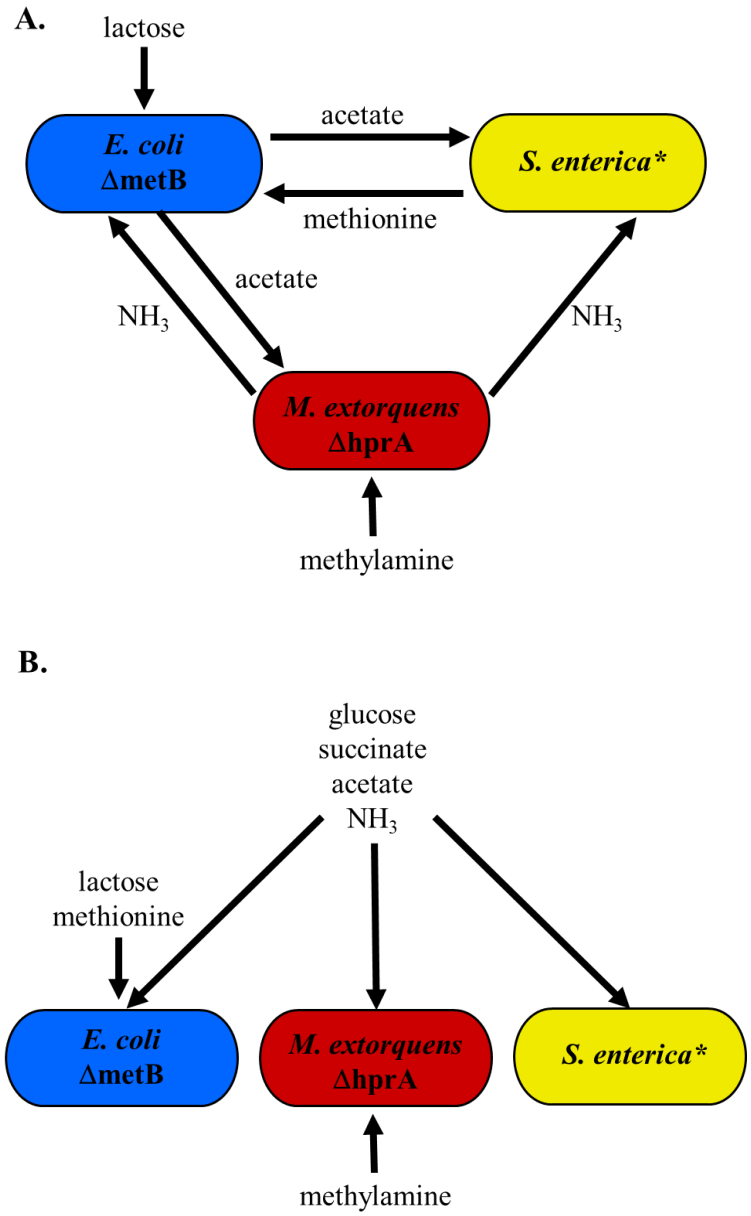

Figure 2.1 Cooperative and competitive model communities. **A.** Cooperative community. Methylamine and lactose are supplied in the growth medium as a nitrogen and a carbon source, respectively. *E. coli* consumes lactose and excretes acetate as a carbon source for *S. enterica* and *M. extorquens*. *S. enterica* secretes methionine for the

methionine auxotroph *E. coli*. *M. extorquens*, which has a deletion in *hprA* which renders it unable to assimilate carbon from methylamine, provides nitrogen to the community via methylamine breakdown. **B.** Competitive community. Growth medium contains all metabolites necessary for growth of each individual species such that no cross-feeding is necessary to support growth.

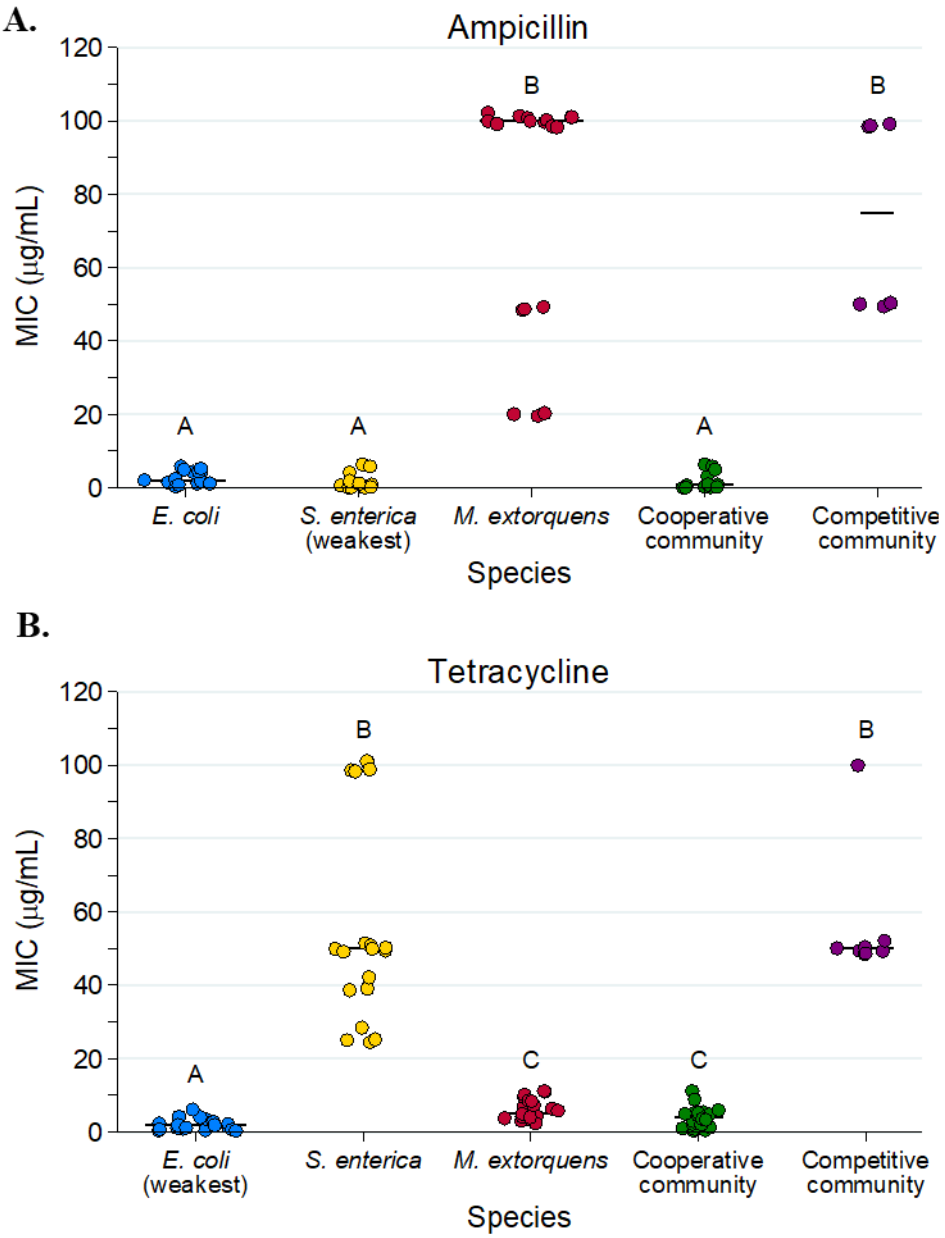

Figure 2.2 Minimum inhibitory concentration (MIC) values for each monoculture and community type in ampicillin (**A**) and tetracycline (**B**) based on total population OD600. The 'weakest link' species (i.e. the species with the lowest median MIC in monoculture) is indicated on the x-axis. Bars represent median values. MIC is defined as the minimum concentration of antibiotic required to inhibit growth by three times the time to

observable growth of the antibiotic free control. Cultures were grown on a Tecan plate reader with measurements every 15 minutes. At least eight replicates were performed for each species/ antibiotic combination. Pairwise comparisons of median MIC were performed using a Mann-Whitney U test, with a Bonferroni correction applied for ten pairwise multiple comparisons. Shared letters indicate nonsignificant differences between groups.

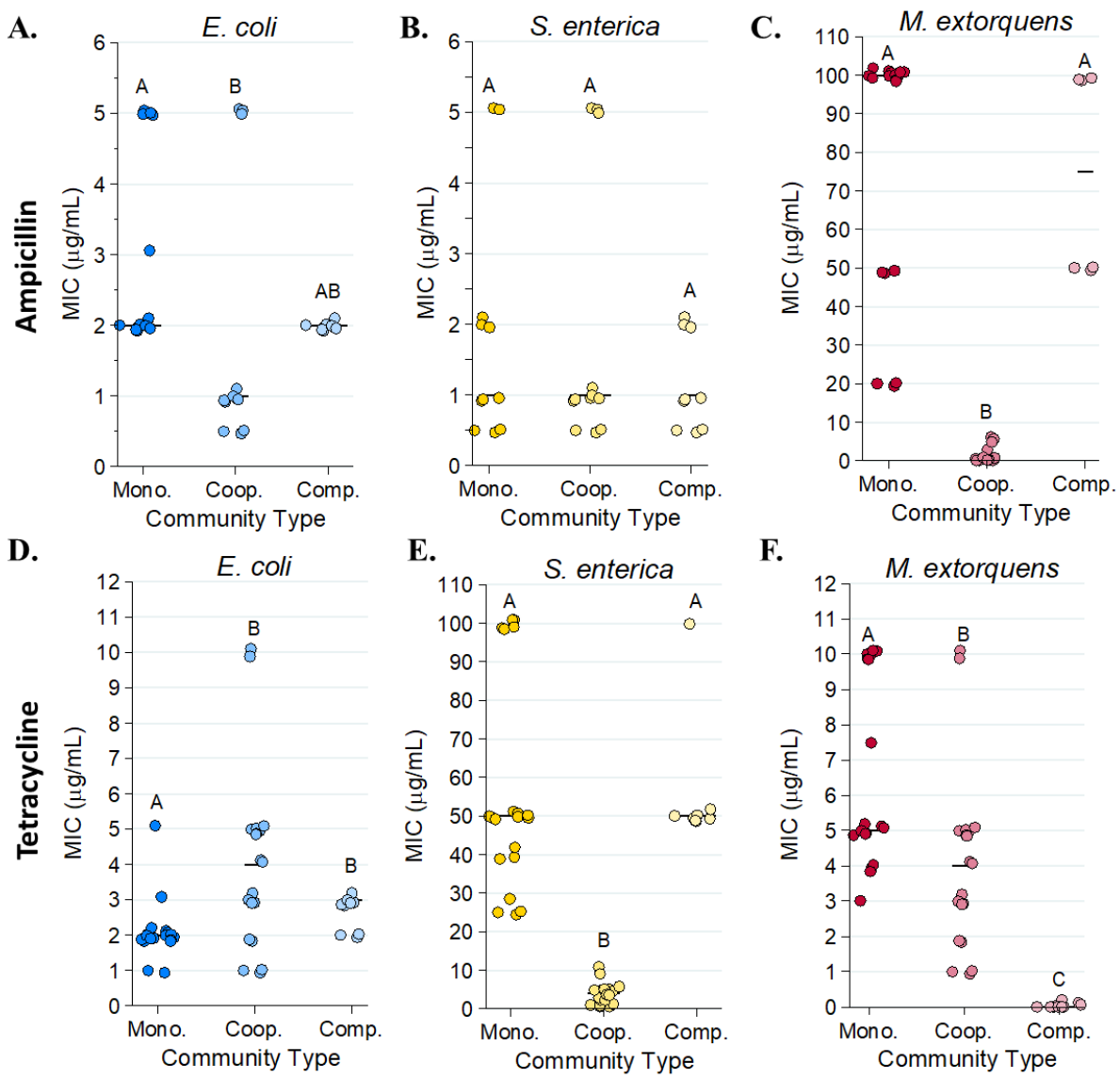

Figure 2.3 Species-specific minimum inhibitory concentration (MIC) values in monoculture, cooperative community, and competitive community in ampicillin (**A-C**) and tetracycline (**D-F**). MIC was defined as the minimum concentration of antibiotic required to inhibit growth by three times the time to detectable growth of the antibiotic free control MICs were calculated based on fluorescence (CFP for *E.* coli, YFP for *S. enterica*, and RFP for *M. extorquens*) recorded on a Tecan plate reader with fluorescence measurements every 15 minutes. Pairwise comparisons of median MIC were performed

using a Mann-Whitney U test, with a Bonferroni correction applied for three multiple comparisons. Shared letters indicate nonsignificant differences between clusters.

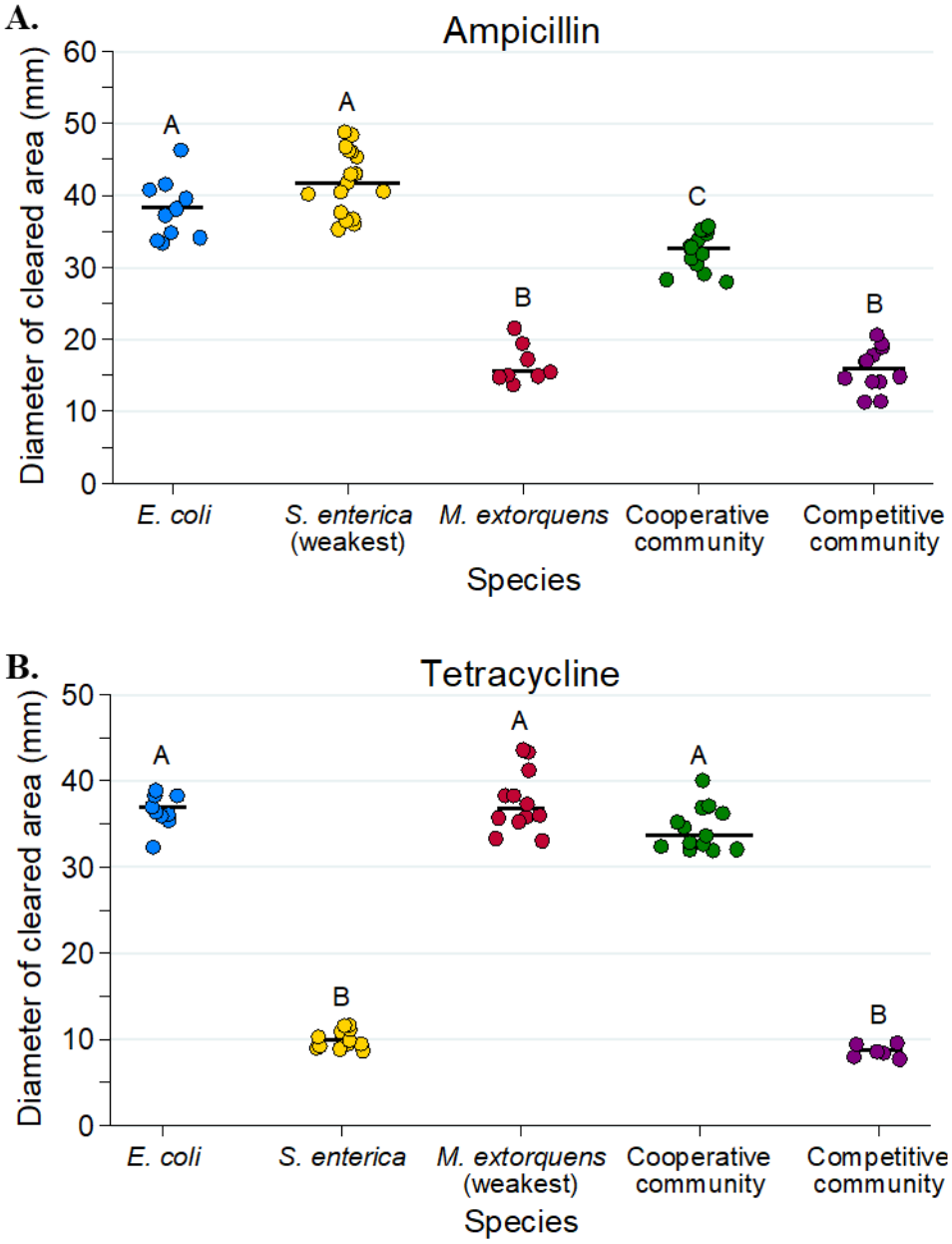

Figure 2.4 Diameters of zones of clearing for ampicillin (**A**) and tetracycline (**B**) disc diffusion assays. The diameter of the zone of clearing was measured three times for each plate and averaged for a single plate measurement. At least eight replicate plates were measured for each monoculture and community type. The 'weakest link' species (i.e. the species with the largest median zone of clearing in monoculture) is indicated on the x-

axis. Pairwise comparisons of the zone of clearing for each monoculture and community was performed with a Mann-Whitney U test with Bonferroni adjustment for multiple comparisons. Significant differences are noted by different letters above each cluster; shared letters represent nonsignificant differences.

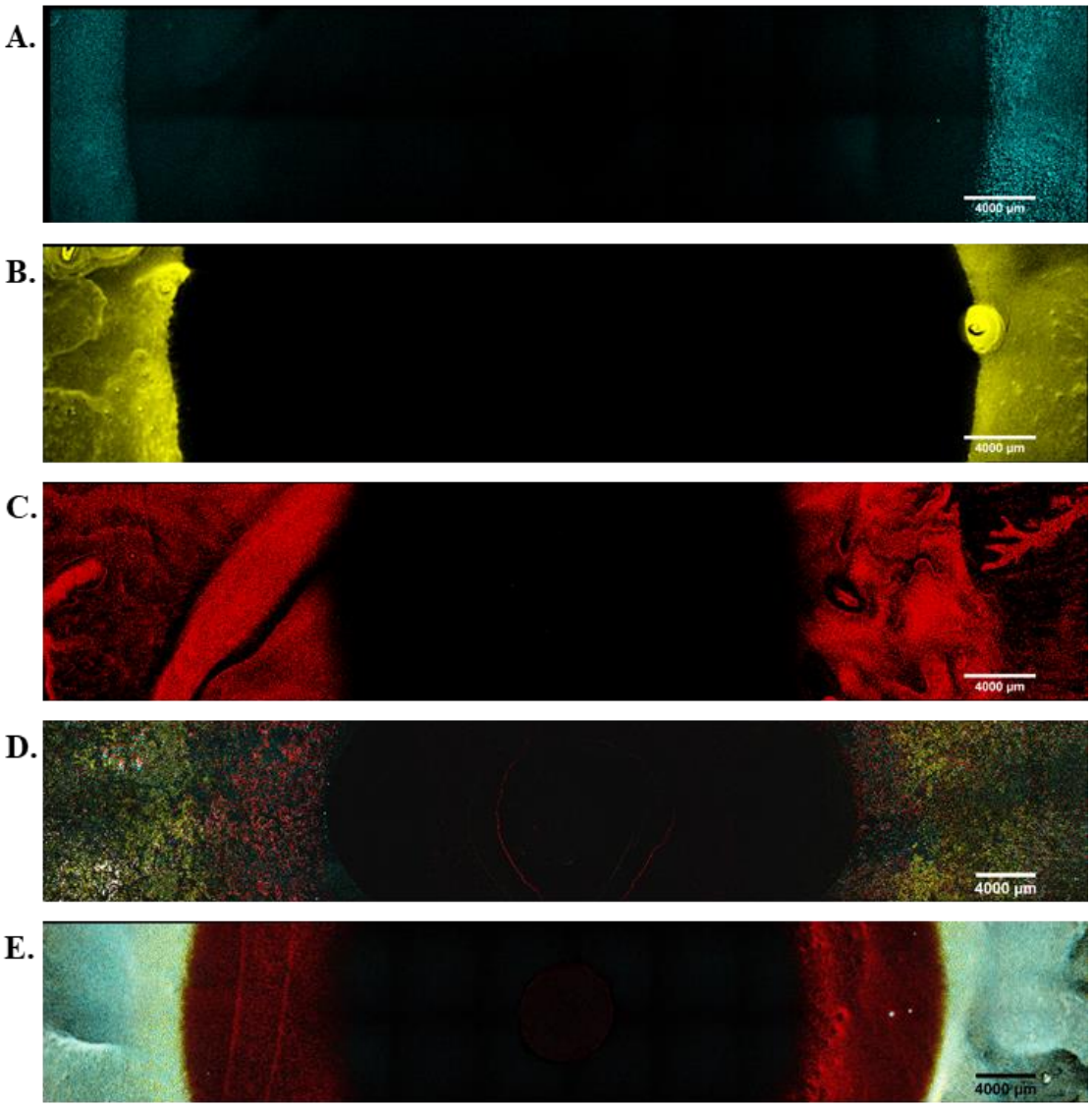
A.
4000 µm
B.
4000 µm
C.
4000 µm
D.
4000 µm
E.
4000 µm

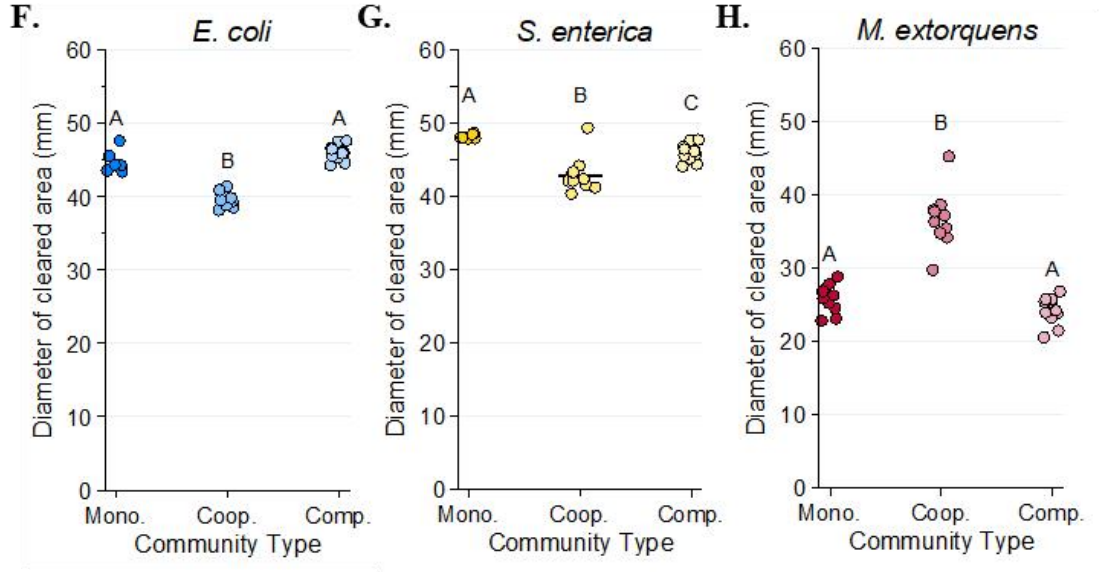
F.
E. coli
G.
S. enterica
H.
M. extorquens
Diameter of cleared area (mm)
0
10
20
30
40
50
60
A
B
A
A
B
C
A
B
A
Mono.
Coop.
Comp.
Community Type

Figure 2.5 Fluorescent microscopy images of Petri plates with ampicillin antibiotic discs. An AZ100 confocal fluorescent macroscope at 3.40x magnification was used to image 12x2 fields of view of each Petri plate to visualize *E. coli* (CFP, in blue), *S. enterica* (YFP, in yellow) or *M. extorquens* (RFP, red). **A**-**E** are representative images of *E. coli* monoculture (**A.**), *S. enterica* monoculture (**B.**), *M. extorquens* monoculture (**C.**), cooperative community (**D.**) and competitive community (**E.**) Quantification of the diameter of the species-specific zone of clearing for *E. coli* (**F.**), *S. enterica* (**G.**), and *M. extorquens* (**H.**) in each growth condition was performed in Elements software. The average of three technical replicate diameters was calculated to obtain a single measurement. At least 6 biological replicates were obtained for each species/ growth condition. Pairwise comparisons of median diameter of clearing were performed using a Mann-Whitney U test, with a Bonferroni correction applied for three multiple comparisons. Significant differences are noted by different letters above each cluster.

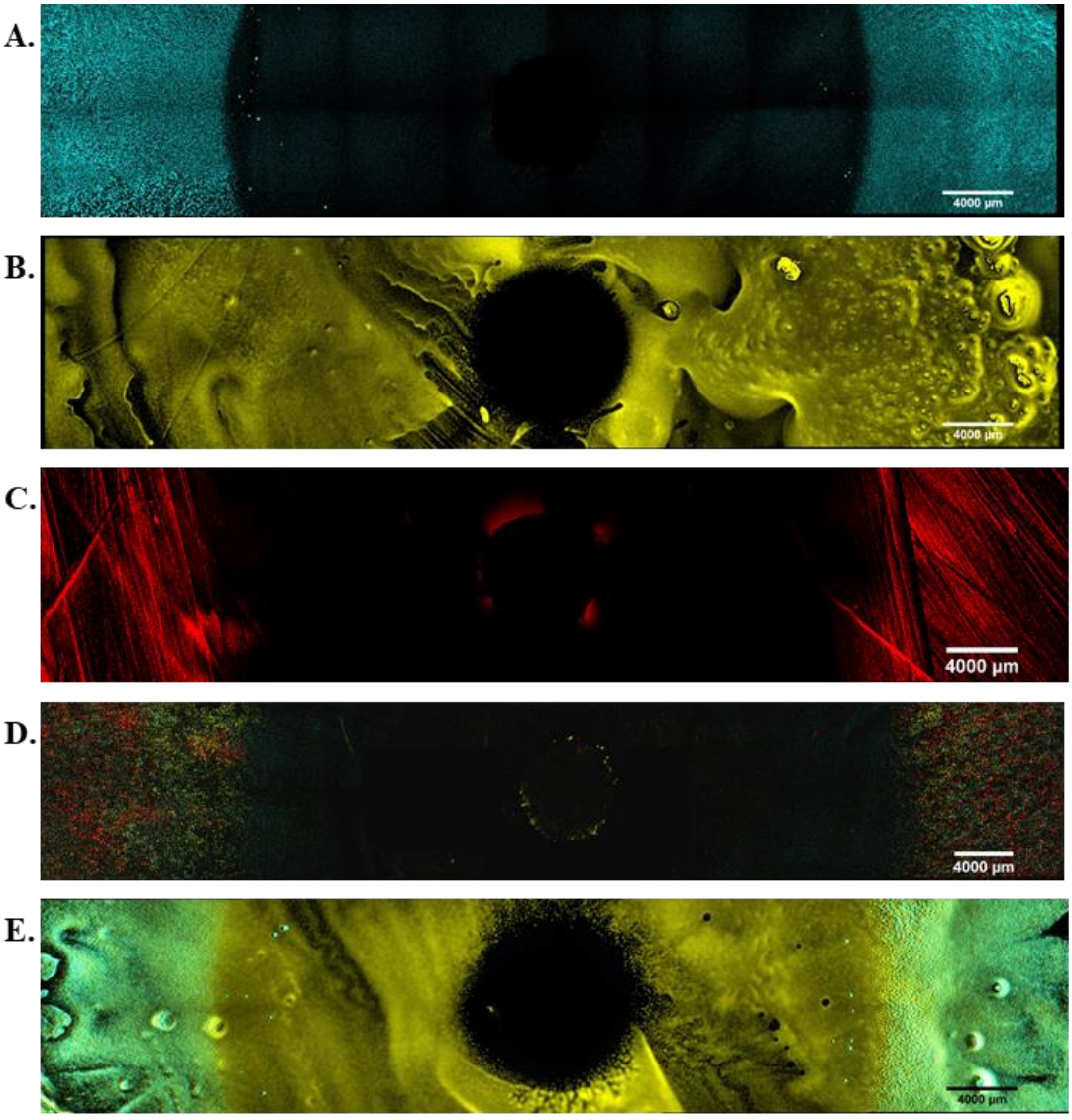
A.
4000 µm
B.
4000 µm
C.
4000 µm
D.
4000 µm
E.
4000 µm

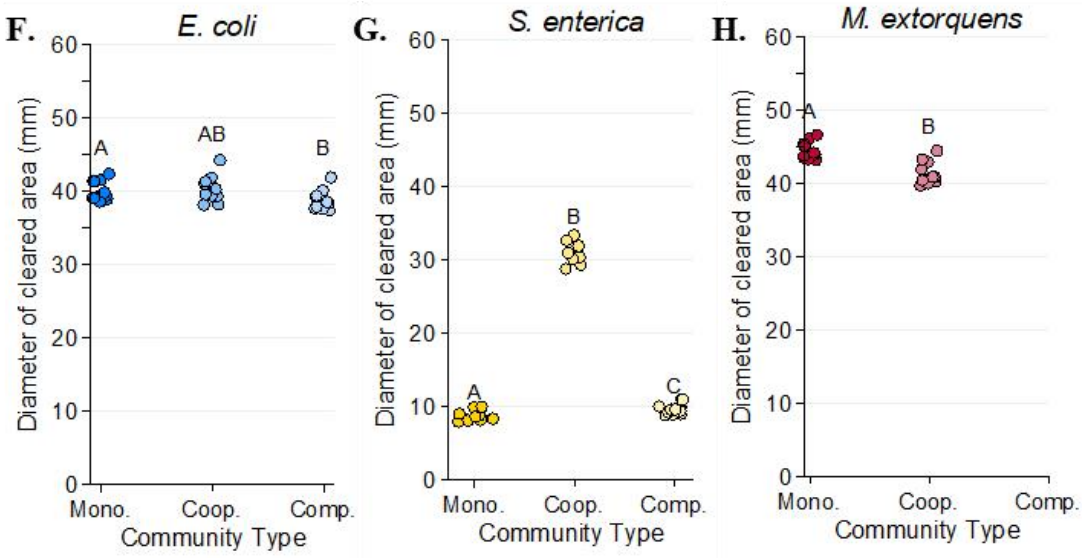
F.
E. coli
Diameter of cleared area (mm)
60
50
40
30
20
10
0
A
AB
B
Mono.
Coop.
Comp.
Community Type
G.
S. enterica
Diameter of cleared area (mm)
60
50
40
30
20
10
0
A
B
C
Mono.
Coop.
Comp.
Community Type
H.
M. extorquens
Diameter of cleared area (mm)
60
50
40
30
20
10
0
A
B
Mono.
Coop.
Comp.
Community Type

Figure 2.6 Fluorescent microscopy images of Petri plates with tetracycline antibiotic discs. An AZ100 confocal fluorescent macroscope at 3.40x magnification was used to image 12x2 fields of view of each Petri plate to visualize *E. coli* (CFP, in blue), *S. enterica* (YFP, in yellow) or *M. extorquens* (RFP, red). **A**-**E** are representative images of *E. coli* monoculture (**A.**), *S. enterica* monoculture (**B.**), *M. extorquens* monoculture (**C.**), cooperative community (**D.**) and competitive community (**E.**) Quantification of the diameter of the species-specific zone of clearing for *E. coli* (**F.**), *S. enterica* (**G.**), and *M. extorquens* (**H.**) in each growth condition was performed in Elements software. The average of three technical replicate diameters was calculated to obtain a single measurement. At least 6 biological replicates were obtained for each species/ growth condition, except for *M. extorquens* in competition in tetracycline, for which no RFP signal could be detected. Pairwise comparisons of median diameter of clearing were performed using a Mann-Whitney U test, with a Bonferroni correction applied for three multiple comparisons. Significant differences are noted by different letters above each cluster.

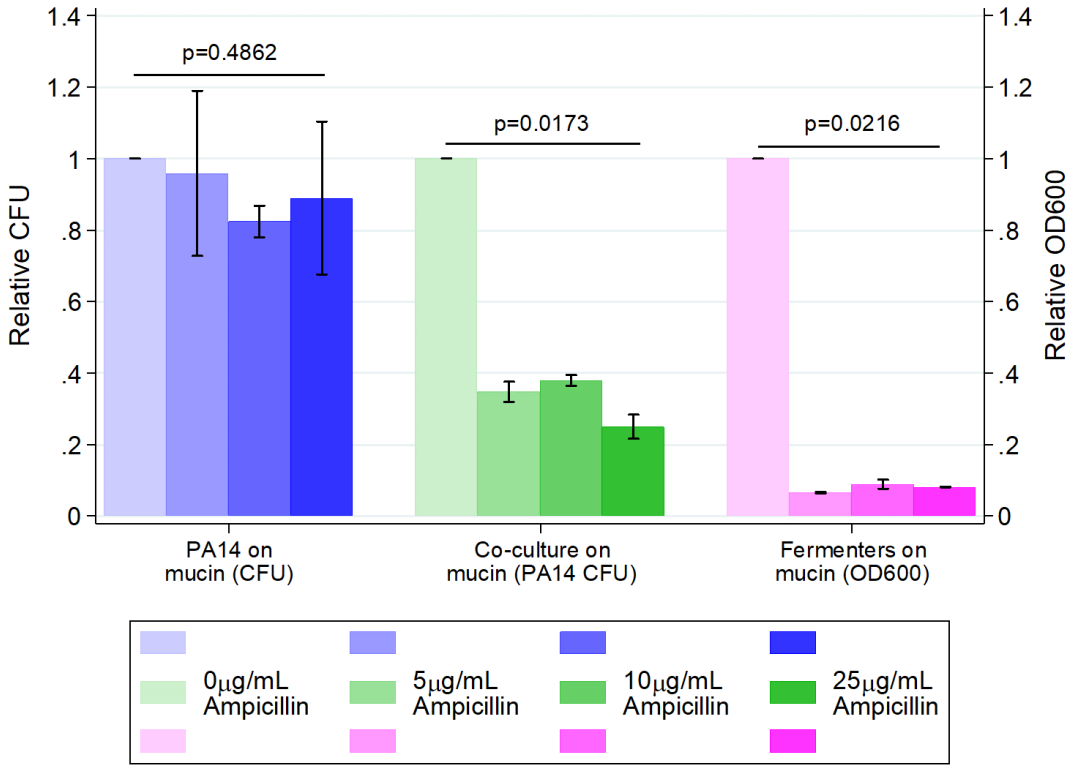

Figure 2.7 Ampicillin tolerance of *Pseudomonas aeruginosa* PA14 grown, PA14 cross-feeding with a mucin-fermenting community, and the mucin-fermenting community alone. PA14 colony-forming units (CFUs) from monocultures and co-cultures were enumerated by plating cells from each ampicillin concentration on LB agar after 16 hours of growth. Fermenter community OD600 was measured with a Biotek Synergy H1 plate reader after 48 hours of growth. Normalized OD600 and colony-forming units (CFU) values were calculated for each concentration of ampicillin by dividing raw values for the OD600 or CFU value at that concentration by the raw OD600 or CFU value of growth at 0μg/mL ampicillin. Each point represents the mean and standard deviation of triplicate samples. *P*-values were calculated using a Kruskal-Wallis test across ampicillin concentrations using relative CFU (for PA14) or OD600 (for fermenters).

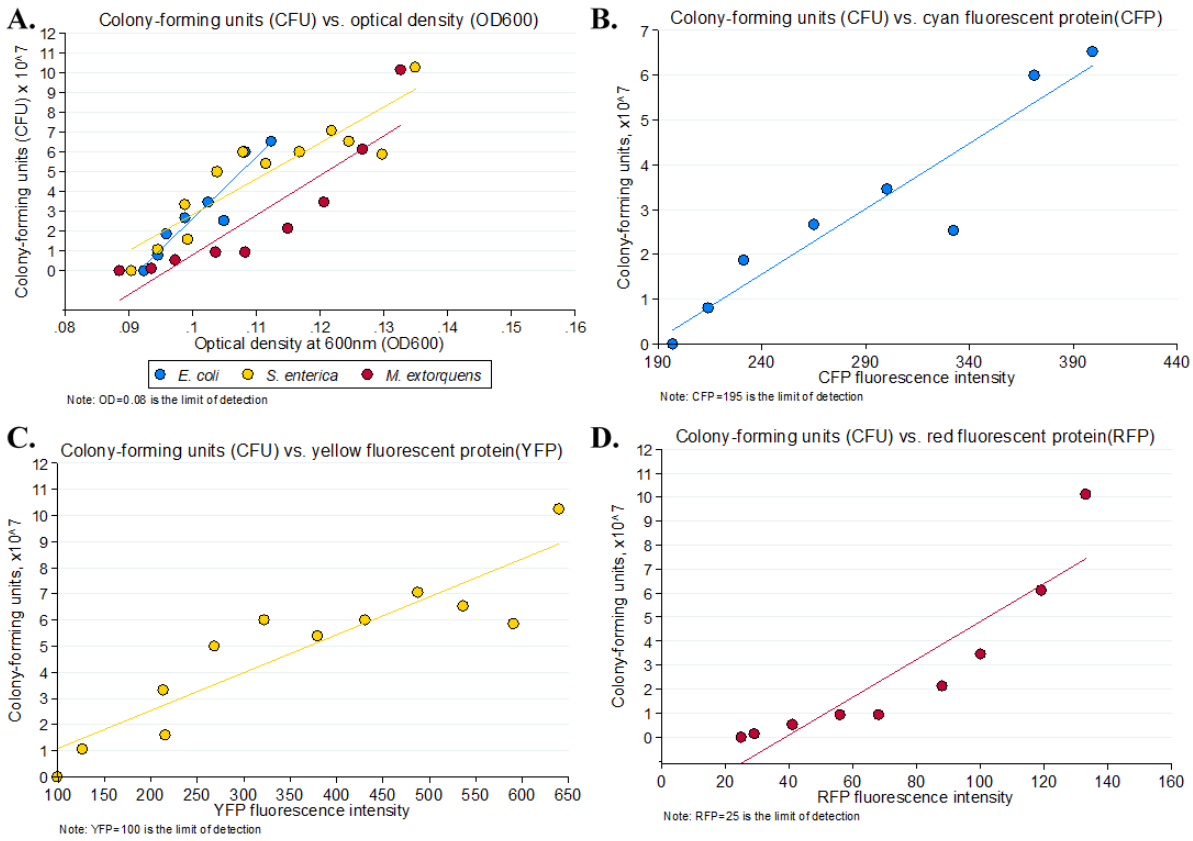

Supplementary figure S2.1 Correlations between colony-forming units (CFU) and optical density (OD600) for each of *E. coli*, *S. enterica*, and *M. extorquens* (**A**), between CFU and cyan fluorescent protein (**B**), between CFU and yellow fluorescent protein (**C**), and between CFU and red fluorescent protein (**D**). Briefly, cultures of each species were grown to mid-log phase at 30°C (OD600~0.2), diluted twofold eleven times, and the dilutions measured for their OD600 and fluorescence in a Tecan plate reader. Each dilution was then plated for CFU and the resulting CFU/mL values were calculated and plotted against measured OD600 and fluorescent protein values.

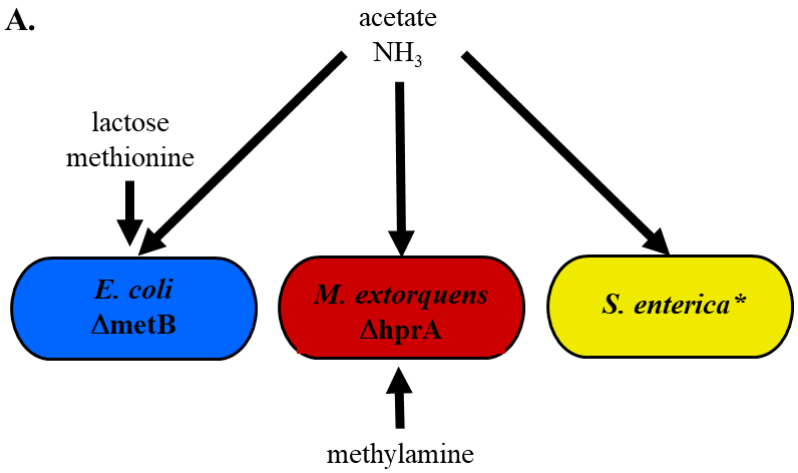
A.
acetate
NH_3
lactose
methionine
E. coli
ΔmetB
M. extorquens
ΔhprA
S. enterica*
methylamine

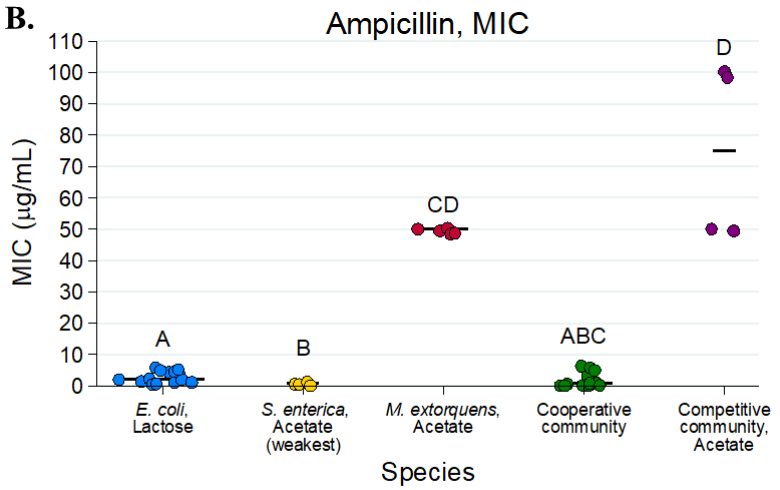
B.
Ampicillin, MIC
MIC (µg/mL)
110
100
90
80
70
60
50
40
30
20
10
0
A
B
CD
ABC
D
E. coli, Lactose
S. enterica, Acetate (weakest)
M. extorquens, Acetate
Cooperative community
Competitive community, Acetate
Species

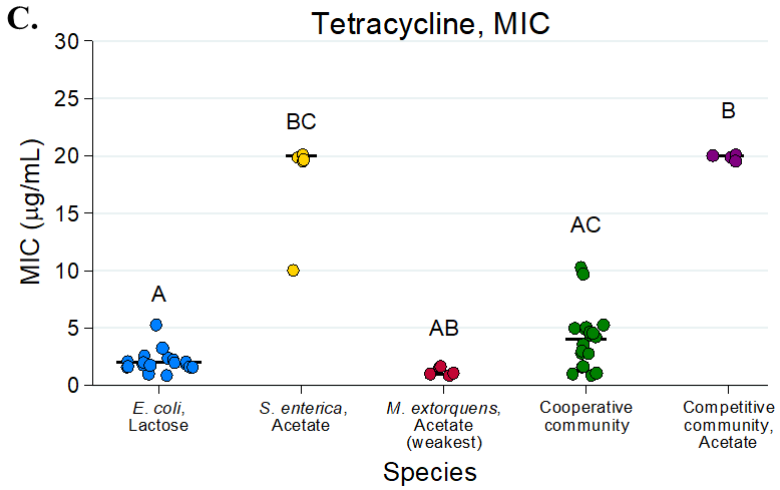
C.
Tetracycline, MIC
MIC (µg/mL)
30
25
20
15
10
5
0
A
BC
AB
AC
B
E. coli, Lactose
S. enterica, Acetate
M. extorquens, Acetate (weakest)
Cooperative community
Competitive community, Acetate
Species

Supplementary figure S2.2 Acetate as the sole carbon source for *M. extorquens* and *S. enterica* in monoculture and competitive community. **A.** Competitively grown three-species community using acetate. Growth medium contains all metabolites necessary for the growth of each individual species, with the carbon sources provided matching that of the carbon sources available to each species in cooperative community via cross-feeding. Minimum inhibitory concentrations (MICs) in for ampicillin (**B.**) and tetracycline (**C.**) were calculated as previously described. At least four replicates were performed for each community type. Matching letters represent statistical non-significance in medians between groups.

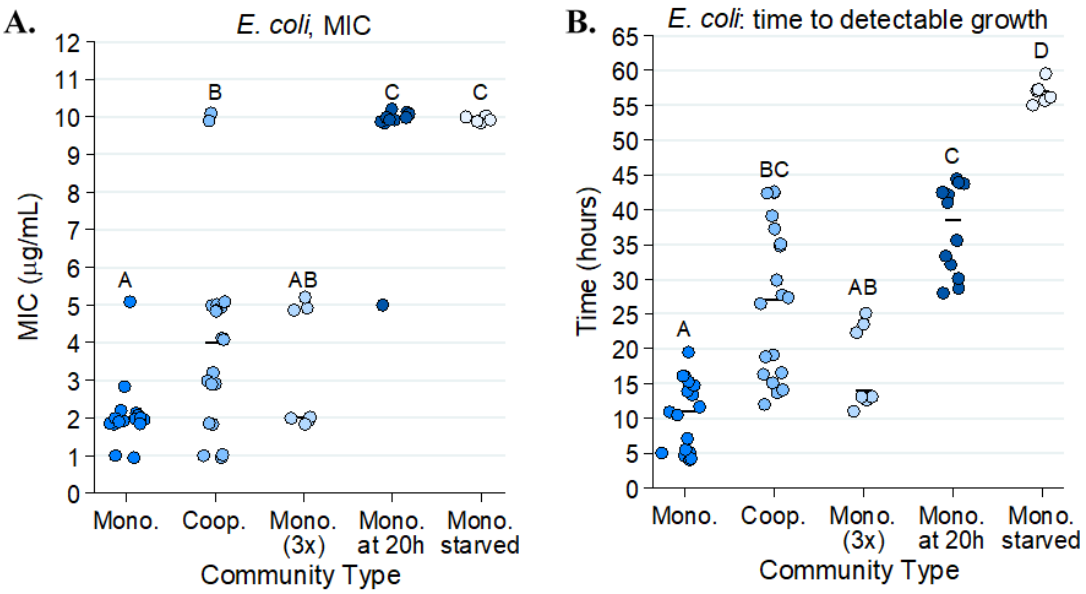

Supplementary figure S2.3 A Minimum inhibitory concentrations (MICs) of tetracycline for *E. coli* in different growth conditions. MIC was calculated as previously described. 3x mono is monoculture *E. coli* at three times the starting density of conventional monocultures. Mono. at 20h is sterile *E. coli* monoculture medium containing antibiotic and incubated for 20 hours prior to *E. coli* inoculation. Mono. starved is *E. coli* monocultures in which nitrogen and methionine are added 20 hours post-*E. coli* inoculation. **B.** Time to detectable growth of *E. coli* in different growth conditions. Cyan fluorescent protein (CFP) was used to monitor the growth of *E. coli*. Time to detectable growth was recorded as the first time point in which CFP above background levels was detected. In the Mono. at 20h and Mono. starved data, the 20 hour incubation period is included in the time to detectable growth. Pairwise MIC comparisons were performed using a Mann-Whitney U test with Bonferroni adjustment for ten multiple comparisons. Shared letters represent nonsignificant differences between groups.

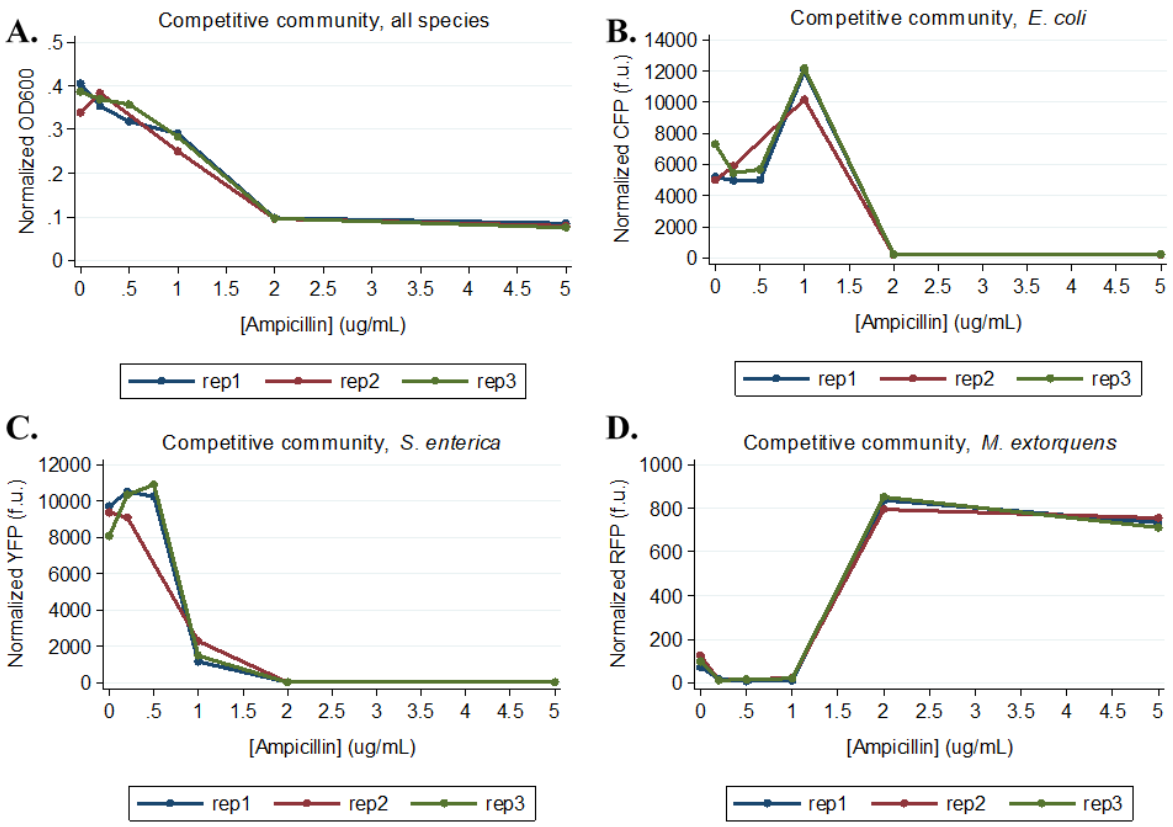

Supplementary figure S2.4 Competitive release of *M. extorquens* at high ampicillin concentrations in competitively grown community. Species were grown together in competitive Hypho medium at a range of ampicillin concentrations for 72 hours at 30^{O}C. A Tecan InfinitePro 200 plate reader was then used to measure OD600 of the entire community and fluorescent markers corresponding to individual species. Normalized OD600 (**A**), cyan fluorescent protein to detect *E. coli* (**B**), yellow fluorescent protein to detect *S. enterica* (**C**), and red fluorescent protein to detect *M. extorquens* (**D**) were calculated by subtracting blank values from cell-free medium.

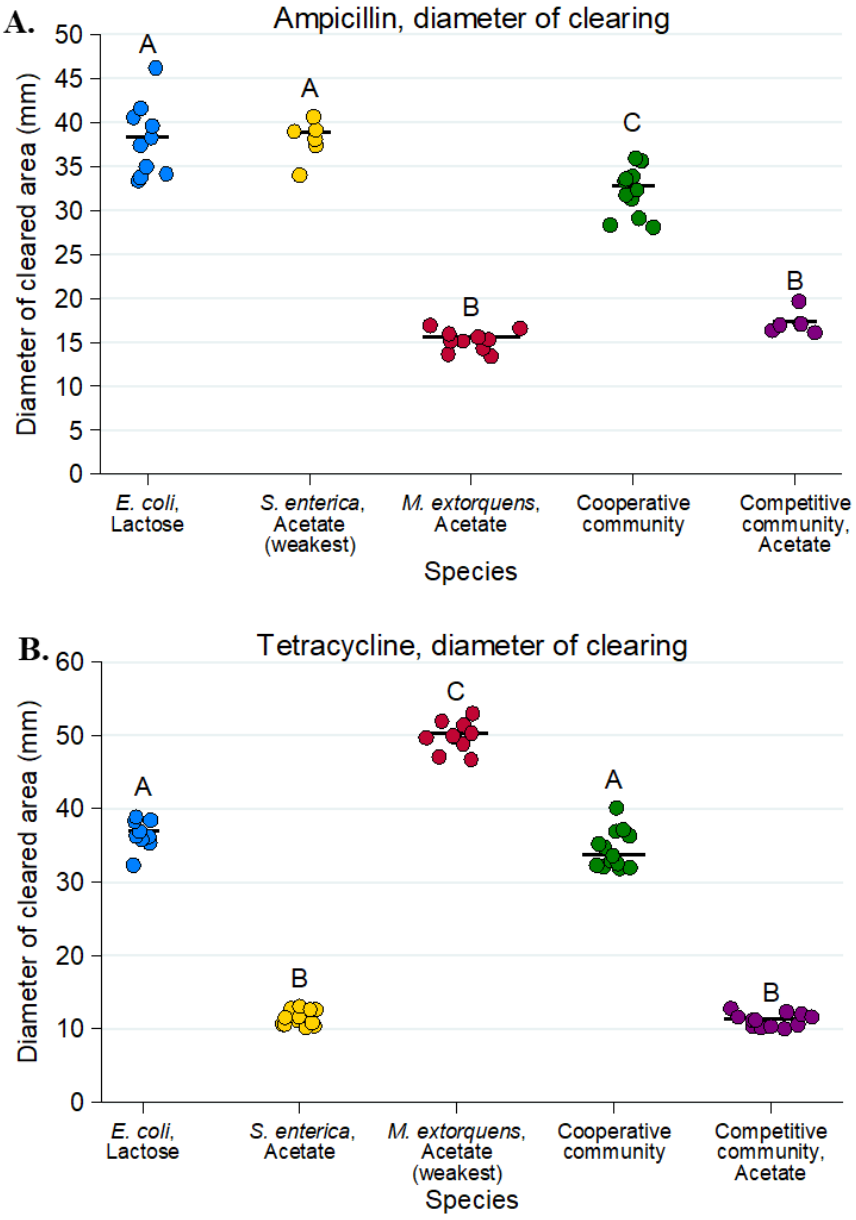

Supplementary figure S2.5 Acetate as the sole carbon source for *M. extorquens* and *S. enterica* in monoculture and competitive community on solid medium. Disc diffusion experiments using ampicillin (**A.**) and tetracycline (**B.**) were performed and analyzed as previously described. The 'weakest link' species (i.e. the species with the largest median zone of clearing in monoculture) is indicated on the x-axis. At least six replicates were performed for each community type. Pairwise comparisons of median zone of clearing

were performed using a Mann-Whitney U test with Bonferroni adjustment for ten multiple comparisons. Matching letters represent statistical non-significance in medians between groups.

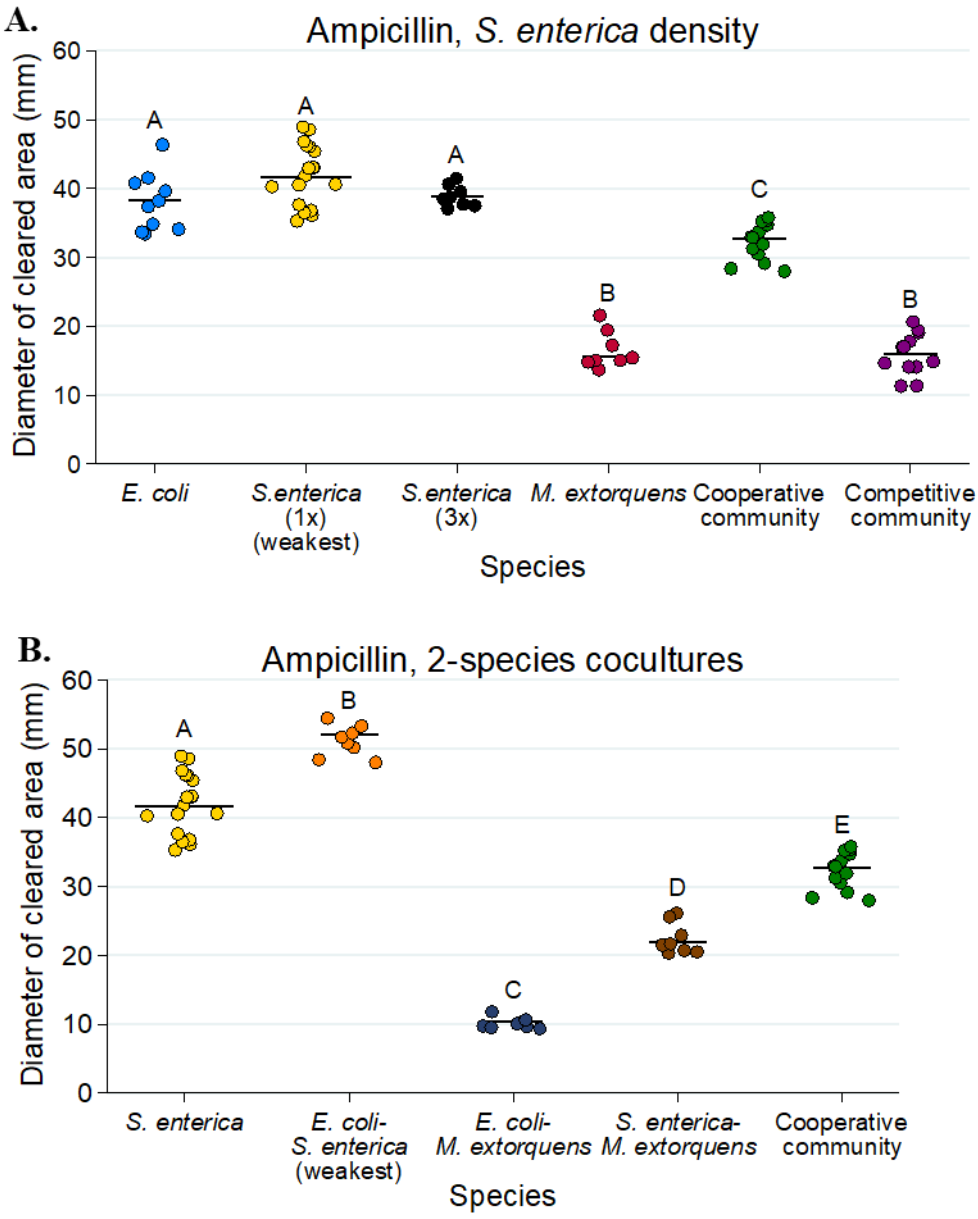

Supplementary figure S2.6 Possible mechanisms of *S. enterica* and *E. coli* protection from ampicillin in cooperative community on solid medium. The 'weakest link' species (i.e. the species with the largest median zone of clearing in monoculture) is indicated on the x-axis. **A.** Comparing monocultures and cooperative/ competitive community zones of clearing to 3x *S. enterica* to match total cell density of *S. enterica* monoculture to total cell density in community. **B.** Two-species cooperative co-cultures as compared to

S. enterica monoculture and cooperative three-species community. Pairwise comparisons of median zone of clearing were performed using a Mann-Whitney U test with Bonferroni adjustment for fifteen (**A.**) or ten (**B.**) multiple comparisons. Matching letters represent statistical non-significance in medians between groups.

Supplementary figure S2.7 Nitrocefin disc assay for *M. extorquens*. Nitrocefin discs were used to determine if *M. extorquens* was producing a β-lactamase (indicated by a color change from yellow to red/ pink). *E. coli* containing the plasmid pBR322 was used as a control; pBR322 contains a *bla* selectable marker encoding a β-lactamase. **A.** *M. extorquens* grown in liquid medium **B.** *M. extorquens* grown on solid medium **C.** *E. coli* with pBR322 on solid medium **D.** *E. coli* with pBR322 in liquid medium. For liquid cultures, 15µL of liquid medium containing cells was pipetted onto the disc and left at room temperature for 15 minutes. For solid cultures, colonies were scraped off plates and dissolved in liquid medium, and 15µL was pipetted onto the discs. All cells were grown in the presence of 50µg/mL ampicillin.

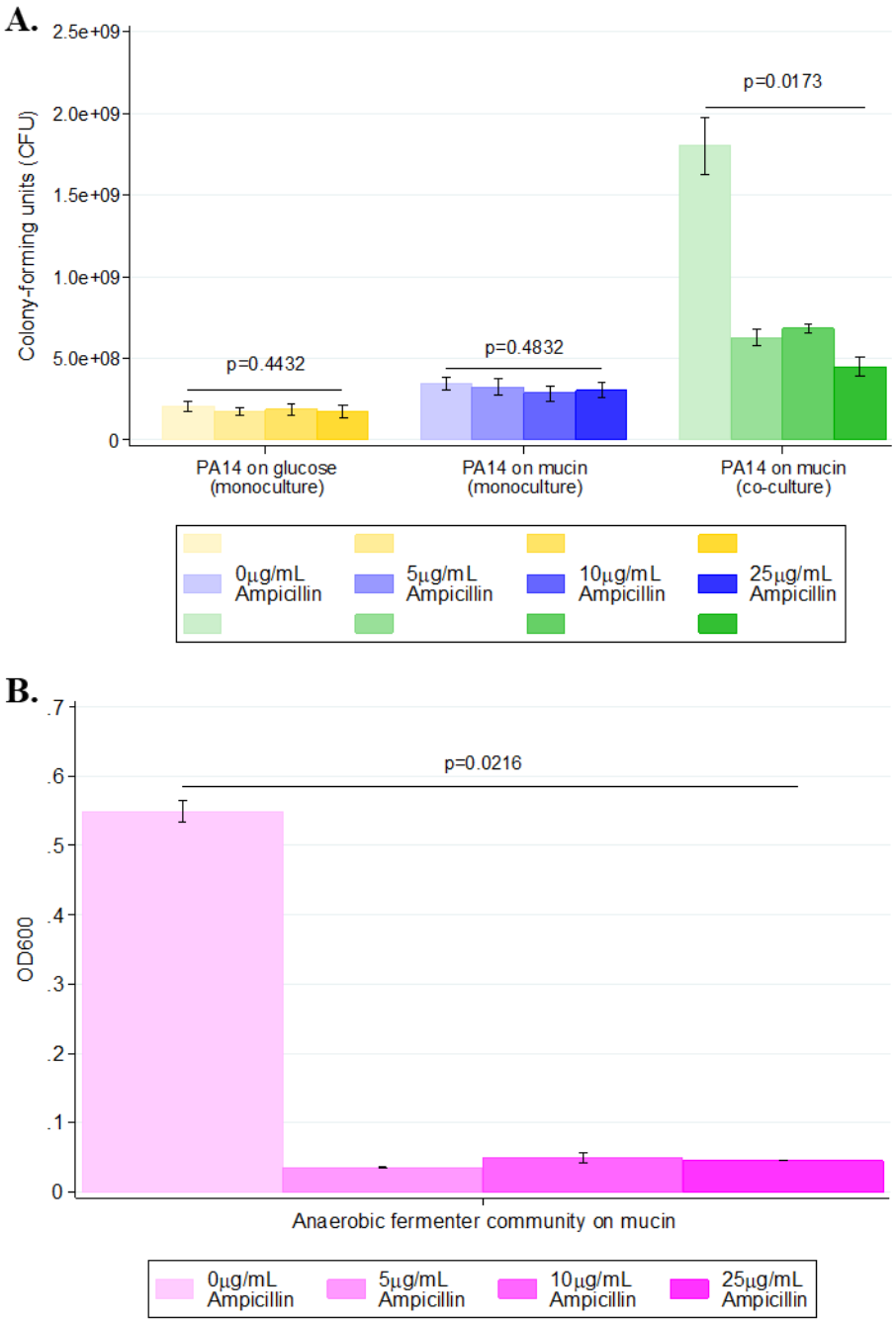

Supplementary Figure S2.8 Raw colony forming unit (CFU) data for *Pseudomonas aeruginosa* PA14 growth on mucin and glucose (**A**) and raw OD600 data for the anaerobic fermenter community on mucin (**B**). PA14 CFU grown alone on glucose and mucin, as well as in co-culture with the fermenter community on mucin. CFU values

were obtained by plating cells from each concertation of ampicillin on Luria Broth agar. Note that CFU values in 0µg/mL ampicillin are higher on mucin than on glucose because of the greater amount of carbon available in 12mM of mucin vs. 12mM of glucose. OD600 values were obtained using a Biotek Synergy H1 plate reader. Each point represents the mean and standard deviation of triplicate samples. *P*-values were calculated using a Kruskal-Wallis test across ampicillin concentrations.

Supplementary table S2.1 Components of Hypho media.

Growth supported	Metabolites	Sulfate solution	Phosphate solution	Trace Metals
E. coli monoculture	2.78mM lactose, 0.020mM methionine	3.78mM $(NH_4)_2SO_4$, 0.814mM $MgSO_4$	14.5mM K_2HPO_4, 16.3mM NaH_2PO_4	1.2µM $ZnSO_4$ 1µM $MnCl_2$ 18µM $FeSO_4$ 2µM $(NH_4)_6Mo_7O_{24}$ 1µM $CuSO_4$ 2mM $CoCl_2$ 0.33µM Na_2WO_4 20µM $CaCl_2$
S. enterica monoculture	5.55mM glucose			
S. enterica monoculture (acetate)	12.04mM acetate			
3-species competitive community	2.78mM lactose, 0.020mM methionine, 5.55mM glucose, 3.70mM succinate, 0.231mM methylamine			
3-species competitive community (acetate)	0.280mM lactose, 0.020mM methionine, 12.0mM acetate, 0.231mM methylamine			
E. coli– *S. enterica* cooperative co-culture	2.78mM lactose			
M. extorquens monoculture	3.70mM succinate, 0.231mM methylamine	3.78mM Na_2SO_4, 0.814mM $MgSO_4$		
M. extorquens monoculture, acetate	12.0mM acetate, 0.231mM methylamine			
3-species cooperative community	2.78mM lactose, 0.231mM methylamine			
E. coli– *M. extorquens* cooperative co-culture	2.78mM lactose, 0.020mM methionine, 0.231mM methylamine			
S. enterica– *M. extorquens* cooperative co-culture	5.55mM glucose, 3.70mM succinate, 0.231mM methylamine			

Supplementary table S2.2 Summary statistics for diameters of zones of clearing obtained by OD600 in ampicillin

Species	mean	std. dev	median	IQR
E. coli	38.06668	3.943439	38.33335	5.666698
S. enterica	42.09259	4.274579	41.66665	7.666698
M. extorquens	16.66668	2.488071	15.6667	2.6667
Cooperative community	32.35896	2.551192	32.6667	2.6667
Competitive community	15.98611	2.801933	16	3.41665

Supplementary table S2.3 Summary statistics for diameters of zones of clearing obtained by OD600 in tetracycline

Species	mean	std. dev	median	IQR
E. coli	36.66666	1.972022	37	1.333302
S. enterica	10.08333	0.8393739	9.916665	1
M. extorquens	37.63888	3.337767	36.8333	3.833349
Cooperative community	34.66668	2.400134	33.6667	4
Competitive community	8.944443	0.9525795	8.83333	2

Supplementary table S2.4 Summary statistics for diameters of zones of clearing obtained by fluorescence in ampicillin

Species	Community type	mean	std. dev	median	IQR
E. coli	monoculture	45.13889	1.709505	44.65	2.433334
E. coli	cooperative	39.7125	0.907629	39.9	1.316668
E. coli	competitive	46.07667	0.878418	46.26667	0.733334
S. enterica	monoculture	48.48333	0.314643	48.56667	0.433334
S. enterica	cooperative	43.03667	2.219301	42.75	1.333332
S. enterica	competitive	46.04	0.994155	46.36667	1.166664
M. extorquens	monoculture	25.86667	1.787612	26.55	2.566666
M. extorquens	cooperative	36.77667	3.72751	37.23333	2.633335
M. extorquens	competitive	24.12	1.820202	24.53333	1.700001

Supplementary table S2.5 Summary statistics for diameters of zones of clearing obtained by fluorescence in tetracycline

Species	Community type	mean	std. dev	median	IQR
E. coli	monoculture	40.17	1.094143	39.9	2.199997
E. coli	cooperative	40.37	1.607809	40.41667	1.933331
E. coli	competitive	38.84	1.091131	38.66667	0.966667
S. enterica	monoculture	8.733333	0.311111	8.666667	0.366667
S. enterica	cooperative	41.53667	1.334115	41.16667	1.266666
S. enterica	competitive	9.65	0.488447	9.85	0.733333
M. extorquens	monoculture	44.59	0.903772	44.43333	1.666668
M. extorquens	cooperative	31	1.428063	31.16667	2.399999
M. extorquens	competitive	.	.	.	.

Chapter 3. Cross-feeding modulates the rate and mechanism of antibiotic resistance evolution in a model microbial community

Summary

With antibiotic resistance rates on the rise, novel strategies are needed to understand and mitigate resistance evolution. A growing appreciation that most bacteria live in multispecies environments, as well as the importance of the interspecies interactions therein, offers a possible avenue of targeting resistance evolution. We have previously shown that "weakest link" dynamics dominate in communities where species are engaged in obligate mutualistic cross-feeding. In these communities, the survival of any one species (regardless of its intrinsic resistance) is contingent on the resistance of its cross-feeding partners, setting the community antibiotic tolerance at that of the "weakest link" species. In this study, we extended that hypothesis to see whether obligate cross-feeding would limit the extent and mechanisms of antibiotic resistance evolution. Under both rifampicin and ampicillin selection, we observed slower rates of resistance acquisition in obligate co-cultures of *E. coli* and *S. enterica* versus monocultures. These results were recapitulated in a mathematical model of our experiments. Further, while we observed similar mechanisms of resistance arising under rifampicin selection, monocultures and co-cultures under ampicillin selection evolved different resistance mechanisms. An *ftsI* penicillin-binding protein mutation arose in *S. enterica* only in co-culture; this mutation was lethal in monoculture unless cells were grown in an acidic environment. Using our model, we also showed that adding a growth rate cost to big-benefit resistance mutations and making big-benefit mutations rarer can also select for different mechanisms of resistance. Our results demonstrate that cooperative metabolic interactions may be an important modulator of resistance evolution in natural microbial communities.

Introduction

The seemingly unstoppable ability of pathogens to rapidly evolve antibiotic resistance is an increasingly pressing global challenge. While resistance frequently evolves in complex microbial communities, relatively little is known about how species interactions influence the evolution of antibiotic resistance (182–184). Most of the studies that do incorporate multiple species focus on the role of horizontal transfer of antibiotic resistance between species, and less on the *de novo* evolution of resistance within genomes (102, 184–187). Additionally, antibiotic resistance studies in multispecies systems typically involve unknown interactions between species, with some exceptions in modeling (55, 133, 188, 189). The specific role of interspecies interactions in the evolution of antibiotic resistance in microbial communities, therefore, remains largely unexplored.

Positive interspecies interactions are common in bacterial communities (43), and relatively understudied in terms of their role in modulating the evolution of resistance. One such interaction is cross-feeding, wherein two species exchange essential metabolites (44). The resilience of metabolically interdependent microbial systems to environmental disturbances is a growing field of study, with research being conducted into how these systems resist invasion (190, 191) and respond to abiotic environmental changes (45, 55, 120, 192). Over short time-scales (e.g. within a single growth curve), we previously showed that obligate cross-feeding produces “weakest link” dynamics (120), wherein the least resistant member of an obligate cross-feeding community constrains the ability of more resistant community members to grow at high antibiotic concentrations. In this case, the resistance (genetic mechanisms conferring an ability to

grow at higher antibiotic concentrations) did not change for each species, but the tolerance (a phenotypic trait describing their ability to grow at high antibiotic concentrations) was limited by the dependence on the least resistant species. This idea has also been demonstrated by others through modeling approaches (55).

We hypothesize that the weakest link pattern described above should also hold over evolutionary timescales; that is, at any given point during the evolution of resistance in a metabolically interdependent community, one "weakest link" species should set the tolerance of the whole community. The obligate cross-feeding interactions would then require that each individual species develop its own resistance mechanism before the tolerance of the community can increase. We therefore hypothesize that metabolically interdependent communities will be slower to adapt to rising antibiotic levels than their single-species counterparts, leading to higher rates of extinction in these communities.

We also hypothesize that weakest link dynamics should affect the mechanisms of resistance evolution. For example, the evolution of some shared resistance mechanism such as an antibiotic-degrading enzyme (121, 122, 184) or an induction of tolerance mechanism in a partner species (123, 125) could be uniquely selected for in co-culture. Cross-feeding may also limit the types of resistance mutations available to mutualistic networks of bacteria; for example, cross-feeding could make some resistance mechanisms more costly. Evolution of resistance by altering cell wall permeability may be particularly maladaptive in cross-feeding communities, where exchanged nutrients will typically be at low concentrations (40, 47, 193). Finally, a reduction in the rate of adaptation may drive different mechanisms of resistance to evolve. Varying the rate at which antibiotics are increased has been shown to lead to different evolutionary

trajectories (23-28). More rapid changes in antibiotic concentration tend to select for mutations with larger effects that are more costly (23-28). These big–effect mutations can trap populations on sub-optimal fitness peaks (67). We therefore hypothesize that we will see different mechanisms of resistance evolve in co-culture vs. monoculture, though the exact nature of these differences is unclear.

We sought to investigate whether obligate cross-feeding altered the rate and mechanism of antibiotic resistance evolution. We used a previously engineered two-species system of *E. coli* and *S. enterica*, wherein *E. coli* consumes lactose and excretes acetate for *S. enterica* to use as a carbon and energy source, and *S. enterica* overproduces methionine for the methionine-auxotrophic *E. coli*. We evolved six replicate populations of each species growing in monoculture (providing *E. coli* with lactose and methionine, and *S. enterica* with glucose) and in obligately cross-feeding co-culture (providing both species with lactose only, hereafter referred to as 'co-culture') along increasing antibiotic gradients of rifampicin or ampicillin for 20 (rifampicin) or 10 (ampicillin) passages of 48 hours each. At each passage, the MIC (minimum inhibitory concentration, the lowest concentration of antibiotic at which 90% of growth was inhibited relative to the antibiotic–free control) was assessed. We also constructed a mathematical model of resistance evolution in monoculture versus co-culture populations and used it to predict some mechanistic differences that might explain the differences in rate of resistance acquisition that we observed in monoculture versus co-culture populations. Our results show that growth in an obligate co-culture slows the rate of adaptation, and sometimes leads to different mechanisms of resistance.

Methods

Bacterial Strains and media

The *Escherichia coli* and *Salmonella enterica* strains used in this study have been described previously (159). Briefly, the *E. coli* str. K12 was the Δ*metB* strain from the Keio collection (194) that was mated with an Hfr line to reinsert the lac operon (29). The *S. enterica* LT2 mutant was selected and engineered to excrete methionine (137). Each strain is fluorescently labelled with a genomic integration of a fluorophore; *E. coli* is labelled with cyan fluorescent protein (CFP) and *S. enterica* is labelled with yellow fluorescent protein (YFP). Bacteria were grown in minimal Hypho medium containing phosphate and varying amounts and types of carbon and nitrogen as previously described (159). Co-culture media contained 2.78mM of lactose, *E. coli* monoculture medium contained 2.78mM of lactose and 0.020mM of methionine, and *S. enterica* medium contained 5.55mM of glucose.

Experimental Evolution[1]

Three different culture conditions (*E. coli* monoculture, *S. enterica* monoculture, and obligate co-culture) were each evolved across two antibiotic gradients (rifampicin, Chem-Impex International Inc. 00260, and ampicillin, Fisher BP1760). Six replicate populations were evolved for each antibiotic/ culture condition combination. Each antibiotic gradient began with an antibiotic–free control well and increased twofold with each subsequent well, starting at 0.25µg/mL and ending at 64µg/mL. When populations evolved to grow at 64µg/mL, the upper end of the gradient was increased to 1024µg/mL and the lowest concentrations were removed. To minimize differences in concentration

between passages caused by pipetting errors, stocks of antibiotic gradients were prepared in advance and diluted such that 2µL of stock constituted the desired concentration when diluted 1/100 in the bacterial growth plate. Fresh antibiotic stocks were prepared and filter-sterilized immediately before the experiment began.

Initial bacterial cultures were inoculated from DMSO freezer stocks in 10mL of monoculture minimal Hypho medium for approximately 48 hours at 30^{O}C, to stationary phase (OD~0.4). Cells were then distributed into 96 well cell culture plates. For monocultures, 2µl of bacterial cells (~$2x10^{5}$ cells) were inoculated into 196µl of the appropriate monoculture medium with 2µL of antibiotic stock. In co-cultures plates, 1µl of *E. coli* and 1µl of *S. enterica* were inoculated into 196µL medium. The plates were then incubated for 48 hours at 30°C with shaking at 450 rpm. After each growth phase, cells were then transferred to a new 96-well plate with fresh media. 1µL cells were transferred to a new well with the same antibiotic concentration, and 1µL cells were transferred to a new well that was one step higher on the antibiotic gradient (see **Figure 3.1**). This regimen challenged bacterial populations with increasing antibiotic concentrations at each transfer, but also allowed for populations to be maintained throughout the experiment if resistance was not acquired during a given transfer. The 96-well plate from each growth phase was frozen down in 10% DMSO for future analysis. After each 48-hour growth period, each plate was also placed onto a Tecan InfinitePro 200 plate reader where OD600 and species-specific fluorescence measurements were obtained. These readings were used to calculate the 90% minimum inhibitory concentration (MIC_{90}) for each replicate; growth at a given antibiotic concentration was confirmed if the well OD600 was above 10% of the OD600 of the

antibiotic–free control well for a given replicate. Statistical analysis of rate of resistance evolution between monocultures and obligate co-cultures for each antibiotic was performed in R. A linear mixed-effects model with a random slope for each replicate within a treatment group was used to test the relationship between MIC and transfer, culture type (monoculture or co-culture), and a transfer-culture type interaction.

Sequencing

To identify mutations which conferred antibiotic resistance in each evolved population, the most resistant population of each replicate in each antibiotic-growth condition combination was whole-genome sequenced. Two antibiotic–free populations per antibiotic-growth condition combination were also sequenced to identify any mutations which may have arisen during passaging but are not related to antibiotic resistance. Each population to be sequenced was scraped from 10% DMSO freezer stock and grown up in 10mL Hypho at the appropriate antibiotic concentration for 48 hours at 30^{O}C. gDNA was then extracted from each population using Zymo Quick-gDNA Miniprep Kit (Zymo 11-317C). The gDNA was then used to prepare Illumina sequencing libraries according to the Nextera XT DNA Library Prep Kit protocol. Libraries were submitted to the University of Minnesota Genomics Center for QC analysis and sequenced on an Illumina Hi-Seq with 125bp paired-end reads.

Sequence analysis was performed using BreSeq (195) to align Illumina reads to reference *E. coli* and *S. enterica* genomes as previously described (196). Briefly, mutation lists for resistant populations were filtered such that variation between our ancestral strains and the reference genome were removed, as well as any mutations

which also arose in the antibiotic–free populations. Mutation lists were then assembled for each population (**Supplementary table S3.1**) and any known functions described (**Supplementary table S3.2**). Mutations which rose to above 80% frequency (for rifampicin) or above 50% frequency (in ampicillin, due to the fewer number of transfers) were examined for their possible role in conferring antibiotic resistance (**Table 3.1**).

Isolation and phenotyping of isolates

Obtaining isolates

At the final transfer of each evolution experiment, the well in each replicate displaying growth at the highest antibiotic concentration, according the MIC_{90}, was identified as the "resistant population". These resistant populations, as well as the corresponding antibiotic–free control populations from each replicate, were plated onto minimal Hypho medium containing X-Gal (5-Bromo-4-chloro-3-indolyl β-D-galactopyranoside, Teknova X1220), which allowed us to differentiate between β-galactosidase-positive *E. coli* and β-galactosidase-negative *S. enterica* through a colorimetric change. Three isolates of each species each from the resistant and antibiotic–free wells were selected from these plates and frozen down in 10% DMSO for further analysis.

For ampicillin-evolved populations in which we were unable to obtain *S. enterica* isolates on pH neutral medium, we prepared acidic Hypho plates by adding 6M HCl to the growth medium until the pH reached ~4.7. Growth medium was then autoclaved, and X-gal was added as described above. For growth of these isolates in liquid medium, 6M HCl was added to autoclaved Hypho medium to a pH of ~4.7.

Phenotyping Isolates

Isolate growth rates and yields

Evolved isolates were scraped from DMSO freezer stocks onto solid agar plates and grown up overnight, then inoculated into 96-well plates containing the appropriate species-specific Hypho and grown at 30°C for 48 hours at 450rpm to acclimatize them to minimal media growth and standardize cell density. 2µL of stationary-phase cells was then used to inoculate a new 96-well plate containing 198µL monoculture growth medium. These plates were then placed in a Tecan InfinitePro 200 for 48 hours at 30°C with shaking at 300rpm; OD600, CFP, and YFP were measured every 20 minutes. After 48 hours, 1µL from the wells of monoculture isolate plates were transferred to new 96-well plates. These plates contained 198µL of fresh co-culture Hypho medium and 1µL of either ancestor strain of *E. coli* or *S. enterica.* If the monoculture isolate was *E. coli,* the ancestor strain of *S. enterica* was added, and vice-versa. The plates were then placed into a Tecan InfinitePro 200 for 48 hours at 30°C, and OD600 and florescent data was obtained every 20 minutes. Growth rates and yields were then calculated using Baranyi curves in R software using an in-house script. Statistical analyses and graphs were prepared in Stata version 14.

Isolate Minimum Inhibitory Concentrations (MICs)

Evolved isolates were prepared for inoculation as described above for beginning monoculture growth rate experiments. Based on the MIC_{90} of the population from which they originated, 2µL of each isolate culture was then inoculated across an antibiotic gradient such that the antibiotic concentration equaling the population MIC_{90} was in the

middle of the gradient. An antibiotic–free control well was also included for each gradient. If the gradient used was insufficient to calculate MIC (e.g. cells grew at all concentrations, or at none of them), the experiment was repeated with the antibiotic gradient shifted up or down as necessary. MIC of isolates was determined using MIC_{90} as described above. Statistical analyses and graphs were prepared in Stata version 14.

Evolution Model[2]

We used an evolution simulation to examine the rate at which antibiotic resistance evolved as a function of the number of interdependent species and other variables. There were two timescales in this model; the "within-transfer" timescale, and the "between-transfer" timescale.

Within a transfer, evolution was simulated in any given "well" using a modified haploid Wright-Fisher simulation with selection. A well was initiated with N individuals (default N = 1000). If this was the first transfer, these individuals were clones of a genotype with growth rate (s) = 1 and MIC = 0. Each well had a pre-determined antibiotic concentration. Evolution occurred over a predetermined number of generations. Each generation, the population was fully replaced. The new population was picked from the previous generation depending on the frequency of each genotype and its growth rate. The unscaled fitness of individual *i* was determined by $w_i = s_i / \sum_{j=1}^{N} s_j$. This was scaled to get expected frequency $w_i = w_i / \sum_{j=1}^{N} w_j$. In other words, $\sum_{j=1}^{N} w_j = 1$. The next generation was then created by generating N random numbers from a uniform distribution on [0,1] and choosing genotypes from the previous generation based on their w_j. Prior to calculating w, each genotype's MIC was compared to the antibiotic

concentration in the well. If the genotype's MIC was less than the antibiotic concentration, its $s = 0$ for the fitness calculation.

Once the new population was generated, some of the new individuals may be mutated. Each simulation used a pre-determined mutation rate u (default = 0.001 mutations per individual per generation). We generated N random numbers from a uniform distribution on [0,1]. Any random numbers less than u meant those individuals gained a mutation. In all cases, mutations could be either a growth rate mutation or an MIC mutation with a 50:50 chance. Growth rate mutations were simulated by adding a random number from a normal distribution with mean 0 and standard deviation 0.1 to the current growth rate (i.e. deleterious growth rate mutations were equally as likely as advantageous). MIC mutations altered either the MIC of the individual alone or both the MIC and the growth rate, as described in the results. We tracked the genealogy of all individuals.

To simulate interdependence, we simulated >1 species per well. Each species had N individuals, and the dynamics of each species were independent of the other species, *except* that there must be individuals of all species with an MIC > the antibiotic concentration for any species to grow.

The second time scale—the transfer scale—was simulated to approximate the wet-lab experiments. Individuals were transferred from one well to two wells: the same antibiotic concentration, and the next higher antibiotic concentration. Therefore, wells received individuals from two wells. If there were surviving species in both source wells, N/2 individuals were randomly chosen from each well to populate the new well. If there were surviving species in only one source well, all N individuals were transferred

from that well to the new well. If no source wells had surviving species, the destination well was sterile. Simulations were conducted in R.

Statistical analyses of the simulation data were performed as follows. We analyzed the rate of evolution of antibiotic tolerance as was done in the wet-lab experiments. To examine the effect of mutation rate or population size on antibiotic tolerance, we measured the maximum tolerance observed (highest antibiotic concentration survivable) at the final transfer for each replicate. This response variable was predicted using mutation rate or population size as categorical independent variables, crossed with the number of species, in a two-way analysis of variance. A one-way analysis of variance tested the amount of mutations observed in the most-tolerant population, with an independent variable of the # of interdependent species. To calculate the relative tolerance of two-species simulations versus one-species simulations (**Figure 3.5B, C**), we first found the mean and standard error in the tolerance in each set of simulations. Then, the mean of the two-species community was divided by the mean of the one-species community. The error was propagated using (mean_relative_tolerance)*sqrt((SEM[two species]/mean_tolerance[two_species])^2 + (SEM[one species]/mean_tolerance[one_species])^2). The average MIC mutation size was the (**Figure 3.6D**) was average MIC in a surviving population divided by the average number of mutations in that population. In all cases, since species were functionally equivalent, we arbitrarily chose one species to assess. Statistics were performed in R.

Results

Antibiotic resistance evolves more quickly in monoculture than in obligate co-culture

First, we tested the rate at which antibiotic resistance evolved in monocultures of *E. coli* and *S. enterica* as well as obligate co-cultures of the two species. We established six replicate cultures of each monoculture, and the co-culture. Each culture was distributed along an antibiotic gradient of either ampicillin or rifampicin. After 48 hours of growth, we transferred cells in a 1/200 dilution to fresh medium in the same antibiotic concentration, as well as double that concentration (**Figure 3.1A**). We transferred populations for 20 transfers (approximately 180 generations) in rifampicin, and 10 transfers (approximately 90 generations) in ampicillin. At each transfer, we measured total population density spectrophotometrically (by OD600) and calculated MIC_{90} based on the density in wells along each gradient. After the final transfer, three colonies of each species were isolated from each replicate population and their MIC_{90} values measured. Due to contamination, we removed one replicate of rifampicin-evolved *S. enterica* in monoculture.

In rifampicin, we found that resistance evolved more quickly in monoculture populations than in co-cultures (**Figure 3.2A,B**). *For E. coli*, growth in monoculture vs. co-culture was associated with a 1.06µg/mL greater increase in MIC per passage (+/- SEM of 1.02, $t(df = 11) = 2.431$, $P = 0.0328$). There was also a significant, positive effect of growing in monoculture vs. obligate co-culture, as monoculture–evolved *E. coli* had a 1.98 +/- 1.19µg/mL higher MIC overall than co-culture–evolved *E. coli* (**Figure**

3.2A, see **Supplementary table S3.3** for all statistical results**)**. Similarly, for *S. enterica*, growth in monoculture was associated with a significantly higher increase in MIC per passage versus growth in co-culture (1.09 +/- 1.02µg/mL, t(df=11) =3.08, *P*= 0.01). However, the difference in monoculture vs co-culture MIC was not significant (1.22 +/- 1.13µg/mL, df=207, t=1.63, *P*= 0.1054). In ampicillin, monoculture resistance in both species also rose more quickly than co-culture resistance, even over just ten transfers. The per-passage increase in MIC of both monocultures was higher than that of co-cultures (*P*= 0.007 for *E. coli*, *P*= 0.0272 for *S. enterica*) (**Figure 3.2B**). Growth in monoculture was also associated with a significantly higher MIC overall than co-culture for *E. coli* (*P*= 0.0001), but not *S. enterica* (*P*= 0.4942).

Similar mechanisms of rifampicin resistance evolve in monoculture and obligate co-culture

Given the consistently lower average MIC in co-culture–evolved populations than in monoculture–evolved populations, we hypothesized that these differences might be due to a difference in time under selection of species grown alone vs. cooperatively (**Figure 3.1B-D**). To identify whether cross-feeding selected for different resistance mechanisms we sequenced resistant populations at transfer 10 (ampicillin) and 20 (rifampicin). Genomic DNA was extracted from the well that grew at the highest concentration of antibiotic for each replicate population. For each resistant population we created a list of mutations excluding any mutations also observed in antibiotic free controls (**Supplementary Tables S3.1 and S3.2).** For further analysis, we focused on genes that acquired mutations multiple times within a treatment, as parallel evolution is a signature of adaptation (197). We included mutations which rose above 80% frequency under

rifampicin selection and those which rose above 50% frequency under ampicillin selection (with the lower threshold for the latter due to the fewer number of transfers occurring under the latter). We hypothesized that, if time under selection were sufficient to explain differences in mutational spectra between monoculture and co-culture–evolved lines, we should see more mutations arising in monoculture, and co-culture mutations would largely be a subset of monoculture–evolved mutations. If, however, different mechanisms of resistance were arising in monoculture vs. co-culture, these different mechanisms might also be driving the different levels of resistance we observed.

Under rifampicin pressure, the genes that acquired mutations in co-culture were a subset of those that acquired mutations in monoculture for both species (**Figure 3.3A,B**). The most clearly identifiable resistance-associated mutation was *rpoB*, a component of RNA polymerase and the most common mutational target for rifampicin resistance (103). Mutations in this gene arose in four out of the six replicates each in monoculture and co-culture (**Figure 3.3A**) and were strongly tied to higher levels of resistance (**Figure 3.3C,D**). A mutation in a prophage tail-specific protein, *prc*, was also repeatedly observed in both monoculture and co-culture (**Supplementary figure S3.1)**. The overlap in mutations suggest that co-cultures and monocultures are evolving along similar adaptive trajectories.

Monoculture lines also evolved more mutations than co-culture lines in rifampicin. Mutations in *mdoG* and *mdoH* were only observed in monocultures of *E. coli* and *S. enterica*. Both *mdoG* and *mdoH* likely influence cell membrane permeability. *mdoG*, also known as *opgG*, is a glucan biosynthesis protein in *E. coli* which antagonizes the

FtsZ-mediated assembly of the divisome in rich growth medium (198). *mdoH* (or *opgH*) encodes a membrane-bound glycosyltransferase that functions in synthesis of membrane-derived oligosaccharides (199). However, we found no changes in monoculture or co-culture growth rate associated with these mutations (**Supplementary figure S3.2**). Taken together, the pattern of rifampicin resistance mutations suggests that populations were moving along the same evolutionary trajectory in monoculture and co-culture but reached further along that trajectory in monocultures.

Different mechanisms of ampicillin resistance arise in monocultures vs. obligate co-cultures

In contrast to our results from rifampicin, the mutational spectra that we obtained from sequencing ampicillin-resistant populations suggests different resistance mechanisms arose in monoculture vs. co-culture. We observed more mutations in ampicillin than in rifampicin due to our lowered threshold for inclusion (above 50% frequency, versus above 80% in ampicillin); we used this cut-off to be able to detect resistance mutational signatures even with the fewer number of transfers in ampicillin. We had fewer transfers in ampicillin due to contamination in transfers 13 and beyond. Nevertheless, we observed distinct mutational signatures in both *E. coli* and *S. enterica* monocultures and co-cultures.

Very few genes acquired mutations more than once in the *E. coli* replicates. Two co-culture replicates evolved mutations in *proQ*, a regulator of efflux pumps (200) **(Figure 3.4A**). In monoculture, resistance evolution repeatedly involved in a gene associated with stress response (*rne*). Given the relative paucity of mutations there is at best only a

weak signature of differential resistance mechanisms evolving in *E. coli* in monoculture and co-culture.

The evidence for differential mechanisms of resistance was stronger in *S. enterica*, despite more overlap in mutated genes (**Figure 3.4B**). Mutations in efflux pump genes (*acrB, ramR*), and an unnamed dehydratase, arose in *S. enterica* monoculture but not in co-culture. Mutations in some genes associated with cell membrane permeability (*envZ, ompR*) were also observed exclusively in monoculture. None of these mutations were associated with a significant increase in resistance except for *ramR*, wherein mutants had a higher median MIC than wild-type isolates (P= 0.0491, **Supplementary figure S3.3**). Conversely, mutations in *ftsI*, a penicillin-binding protein, was only observed in co-culture. *ftsI* is an essential gene and encodes a penicillin-binding protein (PBP3) which is known to be a target site for β-lactam antibiotics (201). Interestingly, the mutations we observed in *ftsI* in our whole-genome sequencing were a combination of point mutations (D534Y at 75% frequency in rMM158) and mutations which should have ablated gene function (+A at 100% frequency in rMM127 and Q142* in rMM158). While we were able to identify these mutations from whole-genome sequencing of co-cultures, we were unable to identify them from *S. enterica* isolates from these populations (see Methods for information on how isolates were obtained). *S. enterica* isolates were difficult to obtain from these populations in general, and isolates which we did manage to isolate either did not contain the +A or Q142* mutations, or had a suppressor mutation in the same codon as the Q142* mutation site which eliminated the stop codon (**Supplementary table S3.1).**

Castanheira et al. recently demonstrated that the lethality associated with *ftsI* loss in *S. enterica* could be mitigated by growing *S. enterica* under acidic conditions (pH<5.8); under these conditions, a second PBP3, which they called $PBP3_{SAL}$, is expressed (202). Considering this, we plated co-culture populations containing Q142* or +A mutations in *ftsI* on LB of pH 4.7. We were able to obtain *S. enterica* isolates at roughly equal frequencies to what we would expect in the population, and Sanger sequencing demonstrated that these isolates did contain the loss-of-function Q142* or +A mutations. These isolates did not show detectable growth in monoculture unless the growth medium was acidified (**Figure 3.4C)** and were associated with increased MICs versus isolates with wild-type *ftsI*, though this difference was not statistically significant (**Figure 3.4D**, $P = 0.0603$). Interestingly, *ftsI* mutant isolates had co-culture growth rates comparable to wild-type when paired with an *E. coli* ancestor (**Supplementary figure S3.4**). This suggests that *ftsI* knockout mutations were non-viable in monoculture but conferred little cost in co-culture.

An evolutionary model suggests that differences in time under selection for monocultures vs. co-cultures is sufficient to explain differences in evolved resistance

To test the effect of interdependence on evolution of antibiotic resistance in the absence of species-specific biological details, we developed a simple model. The model is based upon the haploid Wright-Fisher model with selection, but populations at a fixed density evolved with a transfer regimen similar to the evolution experiments above. Individuals had two genes containing positive real numbers: a growth rate and an MIC, both of which could mutate upon reproduction. Growth rate determined fitness, and MIC

determined whether an individual could reproduce at all in a well with a given antibiotic concentration. When simulations had more than one species, they were interdependent, such that a species was unable to grow if there were no viable individuals of the other species (see Methods for details).

We first examined the relationship between the number of interdependent species and the rate of evolution of antibiotic resistance. Here, MIC–increasing mutations were free of cost, and were pulled from a uniform distribution ranging from zero to 1.1 (with 1 being the step size at which antibiotic concentration increased across wells). One thousand individuals of each species were simulated per well. Ten generations occurred within a transfer, and we conduced nine transfers. Mutations occurred at a rate of $u = 0.001$ per individual per generation. Thirty-five replicates were simulated. We found that antibiotic tolerance (the highest antibiotic concentration at which a species grew) evolved more slowly as more interdependent species were simulated (**Figure 3.5A**). We also observed that increasing the mutation rate (**Figure 3.5B)** or the population size (**Figure 3.5C)** increased the difference in antibiotic tolerance at the final transfer between monocultures and co-cultures (mutation rate, main effect of u: $F(2,204) = 62.88$, $P < 1e\text{-}10$; main effect of # species: $F(1,204) = 49.06$, $P < 1e\text{-}10$; interaction: $F(2,204) = 10.52$, $P = 4.49e\text{-}5$; population size, main effect of N: $F(2,204) = 39.9$, $P < 1e\text{-}10$; main effect of # species: $F(1,204) = 47.6$, $p < 1e\text{-}10$; interaction: $F(2,204) = 5.48$, $P = 0.0048$). Additionally, we showed that more mutations accumulated in the population with highest antibiotic tolerance when there were fewer species present (**Supplementary figure S3.5A**, $F(2,102) = 20.98$, $P < 1e\text{-}7$); this parallels what we observed in our experimental data (**Supplementary figure S3.5B).**

MIC-increasing mutations are unlikely to be drawn from a uniform distribution and have no pleiotropy. Therefore, we wondered about the rate of evolution of antibiotic resistance when either (1) big-benefit mutations were less common, or (2) incurred a growth rate cost. To that end, we tested two additional situations: one, "nexp," in which big-benefit mutation were rarer, and two, "tradeoff," in which all MIC mutations were equally likely, but greater changes to MIC incurred a disproportionally larger growth rate cost **(Figure 3.6A)**. Either constraint reduced the tolerance achieved through time by one or two species communities **(Figure 3.6B)**. Interestingly, not only were the absolute tolerances altered, but so were the relative tolerances: tolerance developed proportionally more slowly in the "nexp" or "tradeoff" model than in the "null" model **(Figure 3.6C)**. Finally, in any model, the average size of an MIC-changing mutation was smaller when there were more species (**Figure 3.6D**, main effect in two-way ANOVA, $F(1,572) = 119.7$, $P < 1e\text{-}10$; main effect of mutant function, and interaction, were also significant). Overall, our model showed that cross-feeding (i.e. dependence on another species for growth) is sufficient to slow the rate of resistance evolution versus monoculture, and that adding a cost to resistance (tradeoff) or making big-benefit resistance mutations rarer (nexp) reduced the rate of resistance acquisition overall.

Discussion

Our results demonstrate that obligate cross-feeding changes the rate and mechanisms of resistance evolution relative to that of monoculture. We showed that the obligate interspecies interactions resulted in a slower rate of adaptation to two different drugs and in an evolution model unbounded by species–specific details. In rifampicin, the resistance mechanisms remained similar between monoculture and co-culture–evolved lines; genes that acquired resistance mutations in co-culture were a subset of the genes involved in adaptation in monoculture. In ampicillin, in contrast, we observed different resistance mechanisms arising in monoculture and in co-culture, likely due in part to different costs of resistance mutations in monoculture and co-culture. We showed that *ftsI* mutations provide high levels of ampicillin resistance, but are only selected for in co-culture. In this environment, we expect that a second acid–induced penicillin binding protein is induced and can compensate for the loss of the essential *ftsI* gene. Overall, the fact that monocultures evolved more resistance than co-cultures, irrespective of species and antibiotic identity, suggests that slower resistance evolution in cross-feeding co-cultures is a general phenomenon.

Our results demonstrate that mutualistic interactions between species can result in slower evolution of antibiotic resistance and, in the case of ampicillin, the selection of different antibiotic resistance mechanisms altogether. This emphasizes the importance of taking ecological context into account when studying antibiotic resistance and suggests that species interactions may play an important role in shaping resistance evolution trajectories. Interestingly, the most significant impact that cross-feeding appears to have on the evolution of resistance is simply delaying it— when an increase in MIC of the

community requires two mutations in two different species, it makes sense that resistance evolution would be slowed. This phenomenon depends on the interactions between species being obligate, which is unlikely in nature; however, this does provide a novel possible strategy for slowing the evolution of resistance— namely, using a broad-spectrum antibiotic that targets both a pathogen and its cross-feeding partners.

Our findings that *rpoB* mutations confer resistance to rifampicin in both monocultures and co-cultures are not unexpected; indeed, there is an extensive field of research solely focusing on this topic (67, 103, 203–205). However, it is worth noting that there was a separation of the specific *rpoB* mutations which arose in monoculture vs. co-culture. S547Y arose in three co-culture *E. coli* populations, and I572N arose in one; neither of these mutations were observed in monoculture, though an I572L mutation did arise in one monoculture population. A previous study showed that I572L conferred high levels of rifampicin resistance, whereas I572N conferred only a moderate increase in resistance (203); this supports our hypothesis that high-level resistance is more commonly selected for in monoculture (**Figure 3.6D**). It is interesting that all of our *rpoB* mutations identified in Lindsey et al. 2013 are associated with gradual or moderate rifampicin exposure, rather than sudden exposure. This may explain the high level of variation in growth rate among replicate populations in our study; Lindsey et al also found that populations evolved under gradual and moderate rifampicin exposure had a greater diversity of growth rates and *rpoB* mutations than populations evolved under sudden antibiotic exposure (67). Similarly, in *S. enterica*, the mutations which arose in monoculture differed from those which arose in co-culture (**Supplementary table S3.1**). The specific fitness costs of each of these mutations is beyond the scope of this paper,

but it is possible that some aspect of co-culture vs. monoculture growth may be driving these differences in specific *rpoB* mutations. Given that *rpoB* mutations generally up-regulate the production of central metabolism enzymes, detoxification pathways, and cell membrane processes (132), the need to maintain cross-feeding and/or the different physiological states of cross-feeding vs. monoculture cells may be changing the fitness landscape of *rpoB* mutations in these cells.

One resistance mechanism that consistently arose in our evolved lines was modulation of cell wall permeability, either through changes in cell membrane composition or mutations affecting porin and efflux pump expression/regulation. Cell membrane composition changes are expected to be particularly relevant for hydrophobic antibiotics, such as erythromycin, aminoglycosides, and rifampicin; hydrophilic antibiotics such as β-lactams are more likely to use porins as entry points into the cell (206, 207). The resistance mechanisms which arose during our experimental evolution reflect this; mutations in *ompR* and *ompF* only arose under ampicillin selection, whereas mutations in *mdoG* and *mdoH*, which alter membrane biochemical composition, only arose under rifampicin selection. Similarly, changes in membrane phospholipid composition was recently shown to increase *Staphylococcus aureus* resistance to daptomycin (208), and changes in LPS biosynthesis in *E. coli* increased sensitivity to bacitracin and rifampicin (199). While modulation of cell wall permeability through changes in porin regulation (65, 207) and expression of efflux pumps (209) are well-established resistance mechanisms, less is known about how modification of cell membrane biochemistry affects resistance. The potential cross–resistance provided by each of these mutations could provide answers to this question.

It is worth noting that the *ftsI* mutation we identified in *S. enterica* only arose in co-culture environments, despite being associated with increased ampicillin resistance (albeit non-significantly). This raises an interesting possible evolutionary conflict for *S. enterica* in its role as a facultative intracellular pathogen. Our study demonstrated that mutations in *ftsI* confer high-level resistance (**Figure 3.4B**); however, this mutation is lethal outside of an acidic environment. A previous study identified a compensatory penicillin-binding protein, called $PBP3_{Sal}$, which is induced in acidic environments such as macrophages (202). Loss of *ftsI* might provide high-level resistance but prevent *S. enterica* from reproducing outside the acidic macrophage environment, making *S. enterica* into an obligate intracellular pathogen. Antibiotic pressure in a patient might therefore select for antibiotic-resistant *ftsI* mutants which are unable to spread. Other studies have demonstrated that resistance mutations have associated fitness costs in specific environments (210, 211). However, further research is needed into how these context-dependent costly mutations might be disproportionately selected for in multispecies environments where those costs are not realized until an infection situation.

Our mathematical model identified the same difference in rate of resistance acquisition between monocultures and co-cultures as did our experimental results. This shows that our experimental findings were not driven by system–specific parameters such as species identity, differences in carbon source between monocultures and co-cultures, or population size. This is particularly important given that Zampieri et al have previously shown that growth on different carbon sources (such as glucose in our *S. enterica* monoculture vs. acetate in the co-culture) can select for different resistance mechanisms (212). Our findings that obligate metabolic dependencies slow the rate of resistance

evolution may therefore be widely generalizable. Additionally, the model offers a generalized framework with which to investigate the impact of parameters such as mutation effect size, mutation rate, and population size, which may be difficult to modulate experimentally. Unexpectedly, the addition of a cost to resistance (tradeoff model) or a mutation distribution where large-effect mutations were rarer (nexp model) did not affect the pattern of monocultures evolving resistance more quickly. In all cases, monocultures also evolved more big benefit mutations than co-cultures, even when there was not an associated increase in cost. This suggests that bacteria engaged in mutualisms likely evolve resistance via many small-step mutations, rather than fewer large-step mutations. We are currently investigating this hypothesis in our system by engineering the evolved resistance mutations into the ancestral strain and testing the individual MIC benefits of each resistance mutation. We predict that single monoculture–evolved mutations will confer higher resistance than single co-culture–evolved mutations.

Studying how mutualisms evolve resistance to environmental stresses has significant implications not only for the evolution of antibiotic resistance in microbial communities, but also for the impact of climate change on symbiotic relationships at the macroscopic level. For example, the relationships between arbuscular mycorrhizal fungi (AMF) and wine grapevines is likely to be modified by climate change via AMF-mediated changes in grapevine metabolism and subsequent changes in grape quality. Understanding the nature of these interactions, and developing a better framework to predict the effects of climate change on them, will be essential in maintaining grape quality under changing climatic conditions (213). Climate change may also result in asynchronicity of plant flowering and pollinator flight seasons, causing timing mismatches between mutualistic

partners that may affect the stability of the mutualism. This is particularly likely if environmental changes in temperature, precipitation, and interactions with other species disproportionately and/or differentially affect one mutualistic partner over another (214). Microbial communities offer an intermediate between theoretical models and long-term macroscopic mutualism studies, which allow us to test the predictions made by models in a more reasonable time frame and potentially develop a predictive framework for the coevolution of mutualisms that extends to macroscopic communities.

Footnotes

[1]Experiments were performed in conjunction with Michaela Muza

[2]Model development, execution, and analysis was done by Dr. Jeremy Chacon

Chapter 3 Figures and Tables

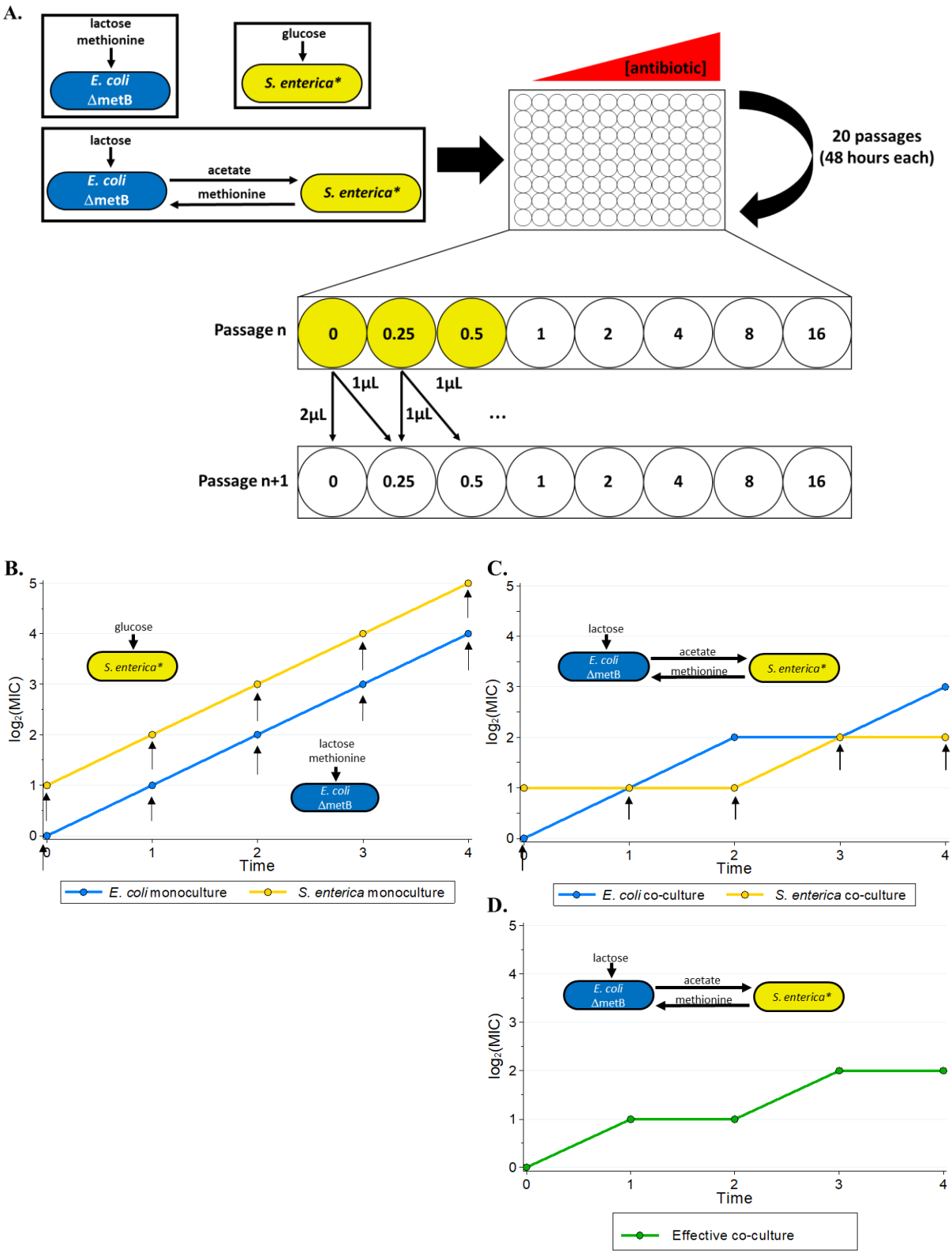

Figure 3.1 A. Schematic of evolution experiment setup. Monocultures of *E. coli* and *S. enterica*, as well as cross-feeding co-cultures, were distributed in six replicate populations along an antibiotic gradient. The antibiotics tested included rifampicin and ampicillin, and the concentration of antibiotic increased twofold at each well. 96-well plates were incubated with shaking at 30°C for 48 hours, then cells were transferred to fresh medium and antibiotic in a new plate. The passaging regimen was to transfer 1µL of culture to a fresh well containing the same concentration of antibiotic at which it had previously grown, and 1µL to a fresh well containing one concentration step higher antibiotic. At each passage, the OD600 of the plate was measured, as well as species-specific fluorescence (CFP for *E. coli*, YFP for *S. enterica*). **B-D.** Hypothesis on why time under selection may be sufficient to explain MIC differences between monocultures and co-cultures. **B.** In monoculture, each species is under selection at every time step, thus selecting for increasing resistance with each passage. **C**. In obligate co-culture, only the more antibiotic-sensitive species is under selection at a given time, and effective co-culture resistance requires an increase in MIC in both species. This leads to the slower rise in resistance for the co-culture observed in **D.**

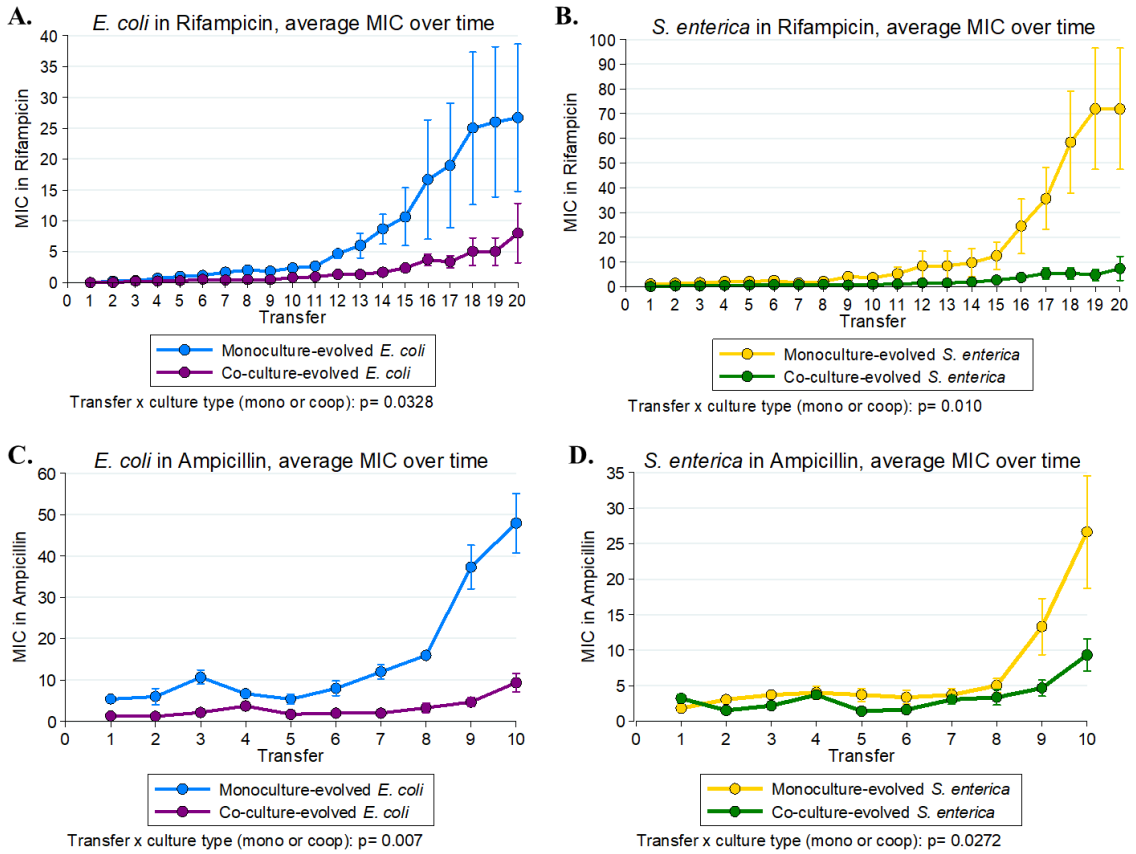

Figure 3.2. Resistance evolves more slowly, and to a lesser extent, in co-culture–evolved populations vs. monoculture–evolved populations. Six replicate populations each of monocultures and co-cultures were evolved along a Rifampicin gradient (**A-B**) or an Ampicillin gradient (**C-D**). Population MICs for each species (*E. coli* **A, C**; *S. enterica* **B, D**) were measured each passage and the resulting MICs plotted (rifampicin **A, B**; ampicillin **C, D**). Statistical analysis was performed using a mixed-effects model with a randomized slope for each replicate within a culture type. P-values are for the interaction term between passage and culture type.

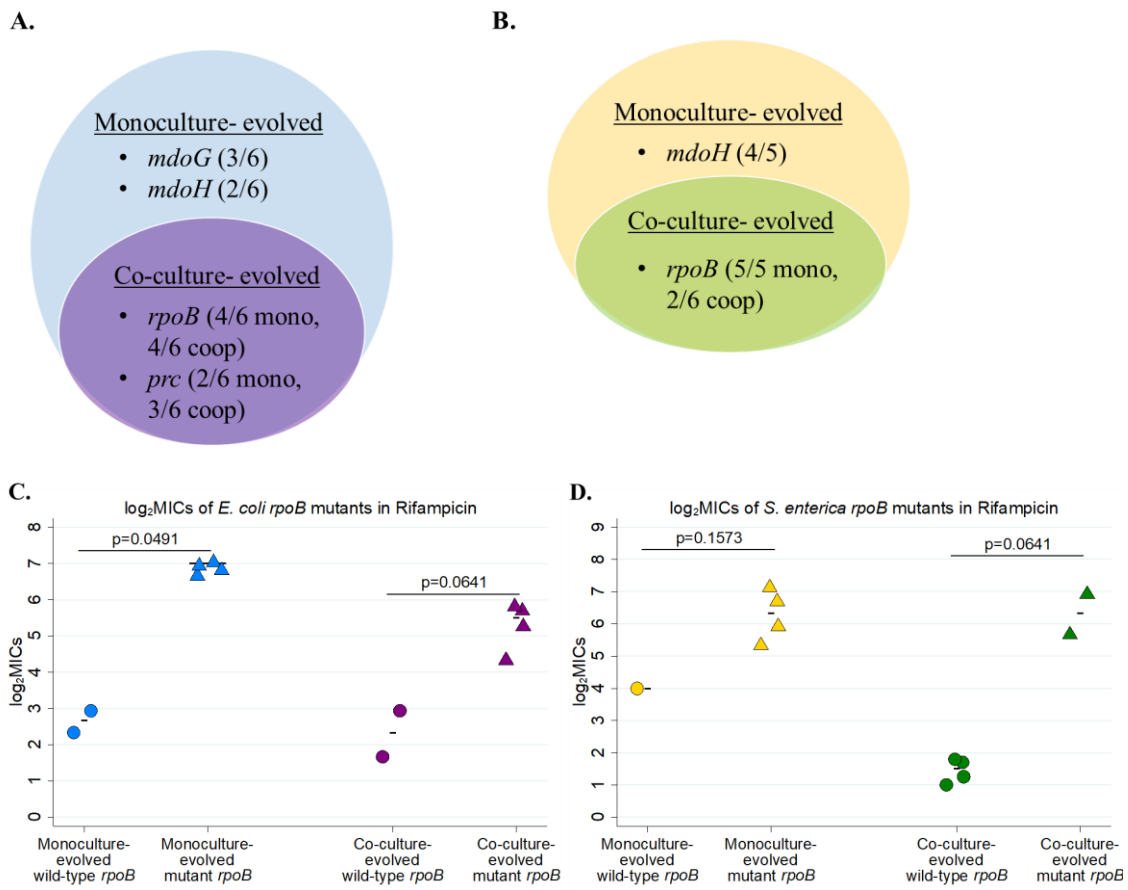

Figure 3.3 Resistance– associated mutations in rifampicin-resistant evolved populations **A-B.** Venn diagrams of mutations which arose in *E. coli* (**A**) or *S. enterica* (**B**) monoculture only, co-culture only, or both. Putative resistance mutations which arise in more than one population are are named; other mutations may be found in **Supplementary table 1**. Rifampicin MICs of isolates with wild-type vs. mutant *rpoB* genes in *E. coli* (**C**) and *S. enterica* (**D**). Isolates were obtained from passage 20 populations by streaking onto selective medium and picking isolated colonies. MIC_{90} values for isolates were defined as the lowest concentration of antibiotic which decreased growth by greater than 90% by 48 hours at $30^{O}C$. Each point represents the average MIC of three isolates from a single population.

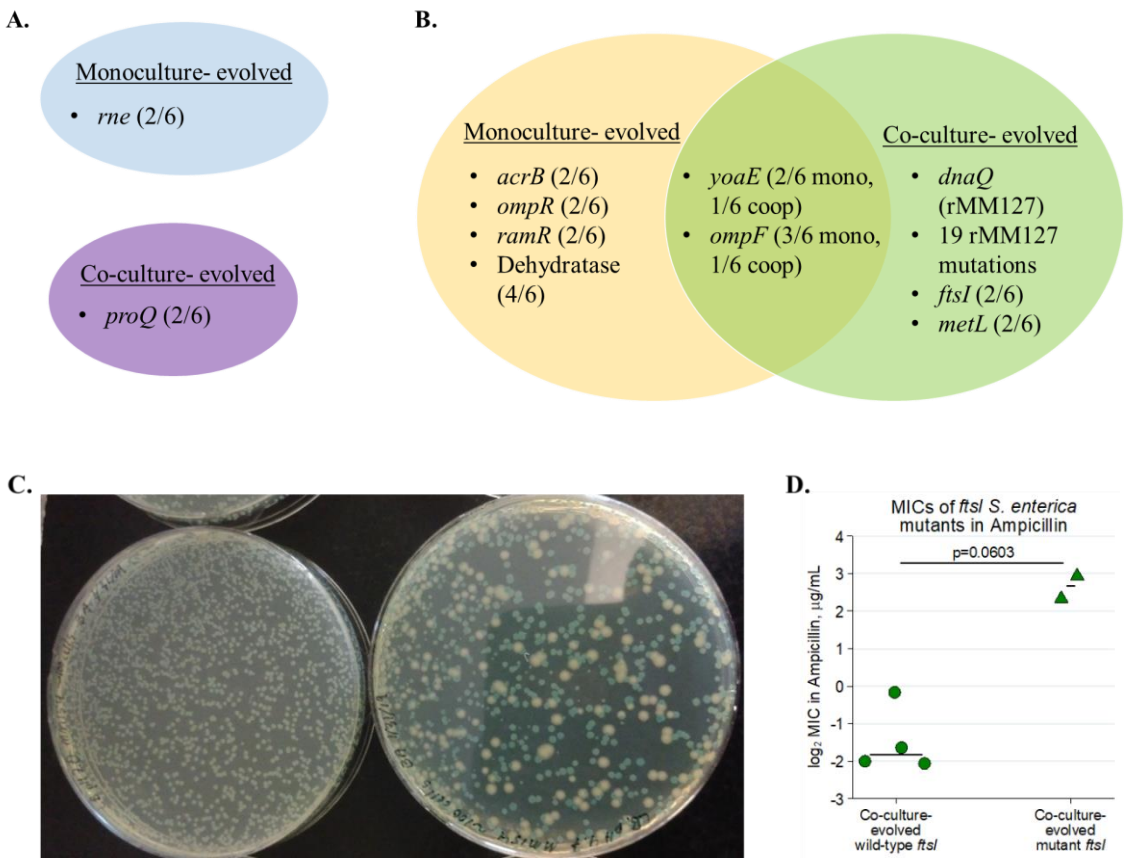

Figure 3.4 Resistance– associated mutations in ampicillin-resistant evolved populations. Venn diagrams of mutations which arose in *E. coli* (**A**) or *S. enterica* (**B**) monoculture only, co-culture only, or both. Mutation descriptions may be found in **Supplementary table 1-2**. **C.** Image of co-culture populations containing *ftsI* mutations on Petri plates with LB pH= 7 (left) and pH= 4.7 (right). Blue colonies are *E. coli* which metabolize X-gal to a blue color; white colonies are *S. enterica*. **D.** MICs of isolates from libraries containing *ftsI* mutations in pH= 7 or pH= 4.7 medium. Isolates were obtained from passage 10 populations by streaking onto selective medium and picking isolated colonies. MIC_{90} values were defined as the lowest concentration of antibiotic which decreased growth by greater than 90% by 48 hours at 30^{O}C. Each point represents the average MIC of three isolates from a single population. *P*= 0.0603, Mann-Whitney U.

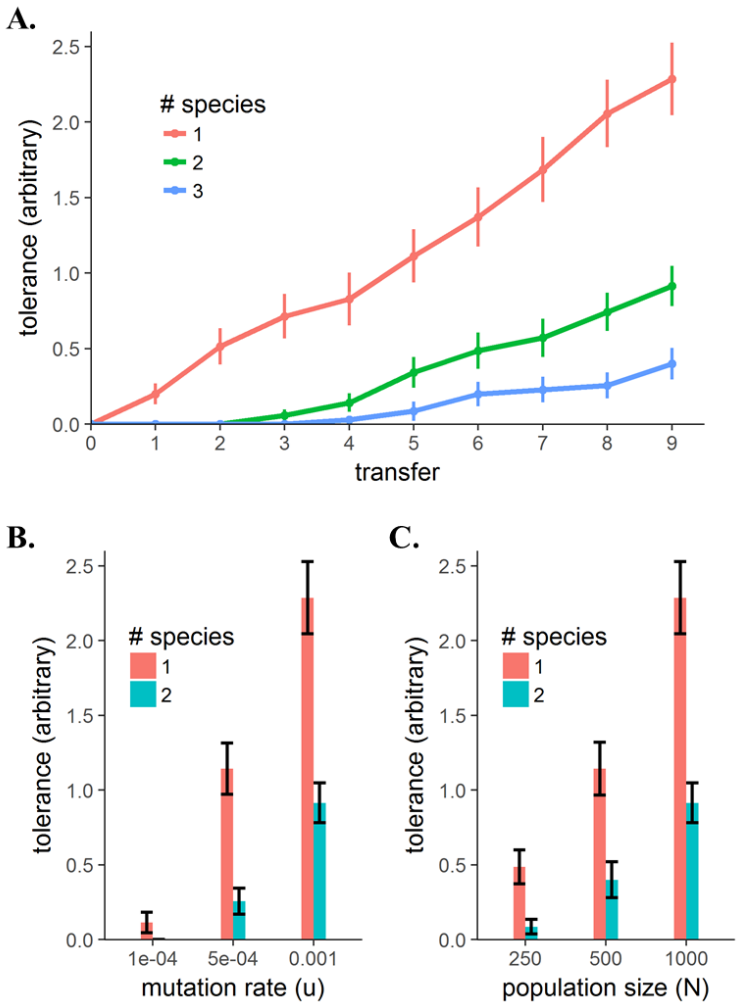

Figure 3.5 Simulation model of the evolution of antibiotic resistance in single-species vs. multispecies obligately dependent communities. **A.** A 9-season simulated evolution experiment with 35 replicate populations shows that increasing the number of interdependent species in a consortium results in a slower increase in the average MIC over time. **B, C.** Effect of mutation rate and population size on resistance evolution in model. **B.** As mutation rates increase in our model, the difference between average MIC of monoculture–evolved vs. co-culture–evolved populations also increase. **C.** As population size increases, the difference between average MIC of monoculture–evolved vs. co-culture–evolved populations decrease.

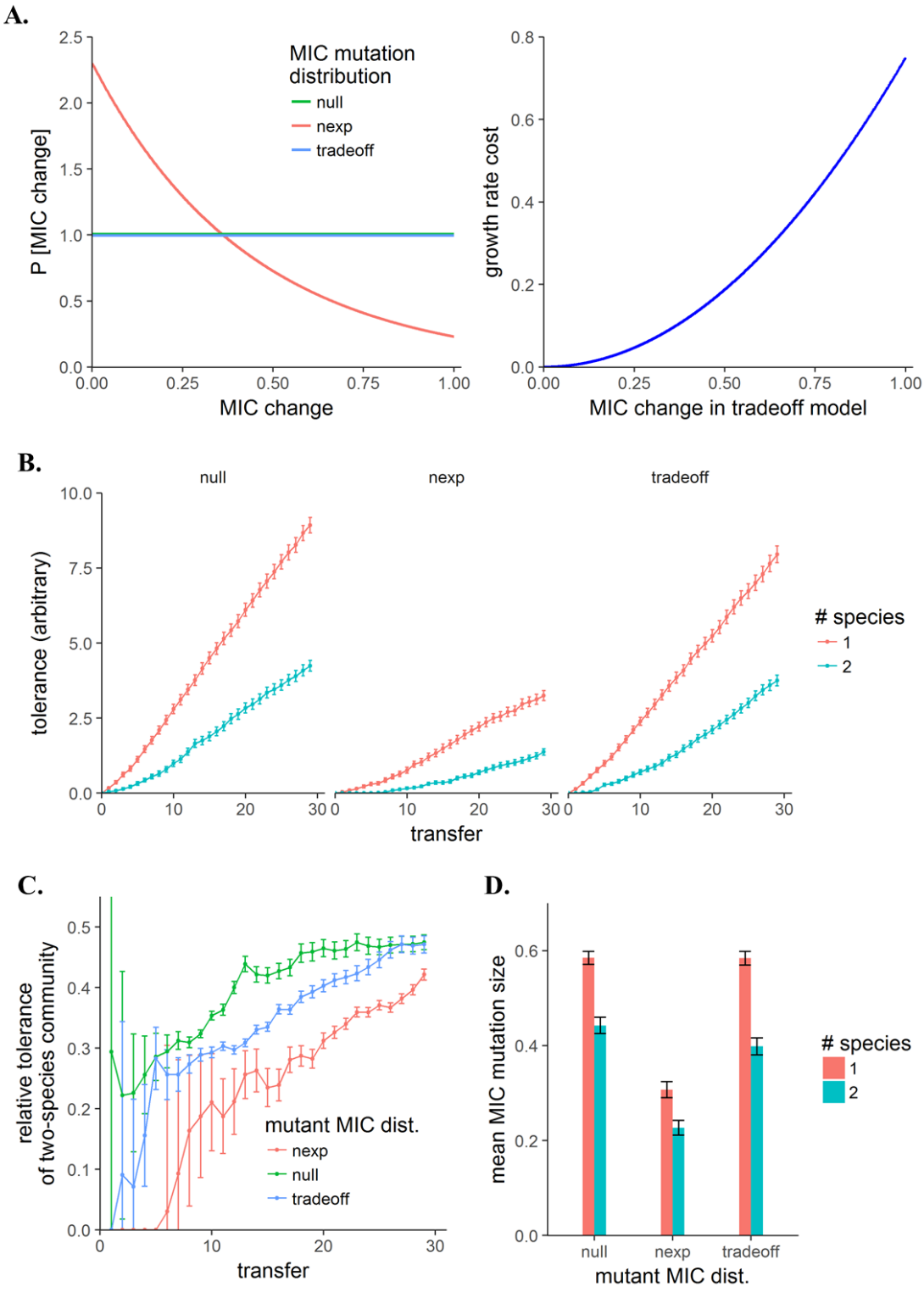
A.
MIC mutation distribution
null
nexp
tradeoff
P [MIC change]
MIC change
growth rate cost
MIC change in tradeoff model
B.
null
nexp
tradeoff
tolerance (arbitrary)
transfer
species
1
2
C.
relative tolerance of two-species community
mutant MIC dist.
nexp
null
tradeoff
transfer
D.
mean MIC mutation size
null
nexp
tradeoff
mutant MIC dist.
species
1
2

Figure 3.6. Effect of different mutation distributions on the rate of evolution of antibiotic resistance. Tradeoff mutation models in evolution simulation. **A. (left)** Distributions from which MIC-altering mutations were randomly pulled. The x-axis is relative to the maximum MIC change possible in one mutation. Both the "null" and the "tradeoff" model used uniform distributions. The "nexp" used a truncated negative exponential distribution with rate parameter 2.3, which kept 90% of random numbers less than the max MIC change of 1.0. During simulations, random pulls higher than this value were resampled **(right).** In the trade-off model, mutations which altered MIC had a deterministic cost to growth rate, using the function 0.75*(MIC change)^2, meaning larger mutations were disproportionally more costly, and the maximum cost to growth rate was 0.75, **B.** The absolute increase in antibiotic tolerance for each mutation distribution, simulated for one or two species communities and using 100 replicates per treatment. Points are mean +/- SEM. **C.** The tolerance achieved by two-species communities divided by the tolerance achieved by one-species communities, using the data from B. **D.** The average change in MIC for any mutation as a function of the mutation distribution and the number of species.

Supplementary table S3.1 Mutations evolved under antibiotic selection

Anti-biotic	Evolution condition	Library	Species	Gene	Description	Mutation	Position	Freq
Rif	*E. coli* monoculture	BA010	*E. coli*	*mdoH* →	glucosyltransferase	+T	1,107,543:1	94.10%
Rif	*E. coli* monoculture	BA010	*E. coli*	*prc* ←	tail-specific protease	Δ2 bp	1,908,859	100%
Rif	*E. coli* monoculture	BA010	*E. coli*	*rpoB* →	DNA-directed RNA polymerase subunit beta	A→C	4,172,886	93.90%
Rif	*E. coli* monoculture	BA017	*E. coli*	*rpoB* →	DNA-directed RNA polymerase subunit beta	C→T	4,172,863	100%
Rif	*E. coli* monoculture	BA030	*E. coli*	*mdoG* →	glucan biosynthesis protein G mdoG →	+TT	1,106,042:1	100%
Rif	*E. coli* monoculture	BA030	*E. coli*	*rpoB* →	DNA-directed RNA polymerase subunit beta	G→A	4,172,781	100%
Rif	*E. coli* monoculture	BA036	*E. coli*	*glpA* →	anaerobic glycerol-3-phosphate dehydrogenase subunit A	+CTGCGCGGG	2,346,218	100%
Rif	*E. coli* monoculture	BA036	*E. coli*	*mdoG* →	glucan biosynthesis protein G mdoG →	G→C	1,105,310	64.80%
Rif	*E. coli* monoculture	BA036	*E. coli*	*prc* ←	tail-specific protease	Δ11 bp	1,907,811	100%
Rif	*E. coli* monoculture	BA049	*E. coli*	*mdoG* →	glucan biosynthesis protein G mdoG →	Δ8 bp	1,105,573	100%
Rif	*E. coli* monoculture	BA049	*E. coli*	*rpoB* →	DNA-directed RNA polymerase subunit beta	A→G	4,172,719	100%

Rif	*E. coli* monoculture	BA056	*E. coli*	*fre* →	NAD(P)H-flavin reductase	Δ13 bp	4,019,988	86.50%
Rif	*E. coli* monoculture	BA056	*E. coli*	*mdoH* →	glucosyltransferase	Δ6 bp	1,107,321	100%
Rif	*S. enterica* monoculture	BA067	*S. enterica*	*mdoH* →	gucans biosynthesis glucosyltransferase H	G→T	1,239,272	100%
Rif	*S. enterica* monoculture	BA067	*S. enterica*	*rpoB* →	DNA-directed RNA polymerase subunit beta	T→G	4,367,622	100%
Rif	*S. enterica* monoculture	BA079	*S. enterica*	*ispD* ←	2-C-methyl-D-erythritol 4-phosphate cytidylyltransferase	C→T	3,070,986	100%
Rif	*S. enterica* monoculture	BA079	*S. enterica*	*mdoH* →	gucans biosynthesis glucosyltransferase H	G→T	1,239,272	100%
Rif	*S. enterica* monoculture	BA079	*S. enterica*	*rpoB* →	DNA-directed RNA polymerase subunit beta	A→G	4,367,454	100%
Rif	*S. enterica* monoculture	BA079	*S. enterica*	*STM4466* ←	carbamate kinase	A→G	4,708,815	100%
Rif	*S. enterica* monoculture	BA098	*S. enterica*	*mdoH* →	gucans biosynthesis glucosyltransferase H	G→T	1,239,272	100%
Rif	*S. enterica* monoculture	BA098	*S. enterica*	*rpoB* →	DNA-directed RNA polymerase subunit beta	C→T	4,367,442	100%
Rif	*S. enterica* monoculture	BA108	*S. enterica*	*rpoB* →	DNA-directed RNA polymerase subunit beta	C→T	4,367,511	90.00%
Rif	*S. enterica* monoculture	BA108	*S. enterica*	*rpoB* →	DNA-directed RNA polymerase subunit beta	T→G	4,367,622	100%
Rif	*S. enterica* monoculture	BA108	*S. enterica*	*ramR* ←	regulatory protein	Δ4 bp	638,200	86.10%

Rif	*S. enterica* monoculture	BA115	*S. enterica*	*mdoH* →	glucans biosynthesis glucosyltransferase H	G→T	1,239,272	100%
Rif	*S. enterica* monoculture	BA115	*S. enterica*	*rpoB* →	DNA-directed RNA polymerase subunit beta	C→T	4,367,504	100%
Rif	Co-culture	BA125	*E. coli*	*pnp* ←	polyribonucleotide nucleotidyltransferase	+G	3,303,449:1	90.10%
Rif	Co-culture	BA125	*E. coli*	*rpoB* →	DNA-directed RNA polymerase subunit betat	T→A	4,172,887	100%
Rif	Co-culture	BA139	*E. coli*	*rfaQ* ←	LPS core heptosyltransferase RfaQ	Δ1 bp	3,800,489	100%
Rif	Co-culture	BA139	*E. coli*	*rpoB* →	DNA-directed RNA polymerase subunit beta	C→A	4,172,893	100%
Rif	Co-culture	BA139	*S. enterica*	*rpoB* →	DNA-directed RNA polymerase subunit beta	A→G	4,366,350	100%
Rif	Co-culture	BA145	*E. coli*	*prc* ←	tail-specific protease	Δ2 bp	1,908,859	100%
Rif	Co-culture	BA145	*E. coli*	*prs* ←	ribose-phosphate pyrophosphokinase	A→T	1,256,880	100%
Rif	Co-culture	BA145	*E. coli*	*rpoB* →	DNA-directed RNA polymerase subunit beta	C→A	4,172,893	100%
Rif	Co-culture	BA155	*E. coli*	*prc* ←	tail-specific protease	Δ10 bp	1,907,831	64.40%
Rif	Co-culture	BA165	*E. coli*	*rplK* →	50S ribosomal protein L11	C→T	4,168,451	100%
Rif	Co-culture	BA165	*E. coli*	*rpoB* →	DNA-directed RNA polymerase subunit beta	C→A	4,172,893	92.80%
Rif	Co-culture	BA165	*E. coli*	*BW25113_RS13710* ←	CP4-57 defective prophage, DUF4297/DUF1837	+GCACTATG	2,758,778	87.60%

				/ ← BW2511 3_RS13715	polymorphic toxin family protein/hypothetical protein			
Rif	Co-culture	BA176	*E. coli*	*prc* ←	tail-specific protease	Δ11 bp	1,908,656	100%
Rif	Co-culture	BA176	*S. enterica*	*rpoB* →	DNA-directed RNA polymerase subunit beta	C→A	4,367,483	100%
Amp	*E. coli* monoculture	rMM010	*E. coli*	*acrB* ←	multidrug efflux RND transporter permease subunit	A→C	479,480	100%
Amp	*E. coli* monoculture	rMM010	*E. coli*	*rne* ←	ribonuclease E	repeat_region (+) +5 bp :: Δ1 bp	1,138,341	100%
Amp	*E. coli* monoculture	rMM020	*E. coli*	*envZ* ←	two-component sensor histidine kinase	C→G	3,528,288	100%
Amp	*E. coli* monoculture	rMM039	*E. coli*	*mdoH* →	glucosyltransferase	Δ1 bp	1,107,469	100%
Amp	*E. coli* monoculture	rMM049	*E. coli*	*ilvN* ←	acetolactate synthase isozyme 1 small subunit	Δ5 bp	3,844,420	72.20%
Amp	*E. coli* monoculture	rMM060	*E. coli*	*eda* ←	2-keto-3-deoxy-L-rhamnonate aldolase	Δ47 bp	2,351,941	67.60%
Amp	*E. coli* monoculture	rMM060	*E. coli*	*ompF* ←	outer membrane protein F	Δ2 bp	982,235	100%
Amp	*E. coli* monoculture	rMM060	*E. coli*	*prlF* →	antitoxin PrlF	repeat_region (–) +4 bp :: Δ3 bp	3,270,368	59.20%
Amp	*E. coli* monoculture	rMM060	*E. coli*	*rne* ←	ribonuclease E	repeat_region (+) +5 bp :: Δ1 bp	1,138,341	100%
Amp	*S. enterica* monoculture	rMM067	*S. enterica*	*ompF/IS10*	outer membrane protein F/ repeat region	IS element insertion	1090025 = = 1090033	85%

Amp	*S. enterica* monoculture	rMM078	*S. enterica*	*ompF/IS10*	outer membrane protein F/ repeat region	IS element insertion	1090025 = = 1090033	95%
Amp	*S. enterica* monoculture	rMM078	*S. enterica*	*ramR* ←	regulatory protein	coding (511-554/582 nt)	638,174	100%
Amp	*S. enterica* monoculture	rMM078	*S. enterica*	*STM2273/ IS10*	dehydratase/ repeat region	IS element insertion	2377331 = = 2377339	98%
Amp	*S. enterica* monoculture	rMM090	*S. enterica*	*acrB* ←	RND family acridine efflux pump	W634R (TGG→CGG)	530,497	100%
Amp	*S. enterica* monoculture	rMM090	*S. enterica*	*ompR* ←	osmolarity response regulator OmpR	R210L (CGT→CTT)	3,659,697	100%
Amp	*S. enterica* monoculture	rMM090	*S. enterica*	*ramR* ←	regulatory protein	Q19* (CAG→TAG)	638,673	100%
Amp	*S. enterica* monoculture	rMM090	*S. enterica*	*STM2273/ IS10*	dehydratase/ repeat region	IS element insertion	2377331 = = 2377339	98%
Amp	*S. enterica* monoculture	rMM090	*S. enterica*	*yoaE*	inner membrane protein	Intragenic inversion	= 1926896	100%
Amp	*S. enterica* monoculture	rMM098	*S. enterica*	*STM2273/ IS10*	dehydratase/ repeat region	IS element insertion	2377331 = = 2377339	98%
Amp	*S. enterica* monoculture	rMM108	*S. enterica*	*ompF/IS10*	outer membrane protein F/ repeat region	IS element insertion	1090025 = = 1090033	73%
Amp	*S. enterica* monoculture	rMM108	*S. enterica*	*STM2273/ IS10*	dehydratase/ repeat region	IS element insertion	2377331 = = 2377339	98%
Amp	*S. enterica* monoculture	rMM108	*S. enterica*	*yoaE*	inner membrane protein	Intragenic inversion	= 1926896	84%

Amp	*S. enterica* monoculture	rMM119	*S. enterica*	*acrB* ←	RND family acridine efflux pump	F615S (TTC→TCC)	530,553	100%
Amp	*S. enterica* monoculture	rMM119	*S. enterica*	*ompR* ←	osmolarity response regulator OmpR	R210L (CGT→CTT)	3,659,697	100%
Amp	Co-culture	rMM127	*S. enterica*	*ahpF* →	alkyl hydroperoxide reductase subunit F	G→A	672,700	94.60%
Amp	Co-culture	rMM127	*S. enterica*	*amn* ←	AMP nucleosidase	T→C	2,092,111	100%
Amp	Co-culture	rMM127	*S. enterica*	*dnaQ* →	DNA polymerase III subunit epsilon	T→A	303,499	100%
Amp	Co-culture	rMM127	*S. enterica*	*envZ* ←	osmolarity sensor protein EnvZ	A→G	3,659,359	100%
Amp	Co-culture	rMM127	*S. enterica*	*ftsI* →	peptidoglycan synthase FtsI	+A	143,219:1	100%
Amp	Co-culture	rMM127	*S. enterica*	*ftsZ* →	cell division protein FtsZ	C→T	155,877	100%
Amp	Co-culture	rMM127	*S. enterica*	*gldA* ← / → *STM3531*	glycerol dehydrogenase/ dihydroxyacid dehydratase	G→A	3,694,118	94.40%
Amp	Co-culture	rMM127	*S. enterica*	*metL* →	bifunctional aspartate kinase II/ homoserine dehydrogenase II	G→A	4,312,839	100%
Amp	Co-culture	rMM127	*S. enterica*	*rtn* →	lambda/N4 phages resistance membrane protein	T→C	2,315,609	92.40%
Amp	Co-culture	rMM127	*S. enterica*	*sppA* ←	protease 4	G→A	1,373,495	54.20%
Amp	Co-culture	rMM127	*S. enterica*	*STM0019* →	hydroxymethyltransferase	A→G	20,208	100%
Amp	Co-culture	rMM127	*S. enterica*	*STM0566* →	inner membrane protein	G→A	622,193	100%

Amp	Co-culture	rMM127	*S. enterica*	*STM1552* → / ← *STM0555*	cytoplasmic protein/hypothetical protein	A→G	1,629,730	100%
Amp	Co-culture	rMM127	*S. enterica*	*STM2179* ←	sugar transporter	T→C	2,275,700	93.00%
Amp	Co-culture	rMM127	*S. enterica*	*STM2700* ←	phage tail fiber-like protein	T→C	2,850,036	94.00%
Amp	Co-culture	rMM127	*S. enterica*	*STM2739* →	phage tail-like protein	C→A	2,877,206	100%
Amp	Co-culture	rMM127	*S. enterica*	*STM2756* ←	sugar phosphate aminotransferase	C→T	2,894,787	100%
Amp	Co-culture	rMM127	*S. enterica*	*STM3052* ←	outer membrane protein	T→C	3,211,576	94.00%
Amp	Co-culture	rMM127	*S. enterica*	*STM3631* ←	xanthine permease	T→C	3,817,700	94.60%
Amp	Co-culture	rMM127	*S. enterica*	*STM3653* ← / ← *glyS*	acetyltransferase/glycine--tRNA ligase subunit beta	A→G	3,839,640	100%
Amp	Co-culture	rMM127	*S. enterica*	*STM4419* →	sugar transporter	C→T	4,662,084	100%
Amp	Co-culture	rMM127	*S. enterica*	*xylA* ← / → *xylR*	xylose isomerase/xylose operon regulatory protein	T→C	3,848,052	100%
Amp	Co-culture	rMM127	*S. enterica*	*yeaQ* →	inner membrane protein	T→C	1,353,286	54.60%
Amp	Co-culture	rMM127	*S. enterica*	*yhiP* →	dipeptide/tripeptide permease B	C→T	3,762,685	52.60%
Amp	Co-culture	rMM137	*E. coli*	*proQ* ←	RNA chaperone ProQ	Δ5 bp	1,909,389	19.70%
Amp	Co-culture	rMM137	*S. enterica*	*metL* →	bifunctional aspartate kinase II/ homoserine dehydrogenase II	Δ4 bp	4,311,847	59.20%
Amp	Co-culture	rMM146	*S. enterica*	*ompF* ←	outer membrane protein F	Δ116 bp	1,090,110	64.50%
Amp	Co-culture	rMM158	*E. coli*	*proQ* ←	RNA chaperone ProQ	C→A	1,909,737	86.50%

Amp	Co-culture	rMM158	*S. enterica*	*ftsI* →	peptidoglycan synthase FtsI	G→T	143,325	75.30%
Amp	Co-culture	rMM167	*S. enterica*	*yoaE*	inner membrane protein	Intragenic inversion	= 1926896	100%

Supplementary table S3.2 Functions of genes mutated under antibiotic selection.

Gene	Mutated in	Description	Function
fre →	*E. coli*: BA056	NAD(P)H-flavin reductase	May be involved in iron homeostasis and oxidative stress response (UniProt)
rpoB →	*E. coli*: BA010, BA017, BA030, BA049, BA125, BA139, BA145, BA165 *S. enterica*: BA067, BA079, BA098, BA108, BA115, BA139, BA176	DNA-directed RNA polymerase subunit beta	RNA polymerase beta subunit; commonly mutated in rifampicin-resistant lines (215)
prc ←	*E. coli*: BA010, BA036, BA145, BA155, BA176	tail-specific protease	Cleaves precursor to form a functional PBP3; involved in thermal and osmotic stress response (216); mutations lead to increased antibiotic susceptibility (217)
mdoH →	*E. coli*: BA010, BA056, rMM039 *S. enterica*: BA067, BA079, BA098, BA115	glucosyltransferase	Also called *mdoH/opgH*; involved in regulating cell wall osmolarity and likely modulates cellular penetration of rifampicin (199)
mdoG →	*E. coli*: BA030, BA036, BA049	glucan biosynthesis protein G MdoG →	Required for the synthesis of osmoregulated periplasmic glucans; may function in biofilm formation (218)
glpA →	*E. coli*: BA036	anaerobic glycerol-3-phosphate dehydrogenase subunit A	Involved in utilization of glycerol as a carbon source; deletions lead to decreased persister formation (219)
pnp ←	*E. coli*: BA125	polyribonucleotide nucleotidyltransferase	Involved in mRNA degradation and tRNA processing; contributes to rRNA quality control during steady-state growth (220)
rfaQ ←	*E. coli*: BA139	LPS core heptosyltransferase RfaQ	Also called *waaQ*; involved in LPS biosynthesis (UniProt)
prs ←	*E. coli*: BA145	ribose-phosphate pyrophosphokinase	Involved in central metabolism (UniProt)
BW25113_RS13710 ← / ← BW25113_RS13715	*E. coli*: BA165	CP4-57 defective prophage, DUF4297/DUF1837 polymorphic toxin family protein/hypothetical protein	

rplK →	*E. coli*: BA165	50S ribosomal protein L11	Regulator of the stringent response and signals increased ppGpp production, which increases antibiotic tolerance (221)
rne ←	*E. coli*: rMM010, rMM060	ribonuclease E	Small regulatory RNA that functions in SOS initiation (222)
acrB ←	*E. coli*: rMM010 *S. enterica*: rMM090, rMM119	multidrug efflux RND transporter permease subunit	Efflux transporter protein component of the TolC-AcrAB multidrug efflux pump (223)
envZ ←	*E. coli*: rMM020 *S. enterica*: rMM127	two-component sensor histidine kinase	Sensor kinase in two-component signalling control of *ompF/ompC* expression regulation (223)
ilvN ←	*E. coli*: rMM049	acetolactate synthase isozyme 1 small subunit	Catalyzes the first step in valine biosynthesis and the second step in isoleucine biosynthesis (UniProt)
eda ←	*E. coli*: rMM060	2-keto-3-deoxy-L-rhamnonate aldolase	Involved in glucose degradation through the Entner-Doudoroff pathway (UniProt)
prlF →	*E. coli*: rMM060	antitoxin PrlF	Antitoxin component of an mRNA degradation toxin system (224)
ompF ←	*E. coli*: rMM060 *S. enterica*: rMM146	outer membrane protein F	Classic trimeric porin commonly lost in beta-lactam resistant strains (225)
proQ ←	*E. coli*: rMM137, rMM158	RNA chaperone ProQ	Small regulatory RNA that controls efflux pump expression (200)
ispD ←	*S. enterica*: BA079	2-C-methyl-D-erythritol 4-phosphate cytidylyltransferase	Functions in isoprene biosynthesis (UniProt)
STM4466 ←	*S. enterica*: BA079	carbamate kinase	Functions in the arginine deaminase pathway (UniProt)
ramR ←	*S. enterica*: BA108, rMM078, rMM090	regulatory protein	Negative repressor of *ramA*, which positively regulates *acrAB* expression- knockouts result in constitutive *acrAB* expression (226)
ompF/IS10	*S. enterica*: rMM067, rMM078, rMM108	outer membrane protein F/ repeat region	Classic trimeric porin commonly lost in beta-lactam resistant strains (225)
STM2273/ IS10	*S. enterica*: rMM078, rMM090, rMM098, rMM108	dehydratase/ repeat region	-
yoaE	*S. enterica*: rMM090, rMM108, rMM167	inner membrane protein	Integral membrane protein, putative transporter (UniProt)

ompR ←	*S. enterica*: rMM090, rMM119	osmolarity response regulator OmpR	Response regulator in two-component signalling of *ompF/ompC* expression (223)
ahpF →	*S. enterica*: rMM127	alkyl hydroperoxide reductase subunit F	Functions in protecting cells from hydrogen peroxide toxicity (227)
amn ←	*S. enterica*: rMM127	AMP nucleosidase	Loss of function mutations allow greater cold tolerance in *E. coli* (228)
dnaQ →	*S. enterica*: rMM127	DNA polymerase III subunit epsilon	Encodes proofreading DNA polymerase III; mutations lead to high mutation rates and are often observed under antibiotic selection (229)
ftsZ →	*S. enterica*: rMM127	cell division protein FtsZ	Essential component of cell division (forms septum Z-ring); target of antimicrobial development (230)
gldA ← / → *STM3531*	*S. enterica*: rMM127	glycerol dehydrogenase/dihydroxyacid dehydratase	-
rtn →	*S. enterica*: rMM127	lambda/N4 phages resistance membrane protein	-
sppA ←	*S. enterica*: rMM127	protease 4	Signal peptide peptidase (UniProt)
STM0019 →	*S. enterica*: rMM127	hydroxymethyltransferase	-
STM0566 →	*S. enterica*: rMM127	inner membrane protein	-
STM1552 → / ← *STM05155*	*S. enterica*: rMM127	cytoplasmic protein/hypothetical protein	-
STM2179 ←	*S. enterica*: rMM127	sugar transporter	4-hydroxybenzoate transporter (UniProt)
STM2700 ←	*S. enterica*: rMM127	phage tail fiber-like protein	-
STM2739 →	*S. enterica*: rMM127	phage tail-like protein	Putative integrase (UniProt)
STM2756 ←	*S. enterica*: rMM127	sugar phosphate aminotransferase	-
STM3052 ←	*S. enterica*: rMM127	outer membrane protein	May be involved in phenol degradation (UniProt)
STM3631 ←	*S. enterica*: rMM127	xanthine permease	-
STM3653 ← / ← *glyS*	*S. enterica*: rMM127	acetyltransferase/glycine--tRNA ligase subunit beta	-
STM4419 →	*S. enterica*: rMM127	sugar transporter	Carbohydrate/proton symporter (UniProt)
xylA ← / → *xylR*	*S. enterica*: rMM127	xylose isomerase/xylose operon regulatory protein	-
yeaQ →	*S. enterica*: rMM127	inner membrane protein	Putative integral membrane protein (UniProt)

yhiP →	*S. enterica*: rMM127	dipeptide/tripeptide permease B	Putative transporter (UniProt)
metL →	*S. enterica*: rMM127, rMM137	bifunctional aspartate kinase II/homoserine dehydrogenase II	Catalyzes the first step in lysine/homoserine biosynthesis, the last step in homoserine biosynthesis, and indirectly functions in methionine and threonine biosynthesis (UniProt)
ftsI →	*S. enterica*: rMM127, rMM158	peptidoglycan synthase FtsI	Penicillin-binding protein 3 (PBP3); mutations confer β-lactam resistance (201)

Supplementary table S3.3. Statistics for mixed–effects model analyzing rate of MIC increase over 20 rifampicin passages and 10 ampicillin passages.

E. coli in Rifampicin					
	Estimate	Std. Error	df	t	value
(Intercept)	0.77227	1.05741	226	-4.63	6.2E-06
evol_condition	1.067	1.08214	226	0.822	0.41221
passage	1.09838	1.01694	11.2929	5.584	0.00015
evol_condition: passage	1.05947	1.02405	11.2929	2.431	0.03285
S. enterica in Rifampicin					
	Estimate	Std. Error	df	t	value
(Intercept)	0.90274	1.08656	207	-1.232	0.21921
evol_condition	1.22175	1.13104	207	1.626	0.10537
passage	1.08845	1.01818	11.4501	4.705	0.00058
evol_condition: passage	1.08584	1.02707	11.4501	3.082	0.00998
E. coli in Ampicillin					
	Estimate	Std. Error	df	t	value
(Intercept)	1.8614	1.12912	106	5.116	1.4E-06
evol_condition	1.97848	1.18738	106	3.973	0.00013
passage	1.11823	1.02495	36.0446	4.535	6.1E-05
evol_condition: passage	1.10477	1.03546	36.0446	2.859	0.00701
S. enterica in Ampicillin					
	Estimate	Std. Error	df	t	value
(Intercept)	2.39983	1.12832	106	7.251	7.1E-11
evol_condition	0.88947	1.18617	106	-0.686	0.49417
passage	1.08302	1.02837	25.1259	2.851	0.00859
evol_condition: passage	1.09727	1.04036	25.1259	2.346	0.02716

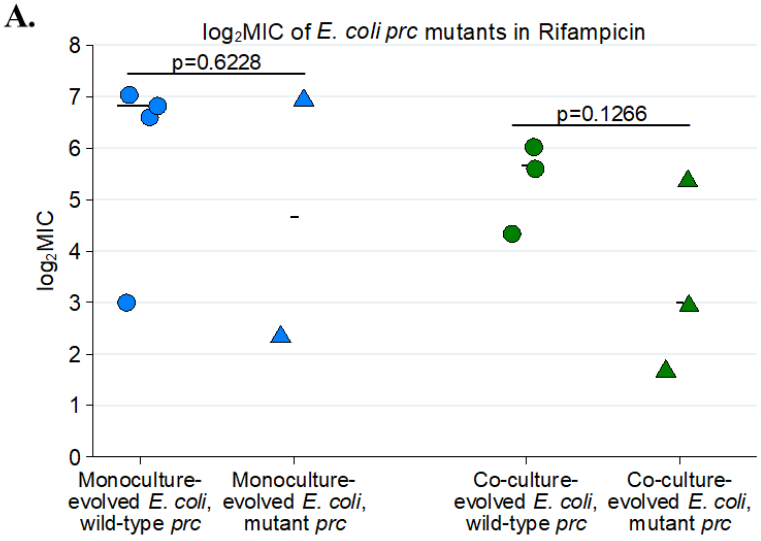
A.
log2MIC of E. coli prc mutants in Rifampicin
p=0.6228
p=0.1266
log2MIC
0
1
2
3
4
5
6
7
8
Monoculture-evolved E. coli, wild-type prc
Monoculture-evolved E. coli, mutant prc
Co-culture-evolved E. coli, wild-type prc
Co-culture-evolved E. coli, mutant prc

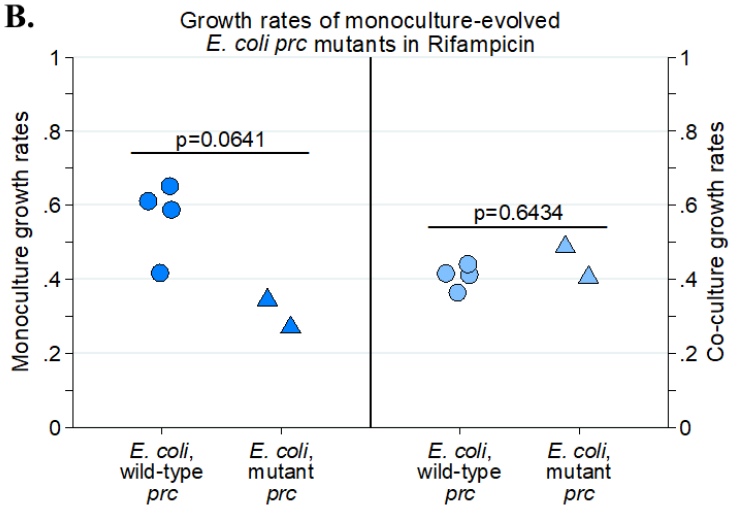
B.
Growth rates of monoculture-evolved E. coli prc mutants in Rifampicin
p=0.0641
p=0.6434
Monoculture growth rates
Co-culture growth rates
0
.2
.4
.6
.8
1
E. coli, wild-type prc
E. coli, mutant prc
E. coli, wild-type prc
E. coli, mutant prc

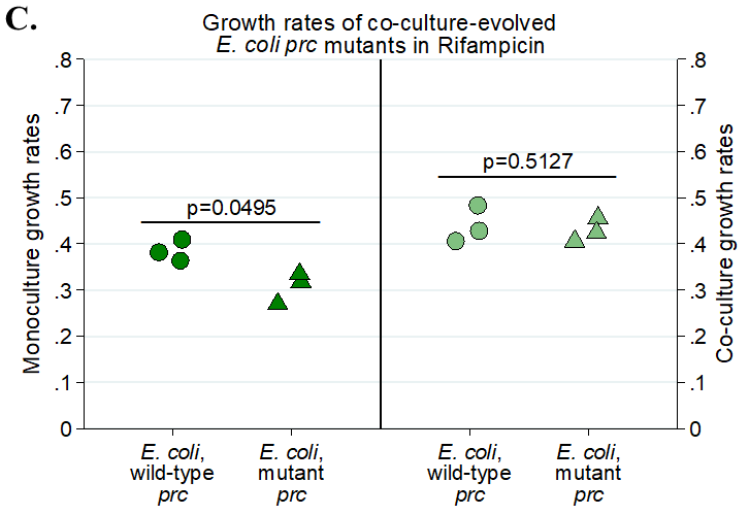
C.
Growth rates of co-culture-evolved E. coli prc mutants in Rifampicin
p=0.0495
p=0.5127
Monoculture growth rates
Co-culture growth rates
0
.1
.2
.3
.4
.5
.6
.7
.8
E. coli, wild-type prc
E. coli, mutant prc
E. coli, wild-type prc
E. coli, mutant prc

Supplementary figure S3.1 A. MICs of monoculture– and co-culture– evolved *E. coli* isolates containing wild-type or mutant *prc*. **B.** Monoculture and co-culture growth rates of monoculture–evolved *E. coli* isolates containing wild-type or mutant *prc*. **C.** Monoculture and co-culture growth rates of co-culture–evolved *E. coli* isolates containing wild-type or mutant *prc.* All p-values based on Mann-Whitney U tests. Points represent the average growth rate or MIC values of three isolates from the same population.

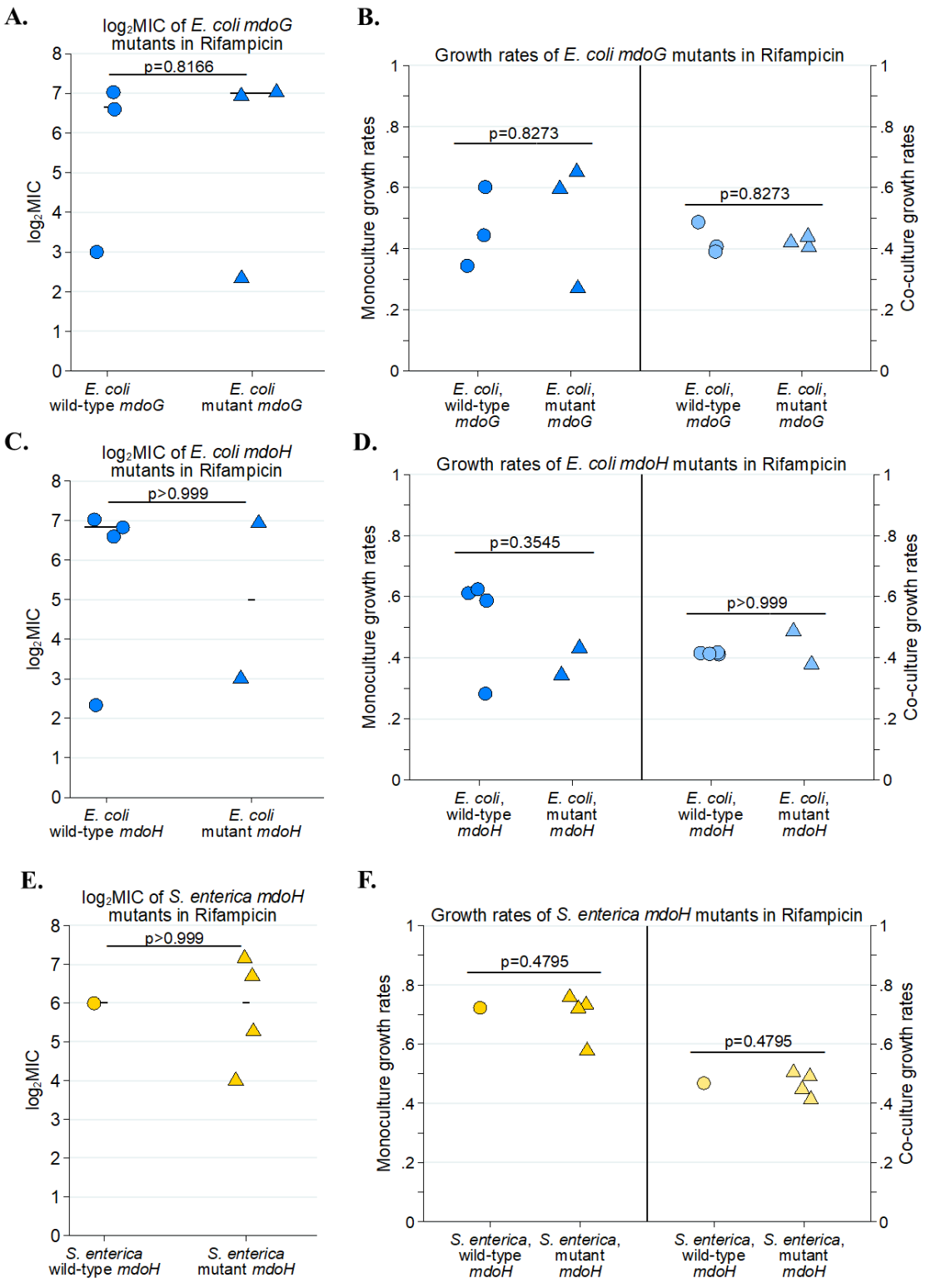
A.
log2MIC of E. coli mdoG mutants in Rifampicin
p=0.8166
log2MIC
E. coli wild-type mdoG
E. coli mutant mdoG
B.
Growth rates of E. coli mdoG mutants in Rifampicin
p=0.8273
p=0.8273
Monoculture growth rates
Co-culture growth rates
E. coli, wild-type mdoG
E. coli, mutant mdoG
E. coli, wild-type mdoG
E. coli, mutant mdoG
C.
log2MIC of E. coli mdoH mutants in Rifampicin
p>0.999
log2MIC
E. coli wild-type mdoH
E. coli mutant mdoH
D.
Growth rates of E. coli mdoH mutants in Rifampicin
p=0.3545
p>0.999
Monoculture growth rates
Co-culture growth rates
E. coli, wild-type mdoH
E. coli, mutant mdoH
E. coli, wild-type mdoH
E. coli, mutant mdoH
E.
log2MIC of S. enterica mdoH mutants in Rifampicin
p>0.999
log2MIC
S. enterica wild-type mdoH
S. enterica mutant mdoH
F.
Growth rates of S. enterica mdoH mutants in Rifampicin
p=0.4795
p=0.4795
Monoculture growth rates
Co-culture growth rates
S. enterica, wild-type mdoH
S. enterica, mutant mdoH
S. enterica, wild-type mdoH
S. enterica, mutant mdoH

Supplementary figure S3.2 Impact of *mdoG* and *mdoH* mutations on MICs and growth rates in rifampicin-resistant evolved *E. coli* and *S. enterica*. **A.** MIC of *mdoG* wild-type vs. mutant *E. coli* isolates, averaged by population (three isolates per population were used). **B.** Monoculture and co-culture growth rates of *mdoG* wild-type vs. mutant *E. coli* isolates. **C.** MIC of *mdoH* wild-type vs. mutant *E. coli* isolates. **D.** Monoculture and co-culture growth rates of *mdoH* wild-type vs. mutant *E. coli* isolates. E**.** MIC of *mdoH* wild-type vs. mutant *S. enterica* isolates. **F.** Monoculture and co-culture growth rates of *mdoH* wild-type vs. mutant *S. enterica* isolates.

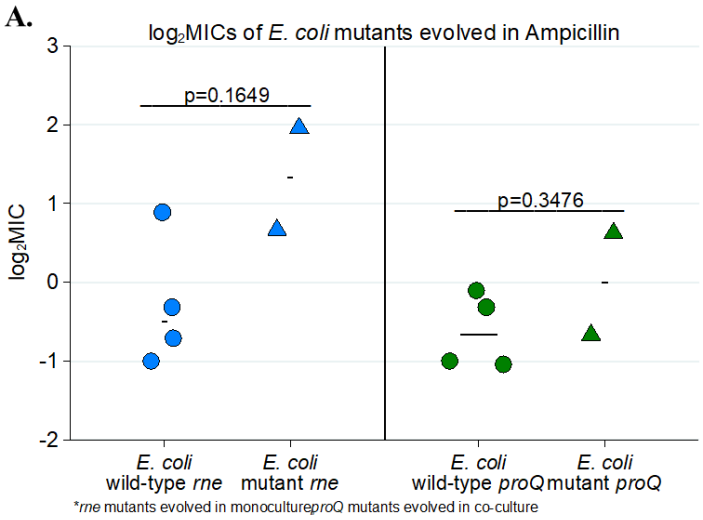
A.
log2MICs of E. coli mutants evolved in Ampicillin
log2MIC
p=0.1649
p=0.3476
E. coli wild-type rne
E. coli mutant rne
E. coli wild-type proQ
E. coli mutant proQ
*rne mutants evolved in monoculture proQ mutants evolved in co-culture

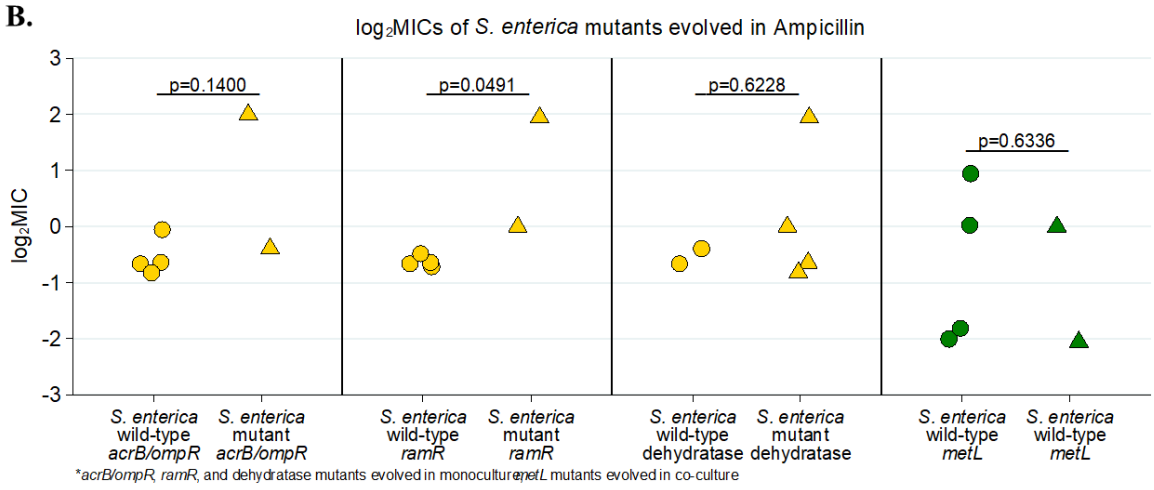
B.
log2MICs of S. enterica mutants evolved in Ampicillin
log2MIC
p=0.1400
p=0.0491
p=0.6228
p=0.6336
S. enterica wild-type acrB/ompR
S. enterica mutant acrB/ompR
S. enterica wild-type ramR
S. enterica mutant ramR
S. enterica wild-type dehydratase
S. enterica mutant dehydratase
S. enterica wild-type metL
S. enterica wild-type metL
*acrB/ompR, ramR, and dehydratase mutants evolved in monoculture metL mutants evolved in co-culture

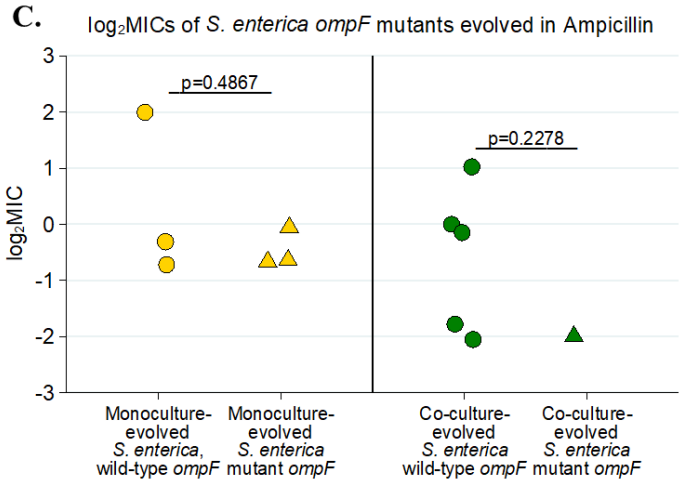
C.
log2MICs of S. enterica ompF mutants evolved in Ampicillin
log2MIC
p=0.4867
p=0.2278
Monoculture-evolved S. enterica, wild-type ompF
Monoculture-evolved S. enterica mutant ompF
Co-culture-evolved S. enterica wild-type ompF
Co-culture-evolved S. enterica mutant ompF

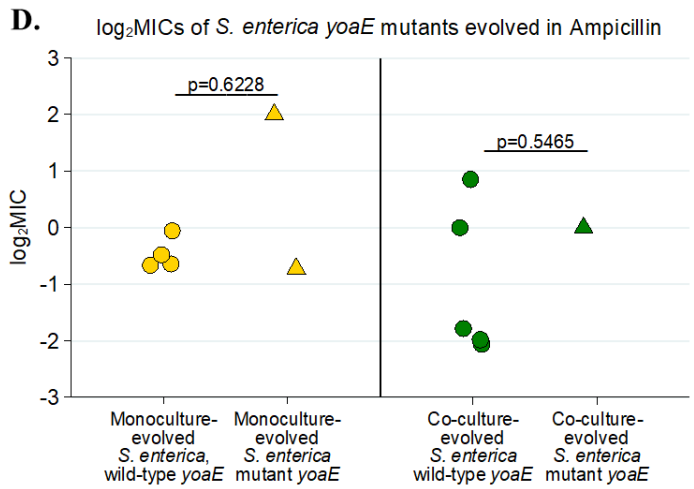

Supplementary figure S3.3 Effect of other mutations on MICs of ampicillin-evolved isolates. **A.** MICs of wild-type vs. mutant *E. coli* with mutations in *rne* (monoculture–evolved, in blue) and *proQ* (co-culture–evolved, in green). **B.** MICs of wild-type vs. mutant *S. enterica* with mutations in *acrB/ompR*, *ramR*, an unnamed dehydratase (all evolved in monoculture only), and *metL* (evolved in co-culture only). **C.** MICs of wild-type vs. mutant *S. enterica* with mutations in *ompF* evolved in monoculture (gold) or co-culture (green). **D.** MICs of wild-type vs. mutant *S. enterica* with mutations in *yoaE* evolved in monoculture (gold) or co-culture (green).

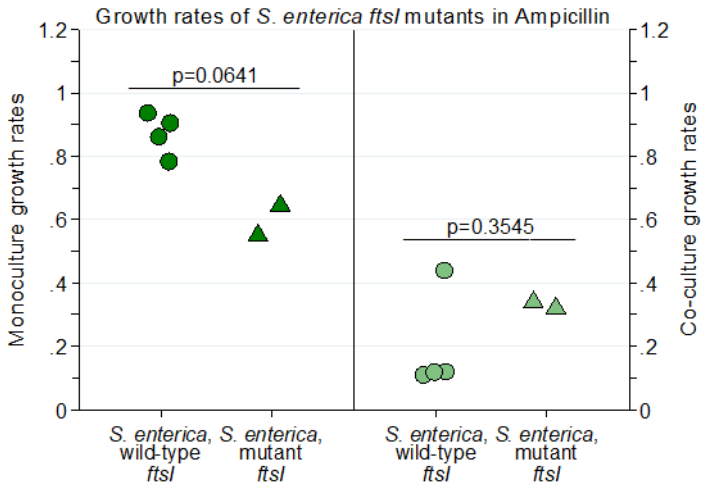

Supplementary figure S3.4 Monoculture and co-culture growth rates of *ftsI* mutant isolates in pH=4.7 growth medium. *P*= 0.0614 for monocultures, *P*= 0.3545 for co-cultures, Mann-Whitney U test.

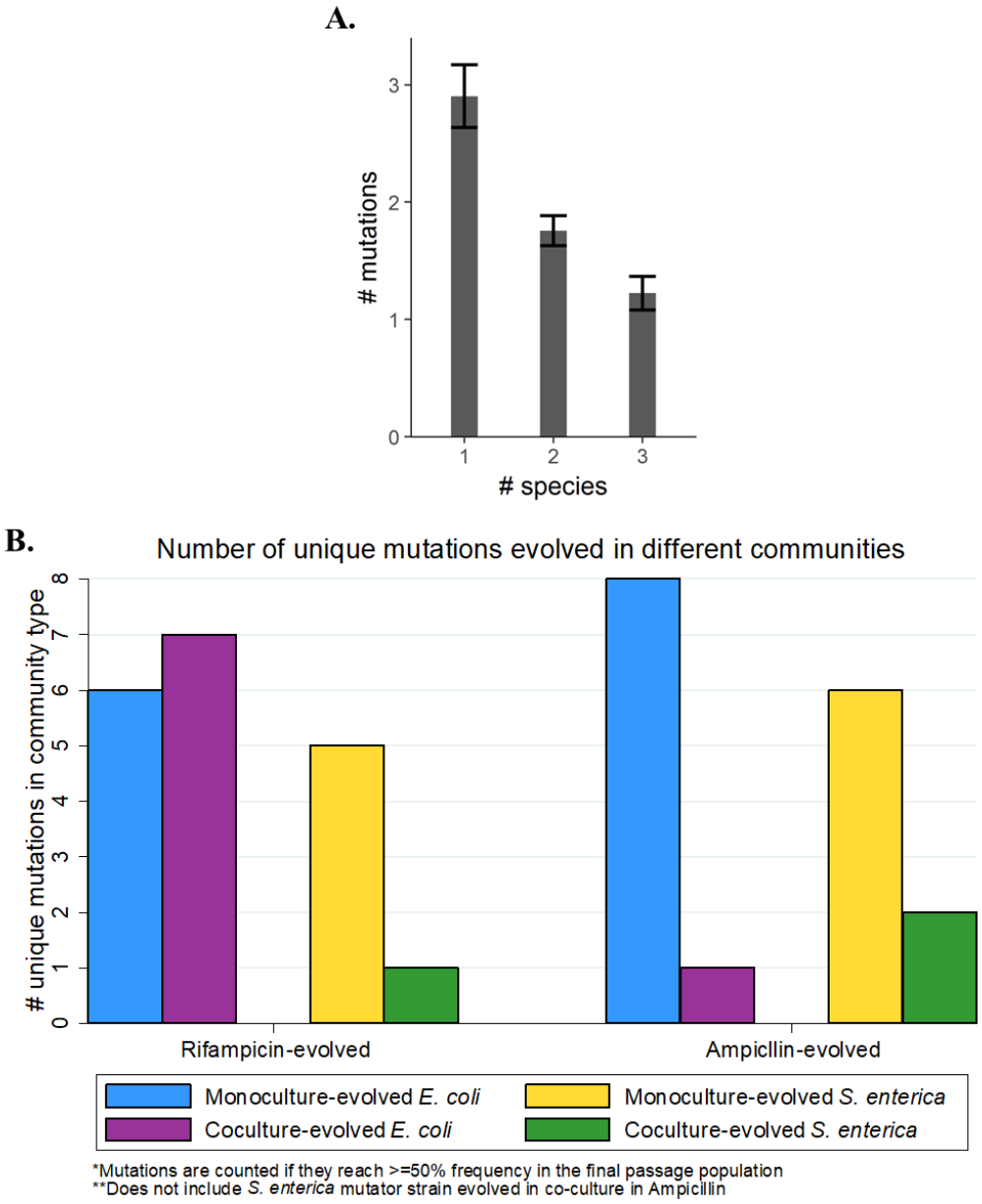

Supplementary figure S3.5 Number of mutations in monoculture vs. co-culture in simulation and in experimental evolution. **A.** The number of mutations (mean + SEM) accumulated in a species in simulations with one-three interdependent species. **B.** Experimental data showing the total number of unique mutations which arose in six replicate populations of each monocultures and co-cultures under rifampicin (left) and ampicillin (right) selection.

Chapter 4. Weakest link dynamics predict apparent antibiotic interactions in a model cross-feeding community

Summary

With the growing global threat of antimicrobial resistance, novel strategies are required for combatting resistant pathogens. Combination therapy, wherein multiple drugs are used to treat an infection, has proven highly successful in the treatment of cancer and HIV. However, this practice has proven challenging for the treatment of bacterial infections due to difficulties in selecting the correct combinations and dosages. An additional challenge in infection treatment is the polymicrobial nature of many infections, which may respond to antibiotics differently than a monoculture pathogen. This study tests whether patterns of antibiotic interactions (synergy, antagonism, or independence/additivity) in monoculture can be used to predict antibiotic interactions in an obligate cross-feeding co-culture. Using our previously described weakest link hypothesis, we hypothesized antibiotic interactions in co-culture based on the interactions we observed in monoculture. We then compared our predictions to observed antibiotic interactions in co-culture. We tested the interactions between ten previously identified antibiotic combinations using checkerboard assays. Although our antibiotic combinations interacted differently than predicted in our monocultures, our monoculture results were generally sufficient to predict co-culture patterns based solely on the weakest link hypothesis. These results suggest that combination therapy for cross-feeding multispecies infections may be successfully designed based on antibiotic interaction patterns for their component species.

Introduction

Antibiotic resistance is a growing global threat. It is estimated that, by 2050, 10 million deaths per year worldwide will be attributable to antibiotic-resistant infections (58). Many previously treatable infections, such as tuberculosis (231), urinary tract infections (232), and even *Staphylococcus*-mediated skin infections (233) now require higher doses of more powerful antibiotics. More concerning is that the patients most at risk for multidrug resistant infections are those with complex medical histories and increased risk of side effects (89). This arms race against pathogens by clinicians is proving a losing battle, as resistance is acquired rapidly, and the development of novel antimicrobials is limited (88, 90). The demand for novel treatment strategies is, therefore, an ever–increasing issue.

One treatment strategy that has proven particularly successful in the treatment of viral infections is the use of drug combinations. The best example of this is perhaps in HIV, where the advent of highly active antiretroviral therapy (HAART) dramatically improved the longevity and quality of life for HIV patients (234). The theory behind this treatment is based on simple probability — even in a highly mutable and therefore rapid resistance-acquiring virus such as HIV, it is much less likely that a viral population will acquire resistance to multiple antivirals than a single one, assuming an independent mutation is required for resistance to each drug (235). In line with this theory, HAART regimens typically involve drugs targeting different viral targets, including the HIV protease required for virion maturation, the reverse transcriptase required for replication, and the integrase required for viral insertion into the host genome (234). This approach, of using multiple drugs to target multiple essential targets, has also been used in cancer

chemotherapy to manage drug-resistant and genetically heterogeneous tumors (236). For example, treatment for metastatic colon cancer may involve a growth factor inhibitor to block cell division signals, a nucleoside analog to induce hypermutation and apoptosis of cancer cells, and a topoisomerase inhibitor to inhibit DNA replication (237).

The success of combination therapy is affected by interactions between drugs, wherein the activity and effectiveness of one drug is impacted by the presence or absence of another (238). There are several mechanisms by which antibiotics may synergize (work more effectively or at lower doses together than separately) or antagonize (work less effectively or at higher doses together than separately). Antibiotic interactions may arise as a result of chemical interactions (e.g. two similar drugs compete for the same enzymatic target) (238), or biological constraints (e.g. bacteriostatic drugs slow cellular growth sufficiently for cells to become transiently tolerant to bactericidal drugs) (239). While the precise nature of these interactions depends on the drugs and the bacterial species being targeted, some general mechanisms have been described for different classes of antibiotics (240). For example, cell wall inhibitors such as β-lactam antibiotics may synergize with aminoglycosides by permeabilizing the cell membrane, thus allowing increased aminoglycoside penetration (241, 242) or co-inducing cell envelope stress (243). Co-administration of β-lactam antibiotics and β-lactamase inhibitors such as tazobactam maintains β-lactam efficacy even in β-lactamase–containing pathogens (244). Antibiotics targeting similar cellular processes or pathways may also synergize (245, 246). Conversely, antagonism may occur when the cellular response to one antibiotic involves induction of tolerance or resistance mechanisms to another (240, 247, 248). Physiological disruptions induced by one drug may also be corrected for via the

response to a second drug, leading to antagonistic interactions (249). These are general trends only, however, and many species– and drug – specific exceptions apply, making it challenging to predict drug interactions *a priori* in new systems.

In cases of bacterial infections, multidrug therapy has been adopted only in a few specific infections. Standard treatment for drug–sensitive tuberculosis, for example, includes two months of isoniazid, rifampicin, pyrazinamide, and ethambutol, followed by four months of isoniazid and rifampicin (231). However, clinical trials of combination therapy in the treatment of bacterial infections in patients have been limited for a few reasons (240). One is that combination therapy is most useful in infections which do not respond to single drugs at tolerable concentrations; many bacterial infections are still treatable by single antibiotics at non– or minimally toxic doses (86). Another is the inherent difficulty in choosing the correct antibiotic combinations and doses for a specific infection (86, 250). Perhaps most importantly, however, is that the evidence for the effectiveness of multidrug treatment regimens, particularly for Gram-negative pathogens, is mixed at best and leads to increased side effects in several cases (87). However, there has been some evidence that combination therapy is effective at reducing mortality for septic patients, possibly due to increased likelihood of administering the correct antibiotic to treat a pathogen(s) whose resistance profile is unknown (251). Further research into the precise mechanisms of bacterial suppression in combination therapy may therefore have clinical impacts in cases of severe bacteremia.

Another increasingly appreciated feature of bacterial infections is their polymicrobial nature. Numerous clinically relevant infections are now known to involve multiple species, consisting of a single pathogen and various commensal partners, or several co-

infecting pathogens (11, 12). Polymicrobial infections have been observed to have worse clinical outcomes in some cases (115–117), though these results are mixed (252, 253). The metabolic interactions (both positive and negative) among these species have been demonstrated to impact antibiotic response. For example, in a co-culture model of *Candida albicans* and *Candida glabrata*, competition for glucose changes the ability of each species to survive and invade a community during antifungal treatment (134). While negative interactions such as resource competition might be more common in infection scenarios, where a pathogen (or pathogens) is likely to be invading an established community, positive ecological interactions may also be occurring. One such interaction is cross-feeding, wherein one species produces an essential metabolite for another; this also occurs in infection contexts (13). For example, in a cystic fibrosis model where the pathogen *Pseudomonas aeruginosa* depends on the mucin degradation products supplied by a community of anaerobic commensals, antibiotics specifically targeting the anaerobes decreased *P. aeruginosa* abundance despite its intrinsic resistance to the antibiotic (120). Treatment regimens might, therefore, be more effective if metabolic interactions among species are taken into account; however, little research has been done on how cross-feeding might impact combination therapy.

To this end, we aimed to test whether cross-feeding interactions in a model bacterial community might influence antibiotic interactions. We selected ten combinations of six antibiotics based on the work of Yeh et al. (238); this study quantitatively tested the pairwise interactions between 21 different antibiotics which altered *E. coli* growth rate. Yeh et al then developed a drug interaction network wherein interactions were found to correspond to the cellular targets of each drug, providing both a predictive and

mechanistic framework for future interaction studies. Three of the combinations we selected from this study were predicted to synergize (greater antibiotic efficacy in combination than alone); three were predicted to antagonize (lower antibiotic efficacy in combination than alone), and four to interact additively or independently in *E. coli* monoculture. Our model system, consisting of an *E. coli* methionine auxotroph strain that produces acetate from lactose, and an *S. enterica* that produces methionine, has been previously described (120, 137, 159).We first tested each of these combinations for their drug interactions in *E. coli* and *S. enterica* monoculture, and used fractional inhibitory concentration indices (FICIs) to identify any drug interactions. We then used our "weakest link" hypothesis to predict the growth patterns of the co-culture and the subsequent antibiotic interactions. Briefly, the weakest link hypothesis states that the "weakest link" species in an obligate cross-feeding community will define the tolerance (i.e. the ability to grow at high antibiotic concentrations) of the entire community. The weakest link species is defined as the species with the lowest antibiotic tolerance in monoculture. We previously showed that this hypothesis holds true for different individual drugs in our system and others (120). In this study, we found that only three antibiotic combinations showed non-additive interactions, likely due to the different antibiotic interaction metrics that we used versus those used by Yeh et al. (238). However, in those non-additive combinations, weakest link dynamics successfully predicted co-culture growth and antibiotic interactions. While more antibiotic combinations need to be explored, these results suggest that the responses of individual community members to combination therapy might be sufficient to predict the antibiotic interactions in the larger microbial community.

Methods

Our model microbial community has been previously described (137). Briefly, our system consists of an *E. coli* methionine auxotroph, and an *S. enterica* strain which has been evolved to secrete excess methionine. In a lactose environment, *E. coli* metabolizes lactose to produce acetate for *S. enterica*, which in turn supplies methionine for *E. coli*. Each species can also be grown in monoculture by supplying *E. coli* with methionine and lactose, and *S. enterica* with acetate.

We performed checkerboard assays (described below) with six antibiotics in ten different combinations predicted to synergize (3), antagonize (3), or not interact (4)—see **Table 4.1** for these combinations. For each drug combination, we tested *E. coli* and *S. enterica* in monocultures, and the two-species in obligate co-culture. Each antibiotic combination/culture type was tested in triplicate. Seven two-fold dilutions of each antibiotic, along with an antibiotic–free control for each, were used in orthogonal gradients on a 96-well plate such that the antibiotic concentrations increased from left-to-right and top-to-bottom. The first row and column of each plate were antibiotic–free wells for the vertically– and horizontally– distributed antibiotics, respectively. The minimum inhibitory concentrations (MICs) for each antibiotic were determined in the absence of the other antibiotic. Mid-log–phase cells (OD~0.4) were grown up on the day of the experiment in species–specific Hypho growth medium (120) and 2µL was inoculated into 194µL fresh species-specific Hypho. Antibiotic stocks were prepared within two days of the experiment such that 2µL of stock could be added to each well to achieve the desired gradient concentrations. Plates were then incubated at 30°C with shaking for 48 hours. A Tecan plate reader was then used to measure the OD600 and

species-specific fluorescence (CFP for *E. coli* and YFP for *S. enterica*). The 90% minimum inhibitory concentration (MIC_{90}) was then used to establish which wells showed growth. Any well that had an OD600 or fluorescent protein value above 10% of the highest plate value was considered growth. We used the highest plate value rather than the antibiotic–free well because we consistently saw a slight increase in OD600 in the co-cultures at sublethal concentrations, possibly due to a low level of cell lysis and subsequent boost for the cross-feeding partner (196, 254).

We used the Loewe additivity method to identify the nature of our antibiotic interactions as previously described (88). Briefly, we calculated the fractional inhibitory concentration (FIC) for antibiotics A and B as follows: $FIC_A = (MIC_{A\ in\ combination} / MIC_{A\ alone})$, and $FIC_B = (MIC_{B\ in\ combination} / MIC_{B\ alone})$. FIC values were obtained for each well at the edge of growth, as shown in **Figure 4.1.** The FICI is the sum of FIC_A and FIC_B (255). As there are multiple FICI values per plate, we chose to report the median FICI value as the plate value. We did not use the minimum or maximum FICI value so that we would not over-interpret synergy or antagonism results, respectively (256). Minimum FICI values can be found in **Supplementary table S4.3**. Our cut-off values were designed as follows: $FICI < 0.8$ represents synergy; FICI between 0.8 and 2 represent additive interactions, FICI between 1 and 2 represent independent interactions, and $FICI \geq 2$ represents antagonism (255–258). Isobolograms were generated by plotting the FIC_A and FIC_B values as x,y coordinates. A straight line connecting the FIC values represents additive interactions; a concave line represents synergy; and a convex line represents antagonism.

Based on observed monoculture growth patterns (MICs and FICs in each antibiotic combination), we predicted co-culture growth patterns assuming weakest link dynamics; that is, co-cultures should only grow at concentrations of both antibiotics where both species are able to grow in monoculture. We then calculated FICs and FICIs for these predicted co-culture plates and compared them to our observed data. We then used a Mann-Whitney U test to compare predicted versus observed FICIs for our co-cultures.

Results

Based on previous results in *E. coli* (238), we tested ten combinations of six antibiotics for synergy or antagonism in *E. coli* and *S. enterica* monocultures (**Table 4.1**). The mechanism of action for each of these antibiotics can be found in **Supplementary table S4.1.** Each combination was tested in triplicate and minimum inhibitory concentrations (MICs), fractional inhibitory concentrations (FICs) and fractional inhibitory concentration indices (FICIs) were obtained after 48 hours of growth at 30°C (**Figure 4.1**). To avoid over– or under– interpretation of the antibiotic interactions, we used the median FICI value for each plate and the mean value from each of the three replicate plates for each antibiotic combination.

Previous work from our lab has shown that co-culture growth in the presence of antibiotics is dependent on weakest link dynamics (120). This hypothesis predicts that the MIC of an obligately cross-feeding co-culture is set by the MIC of the least tolerant species in the community. This phenomenon allows us to determine how antibiotics should interact in co-culture based on how they interact in each monoculture. A sample of these predictions are detailed in **Figure 4.2**. In brief, the co-culture is predicted to grow only where both species can grow individually (see plate diagrams). The impact of weakest link dynamics on antibiotic interactions depends on whether the weakest link species is the same or different in both antibiotics, and how the antibiotics interact with each species. In scenario 1, the weakest link species differs in each antibiotic, but in both species the antibiotic effects are independent of each other; therefore, the antibiotics should also be independent in co-culture. This is seen in the FICI plots (where the median FICI is around 1) and in the isobolograms (where the curve is around the 1-1

line). In scenario 2, the antibiotics synergize in both species, but because weakest link species differs in each antibiotic, the synergism is weakened (though still present) in co-culture. In scenario 3, the antibiotics antagonize in both species. However, in *E. coli*, antibiotic B antagonizes antibiotic A (i.e. as the concentration of B increases, the MIC of A also increases), but not vice versa (i.e. the MIC of B does not change as the concentration of A increases). In *S. enterica*, antibiotic A antagonizes antibiotic B but not vice versa. This leads to a 'cancelling out' of the antagonistic interactions in co-culture and causes the antibiotics to interact independently. In scenario 4, *E. coli* is the weakest link species in both antibiotics. Therefore, the co-culture antibiotic interaction pattern exactly matches that of *E. coli*.

We first tested whether the antibiotic combinations we selected would interact as predicted in the literature in our monocultures. We tested each antibiotic combination in triplicate for *E. coli* and *S. enterica*, then calculated the median FICI value for each plate and combination (**Figure 4.3**). Our categories were designated as follows: FICI < 0.8 represents synergy; FICI between 0.8 and 2 represent additive interactions, FICI between 1 and 2 represent independent interactions, and FICI ≥ 2 represents antagonism. These are less stringent than other FICI results, as we chose median values to minimize the impact of plate-to-plate variation, which tends to bias FICI results towards additive or independent interactions. We also looked at isobolograms (**Figure 3.4**) of each antibiotic combination for each species, to get a more visual/qualitative examination of interactions between antibiotics. **Supplementary tables S4.2** and **S4.3** contain raw median and minimum FICI data, respectively.

Interestingly, we did see some deviations from our prediction. Nalidixic acid/bleomycin and streptomycin/ciprofloxacin were predicted to synergize; however, our FICI and isobologram data show additive/independent interactions for these antibiotics in both species. Nalidixic acid and streptomycin did synergize as predicted in *E. coli*, but not in *S. enterica*. Of the three pairs of antibiotics predicted to antagonize (nalidixic acid/ spectinomycin, nalidixic acid/doxycycline, and spectinomycin/streptomycin), only the last showed potentially antagonistic interactions; the others all interacted independently. Finally, we observed some unexpected synergy in our antibiotic pairs which were predicted to interact additively/independently. Ciprofloxacin/bleomycin synergized in *E. coli*, and spectinomycin/doxycycline synergized in both species; however, this is more evident in the FICI data than in the isobolograms. The isobolograms suggest that low concentrations of doxycyline decrease the MIC of spectinomycin, but not vice versa; that is, doxycyline synergizes with spectinomycin to increase the latter's potency, but spectinomycin does not change the effect of doxycycline.

Based on our results from monoculture and our weakest link hypothesis, we then predicted the antibiotic interactions which would arise in obligate cross-feeding co-culture. To generate these predictions, we examined the monoculture growth patterns in each antibiotic combination (i.e. at which concentrations of each antibiotic monoculture growth occurred). We then generated a predicted growth pattern for the co-culture wherein growth would only occur at antibiotic concentrations where both species could grow. From this predicted growth pattern, we calculated FICIs and generated isobolograms; these can be seen in **Figure 4.5** and **4.6**, respectively. An example of how this was done can be found in **Supplementary figure S4.1.**

According to our predictions, if one species is the weakest link (i.e. the least tolerant) in both antibiotics, the co-culture interaction typically matched that of the weakest link monoculture. This is the case for nalidixic acid/bleomycin and nalidixic acid/ciprofloxacin (where *S. enterica* is the weakest link), and for streptomycin/ciprofloxacin, spectinomycin/streptomycin, streptomycin/doxycyline, and spectinomycin/doxycycline (where *E. coli* is the weakest link). Co-culture predictions were somewhat more complicated for the other combinations (nalidixic acid/ streptomycin, nalidixic acid/spectinomycin, nalidixic acid/doxycycline, and ciprofloxacin/ bleomycin), where each species is the weakest link in a different antibiotic. We were particularly interested in nalidixic acid/streptomycin, as these antibiotics synergize in *E. coli* (which is the weakest link in streptomycin) and interact independently in *S. enterica* (which is the weakest link in nalidixic acid). Based on the differences in MIC in these species in each antibiotic (see **Supplementary table S4.4**), we predicted an independent interaction in co-culture. Similarly, in the ciprofloxacin/ bleomycin combination, the antibiotics verged on antagonizing in *E. coli* and interacted independently in *S. enterica*; however, their MICs were similar in both antibiotics. This provided an opportunity to examine interactions in co-culture where weakest link dynamics might play less of a role.

After generating predicted FICIs based on our monoculture results and weakest link dynamics, we tested antibiotic interactions in co-culture. We then compared our predicted FICIs to those observed experimentally for each antibiotic combination. Qualitatively, our predictions based on weakest link were accurate — the antibiotic interaction category (antagonism/synergy/additive) identified by predicted FICIs

matched the interaction category identified by the observed FICIs (**Figure 4.5,** see **Supplementary Table S4.5** for raw FICI data). This supports our hypothesis that weakest-link dynamics can be used to predict antibiotic interaction categories in co-culture. The one exception to this was in the spectinomycin/ streptomycin combination. While there was no statistical significance in this difference, (P= 0.37), we predicted an independent interaction and observed an antagonistic interaction. Interestingly, the isobologram suggested that antibiotics antagonized much more in co-culture than we predicted. This suggests that weakest-link dynamics may not always predict co-culture outcomes and that some other factor may be determining antibiotic interactions in this case. Quantitatively, our FICI predictions also matched that of our observed data (see **Supplementary Table S4.6** for all P-values), with one exception. The predicted FICI for the nalidixic acid/ spectinomycin combination was significantly higher than predicted (P= 0.037), but this difference still resulted in independent interactions and so is likely not biologically significant. Overall, weakest-link dynamics were generally sufficient to both qualitatively and quantitatively predict antibiotic interactions in co-cultures.

Discussion

The goal of this work was to identify whether our previously identified weakest link hypothesis, wherein the antibiotic tolerance of a mutualistic co-culture is set by the weakest link species, could change drug interaction patterns in antibiotic combinations. We tested previously identified antibiotic combinations in each of our monocultures. Few of the predicted interactions applied to our monocultures, possibly for reasons discussed below. However, we then used the interactions we identified in monoculture, as well as our knowledge of weakest link dynamics, to predict how each set of antibiotics would interact in co-culture. We found that our predictions were qualitatively correct, with predicted and observed FICIs and isobolograms falling into the same antibiotic interaction category (synergistic, additive, independent, or antagonistic). The one exception to this was the spectinomycin/streptomycin combination, which antagonized more strongly in co-culture than we predicted from monoculture.

Our findings demonstrate an important and hitherto unexplored explanation for why *in vivo* antibiotic interactions do not match *in vitro* assay predictions. Many infections are now known to be polymicrobial (11–14) and likely involve some form of cooperative metabolite exchange. These ecological interactions may be at least partially responsible for the difficulty in finding a successful synergistic antibiotic treatment. Indeed, our results suggest that cross-feeding generally ablates any antagonistic/ synergistic antibiotic interactions unless one partner is the weakest link in every antibiotic (**Figure 4.2**); whether or not this is the case in natural microbial communities is unknown. Helpfully, our results suggest that the antibiotic interactions at the community level are predictable given the right information — i.e. if the individual resistances and antibiotic

interaction patterns are known for each species in the community, the antibiotic interaction pattern is generally predictable based on weakest link dynamics. This adds further weight to the argument that microbial ecology must be considered when treating bacterial infections in the clinic.

Unexpectedly, the antibiotic interactions that we observed in our monocultures did not match the interactions that Yeh et al. had previously observed (238). The most likely reason for this is their use of a growth rate-based measurement method, a dose-response curve (86), versus our yield-based checkerboard assay. We elected to do a yield-based method because it allowed us to more highly parallelize our experiments and decrease plate-to-plate variation in cell density and growth phase, both of which are known to significantly impact antibiotic tolerance (81, 259, 260). Much research has been done on the best method for assessing antibiotic synergy/antagonism (86, 92, 239); we selected the checkerboard method also because of its widespread use and ease of interpretation. Future experiments using dose-response curves might be particularly important for cross-feeding systems such as ours, as cross-feeding is known to alter growth rates of member species (140, 261).

An additional challenge in interpreting antibiotic interactions in multispecies contexts is the possibility of antibiotic interactions changing depending on which species is the weakest link at a given combination of antibiotic combinations. Taking the largest FICI value from a plate biases results towards antagonism and taking the smallest value biases towards synergy. Therefore, the median value is useful in avoiding overinterpretation of data; however, it obscures any concentration-specific changes in interactions which might be occurring. We reported isobolograms and FICIs for this reason. Isobolograms

provide more information as to how the antibiotics are interacting at different concentration combinations than FICIs. The isobologram of nalidixic acid/bleomycin in **Figure 4.6** provides a good example of this. The predicted co-culture isobole showed additive-synergistic interactions; however, the observed co-culture isobole showed synergistic interactions at low bleomycin FIC values. A similar pattern is seen with ciprofloxacin/bleomycin in the same figure. While these patterns may be artifacts of our system, it remains possible that checkerboard assays involving multiple species may produce isobologram patterns which deviate from the typical convex/concave, antagonism/synergy pattern seen in monocultures. Mathematical modeling of how different antibiotic interactions and MICs in each species impact co-culture antibiotic interactions may be a useful way to explore this possibility.

The one drug interaction in our study where weakest link dynamics appeared insufficient to predict co-culture interactions was the streptomycin/spectinomycin combination. These drugs were predicted to antagonize in *E. coli*; though they have similar mechanisms of action, spectinomycin ionically inhibits entry of streptomycin into the cell (262). Given that *E. coli* was the weakest link in both antibiotics, we predicted similar dynamics in co-cultures; additive interactions bordering on antagonism (i.e. FICIs between 1.5 and 2). However, the degree of antagonism that we observed was much higher than predicted. There could be several reasons for this. Given that disruptions in protein biosynthesis have pleiotropic effects on cell physiology and metabolism (263), the application of both drugs might have sufficiently disrupted the cross-feeding between our species such that they starved at otherwise sublethal concentrations of each antibiotic. That antibiotics can arrest growth rate (264, 265) and

change metabolic profile (266, 267) of cells is well known; what is less clear is how this might impact metabolite exchange in antibiotic-exposed natural microbial communities. The complex and often non-obligate metabolite exchange food webs in natural communities (268, 269) might make this question difficult to answer, but our study suggests that weakest link dynamics are a useful null hypothesis starting point.

Though much research has been done *in vitro* on antibiotic synergy/antagonism, it remains unclear what the biological/clinical relevance of any of these interactions truly are. With a few exceptions (90, 231), antibiotic synergy has yet to be adopted as a clinically important treatment strategy due to a variety of factors. Differences in drug half-life and bioavailability can impact effective dosages *in vivo* (270), and strain-specific resistance profiles make assessment of antibiotic synergy challenging in the clinic (86). However, antibiotic combinations may become an increasingly critical clinical tool as resistance continues to rise (250). Further research is therefore required not just on how antibiotics interact *in vitro*, but how they interact in natural environments— both within the host, and within a multispecies community.

Chapter 4 Figures and Tables

Table 4.1 Antibiotic combinations used in the study and their predicted interactions in *E. coli* based on Yeh et al. 2006.

Synergy	Antagonism	Additive
Nalidixic acid and streptomycin	Nalidixic acid and spectinomycin	Nalidixic acid and ciprofloxacin
Nalidixic acid and bleomycin	Nalidixic acid and doxycycline	Ciprofloxacin and bleomycin
Streptomycin and ciprofloxacin	Spectinomycin and streptomycin	Streptomycin and doxycyline
		Spectinomycin and doxycyline

A.

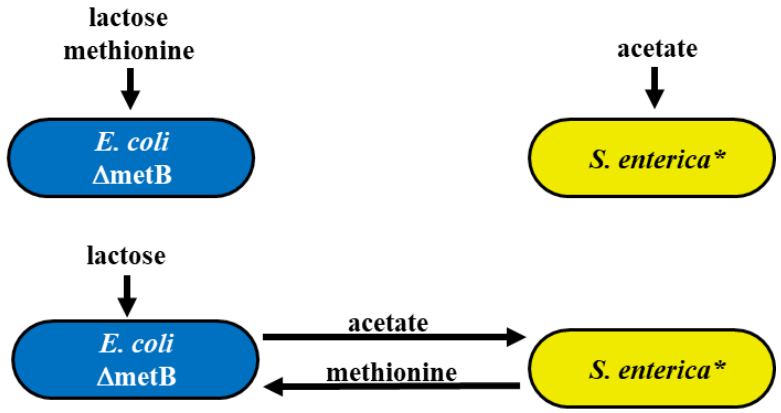

B.

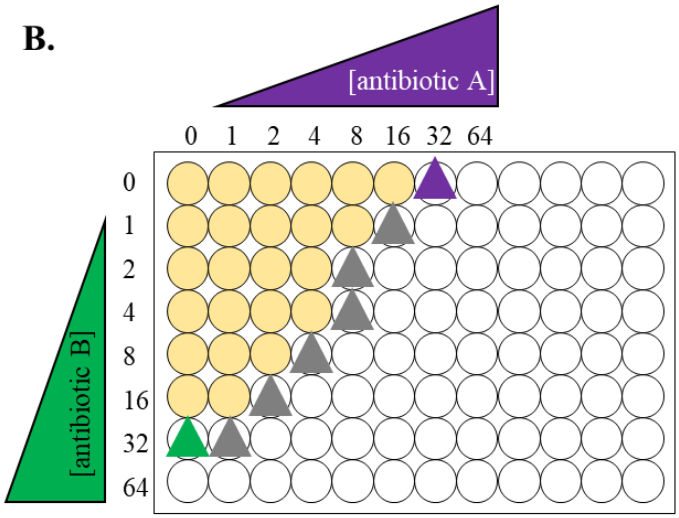

C.

$FIC_A = (MIC_{A \text{ with } B}) / (MIC_{A \text{ alone}})$
$FIC_B = (MIC_{B \text{ with } A}) / (MIC_{B \text{ alone}})$
$FICI = FIC_A + FIC_B$

MIC_A	FIC_A	MIC_B	FIC_B	FICI
0	0	32 ▲	1	1
1	0.03125	32	1	1.03125
2	0.0625	16	0.5	0.5625
4	0.125	8	0.25	0.375
8	0.25	4	0.125	0.375
8	0.25	2	0.0625	0.3125
16 ▲	0.5	1	0.03125	0.53125
32	1	0	0	1

Figure 4.1 Antibiotic interaction experimental setup and hypotheses. **A.** The two-species obligate cross-feeding system. When lactose is supplied, *E. coli* uses it to produce acetate for *S. enterica*, which produces methionine for *E. coli*. Each species can be grown in co-culture or monoculture, depending on the metabolites supplied. **B.** Setup for checkerboard assays. Seven antibiotic concentrations plus one antibiotic–free well were developed for each antibiotic/ species combination, with the MIC approximately in the middle of the gradient. Mid-log phase cells were inoculated into plates containing species-specific growth medium and antibiotic at twofold dilutions. Cells were allowed to grow for 48 hours at 30°C with shaking, and a Tecan plate reader was used to measure growth at OD600. Growth was defined as an OD600 above 10% of the maximum OD600 obtained on each plate. Three replicates of each antibiotic/ culture condition were obtained. **C.** Table of calculations for fractional inhibitory concentrations and formulae used.

	Plate diagram	FICI plots	Isobolograms
Scenario 1: • Species-level: independent interactions • Community level: independent interactions • Each species has a different MIC in each antibiotic	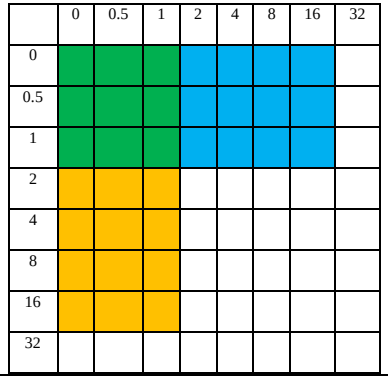	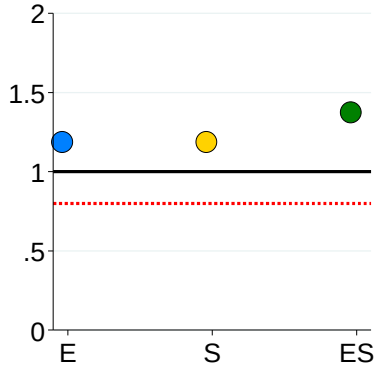	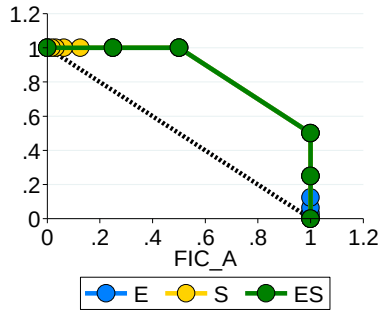
Scenario 2: • Species-level: synergistic interactions • Community level: independent interactions • Each species has a different MIC in each antibiotic	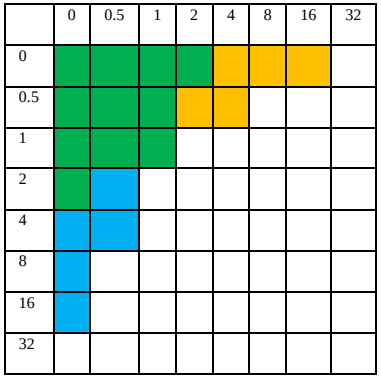	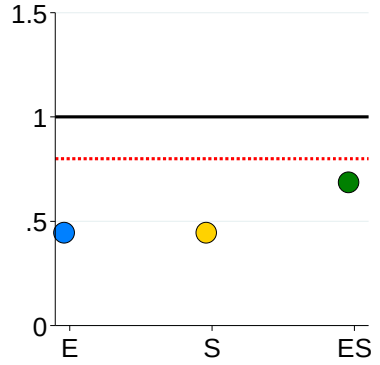	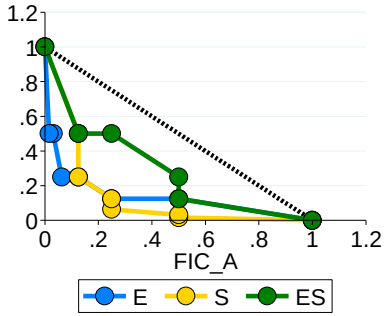

Scenario 3: • Species-level: antagonistic interactions • Community level: independent interactions • Each species has a different MIC in each antibiotic and direction of antagonism differs for each species	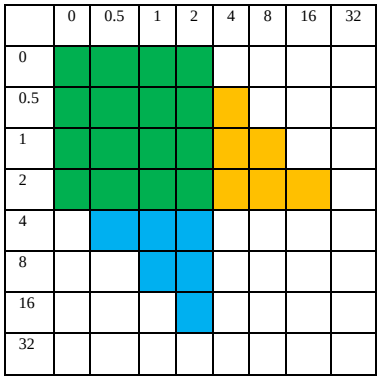	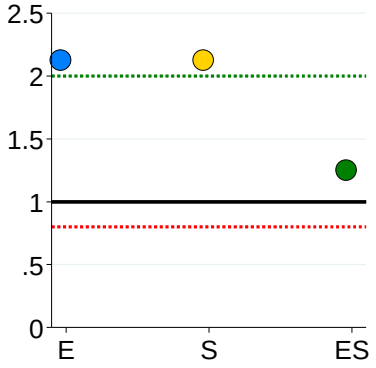	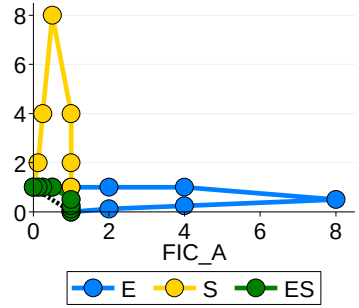
Scenario 4: • Species-level: synergistic interactions in *E. coli*, independent interactions in *S. enterica* • Community level: synergistic interactions • *E. coli* has the lowest MIC in each antibiotic	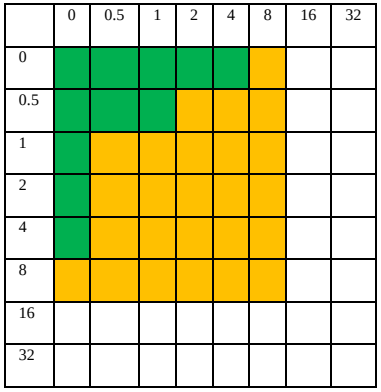	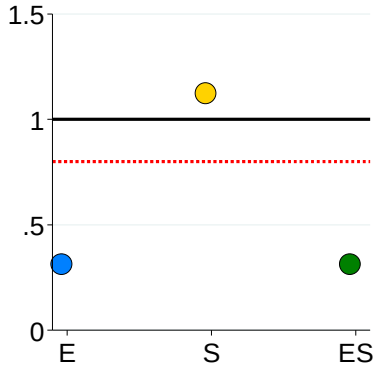	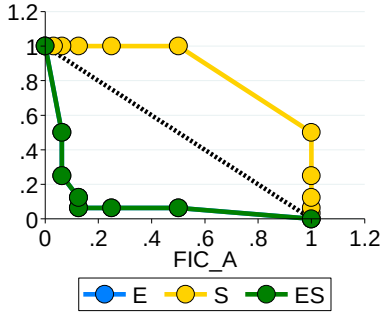

Figure 4.2 Antibiotic interactions at the species level versus the co-culture level. In the plate diagrams (simulated data), blue cells represent concentrations where only *E. coli* can grow; yellow cells represent concentrations where only *S. enterica* can grow, and green cells represent concentrations where the co-culture can grow (i.e. concentrations where both monocultures can grow). Antibiotic A is on the y-axis and antibiotic B is on the X-axis. Points that fall below the red dotted line on FICI plots represent synergistic interactions; points that fall above the green dotted line represent antagonistic interactions. FICI plots and isobolograms were calculated based on the simulated data in plate diagrams (see **Methods**). Concave isoboles represent synergy; convex isoboles represent antagonism.

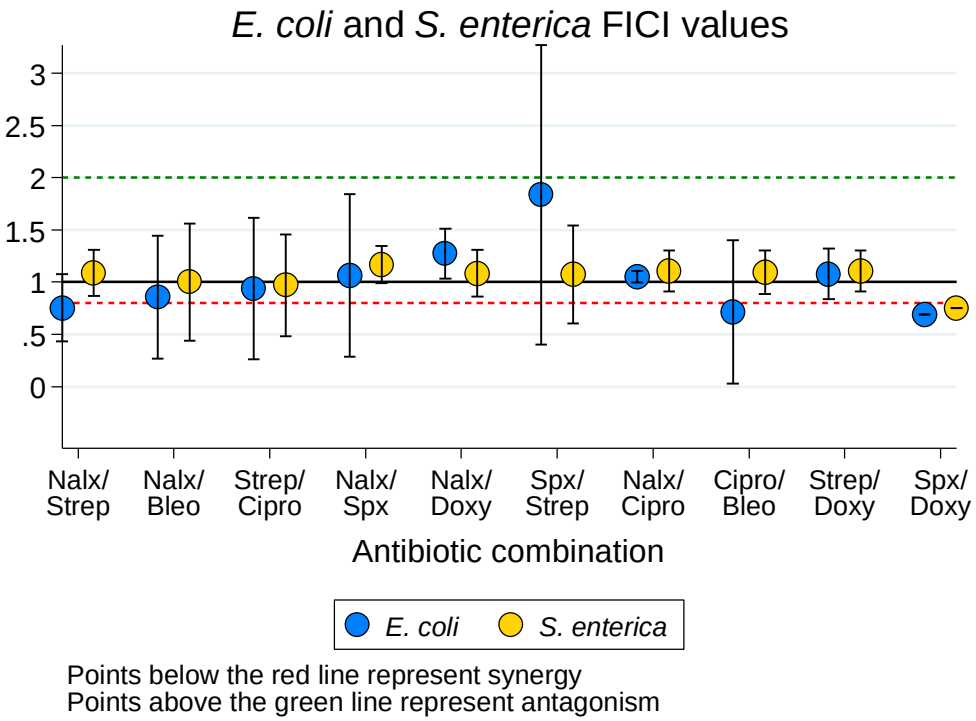

Figure 4.3 Fractional inhibitory concentration index (FICI) plots of *E. coli* and *S. enterica* monocultures across ten antibiotic combinations. Each point represents the mean +/-SE of three replicate FICI values from three biological replicates. FICIs on each plate represent the median FICI value from the plate. Antibiotic abbreviations: Nalx= nalidixic acid; strep= streptomycin; bleo= bleomycin; cipro= ciprofloxacin; spx= spectinomycin; doxy= doxycycline.

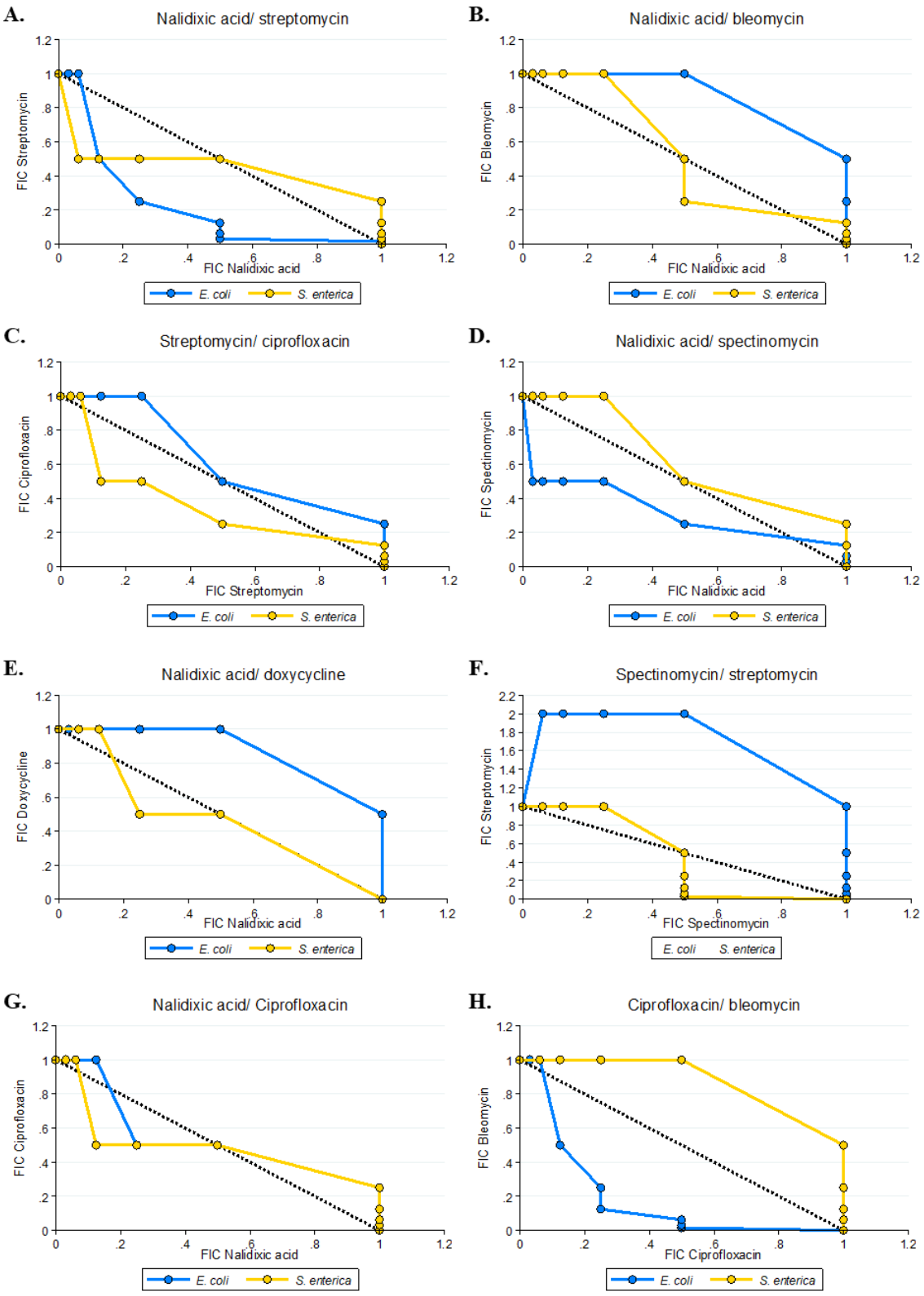
A.
Nalidixic acid/ streptomycin
FIC Streptomycin
FIC Nalidixic acid
E. coli
S. enterica
B.
Nalidixic acid/ bleomycin
FIC Bleomycin
FIC Nalidixic acid
E. coli
S. enterica
C.
Streptomycin/ ciprofloxacin
FIC Ciprofloxacin
FIC Streptomycin
E. coli
S. enterica
D.
Nalidixic acid/ spectinomycin
FIC Spectinomycin
FIC Nalidixic acid
E. coli
S. enterica
E.
Nalidixic acid/ doxycycline
FIC Doxycycline
FIC Nalidixic acid
E. coli
S. enterica
F.
Spectinomycin/ streptomycin
FIC Streptomycin
FIC Spectinomycin
E. coli
S. enterica
G.
Nalidixic acid/ Ciprofloxacin
FIC Ciprofloxacin
FIC Nalidixic acid
E. coli
S. enterica
H.
Ciprofloxacin/ bleomycin
FIC Bleomycin
FIC Ciprofloxacin
E. coli
S. enterica

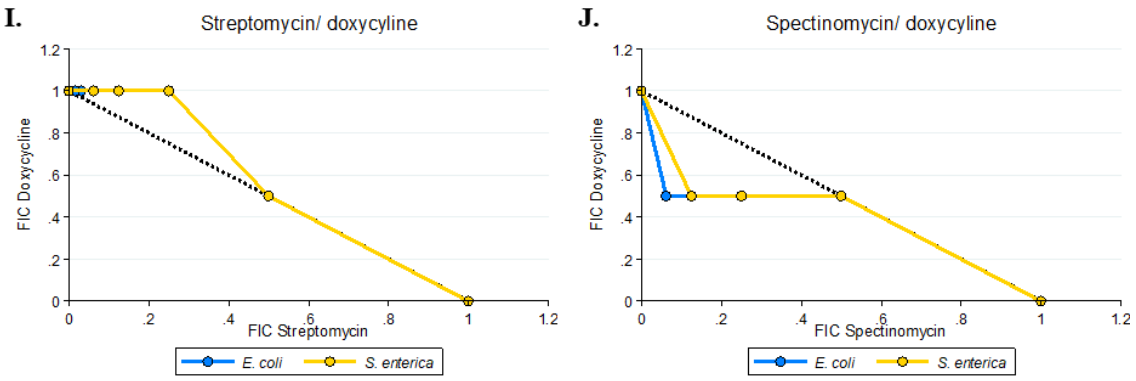

Figure 4.4 Representative isobolograms of *E. coli* and *S. enterica* monoculture fractional inhibitory concentrations (FICs) across ten antibiotic combinations. FICs were calculated based on 48 hours of 30°C growth, and growth was identified as any well which had an OD600 at least 10% of the highest OD600 well on each plate. Each axis corresponds to a fractional inhibitory concentration (FIC) for the antibiotic pair. The black 1-1 line represent a perfectly independent interaction; a concave line towards the origin represents a synergistic interaction, and a convex line away from the origin represents an antagonistic interaction.

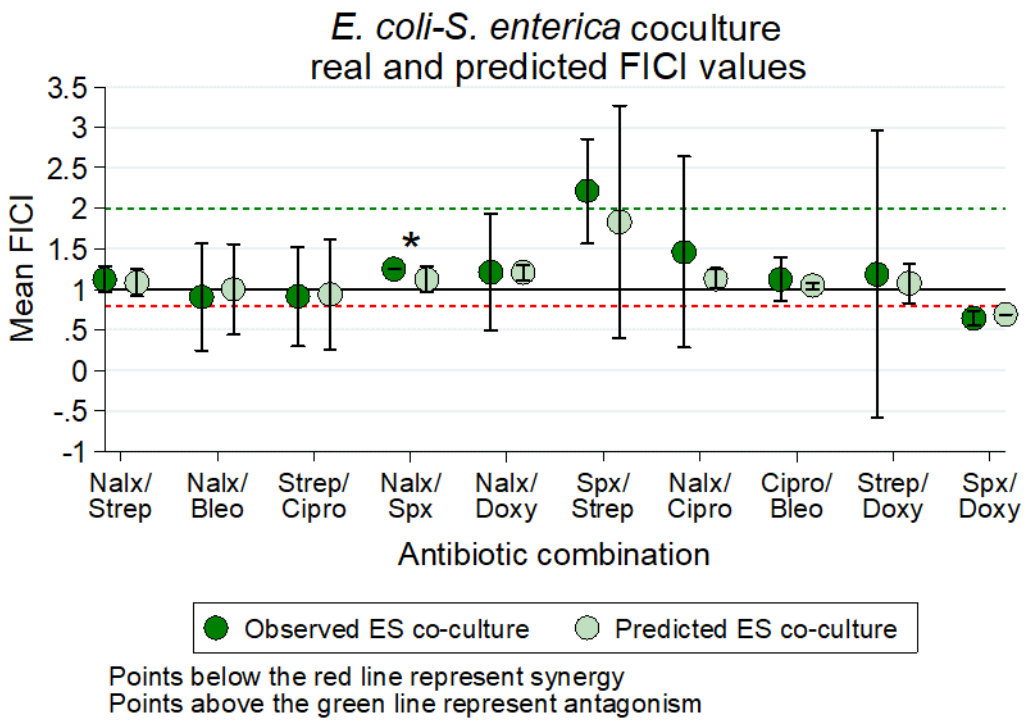

Figure 4.5 Fractional inhibitory concentration index (FICI) plots of predicted and actual co-cultures across ten antibiotic combinations. Each point represents the mean +/-SE of three replicate FICI values from three biological replicates. FICIs on each plate represent the median FICI value from the plate. Asterisks represent $P < 0.05$ for predicted versus observed ES co-culture FICs were compared with a Mann-Whitney U test. *P*-values can be found in **Supplementary table S4.6**. Antibiotic abbreviations: Nalx= nalidixic acid; strep= streptomycin; bleo= bleomycin; cipro= ciprofloxacin; spx= spectinomycin; doxy= doxycycline.

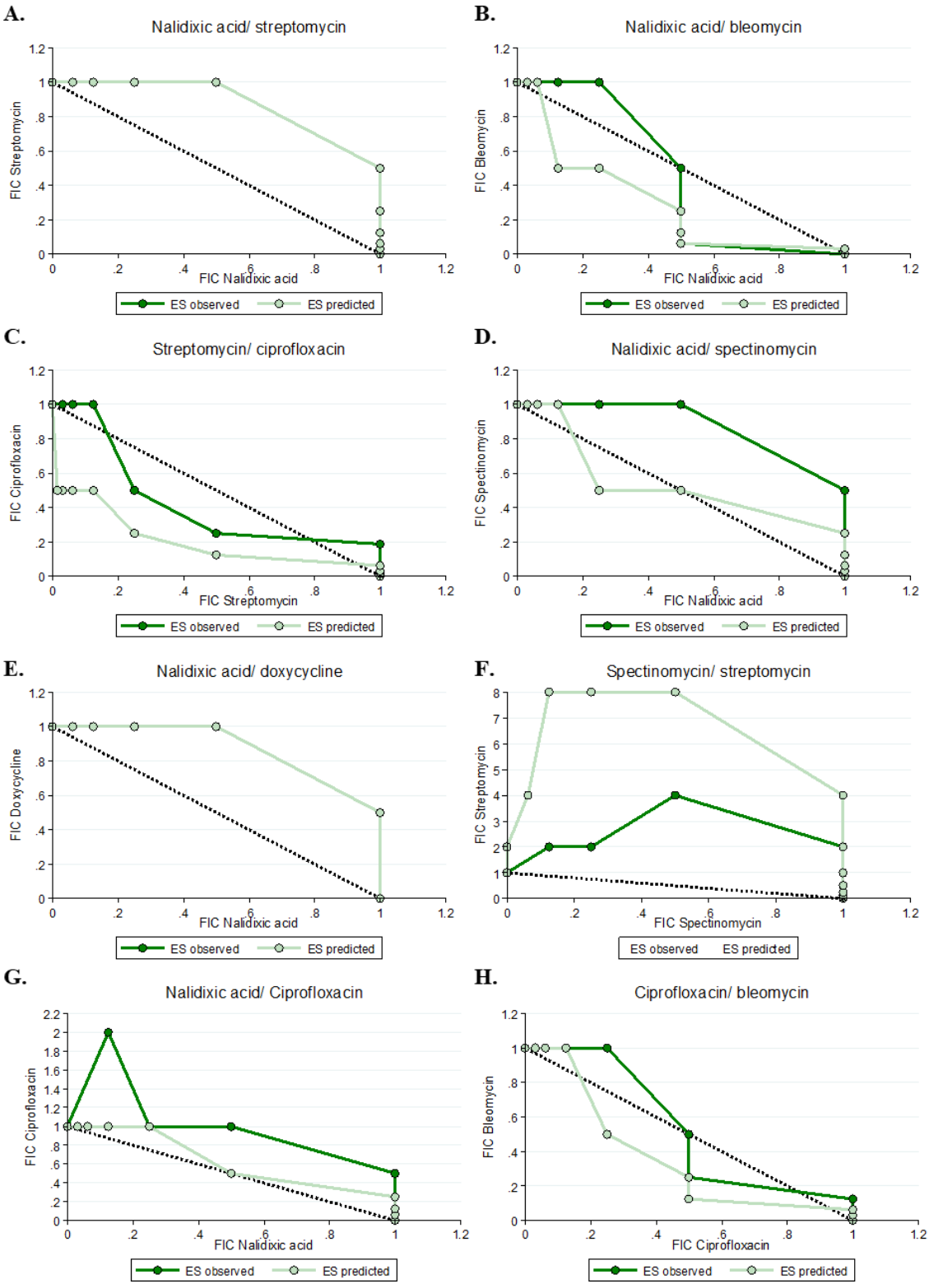
A.
Nalidixic acid/ streptomycin
FIC Streptomycin
FIC Nalidixic acid
ES observed
ES predicted
B.
Nalidixic acid/ bleomycin
FIC Bleomycin
FIC Nalidixic acid
ES observed
ES predicted
C.
Streptomycin/ ciprofloxacin
FIC Ciprofloxacin
FIC Streptomycin
ES observed
ES predicted
D.
Nalidixic acid/ spectinomycin
FIC Spectinomycin
FIC Nalidixic acid
ES observed
ES predicted
E.
Nalidixic acid/ doxycycline
FIC Doxycycline
FIC Nalidixic acid
ES observed
ES predicted
F.
Spectinomycin/ streptomycin
FIC Streptomycin
FIC Spectinomycin
ES observed
ES predicted
G.
Nalidixic acid/ Ciprofloxacin
FIC Ciprofloxacin
FIC Nalidixic acid
ES observed
ES predicted
H.
Ciprofloxacin/ bleomycin
FIC Bleomycin
FIC Ciprofloxacin
ES observed
ES predicted

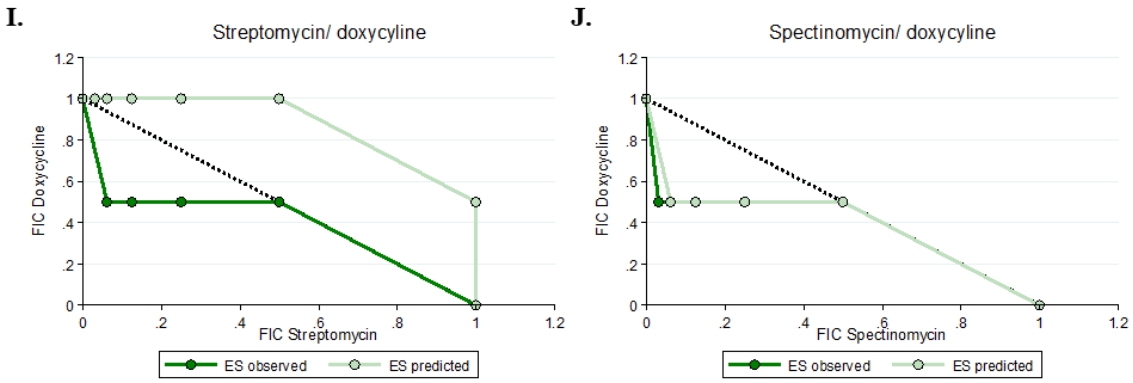

Figure 4.6 Representative isobolograms of predicted and observed co-culture fractional inhibitory concentrations (FICs) across ten antibiotic combinations. Predicted FICs were determined based on monoculture FICs and hypothesized weakest link dynamics (i.e. co-culture growth could only occur at concentrations of both antibiotics where both species could grow alone). Observed co-culture FICs were calculated based on 48 hours of 30°C growth, and growth was identified as any well which had an OD600 at least 10% of the highest OD600 well on each plate.

Supplementary table S4.1 Mechanism of action of antibiotics used in this study.

Antibiotic	Mechanism
Bleomycin	Induces DNA breaks; may inhibit thymidine incorporation into DNA
Ciprofloxacin	Fluoroquinolone: binds DNA gyrase and topoisomerase IV
Nalidixic acid	Naphthyridone: binds DNA gyrase and topoisomerase IV
Doxycycline	Binds 30s ribosomal subunit to prevent protein biosynthesis
Spectinomycin	Binds 30s ribosomal subunit to prevent protein biosynthesis
Streptomycin	Binds 30s ribosomal subunit to prevent protein biosynthesis

Supplementary table S4.2 Median FICIs for *E. coli* and *S. enterica* in monoculture across ten antibiotic combinations and three replicates. FICIs for each replicate are the median FICI value per plate. FICI values below 0.8 are considered synergy; FICIs between 0.8 and 1 are additive interactions, FICIs between 1 and 2 are independent interactions, and FICIs above 2 are antagonistic interactions.

Species	Antibiotic combination	Rep 1	Rep 2	Rep 3
E. coli	Nalidixic acid/ streptomycin	0.75	0.625	0.8828125
	Nalidixic acid/ bleomycin	0.6875	0.75	1.125
	Streptomycin/ ciprofloxacin	1.125	0.625	1.0625
	Nalidixic acid/ spectinomycin	1.0625	0.75	1.375
	Nalidixic acid/ doxycyline	1.25	1.1875	1.375
	Spectinomycin/ streptomycin	2.5	1.5	1.5
	Nalidixic acid/ ciprofloxacin	1.0625	1.0234375	1.0625
	Ciprofloxacin/ bleomycin	0.546875	0.5625	1.03125
	Streptomycin/ doxycyline	1	1.046875	1.1875
	Spectinomycin/ doxycycline	0.6875	0.6875	0.6875
S. enterica	Nalidixic acid/ streptomycin	1.1875	1.015625	1.0625
	Nalidixic acid/ bleomycin	1.1875	0.75	1.0625
	Streptomycin/ ciprofloxacin	1.125	0.75	1.03125
	Nalidixic acid/ spectinomycin	1.25	1.125	1.125
	Nalidixic acid/ doxycyline	1.03125	1.03125	1.1875

	Spectinomycin/ streptomycin	1.25	0.875	1.09375
	Nalidixic acid/ ciprofloxacin	1.1875	1.09375	1.03125
	Ciprofloxacin/ bleomycin	1.1875	1.03125	1.0625
	Streptomycin/ doxycyline	1.1875	1.09375	1.03125
	Spectinomycin/ doxycycline	0.75	0.75	0.75

Supplementary table S4.3 Minimum FICIs for *E. coli* and *S. enterica* in monoculture across ten antibiotic combinations and three replicates. FICIs for each replicate are the minimum FICI value per plate. FICI values below 0.8 are considered synergy; FICIs between 0.5 and 1 are additive interactions, FICIs between 1 and 2 are independent interactions, and FICIs above 2 are antagonistic interactions.

Species	Antibiotic combination	Rep 1	Rep 2	Rep 3
E. coli	Nalidixic acid/ streptomycin	0.5625	0.5	0.5625
	Nalidixic acid/ bleomycin	0.5625	0.5	1.015625
	Streptomycin/ ciprofloxacin	1	0.5	1
	Nalidixic acid/ spectinomycin	0.625	0.53125	1
	Nalidixic acid/ doxycyline	1.0625	1.03125	1.0625
	Spectinomycin/ streptomycin	1.0625	1.015625	1.015625
	Nalidixic acid/ ciprofloxacin	0.75	0.625	0.75
	Ciprofloxacin/ bleomycin	0.375	0.375	0.5
	Streptomycin/ doxycyline	0.625	1	1.03125
	Spectinomycin/ doxycycline	0.5625	0.5625	0.5625
S. enterica	Nalidixic acid/ streptomycin	1.0625	0.5625	1
	Nalidixic acid/ bleomycin	1.0625	0.5625	0.75
	Streptomycin/ ciprofloxacin	1	0.5625	0.625
	Nalidixic acid/ spectinomycin	1.0625	1	1
	Nalidixic acid/ doxycyline	0.75	0.75	1.03125

	Spectinomycin/ streptomycin	1	0.53125	1
	Nalidixic acid/ ciprofloxacin	1.0625	1	0.625
	Ciprofloxacin/ bleomycin	1.0625	0.625	0.75
	Streptomycin/ doxycyline	1.03125	1	0.75
	Spectinomycin/ doxycycline	0.625	0.625	0.625

A.

E. coli	0	6.25	12.5	25	50	100	200	400
0								
2								
4								
8								
16								
32								
64								
128								

B.

S. enterica	0	62.5	125	250	500	1000	2000	4000
0								
0.25								
0.5								
1								
2								
4								
8								
16								

C.

ES (predicted)	0	6.25	12.5	25	50	100	200	400
0								
0.25								
0.5								
1								
2								
4								
8								
16								

D.

ES (observed)	0	6.25	12.5	25	50	100	200	400
0								
0.25								
0.5								
1								
2								
4								
8								
16								

Supplementary figure S4.1 Example of developing predicted FICIs from replicate 1 of nalidixic acid/ spectinomycin combination. Growth patterns of *E. coli* (**A**) and *S. enterica* (**B**)monocultures were used to predict growth patterns for the co-culture (**C**). FICIs and isobolograms were developed from this predicted data as previously described, and these were compared to real data obtained from co-cultures (**D**).

Supplementary table S4.4 Minimum inhibitory concentrations (MICs) of each species in each antibiotic, predictions for co-cultures based on weakest link, and actual co-culture MICs. MICs were defined as the lowest concentration of antibiotic required to inhibit growth below 10% of the densest well (by OD600) within a plate. Medians and ranges are displayed. Predicted co-culture MICs are based on weakest link hypothesis (i.e. the co-culture will be limited by the least resistant monoculture).

Antibiotic	***E. coli* MIC**	***S. enterica* MIC**	**Predicted co-culture MIC**	**Observed co-culture MIC**
Bleomycin (µg/mL)	8 (2-8)	2 (1-2)	2 (1-2)	1 (0.5-2)
Ciprofloxacin (ng/mL)	16 (8-32)	16 (16-32)	16 (8-32)	16 (8-16)
Doxycycline (µg/mL)	0.25 (0.0625-0.25)	2.5 (2.5-5)	0.25 (0.0625-0.25)	0.25 (0.125-0.25)
Nalidixic acid (µg/mL)	32 (32-64)	8 (4-8)	8 (4-8)	2 (1-4)
Spectinomycin (µg/mL)	100 (100-200)	500 (500-1000)	100 (100-200)	100 (50-200)
Streptomycin (µg/mL)	1.5 (0.5-2)	160 (80-160)	1.5 (0.5-2)	0.5 (0.5-8)

Supplementary table S4.5 Observed fractional inhibitory concentration indices (FICIs) for each antibiotic combination in monoculture and co-culture, and predicted co-culture FICIs based on weakest link. FICIs are median values from three biological replicates each. Red cells represent synergistic interactions (median FICI<0.8); green cells represent antagonistic interactions (median FICI>2).

Antibiotic combination	*E. coli* FICI	*S. enterica* FICI	Predicted co-culture FICI	Observed co-culture FICI
Nalidixic acid/ streptomycin	0.75	1.06	1.13	1.13
Nalidixic acid/ bleomycin	0.75	1.06	1.06	0.88
Streptomycin/ ciprofloxacin	1.06	1.03	1.06	1.05
Nalidixic acid/ spectinomycin	1.06	1.13	1.13	1.25
Nalidixic acid/ doxycyline	1.25	1.03	1.19	1.38
Spectinomycin/ streptomycin	1.50	1.09	1.50	2.13
Nalidixic acid/ ciprofloxacin	1.06	1.09	1.13	1.25
Ciprofloxacin/ bleomycin	0.56	1.06	1.05	1.06
Streptomycin/ doxycyline	1.05	1.09	1.05	0.88
Spectinomycin/ doxycycline	0.69	0.75	0.69	0.63

Supplementary table S4.6 Mann-Whitney U statistical test results for predicted vs. observed FICI results.

Antibiotic combination	*P*-value for predicted vs. observed FICI
Nalidixic acid/ streptomycin	0.49
Nalidixic acid/ bleomycin	0.66
Streptomycin/ ciprofloxacin	0.50
Nalidixic acid/ spectinomycin	0.037
Nalidixic acid/ doxycyline	0.50
Spectinomycin/ streptomycin	0.37
Nalidixic acid/ ciprofloxacin	0.18
Ciprofloxacin/ bleomycin	0.10
Streptomycin/ doxycyline	0.51
Spectinomycin/ doxycycline	0.11

Chapter 5. Conclusions and future work

Cross-feeding and antibiotics: more questions raised than answered

Overall, my thesis focused on how obligate metabolic cross-feeding modulates the impact of antibiotics on bacterial communities. Using a model obligate cross-feeding bacterial community, I approached this question in three main ways. First, I examined the ecological impact of cross-feeding; that is, how do monocultures versus communities respond to antibiotics over a single growth phase? I found that community antibiotic tolerance (the ability to grow at a given antibiotic concentration) is generally set by the 'weakest link' species— the most antibiotic-sensitive species in monoculture. Highly resistant species have lowered tolerance in cross-feeding contexts due to their dependence on more sensitive cross-feeding partners. Second, I asked whether the rate and mechanism of resistance evolution could be impacted by cross-feeding. I found that cross-feeding communities evolved resistance more slowly than monocultures (both in wet-lab and modeling experiments) and that mechanisms of resistance may differ between the two. Excitingly, under ampicillin selection, I found that loss-of-function mutations in the penicillin-binding protein *ftsI* only evolved in co-culture due to its conditional lethality in monoculture at neutral pH. Third, I examined how antibiotic synergy/ antagonism might be impacted by cross-feeding interactions using checkerboard assays. I found that weakest link dynamics also generally explained antibiotic interactions in cross-feeding communities, and that this abrogated synergistic or antagonistic interactions unless one species was the weakest link in both antibiotics. This research adds to an already dense body of literature on antibiotic resistance ecology and evolution but makes critical contributions in the often-overlooked impact of cooperative interspecies interactions on antibiotic efficacy.

Despite the plethora of research on antibiotic resistance, and even antibiotic resistance in multispecies contexts, many aspects of this field remain understudied. Even in my own research, there are several outstanding questions that have arisen over the course of my studies which warrant further investigation. Many of these pertain to the evolved mechanisms of resistance which I began investigating in chapter 3, and to how the work in chapters 3 and 4 might be combined to investigate the evolution of broad-spectrum resistance in cross-feeding communities. I also discuss other avenues of research which seem important next steps based on my work, including the impacts of sublethal antibiotic concentrations, mutator strains, the role of competitive interactions on resistance evolution, and some specific antibiotics which should have particularly strong effects in cross-feeding communities. Finally, I discuss possible extensions of my findings into clinical settings and ecological studies on mutualism stability.

Defining resistance in microbial communities: MIC is insufficient

Perhaps the most useful concept that I have taken away from my thesis work is that metrics that purport to measure antibiotic resistance/ tolerance only do so within a narrow set of biological parameters. An MIC, for example, is not actually an objective measure of antibiotic resistance. Rather, it measures the ability of a specific bacterial strain of a specific population size at a specific growth phase to grow to an arbitrary density or within an arbitrary time point, in the presence of an antibiotic that may or may not be at the predicted concentration, depending on whether it degrades over time. The growth rate dependence proved particularly problematic in my experiments in chapter 2 and necessitated the development of a novel MIC metric to contend with the differences in growth rate between *E. coli*/ *S. enterica* and *M. extorquens*. The problems with MIC

are well-established even in monoculture studies (110, 271); this will only get worse as resistance studies begin to include more polymicrobial communities. The definition of resistance/ tolerance, as my research shows, is dependent on how one tests it. *P. aeruginosa* is highly ampicillin-resistant when grown alone in glucose, but highly ampicillin-sensitive when grown on mucin with its cross-feeding partners (chapter 2). Synergy testing is likely to be similarly affected by this issue, particularly synergy assays such as the checkerboard assay which rely on MICs. Our current methodologies for assessing resistance barely consider induced tolerance mechanisms like changes in growth rate or cellular permeability; they are certainly not designed to appropriately assess community resistance.

Ecological theory and experiments on community resistance and resilience may provide some useful alternative ways to describe the impact of abiotic selection pressures on microbial communities. Resistance is defined as the ability of a community to remain unchanged in the face of a disturbance (such as antibiotic administration), whereas resilience describes the ability of a community to return to its pre-disturbance state (52, 272). Both these descriptors are clinically relevant— antibiotics should both eliminate a pathogen (or pathogenic community) and prevent it from recurring. However, prioritizing antibiotic therapy which targets resistance rather than resilience can result in recurring infections which have low resistance but high resilience— for example, due to persister formation of a small percentage of the population. Resilience must therefore also be taken into account when assessing clinical resistance— possibly by redefining MIC as the concentration of antibiotic required to suppress growth of a population and prevent its recovery for at least 48 hours, as suggested by Meredith et al. (272). There

remains much work to be done on determining the appropriate way to define and measure antibiotic resistance, particularly in multispecies communities where interspecies interactions, fitness effects, and many other factors may influence the ability of the pathogen(s) to grow and cause disease.

My finding that *ftsI* mutations only arose in a co-culture study also raises some questions regarding the accurate identification of antibiotic resistance genes (ARGs) from environmental metagenome data. ARGs are typically defined based on monoculture studies and/ or sequence similarity to previously identified ARGs (273). If cross-feeding selects for unique ARGs not found in monoculture studies but ubiquitous in environmental communities where cross-feeding is common, it is likely that such resistance genes will be overlooked in these studies. It is also possible that mutations identified in metagenomic sequence data do confer antibiotic resistance, but only in the context of the whole microbial community; for example, if the ARG/ mutation had high costs in monoculture that were reduced by polyculture growth. If these mutations were investigated in laboratory monocultures, they would likely be missed— possibly because of their different costs/ benefits in monoculture vs. polyculture, as was the case with the *ftsI* mutations we evolved. Future studies investigating novel resistance mechanisms in ARGs might therefore benefit from studying resistance in the context of a microbial ecosystem to better understand how metabolic interactions drive the selection of different resistance mechanisms in natural microbial communities.

Extensions of the antibiotic resistance evolution experiments

One drawback to my experiments in chapter 3 is the lack of molecular biology experiments and data to back up any conclusions that a given mutation confers resistance. The ability to move mutations between the evolved resistant and ancestral strains would facilitate a plethora of future experiments, particularly related to fitness costs and benefits of resistance. I observed many mutations arising in only the resistant populations which, based on their function, seem to have little to do with resistance (the *mdoG* and *mdoH* mutations in monoculture–evolved rifampicin-resistant populations, for example). It would be informative to engineer these mutations into a clean genetic background and test the fitness and growth rate effects of *mdoG* mutants alone versus *mdoG/ rpoB* double mutants. I predict that *mdoG* mutations themselves do not confer high-level resistance, but that they synergize with *rpoB* mutations to decrease the cost of resistance. However, there is some evidence that *mdoG/ mdoH* mutations do contribute to resistance directly. Previous work in *E. coli* has shown that premature stop codon mutations in *mdoH* (*opgH*) led to increased resistance to rifampicin, increased mucoidy (though this was not related to the increased tolerance), and reduced cell size (199). In *Pseudomonas aeruginosa*, the *opgGH* operon is induced under low osmotic conditions and likely contributes to proper cell envelope organization, but does not play a role in resistance to tobramycin (274); however, other periplasmic glucans have been shown to directly interact with and inhibit tobramycin in *P. aeruginosa* biofilms (275, 276). In *Salmonella enterica* and *Shigella flexneri*, deletion of *opgGH* abolished osmoregulated periplasmic glucan (OPG) biosynthesis, increased the lag time of bacterial growth in low-osmolarity conditions, and decreased virulence (277, 278). It is therefore also

possible that *mdoH* and *mdoG* mutations are providing resistance, but we were unable to detect it due to a lack of statistical power and/ or the overwhelming effect of *rpoB* mutations. The generation of a mutant with wild-type *rpoB* and mutant *mdoG* would answer this question.

An additional utility of a mutation-moving system would be to track individual genotypes (such as isogenic strains with wild type vs. putative resistance mutations) using different fluorescent markers. This would allow me to perform competition experiments, both in co-culture and monocultures, to test some hypotheses about the differential fitness costs of resistance mutations in monoculture vs. co-culture (97). For example, I would be particularly interested in whether the different *ftsI* mutants from chapter 3 (the knockout Q142* or the +A frameshift) are more fit than the D534Y mutant. The latter is still able to grow in monoculture at pH 7, unlike the other two mutants which require pH 4.7 to grow in monoculture— this suggests that the D534Y mutant still produces at least some functional *ftsI* protein, and the other mutants do not. In one replicate population of the co-culture evolved under ampicillin, the D534Y mutation was at 75% frequency, while the Q142* mutation was at 9% (and the two did not co-occur in any of the isolates that I sequenced). However, by passage 20 (which was not reported due to contamination issues), the Q142* mutation had swept to fixation and the D534Y mutation had been lost. This suggests that a complete loss-of-function in *ftsI* either is required to provide higher-level resistance, or the loss-of-function mutation is more fit, or additional mutations were evolved between passage 10 and 20 that decreased the cost of the loss-of-function mutation. Having the ability to engineer these

mutants and a way to fluorescently track them individually would allow me to compete them in co-culture in the presence or absence of ampicillin to test these possibilities.

A persistent issue that I encountered when testing the fitness effects of different resistance-associated mutations in this study was the inability to test the fitness of these mutants in the environment in which they evolved. Ideally, to measure the fitness of an antibiotic-resistant mutant, I would measure its growth rate at the concentration of antibiotic at which it was obtained from the evolution experiment (97). However, the appropriate control in this experiment is unclear. An ancestral strain would be ideal, but the antibiotic concentrations at which I obtained my resistant isolates did not allow for any wild-type growth. Another option is using an ancestral strain carrying a resistance plasmid, but that itself likely has fitness costs that would be difficult to control for. Competition experiments between ancestral and evolved resistant isolates pose a similar problem, in addition to the issue of not being able to distinguish different genotypes without screening possibly hundreds of colonies. The best option in this case may be to compete different resistant genotypes and describe their relative fitness, rather than the fitness of the evolved resistant genotype versus that of the ancestor.

During the evolution experiment described in chapter 3, I froze down populations of cells at each passage for further analysis. Though I sequenced the most resistant and antibiotic–free lines at the final passage (10 for ampicillin, 20 for rifampicin), there remains several generations' worth of un-sequenced evolutionary history in populations from earlier passages. Numerous experiments could be done on these, including ones testing the evolution of sublethal resistance as described above. Another, related experiment would be to test the epistatic effects of resistance mutations; that is, what

order do resistance-associated mutations arise in these populations? In an evolution experiment to identify determinants of carbapenem resistance, Adler et al. (279) identified *ompR* or *envZ* as the first-step mutations conferring resistance. Presumed loss-of-function mutations in *ompR* conferred the highest levels of resistance, and *envZ* point mutations conferred lower levels of resistance. Second-step mutations to resistance in *ompR* mutant backgrounds tended to be in *ompF*, whereas mutations in *envZ* backgrounds tended to be in *ompC*. (279). I observed many of these mutations in the ampicillin-evolved populations— sequencing the most resistant population from each replicate at each passage, and perhaps testing isolate growth rates, would be one way to identify similar patterns. It would also be interesting to test whether epistatic patterns are similar in monocultures or co-cultures, as the costs of different mutations (and the associated fitness landscape) might change with the addition of a cross-feeding partner.

Evolution of resistance to multiple drugs: collateral sensitivity and resistance

An important next step in this research will be to combine the work done in chapters 3 and 4 and examine how co-cultures evolve resistance to multiple antibiotics at once. In theory, combination therapy offers a useful tool for limiting the evolution of resistance in bacteria. Combination therapy is based on the assumption that it is more challenging/ less likely that bacteria will evolve resistance to two antibiotics with two different mechanisms of action, thereby necessitating two resistance mutations, than to evolve resistance to a single antibiotic (93). Additionally, the decrease in antibiotic dosages required when antibiotics synergize has obvious advantages in decreasing the evolutionary pressure on bacteria to evolve high-level resistance (88). This approach has proven highly successful in treating HIV (235) and many cancers (236, 237), both of

which are known for rapid drug resistance evolution. However, some research suggests that antibiotics which synergize in the short term may actually facilitate the evolution of resistance, while antagonistic interactions suppress resistance evolution (88, 280, 281). Additionally, multidrug efflux pumps present a unique problem in employing this strategy in bacteria. Many efflux pumps are able to export a variety of structurally unrelated antibiotics and are easily transferred among diverse bacterial species on resistance plasmids (63, 282). Thus, a single mutation in a regulatory region, or acquisition of a plasmid containing a single efflux pump, might confer resistance to multiple drugs at once. The utility of combination therapy, and its potential for treating infections and limiting the evolution of resistance, therefore, remains unclear.

A growing body of research suggests that collateral sensitivity (wherein evolution of high-level resistance to one antibiotic leads to enhanced sensitivity to others) and negative hysteresis (an induced hypersensitivity to one antibiotic induced by pre-exposure to another without an associated genetic change) are common outcomes during multiple antibiotic treatment (104, 283, 284). An example of this is the evolution of hypersensitivity in *E. coli* by Lázár et al. They found that evolution of aminoglycoside resistance involved a decrease in proton motive force (PMF) across the cell membrane. This diminished the effectiveness of PMF-dependent efflux pumps, causing hypersensitivity to other antibiotics applied to aminoglycoside-resistant strains (285). Clinically, the use of antibiotic cycling protocols which involve sequential or alternating administration of different antibiotics have proven highly successful in treating resistant infections (106, 286), though whether cycling or mixing (administration of multiple antibiotics at once) is more successful at clearing infections remains unclear (287–289).

Some of this mixed success may have to do with the fact that antibiotic order, type, dosage, and cycling time strongly influences collateral sensitivity success (290–292); in one study in *P. aeruginosa*, short cycling times selected against resistance whereas longer treatments with each antibiotic selected for high-levels of resistance (293).

Given the already complex and unclear context-dependence of collateral resistance versus sensitivity arising, adding bacterial community context into the mix at first seems unreasonable. If combination therapy success is already challenging to predict in monocultures, how can adding an additional layer of complexity and unpredictability aid in elucidating collateral resistance/ sensitivity research? My results from chapter 4, however, suggest that recognizing and appreciating the community context and metabolic partners of a focal species can inform predictions about antibiotic synergy and antagonism. It is possible that part of the difficulty in determining a single successful multidrug treatment for a given pathogen, for example, is due at least in part to the different commensal species that it interacts with. Studying the evolution of collateral resistance/ sensitivity *in vitro* using not only single species, but species consortia, might produce more reliable predictions for which antibiotic combinations most successfully synergize and/ or limit resistance evolution *in vivo*. Choosing the correct level at which to study the form and function of bacteria in communities remains an open question (294, 295), but in this case the added complexity of a multispecies system may help clarify the variation in efficacy of combination therapy in the clinic. Synergistic interactions among bacterial species may, for example, modulate synergy of antibiotics and the ability of microbial communities to collectively tolerate or evolve antibiotic resistance (296).

Sublethal antibiotic resistance

The impacts of sublethal antibiotic exposure, while not explored in the research described above, is an essential part of understanding resistance evolution in cross-feeding communities. In natural environments such as soil, selection at sublethal levels of antibiotic may be a more realistic scenario as bacteria are exposed to antibiotic runoff from agricultural, industrial, and waste-water treatment runoff , as well as natural production from soil microbes such as *Streptomycetes* (297). More specific to my research, the existence of a weakest link species by extension assumes that there are other, more resistant species in the community. In the presence of antibiotic concentrations which permit community survival, these non-weakest link species must then be growing and surviving at sublethal antibiotic concentrations. In the resistance evolution experiments outlined in chapter 3, the species with the higher resistance in the cross-feeding system is effectively experiencing selection at sublethal antibiotic levels, which has been shown by several groups to confer high levels of resistance (110, 187). This is supported by data showing that individual species-level resistance evolved beyond that of the level of community tolerance in our evolved resistant co-cultures (**Figure 5.1**). Thus, I would hypothesize that the mutants which we observed at passage 20 are most likely mutations which have arisen at sublethal concentrations in prior passages and have moved to the 'most resistant' front well via passaging, rather than mutants which arose and remained at the 'front', as these are mutants which evolved at high antibiotic concentrations and are therefore likely to be less fit. Further studies examining the antibiotic concentration and time point at which these resistance mutations arose will shed light on this question.

Sublethal concentrations of antibiotics have been shown to select for resistance mutations with a lower fitness cost, as their more-fit, susceptible competitors are not killed at sublethal concentrations as they are at near-MIC concentrations (110). Sublethal concentrations of antibiotics also increase mutation rates via induction of the SOS response; not only does this increase the likelihood of a resistance mutation arising in the exposed population (via increased mutation rates and/ or mobilization of transmissible resistance elements), but it also increases the mutation pool available for compensatory mutations to arise (298). In the case of human pathogens, these compensatory mutations might specifically increase survival within the human host, allowing them to outcompete commensal human microbes and transmit more effectively between hosts (102). Sublethal concentrations of antibiotics can also themselves increase the rate/ frequency of resistance acquisition by HGT and mutation (recombination and mutagenesis) (60). This may be a mechanism of niche adaptation, particularly in soil environments; the increased mutation rates and increased expression of efflux pumps may allow bacterial communities to adapt more quickly to changing environments (102). Sublethal antibiotic concentrations can select for resistance mutations which confer similar levels of resistance to lethal antibiotic concentration selection, but also conferred greater levels of cross-resistance; lethal-selected mutations tended to be in antibiotic-specific pathways as well (299).

Evolution at sublethal concentrations has also been shown to change the resistance mechanisms evolved (300); this may also partially explain why co-culture–evolved ampicillin-resistant *S. enterica* evolved different resistance mechanisms than in monoculture. Additional studies on how cross-feeding systems respond to varying

antibiotic concentrations and intensities, such as those done by Lindsey et al. (67), will help answer this question. Given that resistance mutations evolved at sublethal concentrations tend to have a lower fitness cost than those evolved at high antibiotic concentrations, I would predict that the difference between rate of resistance evolution in monocultures and co-cultures would decrease in an environment where sublethal antibiotics were applied.

Mutator strains

An additional feature which I did not explore in chapter 3 was the appearance of mutator strains in our ampicillin-evolved *S. enterica*. Recurring antibiotic pressure is known to select for mutator strains because the increased mutation rates in these strains lead to an increased likelihood that a rare resistant mutant will arise (60). Because sublethal antibiotic concentrations favor resistance evolution via many small-step mutations, mutator strains (which have mutations in DNA repair genes and therefore have greatly increased mutation rates) are enriched for in these environments (297). Interestingly, a recent study showed that mutator strains have a similar rate of resistance acquisition to their non-mutator counterparts; the mutator strain had higher overall numbers of mutations, but the non-mutators showed a stronger bias towards coding (and therefore likely adaptive) mutations (229). These strains are clinically problematic; mutator strains of *Pseudomonas aeruginosa* identified in cystic fibrosis patient lungs were associated with a threefold increase in the rate of antibiotic resistance acquisition and the deterioration of patient lung function (301). Mutator strains also show a lower cost of resistance for some antibiotics (302), likely because compensatory mutations arise quickly after or concurrently with costly resistance mutations. Another study found that

E. coli mutator strains evolved similar mechanisms of resistance as non-mutators, but they did so more quickly and to a higher level with little fitness cost (303); similar results were found in *P. aeruginosa* (304). While mutator phenotypes may prove useful during short-term pulses of environmental stress (such as a course of antibiotics), they are not a viable long-term evolutionary strategy as high mutation rates necessarily lead to high rates of death and accumulation of deleterious mutations (305).

The impact of mutator strains on interspecies interactions remains understudied. One group found that *mutS*– deficient *P. aeruginosa* outcompeted wild-type strains in biofilm formation but not planktonic growth. This success was driven largely by enhanced phenotypic diversification of the mutator strain in biofilms, which the authors suggest led to greater niche expansion and a more specialized set of biofilm functions (306). This result could also apply in multispecies systems, particularly in colonization scenarios. Mutator genotypes may give some species a competitive edge as they attempt to colonize a new environment with a new carbon source, for example. They might also be able to more effectively evolve resistance to antimicrobials produced by competitor species. An analysis of wild-type versus mutator strain growth rates on rich versus minimal media showed that mutators incur a much greater growth deficit on minimal media than wild-type strains (307). This suggests that one of the consequences of the mutator phenotype is a dependence on a rich nutrient environment to compensate for the deleterious effects of an increased mutation rate. Based on this result, I would predict that mutator strains would fare poorly in cooperative communities, where nutrient access is limited to that which a metabolic partner can provide. A spatially structured environment such as a biofilm might ameliorate some of these effects, however— the

concentration of nutrient exchange in these environments might allow mutator strains to survive. However, the greater evolvability of mutator strains also increases the likelihood that cheaters will arise, as was observed in a study of cooperative siderophore production in *P. aeruginosa* (308). Similarly, cheaters evolved more frequently in a mutator population of *P. aeruginosa* infecting a caterpillar, as did increased virulence and growth rate (309). Again, this suggests that mutator strains should fare poorly in metabolically cooperative communities. I suspect that they arose in our evolution experiments as a response to antibiotic pressure, and that if I were to continue evolving the mutator-containing co-cultures in the absence of antibiotic, they would quickly collapse or lose the mutator genotype.

Competition as a driver of resistance ecology and evolution

Some research has been conducted on how inter– and intraspecies interactions, particularly competitive interactions, impact microbial populations. Resource competition decreases the frequency of resistant genotypes within a population in the absence of antibiotic pressure, particularly when resistant genotypes have a fitness cost (133, 188). Additionally, competitors can slow the evolution of resistance within a population simply by reducing population size (133, 188, 310), though competition between co-evolving *Staphylococcus aureus* strains was shown to facilitate the evolution of clinically relevant vancomycin resistance (136). In contrast, competitors that produce antibiotics can increase selection for resistance within a population (20). Nutrient availability and antibiotic concentration can also modulate competitive fitness and species frequencies, as recently demonstrated in a competitive two-species community of fluconazole-resistant *Candida glabrata* and fluconazole-sensitive *Candida albicans*.

C. glabrata was outcompeted in the absence of fluconazole as expected; however, when glucose concentrations were increased, *C. glabrata* dominated the community even in the absence of antifungals (134). The presence of the blue-green alga *Scenedesmus obliquus* was also shown to increase the susceptibility of the primary producer cyanobacterium *Microcystis aeruginosa* to the antibiotic enrofloxacin (311). Changes in carbon source have also been shown to modulate the mechanism and level of resistance evolution (212). This suggests that nutrient exchange and availability may modulate resistance in microbial communities, and that looking at cooperative species interactions may be particularly relevant for resistance studies.

While competitive/ independent microbial communities were addressed somewhat in chapter 2, most of my work has solely focused on obligate cross-feeding interactions. However, in natural microbial communities, and even in our model community, competitive interactions are occurring alongside, and likely more frequently, than cooperative ones (26, 268, 312, 313). Recent work from our lab has illustrated how scaling between cooperative and competitive interactions between our species can change ecological dynamics and even community survival (192). A common mechanism of interference competition that arises in bacteria is antibiotic production (26, 314, 315); what happens when this arises in the context of cross-feeding? An informative experiment could be done wherein two species, cross-feeding for some nutrients (for example, amino acids) and competing for another (for example, carbon) are mixed together. One species produces an antibiotic; the other is susceptible. The stability of this co-culture (in terms of maintaining species ratios) would be contingent on a number of factors, including but not limited to: the fitness costs and ease of resistance acquisition in

the sensitive species; the relative growth rates of each species and their uptake rates for the carbon source (192); and the fitness costs and benefits of antibiotic production (314). A model such as that described in Kosakowski et al. (316), which involved an antibiotic producer, a cheater, and a sensitive strain, might be easily modified to test this possibility. A cross-feeding interaction between the producer/ cheater species and the sensitive species could be engineered, for example, and the ratio of producer to cheater examined over time. Given the complex and environmentally dependent nature of microbial interactions, it is easy to see this scenario arising in, for example, a soil bacterial community where *Streptomyces* species produce a wide array of antibiotics (317, 318) but also frequently exchange metabolites with surrounding species (319, 320). Understanding how these different selection pressures interact, therefore, might have important implications for the discovery of new antibiotics and their effects on microbial communities.

In addition to the monoculture and obligate cooperative co-culture lines in chapter 3, I also evolved a competitive community of *E. coli* and *S. enterica* grown in glucose and methionine. In this experiment, *E. coli* and *S. enterica* competed for both nitrogen and carbon, although nitrogen is not limiting in our growth medium. I performed the evolution experiments but have not yet performed any analyses of these populations; identifying the relative rates of resistance evolution in competitive versus monoculture communities will investigate whether competition increases or decreases rate and level of resistance acquisition. Additionally, sequencing of the resistance mutations in these populations will prove informative for identifying whether different resistance mutations arise as a result of carbon competition in our system.

Antibiotics with disproportionate impacts on cross-feeding communities

The concept of shared/ public-goods resistance, which arose in spatially structured communities in chapter 2, offers some interesting evolutionary dynamics questions in cross-feeding systems. While it is well-established that shared resistance can protect sensitive species in various contexts (120–122, 146, 321–323), the additional influence of metabolic interactions has yet to be explored. In the scenarios cited above, antibiotic degradation can be thought of as a public good, where the producer (the β-lactamase–producing species, say) provides a benefit to other species. This is a cheater scenario, as the producer carries a production cost while likely competing with non-producers for resources. Even if degradation selectively benefits the producer over the non-producer species, as is likely the case where the β-lactamase or other degradation enzymes are confined to the periplasm, the benefits of antibiotic degradation is not limited to the producer species (324). However, β-lactamase production is known to have a high fitness cost, possibly due to its impacts on peptitoglycan metabolism (325–327). What impact might this have on a cross-feeding community, where the non-producer species receive a protective benefit in terms of the β-lactamase, but may be harmed if β-lactamase production disrupts metabolite exchange from the producer species? Alternatively, how might the presence of an obligate cross-feeding partner impact the selection pressure on which resistance mechanisms arise over time? I predict that the metabolic costs of losing a cross-feeding partner would outweigh the fitness costs of producing high quantities of a public-goods resistance mechanism. An experimental evolution study in a cross-feeding community where at least one species has the genetic potential to degrade antibiotics (such as a co-culture of the Harcombe lab *E. coli* and

Methylobacterium extorquens, which I have shown can produce a β-lactamase) would shed light on this question.

In terms of testing the impact of antibiotic combinations in situations where antibiotic degradation occurs, a checkerboard assay may prove insufficient to detect degradation. Another method worth exploring is the E-test method, which involves laying filter paper strips containing gradients of antibiotics at right angles on bacteria growing on Petri plates (258, 328). Particularly in cases where resistant species may produce an antibiotic-degrading enzyme such as a β-lactamase, the least resistant species gains a protective effect from community growth in a spatially structured environment (124, 329). We observed that β-lactamase– based protection of *E.coli* and *S. enterica* by *M. extorquens* only occurred in spatially structured environments, not in liquid (120); others have observed this as well (55). This may also be the case in an E-test scenario, where spatial structure and publicly available resistance might shift the antibiotic interaction towards the resistance-producing species and away from the weakest link species. As many bacterial infections exist in a spatially structured environment (e.g. biofilms), this is an important avenue of research to pursue.

The phenotypic or genetic disruption of metabolism by antibiotics and antibiotic resistance mutations, respectively, is another unexplored area where metabolically interconnected community antibiotic responses might differ from those in monoculture. Sulfa drugs, such as trimethoprim, interfere with folate biosynthesis and resistance to these is often achieved through a metabolic workaround. Cells may acquire mutations in folate biosynthesis gene promoters that increases expression of folate biosynthesis machinery beyond saturation parameters for the drug, or alter their metabolic pathways

to allow for uptake and utilization of exogenous folate sources (61). Either of these changes could potentially change cross-feeding interactions, though whether the interactions are broken or strengthened is an open question. One species might gain an efflux pump resistance mutation to trimethoprim, for example, and might subsequently evolve folate excretion to preserve its sensitive partner. Or, the upregulation of folate biosynthesis machinery in one species might decrease the amount of cross-fed nutrient it is able to provide its partner, leading to a decrease in community productivity. These disruptions are difficult to predict in monoculture, let alone in multispecies cross-feeding systems. However, one study combined metabolic models of *C. difficile* with transcriptomic data from several environments, including exposure to sublethal antibiotics, to predict therapeutic targets that would disrupt *C. difficile* metabolism (330). A similar approach could be used for a defined cross-feeding community such as ours, where the transcriptome of each species could be measured in the presence of sublethal antibiotic concentrations and added to our established metabolic models as described in the above study. I could then use Computation of Microbial Ecosystems in Time and Space (COMETS), a multispecies metabolic modeling platform (159), to predict the metabolic impacts of antibiotics on an obligate co-culture.

Clinical relevance

One of the main challenges (and indeed, one of the main weaknesses of this work that has often been pointed out to me) is that its clinical relevance is unclear due to the model nature of our experimental system. My research assumes and depends on cross-feeding interactions between bacterial species being identified both in terms of their obligacy and their metabolic identity. The cystic fibrosis system described in chapter 2 represents

a rare case of a well-characterized clinically relevant cross-feeding interaction; other examples may be found in dental plaque and *Pseudomonas-Staphylococcus* interactions in skin infections (20), but these are rare. Far more common is a scenario where an infection may be associated with multiple species of bacteria, but the nature of their interaction is either unknown or more complex than metabolic cross-feeding (e.g. involves horizontal gene transfer, toxin production, quorum sensing and quenching, etc.). It is unclear how the weakest link hypothesis would generalize to such a system, where bacteria are likely to be both helping and harming each other. What is clear from my work is that antibiotic pressure has the potential (though not the guarantee) of impacting microbial communities indirectly, particularly when key species in microbial food webs are disrupted. Further research into the microbial ecology of infections might then be informed by my research as to which keystone species would be most effectively targeted to disrupt the community.

An additional layer of complexity in natural systems as opposed to our model community is that of the nutrient environment, which may affect both the obligacy and the stability of cross-feeding interactions. Previous work from our lab has shown that nutrient addition can break even obligate metabolic dependencies under certain conditions (192); therefore, nutrient disruption of the system could nullify weakest link responses to antibiotics. Fortunately, many infection contexts in particular are known to be nutrient-limited environments (331–334); however, in a site such as the human gut, nutrient influxes are likely to be constantly changing metabolic interactions between species (335, 336). This raises the possibility of using prebiotics in combination with antibiotics to treat gut-associated pathogens. Prebiotics have previously been suggested

as a means to selectively boost growth of beneficial bacteria (337, 338), and some studies have found this to be effective at ameliorating dysbioses in human-associated microbial communities such as the gut and the oral cavity (339–341). However, they might also be useful in boosting particular keystone species or altering the metabolic environment of the gut such that pathogens become dependent on cross-fed versus environmentally derived nutrients (as *Pseudomonas* is in the human CF lung), antibiotic-mediated targeting of the pathogen's cross-feeding partner may become much more effective. However, this approach again makes several assumptions that are unlikely to hold true. First, it assumes that the cross-feeding interactions involved in the infection are well-known, which is unlikely; second, it assumes that addition of a prebiotic will sufficiently alter the nutrient environment to affect a shift in cross-feeding interactions, which is unknown; third, it again relies on a narrow-spectrum antibiotic that will target only the pathogen's cross-feeder and not disrupt the rest of the community, which is also unlikely; and fourth, it assumes a single pathogen is solely responsible for causing the disease state, which is may or may not be accurate.

So what, then, can be derived from my research in terms of its application to the clinic? First, in the rare cases where cross-feeding interactions are known in an infection, the weakest link hypothesis at least provides an additional antibiotic target. If a pathogen is difficult to treat due to resistance or drug toxicity, targeting a cross-feeding partner may allow a lower dose or a less toxic antibiotic to be administered successfully. This may be particularly useful in cases where bacterial load is highly predictive of patient outcomes (342–344), or in cases where multiple antibiotics are administered, as shown in chapter 4. Second, it demonstrates the importance of cross-feeding interactions in clinically

relevant microbes and will hopefully motivate further research in the area. Third, it may serve as a useful null hypothesis during infection ecology research— if weakest link eco-evolutionary dynamics are not arising in these systems upon antibiotic application, other factors such as antibiotic breakdown (chapter 2), sublethal resistance evolution (chapter 3), or other factors such as partner-mediated tolerance induction (123, 124) might be useful, testable explanations.

An alternative clinical approach suggested by my research is the development of metabolite exchange inhibitors as antibiotic adjuvants. Indeed, this approach has been suggested as a way to treat *Pseudomonas aeruginosa* infections— blocking species specific central metabolism genes with small-molecule inhibitors might force the pathogen into a more antibiotic-sensitive metabolic state, or kill it outright (345). Metabolic inhibitors might also serve to disrupt the ability of a pathogen to obtain essential metabolites from neighboring species, without the slash-and-burn approach of antibiotics that is known to disrupt microbial community structure (346–351). Amino acid transporters might be a particularly useful target, as amino acids are commonly exchanged in natural microbial communities and amino acid auxotrophies are commonly found in metagenomic studies (44, 352, 353). Metabolic model building with whole-genome sequences from pathogens would allow identification of missing amino acid biosynthesis pathways in specific pathogens; inhibitors could then be designed that prevent uptake of that metabolite in the pathogen (if the import protein is known), or excretion of that metabolite in the neighboring community (again, if known).

While metabolite exchange inhibitors are an intriguing possibility, the substantial amount of research and time required to make them into viable clinical possibilities

suggests a related but more immediately available approach might prove more useful. While my research has not specifically tested or shown this, it is possible that the stability of our cross-feeding system in the face of antibiotic pressure is dependent on the maintenance of a metabolic state wherein the necessary metabolites can be supplied to each species. It stands to reason that, if an antibiotic were to sufficiently shift cellular metabolism away from production and export of these metabolites without killing the producer or receiver species, it is possible that sublethal antibiotic concentrations would be sufficient to disrupt a pathogenic microbial community. Sulfa drugs and other antibiotics known to disrupt microbial metabolism might be particularly useful in this regard, as described above. The advantage of this approach is that the precise nature of the metabolic interaction need not be known, only the direction— possibly making the implementation of this approach more clinically useful.

Despite the strong influence of environmental context on resistance mutation fitness costs, laboratory studies of fitness costs do appear to have clinical relevance as the selected resistance alleles in lab studies are also observed in clinical cases. However, it is less clear whether quantification of resistance, such as by MIC, can be extrapolated from the lab to the clinic (60). This may be for a number of reasons, such as host microenvironments, which are often acidic (pH~5.5), altering the tolerance of pathogenic bacteria to a variety of antibiotics (354), differences in nutrient availability in lab vs. host environments (355), and other *in vivo* pharmacokinetic considerations in drug solubility, metabolism, and excretion (356–358). The evolution of compensatory mutations which decrease the fitness costs of resistance mutations has proven particularly important for developing appropriate antibiotic treatment courses in the

clinic. If treatment regimens are too long, resistant mutants are able to reach large population sizes, which increases the likelihood of compensatory mutations arising which offset the costs of resistance. This is difficult to study in the lab, however, as different compensatory mutations are known to evolve in lab vs. clinical environments (60). A notable example of this is fluoroquinolone resistance in *E. coli* clinical isolates. The most common first resistance mutation is rare (small target size in *gyrA*) but has the largest MIC increase with the smallest fitness cost. The second resistance mutation differs *in vitro* vs. in clinical isolates; in the former, a mutation in an efflux pump (which is more common but more costly) is selected, whereas in the latter, a mutation in another topoisomerase (which is rarer but less costly) is selected (68). Whether the microbial community context has an impact in these cases remains to be seen but may be worth exploring as a way to better predict and screen for resistance mutations in clinical isolates.

Ecological implications

One interesting extension of our weakest link hypothesis is how it might inform the impact of climate change or other abiotic disturbances on symbioses in macroecological contexts. Predicting the effects of climate change on global ecological systems has proven challenging, often because the direct and indirect effects of climate change on mutualistic interactions and the species therein remain unclear (359). Microbes are frequently used as model systems in evolutionary biology because of their large population sizes, rapid generation time, and relative ease of manipulability. Our system, therefore, might be considered as a model for how symbioses respond to abiotic disturbances over ecological and evolutionary time, rather than a clinically informative

study on antibiotic resistance in pathogenic bacteria. Based on my results, I would predict that the mutualism members which are most sensitive to abiotic environmental fluctuations (such as changes in temperature, humidity, etc.) will define whether the mutualism survives a given abiotic disturbance. It would be interesting to examine mechanisms of cross-protection in macroscopic mutualisms that mirror antibiotic degradation in bacterial communities, for example. Mutualists which are able to protect their sensitive partners from environmental changes should be more stable than those without such collective resistance mechanisms.

Northfield and Ives (2002) modelled the effects of climate change/ environmental stresses on mutualistic, competitive, and predator-prey relationships. Their model was able to tune how a trait value of one species impacted the fitness of the other, either detrimentally (conflicting co-evolution) or non-detrimentally (non-conflicting co-evolution). They showed that, under conflicting co-evolution parameters, the impact of environmental change on species densities is decreased. This is because the fitness decrease in species B caused by the change in the species A trait leads species B to evolve to be less invested in the mutualism. In contrast, under nonconflicting co-evolution, the benefits that a change in the species A trait confers on species B leads species B to be more invested in the mutualism. This suggests that, in mutualisms where trait changes caused by climate change have a positive impact on the secondary species, the mutualism will become more susceptible to environmental change due to increased investment in the mutualism by species B (359). I could test this hypothesis by co-evolving our system under different antibiotic selection regimes which selectively target different mutualism members, for example— *M. extorquens* is highly resistant to β-

lactam antibiotics whereas the other two species are highly sensitive, and *S. enterica* is highly resistant to tetracycline. I could also use our system to study how increases in temperature (as a proxy to increasing global temperatures) might affect mutualisms. *M. extorquens* is unable to grow above 30^{O}C, but *E. coli* and *S. enterica* grow optimally at 37^{O}C. An evolution experiment examining the stability of the mutualism in response to rising growth temperatures should yield some interesting insights that could be extrapolated to macroscopic mutualisms wherein partners have discordant temperature sensitivities.

My weakest link hypothesis, in conjunction with the Harcombe lab model microbial system, might also be a useful tool in empirically testing the insurance hypothesis. This theory states that increases in species diversity in an ecosystem should 'insure' ecosystem function against environmental disturbances and prevent ecosystem collapse. This is because a greater number of species increases the likelihood that loss of one species due to the environmental disturbance will be compensated for by another (360–362). While this hypothesis has been tested (and upheld) in numerous microbial communities (52, 363–366), it has yet to be tested in a cooperative microbial community. Cooperation is expected to stabilise species ratios (53, 192), whereas competition is expected to stabilize biomass, as predicted in the insurance hypothesis. An important corollary of the insurance hypothesis is that community biomass is expected to be stabilized along an environmental stressor gradient; species ratios should fluctuate along this gradient as per their individual resistances to the stressor, but total biomass should remain constant provided the species have sufficiently different responses to the stressor (362, 367). An interesting experiment using our system,

therefore, might involve growing our community in obligate versus competitive co-culture along opposing antibiotic gradients. I would predict that the competitive co-culture would maintain total biomass but potentially lose species as the concentration of some antibiotic rose above its tolerance. However, in cooperative co-culture, weakest link dynamics should prevent much growth at all, since scaling across two antibiotic gradients may change the identity of the weakest link species but not the impact of the weakest link on community antibiotic tolerance. Finally, it would be interesting to scale between mutualistic, facilitative, and competitive interactions as described by Hammarlund et al. (192), to see how modulating interspecies interactions influences tolerance to opposing antibiotic gradients. A facilitative community, wherein cross-feeding occurs but is not required for survival, should be able to maintain species richness and biomass most effectively. This community is not constrained by weakest link dynamics but also contains positive interactions, which have been shown to aid in maintenance of biodiversity, particularly in harsh environments (368–370).

Final Thoughts

The challenges of predicting and mitigating the evolution of antibiotic resistance, as well as coping with already resistant bacteria, remains a formidable and imposing problem. The role of interspecies interactions in modulating resistance ecology and evolution, therefore, is increasingly pressing— particularly as the role of microbial communities in human health is growing as well. My research sheds light on how cooperative metabolic interactions might change how bacteria respond to antibiotics, both in the short term and over evolutionary time. Crucially, the existence of weakest link dynamics, wherein the most antibiotic-sensitive member of a microbial community may set the response of the

community to antibiotics, offers a novel target in developing more effective antibiotic treatment strategies. While this body of work represents a critical step forward in this field, there remains much work to be done if we are to avoid returning to a world where bacterial diseases are nearly impossible to treat.

Chapter 5 Figures

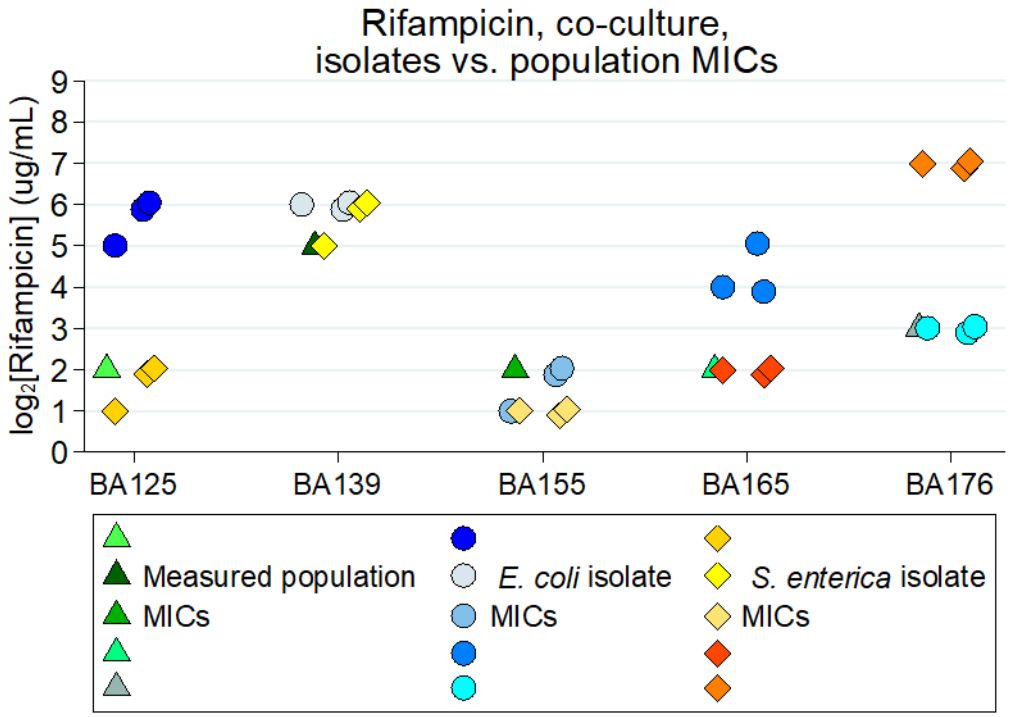

Figure 5.1 Log_2MICs of populations vs. isolates from each population evolved under rifampicin selection in *E. coli*– *S. enterica* obligate co-culture. Population MICs were re-measured from passage 20 isolates frozen and re-grown along a rifampicin gradient for 48 hours with shaking at 30^{O}C. Isolates of each species were also isolated from these populations and their individual MICs measured as above. Colors represent different populations, and shapes represent different culture types (triangle for populations, circle for *E. coli*, diamond for *S. enterica*.)

Bibliography

1. Schloss PD, Girard RA, Martin T, Edwards J, Thrash JC (2016) Status of the archaeal and bacterial census: an update. *mBio* 7(3). doi:10.1128/mBio.00201-16.

2. Locey KJ, Lennon JT (2016) Scaling laws predict global microbial diversity. *Proc Natl Acad Sci U S A* 113(21):5970–5975.

3. Singh NK, et al. (2018) Multi-drug resistant *Enterobacter bugandensis* species isolated from the International Space Station and comparative genomic analyses with human pathogenic strains. *BMC Microbiol* 18(1):175.

4. Varghese NJ, et al. (2015) Microbial species delineation using whole genome sequences. *Nucleic Acids Res* 43(14):6761–6771.

5. Doolittle WF, Papke RT (2006) Genomics and the bacterial species problem. *Genome Biol* 7(9):116.

6. Achtman M, Wagner M (2008) Microbial diversity and the genetic nature of microbial species. *Nat Rev Microbiol* 6(6):431–440.

7. Allen HK, et al. (2010) Call of the wild: antibiotic resistance genes in natural environments. *Nat Rev Microbiol* 8(4):251–259.

8. Surette MD, Wright GD (2017) Lessons from the environmental antibiotic resistome. *Annu Rev Microbiol* 71(1):309–329.

9. Perry J, Waglechner N, Wright G (2016) The prehistory of antibiotic resistance. *Cold Spring Harb Perspect Med* 6(6). doi:10.1101/cshperspect.a025197.

10. Koch R (1932) *The Aetiology of tuberculosis a translation from the German of the original paper announcing the discovery of the tubercle bacillus, read before the Physiological Society in Berlin, March 24, 1882, and published in the Berliner klinische Wochenschrift, 1882, xix, 221 /* (National Tuberculosis Association, New York :).

11. Murray JL, Connell JL, Stacy A, Turner KH, Whiteley M (2014) Mechanisms of synergy in polymicrobial infections. *J Microbiol Seoul Korea* 52(3):188–199.

12. Stacy A, McNally L, Darch SE, Brown SP, Whiteley M (2016) The biogeography of polymicrobial infection. *Nat Rev Microbiol* 14(2):93–105.

13. Gabrilska RA, Rumbaugh KP (2015) Biofilm models of polymicrobial infection. *Future Microbiol* 10(12):1997–2015.

14. Nelson A, De Soyza A, Perry JD, Sutcliffe IC, Cummings SP (2012) Polymicrobial challenges to Koch's postulates: Ecological lessons from the bacterial vaginosis and cystic fibrosis microbiomes. *Innate Immun* 18(5):774–783.

15. de Vos MGJ, Zagorski M, McNally A, Bollenbach T (2017) Interaction networks, ecological stability, and collective antibiotic tolerance in polymicrobial infections. *Proc Natl Acad Sci U S A* 114(40):10666–10671.

16. Caverly LJ, Zhao J, LiPuma JJ (2015) Cystic fibrosis lung microbiome: opportunities to reconsider management of airway infection. *Pediatr Pulmonol* 50 Suppl 40:S31-38.

17. Delhaes L, et al. (2012) The airway microbiota in cystic fibrosis: a complex fungal and bacterial community--implications for therapeutic management. *PloS One* 7(4):e36313.

18. Flynn JM, Niccum D, Dunitz JM, Hunter RC (2016) Evidence and role for bacterial mucin degradation in cystic fibrosis airway disease. *PLoS Pathog* 12(8):e1005846.

19. Ramsey MM, Rumbaugh KP, Whiteley M (2011) Metabolite cross-feeding enhances virulence in a model polymicrobial infection. *PLoS Pathog* 7(3):e1002012.

20. Stacy A, Fleming D, Lamont RJ, Rumbaugh KP, Whiteley M (2016) A commensal bacterium promotes virulence of an opportunistic pathogen via cross-respiration. *mBio* 7(3):e00782-16.

21. Tognon M, Köhler T, Luscher A, van Delden C (2019) Transcriptional profiling of *Pseudomonas aeruginosa* and *Staphylococcus aureus* during *in vitro* co-culture. *BMC Genomics* 20. doi:10.1186/s12864-018-5398-y.

22. Nguyen AT, Oglesby-Sherrouse AG (2016) Interactions between *Pseudomonas aeruginosa* and *Staphylococcus aureus* during co-cultivations and polymicrobial infections. *Appl Microbiol Biotechnol* 100(14):6141–6148.

23. Abisado RG, Benomar S, Klaus JR, Dandekar AA, Chandler JR (2018) Bacterial quorum sensing and microbial community interactions. *mBio* 9(3):e02331-17.

24. Hughes DT, Sperandio V (2008) Inter-kingdom signalling: communication between bacteria and their hosts. *Nat Rev Microbiol* 6(2):111–120.

25. Silva KPT, Chellamuthu P, Boedicker JQ (2017) Quantifying the strength of quorum sensing crosstalk within microbial communities. *PLOS Comput Biol* 13(10):e1005809.

26. Hibbing ME, Fuqua C, Parsek MR, Peterson SB (2010) Bacterial competition: surviving and thriving in the microbial jungle. *Nat Rev Microbiol* 8(1):15–25.

27. Xavier JB, Kim W, Foster KR (2011) A molecular mechanism that stabilizes cooperative secretions in *Pseudomonas aeruginosa*. *Mol Microbiol* 79(1):166–179.

28. Nesme J, Simonet P (2015) The soil resistome: a critical review on antibiotic resistance origins, ecology and dissemination potential in telluric bacteria. *Environ Microbiol* 17(4):913–930.

29. von Wintersdorff CJH, et al. (2016) Dissemination of antimicrobial resistance in microbial ecosystems through horizontal gene transfer. *Front Microbiol* 7:173.

30. Soucy SM, Huang J, Gogarten JP (2015) Horizontal gene transfer: building the web of life. *Nat Rev Genet* 16(8):472–482.

31. Khomyakova M, Bükmez Ö, Thomas LK, Erb TJ, Berg IA (2011) A methylaspartate cycle in Haloarchaea. *Science* 331(6015):334–337.

32. Caro-Quintero A, Konstantinidis KT (2015) Inter-phylum HGT has shaped the metabolism of many mesophilic and anaerobic bacteria. *ISME J* 9(4):958–967.

33. Genilloud O (2017) Actinomycetes: still a source of novel antibiotics. *Nat Prod Rep* 34(10):1203–1232.

34. Katz L, Baltz RH (2016) Natural product discovery: past, present, and future. *J Ind Microbiol Biotechnol* 43(2):155–176.

35. Challinor VL, Bode HB (2015) Bioactive natural products from novel microbial sources. *Ann N Y Acad Sci* 1354(1):82–97.

36. Khoruts A, Sadowsky MJ (2016) Understanding the mechanisms of faecal microbiota transplantation. *Nat Rev Gastroenterol Hepatol* 13(9):508–516.

37. Scott JE, et al. (2019) *Pseudomonas aeruginosa* can inhibit growth of streptococcal species via siderophore production. *J Bacteriol* 201(8):e00014-19.

38. Traxler MF, Seyedsayamdost MR, Clardy J, Kolter R (2012) Interspecies modulation of bacterial development through iron competition and siderophore piracy. *Mol Microbiol* 86(3):628–644.

39. Böttcher T, Clardy J (2014) A chimeric siderophore halts swarming *Vibrio*. *Angew Chem Int Ed Engl* 53(13):3510–3513.

40. D'Souza G, et al. (2014) Less is more: selective advantages can explain the prevalent loss of biosynthetic genes in bacteria. *Evolution* 68(9):2559–2570.

41. Zelezniak A, et al. (2015) Metabolic dependencies drive species co-occurrence in diverse microbial communities. *Proc Natl Acad Sci U S A* 112(20):6449–6454.

42. Schink B (2002) Synergistic interactions in the microbial world. *Antonie Van Leeuwenhoek* 81(1–4):257–261.

43. Seth EC, Taga ME (2014) Nutrient cross-feeding in the microbial world. *Front Microbiol* 5. doi:10.3389/fmicb.2014.00350.

44. D'Souza G, et al. (2018) Ecology and evolution of metabolic cross-feeding interactions in bacteria. *Nat Prod Rep* 35(5):455–488.

45. Hoek TA, et al. (2016) Resource availability modulates the cooperative and competitive nature of a microbial cross-feeding mutualism. *PLoS Biol* 14(8). doi:10.1371/journal.pbio.1002540.

46. Pacheco AR, Moel M, Segrè D (2019) Costless metabolic secretions as drivers of interspecies interactions in microbial ecosystems. *Nat Commun* 10. doi:10.1038/s41467-018-07946-9.

47. Germerodt S, et al. (2016) Pervasive selection for cooperative cross-feeding in bacterial communities. *PLoS Comput Biol* 12(6). doi:10.1371/journal.pcbi.1004986.

48. Mee MT, Collins JJ, Church GM, Wang HH (2014) Syntrophic exchange in synthetic microbial communities. *Proc Natl Acad Sci U S A* 111(20):E2149-2156.

49. Jiménez DJ, Korenblum E, van Elsas JD (2014) Novel multispecies microbial consortia involved in lignocellulose and 5-hydroxymethylfurfural bioconversion. *Appl Microbiol Biotechnol* 98(6):2789–2803.

50. Wongwilaiwalin S, et al. (2010) Analysis of a thermophilic lignocellulose degrading microbial consortium and multi-species lignocellulolytic enzyme system. *Enzyme Microb Technol* 47(6):283–290.

51. Wang Z-W, Chen S (2009) Potential of biofilm-based biofuel production. *Appl Microbiol Biotechnol* 83(1):1–18.

52. Shade A, et al. (2012) Fundamentals of microbial community resistance and resilience. *Front Microbiol* 3. doi:10.3389/fmicb.2012.00417.

53. Chubiz LM, Granger BR, Segrè D, Harcombe WR (2015) Species interactions differ in their genetic robustness. *Front Microbiol* 6:271.

54. Beams AB, Toth DJA, Khader K, Adler FR (2016) Harnessing intra-host strain competition to limit antibiotic resistance: mathematical model results. *Bull Math Biol* 78(9):1828–1846.

55. Estrela S, Brown SP (2018) Community interactions and spatial structure shape selection on antibiotic resistant lineages. *PLoS Comput Biol* 14(6). doi:10.1371/journal.pcbi.1006179.

56. Pena-Miller R, et al. (2013) When the most potent combination of antibiotics selects for the greatest bacterial load: The smile-frown transition. *PLoS Biol* 11(4). doi:10.1371/journal.pbio.1001540.

57. Rosenblatt-Farrell N (2009) The landscape of antibiotic resistance. *Environ Health Perspect* 117(6):A244–A250.

58. Lesho EP, Laguio-Vila M (2019) The slow-motion catastrophe of antimicrobial resistance and practical interventions for all prescribers. *Mayo Clin Proc*. doi:10.1016/j.mayocp.2018.11.005.

59. Brauner A, Fridman O, Gefen O, Balaban NQ (2016) Distinguishing between resistance, tolerance and persistence to antibiotic treatment. *Nat Rev Microbiol* 14(5):320–330.

60. Durão P, Balbontín R, Gordo I (2018) Evolutionary mechanisms shaping the maintenance of antibiotic resistance. *Trends Microbiol*. doi:10.1016/j.tim.2018.01.005.

61. Munita JM, Arias CA (2016) Mechanisms of antibiotic resistance. *Microbiol Spectr* 4(2). doi:10.1128/microbiolspec.VMBF-0016-2015.

62. Dwyer DJ, Kohanski MA, Collins JJ (2009) Role of reactive oxygen species in antibiotic action and resistance. *Curr Opin Microbiol* 12(5):482–489.

63. Li X-Z, Plésiat P, Nikaido H (2015) The challenge of efflux-mediated antibiotic resistance in Gram-negative bacteria. *Clin Microbiol Rev* 28(2):337–418.

64. Cox G, Wright GD (2013) Intrinsic antibiotic resistance: Mechanisms, origins, challenges and solutions. *Int J Med Microbiol* 303(6):287–292.

65. Ghai I, Ghai S (2018) Understanding antibiotic resistance via outer membrane permeability. *Infect Drug Resist* 11:523–530.

66. Hall CW, Mah T-F (2017) Molecular mechanisms of biofilm-based antibiotic resistance and tolerance in pathogenic bacteria. *FEMS Microbiol Rev* 41(3):276–301.

67. Lindsey HA, Gallie J, Taylor S, Kerr B (2013) Evolutionary rescue from extinction is contingent on a lower rate of environmental change. *Nature* 494(7438):463–467.

68. Huseby DL, et al. (2017) Mutation supply and relative fitness shape the genotypes of ciprofloxacin-resistant Escherichia coli. *Mol Biol Evol* 34(5):1029–1039.

69. Flensburg J, Sköld O (1987) Massive overproduction of dihydrofolate reductase in bacteria as a response to the use of trimethoprim. *Eur J Biochem* 162(3):473–476.

70. Yang W, et al. (2004) TetX is a flavin-dependent monooxygenase conferring resistance to retracycline antibiotics. *J Biol Chem* 279(50):52346–52352.

71. Zapun A, Contreras-Martel C, Vernet T (2008) Penicillin-binding proteins and β-lactam resistance. *FEMS Microbiol Rev* 32(2):361–385.

72. Hughes D, Andersson DI (2017) Evolutionary trajectories to antibiotic resistance. *Annu Rev Microbiol* 71(1):579–596.

73. Harms A, Maisonneuve E, Gerdes K (2016) Mechanisms of bacterial persistence during stress and antibiotic exposure. *Science* 354(6318):aaf4268.

74. Rossi NA, Dunlop MJ (2017) Customized regulation of diverse stress response genes by the multiple antibiotic resistance activator *marA*. *PLoS Comput Biol* 13(1). doi:10.1371/journal.pcbi.1005310.

75. Duval V, Lister IM (2013) MarA, SoxS and Rob of *Escherichia coli* – Global regulators of multidrug resistance, virulence and stress response. *Int J Biotechnol Wellness Ind* 2(3):101–124.

76. Zhang Y (2014) Persisters, persistent infections and the Yin–Yang model. *Emerg Microbes Infect* 3(1):e3.

77. Leimer N, et al. (2016) Nonstable *Staphylococcus aureus* small-colony variants are induced by low pH and sensitized to antimicrobial therapy by phagolysosomal alkalinization. *J Infect Dis* 213(2):305–313.

78. Long H, et al. (2016) Antibiotic treatment enhances the genome-wide mutation rate of target cells. *Proc Natl Acad Sci U S A* 113(18):E2498-2505.

79. Laehnemann D, et al. (2014) Genomics of rapid adaptation to antibiotics: convergent evolution and scalable sequence amplification. *Genome Biol Evol* 6(6):1287–1301.

80. Kohanski MA, DePristo MA, Collins JJ (2010) Sublethal antibiotic treatment leads to multidrug resistance via radical-induced mutagenesis. *Mol Cell* 37(3):311–320.

81. Corona F, Martinez JL (2013) Phenotypic resistance to antibiotics. *Antibiot Basel Switz* 2(2):237–255.

82. Vestergaard M, et al. (2017) Inhibition of the ATP synthase eliminates the intrinsic resistance of *Staphylococcus aureus* towards polymyxins. *mBio* 8(5). doi:10.1128/mBio.01114-17.

83. Xu T, Brown W, Marinus MG (2012) Bleomycin sensitivity in *Escherichia coli* is medium-dependent. *PLoS ONE* 7(3). doi:10.1371/journal.pone.0033256.

84. Howe MD, et al. (2018) Methionine antagonizes para-aminosalicylic acid activity via affecting folate precursor biosynthesis in *Mycobacterium tuberculosis*. *Front Cell Infect Microbiol* 8:399.

85. Ali L, et al. (2016) Nutrient-induced antibiotic resistance in *Enterococcus faecalis* in the eutrophic environment. *J Glob Antimicrob Resist* 7:78–83.

86. Katzir I, Cokol M, Aldridge BB, Alon U (2019) Prediction of ultra-high-order antibiotic combinations based on pairwise interactions. *PLoS Comput Biol* 15(1). doi:10.1371/journal.pcbi.1006774.

87. Tängdén T (2014) Combination antibiotic therapy for multidrug-resistant Gram-negative bacteria. *Ups J Med Sci* 119(2):149–153.

88. Singh N, Yeh PJ (2017) Suppressive drug combinations and their potential to combat antibiotic resistance. *J Antibiot (Tokyo)* 70(11):1033–1042.

89. Wright GD (2016) Antibiotic adjuvants: Rescuing antibiotics from resistance. *Trends Microbiol* 24(11):862–871.

90. González-Bello C (2017) Antibiotic adjuvants – A strategy to unlock bacterial resistance to antibiotics. *Bioorg Med Chem Lett* 27(18):4221–4228.

91. Vallejo JA, et al. (2016) LN-1-255, a penicillanic acid sulfone able to inhibit the class D carbapenemase OXA-48. *J Antimicrob Chemother* 71(8):2171–2180.

92. Foucquier J, Guedj M (2015) Analysis of drug combinations: current methodological landscape. *Pharmacol Res Perspect* 3(3). doi:10.1002/prp2.149.

93. Rodriguez de Evgrafov M, Gumpert H, Munck C, Thomsen TT, Sommer MOA (2015) Collateral resistance and sensitivity modulate evolution of high-level resistance to drug combination treatment in *Staphylococcus aureus*. *Mol Biol Evol* 32(5):1175–1185.

94. Zheng X, et al. (2015) Combinatorial effects of arginine and fluoride on oral bacteria. *J Dent Res* 94(2):344–353.

95. Dijk T van, Hwang S, Krug J, Visser JAGM de, Zwart MP (2017) Mutation supply and the repeatability of selection for antibiotic resistance. *Phys Biol* 14(5):055005.

96. Karslake J, Maltas J, Brumm P, Wood KB (2016) Population density modulates drug inhibition and gives rise to potential bistability of treatment outcomes for bacterial infections. *PLoS Comput Biol* 12(10). doi:10.1371/journal.pcbi.1005098.

97. Andersson DI, Levin BR (1999) The biological cost of antibiotic resistance. *Curr Opin Microbiol* 2(5):489–493.

98. Katz S, Hershberg R (2013) Elevated mutagenesis does not explain the increased frequency of antibiotic resistant mutants in starved aging colonies. *PLOS Genet* 9(11):e1003968.

99. Wistrand-Yuen E, et al. (2018) Evolution of high-level resistance during low-level antibiotic exposure. *Nat Commun* 9. doi:10.1038/s41467-018-04059-1.

100. Hughes D, Andersson DI (2017) Environmental and genetic modulation of the phenotypic expression of antibiotic resistance. *FEMS Microbiol Rev* 41(3):374–391.

101. Tay WH, Chong KKL, Kline KA (2016) Polymicrobial–host interactions during infection. *J Mol Biol* 428(17):3355–3371.

102. Bengtsson-Palme J, Kristiansson E, Larsson DGJ (2018) Environmental factors influencing the development and spread of antibiotic resistance. *FEMS Microbiol Rev* 42(1). doi:10.1093/femsre/fux053.

103. Angst DC, Hall AR (2013) The cost of antibiotic resistance depends on evolutionary history in *Escherichia coli*. *BMC Evol Biol* 13(1):163.

104. Pál C, Papp B, Lázár V (2015) Collateral sensitivity of antibiotic-resistant microbes. *Trends Microbiol* 23(7):401–407.

105. Nichol D, et al. (2019) Antibiotic collateral sensitivity is contingent on the repeatability of evolution. *Nat Commun* 10. doi:10.1038/s41467-018-08098-6.

106. Imamovic L, Sommer MOA (2013) Use of collateral sensitivity networks to design drug cycling protocols that avoid resistance development. *Sci Transl Med* 5(204):204ra132-204ra132.

107. Skwark MJ, et al. (2017) Interacting networks of resistance, virulence and core machinery genes identified by genome-wide epistasis analysis. *PLoS Genet* 13(2). doi:10.1371/journal.pgen.1006508.

108. Albarracín Orio AG, Piñas GE, Cortes PR, Cian MB, Echenique J (2011) Compensatory evolution of *pbp* mutations restores the fitness cost imposed by β-lactam resistance in *Streptococcus pneumoniae*. *PLoS Pathog* 7(2). doi:10.1371/journal.ppat.1002000.

109. Tomberg J, Unemo M, Davies C, Nicholas RA (2010) Molecular and structural analysis of mosaic variants of penicillin-binding protein 2 conferring decreased susceptibility to expanded-spectrum cephalosporins in *Neisseria gonorrhoeae*: role of epistatic mutations. *Biochemistry* 49(37):8062–8070.

110. Gullberg E, et al. (2011) Selection of resistant bacteria at very low antibiotic concentrations. *PLOS Pathog* 7(7):e1002158.

111. Jansen G, Barbosa C, Schulenburg H (2013) Experimental evolution as an efficient tool to dissect adaptive paths to antibiotic resistance. *Drug Resist Updat Rev Comment Antimicrob Anticancer Chemother* 16(6):96–107.

112. Westhoff S, et al. (2017) The evolution of no-cost resistance at sub-MIC concentrations of streptomycin in *Streptomyces coelicolor*. *ISME J* 11(5):1168–1178.

113. Greulich P, Waclaw B, Allen RJ (2012) Mutational pathway determines whether drug gradients accelerate evolution of drug-resistant cells. *Phys Rev Lett* 109(8):088101.

114. Keogh D, et al. (2016) Enterococcal metabolite cues facilitate interspecies niche modulation and polymicrobial infection. *Cell Host Microbe* 20(4):493–503.

115. Hardak E, et al. (2016) Polymicrobial pulmonary infection in patients with hematological malignancies: prevalence, co-pathogens, course and outcome. *Infection* 44(4):491–497.

116. Royo-Cebrecos C, et al. (2017) A fresh look at polymicrobial bloodstream infection in cancer patients. *PloS One* 12(10):e0185768.

117. Trifilio S, et al. (2015) Polymicrobial bacterial or fungal infections: incidence, spectrum of infection, risk factors, and clinical outcomes from a large hematopoietic stem cell transplant center. *Transpl Infect Dis Off J Transplant Soc* 17(2):267–274.

118. Penesyan A, Gillings M, Paulsen IT (2015) Antibiotic discovery: combatting bacterial resistance in cells and in biofilm communities. *Molecules* 20(4):5286–5298.

119. Elias S, Banin E (2012) Multi-species biofilms: living with friendly neighbors. *FEMS Microbiol Rev* 36(5):990–1004.

120. Adamowicz EM, Flynn J, Hunter RC, Harcombe WR (2018) Cross-feeding modulates antibiotic tolerance in bacterial communities. *ISME J* 12(11):2723–2735.

121. Stiefel U, Tima MA, Nerandzic MM (2015) Metallo-β-lactamase-producing *Bacteroides* species can shield other members of the gut microbiota from antibiotics. *Antimicrob Agents Chemother* 59(1):650–653.

122. Sorg RA, et al. (2016) Collective resistance in microbial communities by intracellular antibiotic deactivation. *PLOS Biol* 14(12):e2000631.

123. Vega NM, Allison KR, Samuels AN, Klempner MS, Collins JJ (2013) *Salmonella typhimurium* intercepts *Escherichia coli* signaling to enhance antibiotic tolerance. *Proc Natl Acad Sci* 110(35):14420–14425.

124. Perlin MH, et al. (2009) Protection of *Salmonella* by ampicillin-resistant *Escherichia coli* in the presence of otherwise lethal drug concentrations. *Proc R Soc Lond B Biol Sci* 276(1674):3759–3768.

125. Molina-Santiago C, Daddaoua A, Fillet S, Duque E, Ramos J-L (2014) Interspecies signalling: *Pseudomonas putida* efflux pump TtgGHI is activated by indole to increase antibiotic resistance. *Environ Microbiol* 16(5):1267–1281.

126. Christensen BB, Haagensen JAJ, Heydorn A, Molin S (2002) Metabolic commensalism and competition in a two-species microbial consortium. *Appl Environ Microbiol* 68(5):2495–2502.

127. El-Halfawy OM, Valvano MA (2012) Non-genetic mechanisms communicating antibiotic resistance: rethinking strategies for antimicrobial drug design. *Expert Opin Drug Discov* 7(10):923–933.

128. Kong EF, Tsui C, Kucharíková S, Van Dijck P, Jabra-Rizk MA (2017) Modulation of *Staphylococcus aureus* response to antimicrobials by the *Candida albicans* quorum sensing molecule farnesol. *Antimicrob Agents Chemother* 61(12). doi:10.1128/AAC.01573-17.

129. Evans KC, et al. (2018) Quorum-sensing control of antibiotic resistance stabilizes cooperation in *Chromobacterium violaceum*. *ISME J* 12(5):1263.

130. Perkins AE, Nicholson WL (2008) Uncovering new metabolic capabilities of Bacillus subtilis using phenotype profiling of rifampin-resistant *rpoB* mutants. *J Bacteriol* 190(3):807–814.

131. Händel N, Schuurmans JM, Brul S, ter Kuile BH (2013) Compensation of the metabolic costs of antibiotic resistance by physiological adaptation in *Escherichia coli*. *Antimicrob Agents Chemother* 57(8):3752–3762.

132. Derewacz DK, Goodwin CR, McNees CR, McLean JA, Bachmann BO (2013) Antimicrobial drug resistance affects broad changes in metabolomic phenotype in addition to secondary metabolism. *Proc Natl Acad Sci U S A* 110(6):2336–2341.

133. Colijn C, Cohen T (2015) How competition governs whether moderate or aggressive treatment minimizes antibiotic resistance. *eLife* 4. doi:10.7554/eLife.10559.

134. Beardmore RE, et al. (2018) Drug-mediated metabolic tipping between antibiotic resistant states in a mixed-species community. *Nat Ecol Evol*:1.

135. Stubbendieck RM, Straight PD (2015) Escape from lethal bacterial competition through coupled activation of antibiotic resistance and a mobilized subpopulation. *PLoS Genet* 11(12). doi:10.1371/journal.pgen.1005722.

136. Koch G, et al. (2014) Evolution of resistance to a last-resort antibiotic in *Staphyloccocus aureus* via bacterial competition. *Cell* 158(5):1060–1071.

137. Harcombe W (2010) Novel cooperation experimentally evolved between species. *Evolution* 64(7):2166–2172.

138. Douglas SM, Chubiz LM, Harcombe WR, Marx CJ (2017) Identification of the potentiating mutations and synergistic epistasis that enabled the evolution of inter-species cooperation. *PloS One* 12(5):e0174345.

139. Douglas SM, Chubiz LM, Harcombe WR, Ytreberg FM, Marx CJ (2016) Parallel mutations result in a wide range of cooperation and community consequences in a two-species bacterial consortium. *PloS One* 11(9):e0161837.

140. Harcombe WR, Betts A, Shapiro JW, Marx CJ (2016) Adding biotic complexity alters the metabolic benefits of mutualism. *Evol Int J Org Evol* 70(8):1871–1881.

141. World Health Organization (2014) Antimicrobial resistance: global report on surveillance. *Antimicrob Resist Glob Rep Surveill*. Available at: https://www.cabdirect.org/cabdirect/abstract/20143204323.

142. Friman V-P, Guzman LM, Reuman DC, Bell T (2015) Bacterial adaptation to sublethal antibiotic gradients can change the ecological properties of multitrophic microbial communities. *Proc Biol Sci* 282(1806). doi:10.1098/rspb.2014.2920.

143. Hughes D, Andersson DI (2012) Selection of resistance at lethal and non-lethal antibiotic concentrations. *Curr Opin Microbiol* 15(5):555–560.

144. Radlinski L, et al. (2017) *Pseudomonas aeruginosa* exoproducts determine antibiotic efficacy against *Staphylococcus aureus*. *PLOS Biol* 15(11):e2003981.

145. Yurtsev EA, Conwill A, Gore J (2016) Oscillatory dynamics in a bacterial cross-protection mutualism. *Proc Natl Acad Sci U S A* 113(22):6236–6241.

146. Medaney F, Dimitriu T, Ellis RJ, Raymond B (2016) Live to cheat another day: bacterial dormancy facilitates the social exploitation of β-lactamases. *ISME J* 10(3):778–787.

147. Lee KWK, et al. (2014) Biofilm development and enhanced stress resistance of a model, mixed-species community biofilm. *ISME J* 8(4):894–907.

148. Bernier SP, Létoffé S, Delepierre M, Ghigo J-M (2011) Biogenic ammonia modifies antibiotic resistance at a distance in physically separated bacteria. *Mol Microbiol* 81(3):705–716.

149. Hong H, Jung J, Park W (2014) Plasmid-encoded tetracycline efflux pump protein alters bacterial stress responses and ecological fitness of *Acinetobacter oleivorans*. *PloS One* 9(9):e107716.

150. Peng B, et al. (2015) Exogenous alanine and/or glucose plus kanamycin kills antibiotic-resistant bacteria. *Cell Metab* 21(2):249–261.

151. Straight PD, Kolter R (2009) Interspecies chemical communication in bacterial development. *Annu Rev Microbiol* 63(1):99–118.

152. Manor O, Levy R, Borenstein E (2014) Mapping the inner workings of the microbiome: genomic- and metagenomic-based study of metabolism and metabolic interactions in the human microbiome. *Cell Metab* 20(5):742–752.

153. Rosenzweig RF, Sharp RR, Treves DS, Adams J (1994) Microbial evolution in a simple unstructured environment: Genetic differentiation in *Escherichia coli*. *Genetics* 137(4):903–917.

154. Pande S, et al. (2014) Fitness and stability of obligate cross-feeding interactions that emerge upon gene loss in bacteria. *ISME J* 8(5):953–962.

155. Kaeberlein T, Lewis K, Epstein SS (2002) Isolating “uncultivable” microorganisms in pure culture in a simulated natural environment. *Science* 296(5570):1127–1129.

156. Oliveira NM, Niehus R, Foster KR (2014) Evolutionary limits to cooperation in microbial communities. *Proc Natl Acad Sci U S A* 111(50):17941–17946.

157. Koropatkin NM, Cameron EA, Martens EC (2012) How glycan metabolism shapes the human gut microbiota. *Nat Rev Microbiol* 10(5):323–335.

158. Milani C, et al. (2015) Bifidobacteria exhibit social behavior through carbohydrate resource sharing in the gut. *Sci Rep* 5:15782.

159. Harcombe WR, et al. (2014) Metabolic resource allocation in individual microbes determines ecosystem interactions and spatial dynamics. *Cell Rep* 7(4):1104–1115.

160. Nguyen F, et al. (2014) Tetracycline antibiotics and resistance mechanisms. *Biol Chem* 395(5):559–575.

161. Mukerji S, et al. (2017) Development and transmission of antimicrobial resistance among Gram-negative bacteria in animals and their public health impact. *Essays Biochem* 61(1):23–35.

162. Marx CJ (2008) Development of a broad-host-range *sacB*-based vector for unmarked allelic exchange. *BMC Res Notes* 1:1.

163. Rahme LG, et al. (1995) Common virulence factors for bacterial pathogenicity in plants and animals. *Science* 268(5219):1899–1902.

164. Schindelin J, et al. (2012) Fiji: an open-source platform for biological-image analysis. *Nat Meth* 9(7):676–682.

165. O'Callaghan CH, Morris A, Kirby SM, Shingler AH (1972) Novel method for detection of β-lactamases by using a chromogenic cephalosporin substrate. *Antimicrob Agents Chemother* 1(4):283–288.

166. Marsili E, Rollefson JB, Baron DB, Hozalski RM, Bond DR (2008) Microbial biofilm voltammetry: direct electrochemical characterization of catalytic electrode-attached biofilms. *Appl Environ Microbiol* 74(23):7329–7337.

167. Artemova T, Gerardin Y, Dudley C, Vega NM, Gore J (2015) Isolated cell behavior drives the evolution of antibiotic resistance. *Mol Syst Biol* 11(7):822.

168. Oka H, et al. (1989) Photodecomposition products of tetracycline in aqueous solution. *J Agric Food Chem* 37(1):226–231.

169. Langton Hewer SC, Smyth AR (2017) Antibiotic strategies for eradicating *Pseudomonas aeruginosa* in people with cystic fibrosis. *Cochrane Database Syst Rev* 4:CD004197.

170. Krogfelt KA, Utley M, Krivan HC, Laux DC, Cohen PS (2000) Specific phospholipids enhance the activity of β-lactam antibiotics against *Pseudomonas aeruginosa*. *J Antimicrob Chemother* 46(3):377–384.

171. Yılmaz Ç, Özcengiz G (2017) Antibiotics: pharmacokinetics, toxicity, resistance and multidrug efflux pumps. *Biochem Pharmacol* 133:43–62.

172. Chang JY, et al. (2008) Decreased diversity of the fecal microbiome in recurrent *Clostridium difficile*-associated diarrhea. *J Infect Dis* 197(3):435–438.

173. Mills JP, Rao K, Young VB (2018) Probiotics for prevention of *Clostridium difficile* infection. *Curr Opin Gastroenterol* 34(1):3–10.

174. Cox C, Watt AP, McKenna JP, Coyle PV (2016) *Mycoplasma hominis* and *Gardnerella vaginalis* display a significant synergistic relationship in bacterial vaginosis. *Eur J Clin Microbiol Infect Dis Off Publ Eur Soc Clin Microbiol* 35(3):481–487.

175. Brotons P, et al. (2016) Differences in *Bordetella pertussis* DNA load according to clinical and epidemiological characteristics of patients with whooping cough. *J Infect* 72(4):460–467.

176. Weber J, Tatoud R, Fidler S (2010) Postexposure prophylaxis, preexposure prophylaxis or universal test and treat: the strategic use of antiretroviral drugs to prevent HIV acquisition and transmission. *AIDS Lond Engl* 24 Suppl 4:S27-39.

177. Priest D, et al. (2017) *Neisseria gonorrhoeae* DNA bacterial load in men with symptomatic and asymptomatic gonococcal urethritis. *Sex Transm Infect*. doi:10.1136/sextrans-2016-052950.

178. Pan CQ, et al. (2016) Tenofovir to prevent Hepatitis B transmission in mothers with high viral load. *N Engl J Med* 374(24):2324–2334.

179. Silverstein RN, Cunning R, Baker AC (2015) Change in algal symbiont communities after bleaching, not prior heat exposure, increases heat tolerance of reef corals. *Glob Change Biol* 21(1):236–249.

180. Gehring C, et al. (2014) Plant genetics and interspecific competitive interactions determine ectomycorrhizal fungal community responses to climate change. *Mol Ecol* 23(6):1379–1391.

181. Kikuchi Y, et al. (2016) Collapse of insect gut symbiosis under simulated climate change. *mBio* 7(5). doi:10.1128/mBio.01578-16.

182. Hiltunen T, Virta M, Laine A-L (2017) Antibiotic resistance in the wild: an eco-evolutionary perspective. *Philos Trans R Soc B Biol Sci* 372(1712). doi:10.1098/rstb.2016.0039.

183. Crofts TS, Gasparrini AJ, Dantas G (2017) Next-generation approaches to understand and combat the antibiotic resistome. *Nat Rev Microbiol* 15(7):422–434.

184. Klümper U, et al. (2019) Selection for antibiotic resistance is reduced when embedded in a natural microbial community. *bioRxiv*:529651.

185. Dantas G, Sommer MOA (2012) Context matters - the complex interplay between resistome genotypes and resistance phenotypes. *Curr Opin Microbiol* 15(5):577–582.

186. Peterson E, Kaur P (2018) Antibiotic resistance mechanisms in bacteria: Relationships between resistance determinants of antibiotic producers, environmental bacteria, and clinical pathogens. *Front Microbiol* 9. doi:10.3389/fmicb.2018.02928.

187. Murray AK, et al. (2018) Novel insights into selection for antibiotic resistance in complex microbial communities. *mBio* 9(4). doi:10.1128/mBio.00969-18.

188. Gomes ALC, Galagan JE, Segrè D (2013) Resource competition may lead to effective treatment of antibiotic resistant infections. *PLoS ONE* 8(12). doi:10.1371/journal.pone.0080775.

189. Spicknall IH, Foxman B, Marrs CF, Eisenberg JNS (2013) A modeling framework for the evolution and spread of antibiotic resistance: Literature review and model categorization. *Am J Epidemiol* 178(4):508–520.

190. Özkaya Ö, Xavier KB, Dionisio F, Balbontín R (2017) Maintenance of microbial cooperation mediated by public goods in single- and multiple-trait scenarios. *J Bacteriol* 199(22). doi:10.1128/JB.00297-17.

191. Pande S, et al. (2016) Privatization of cooperative benefits stabilizes mutualistic cross-feeding interactions in spatially structured environments. *ISME J* 10(6):1413–1423.

192. Hammarlund SP, Chacón JM, Harcombe WR (2018) A shared limiting resource leads to competitive exclusion in a cross-feeding system. *Environ Microbiol*. doi:10.1111/1462-2920.14493.

193. Henson MA, Phalak P (2017) Byproduct cross feeding and community stability in an *in silico* biofilm model of the gut microbiome. *Processes* 5(1):13.

194. Baba T, et al. (2006) Construction of *Escherichia coli* K-12 in-frame, single-gene knockout mutants: the Keio collection. *Mol Syst Biol* 2(1):2006.0008.

195. Deatherage DE, Barrick JE (2014) Identification of mutations in laboratory-evolved microbes from next-generation sequencing data using breseq. *Methods Mol Biol Clifton NJ* 1151:165–188.

196. Fazzino L, Anisman J, Chacón JM, Heineman RH, Harcombe WR (2019) Lytic bacteriophage have diverse indirect effects in a synthetic cross-feeding community. *bioRxiv*:560037.

197. Lenski RE (2017) Experimental evolution and the dynamics of adaptation and genome evolution in microbial populations. *ISME J* 11(10):2181–2194.

198. Hill NS, Buske PJ, Shi Y, Levin PA (2013) A moonlighting enzyme links *Escherichia coli* cell size with central metabolism. *PLoS Genet* 9(7). doi:10.1371/journal.pgen.1003663.

199. Falchi FA, et al. (2017) Mutation and suppressor analysis of the essential lipopolysaccharide transport protein LptA reveals strategies to overcome severe outer membrane permeability defects in *Escherichia coli*. *J Bacteriol* 200(2). doi:10.1128/JB.00487-17.

200. Dersch P, Khan MA, Mühlen S, Görke B (2017) Roles of regulatory RNAs for antibiotic resistance in bacteria and their potential value as novel drug targets. *Front Microbiol* 8. doi:10.3389/fmicb.2017.00803.

201. Sun S, Selmer M, Andersson DI (2014) Resistance to β-lactam antibiotics conferred by point mutations in penicillin-binding proteins PBP3, PBP4 and PBP6 in *Salmonella enterica*. *PLoS ONE* 9(5). doi:10.1371/journal.pone.0097202.

202. Castanheira S, et al. (2017) A specialized peptidoglycan synthase promotes *Salmonella* cell division inside host cells. *mBio* 8(6):e01685-17.

203. Rodríguez-Verdugo A, Gaut BS, Tenaillon O (2013) Evolution of *Escherichia coli* rifampicin resistance in an antibiotic-free environment during thermal stress. *BMC Evol Biol* 13:50.

204. Alifano P, Palumbo C, Pasanisi D, Talà A (2015) Rifampicin-resistance, *rpoB* polymorphism and RNA polymerase genetic engineering. *J Biotechnol* 202:60–77.

205. Goldstein BP (2014) Resistance to rifampicin: a review. *J Antibiot (Tokyo)* 67(9):625–630.

206. Delcour AH (2009) Outer membrane permeability and antibiotic resistance. *Biochim Biophys Acta* 1794(5):808–816.

207. Pagès J-M, James CE, Winterhalter M (2008) The porin and the permeating antibiotic: a selective diffusion barrier in Gram-negative bacteria. *Nat Rev Microbiol* 6(12):893–903.

208. Jiang J-H, et al. (2019) Antibiotic resistance and host immune evasion in *Staphylococcus aureus* mediated by a metabolic adaptation. *Proc Natl Acad Sci*:201812066.

209. Nicolas-Chanoine M-H, Mayer N, Guyot K, Dumont E, Pagès J-M (2018) Interplay between membrane permeability and enzymatic barrier leads to antibiotic-dependent resistance in *Klebsiella pneumoniae*. *Front Microbiol* 9:1422.

210. Hall AR, Angst DC, Schiessl KT, Ackermann M (2015) Costs of antibiotic resistance – separating trait effects and selective effects. *Evol Appl* 8(3):261–272.

211. Trindade S, Sousa A, Gordo I (2012) Antibiotic resistance and stress in the light of Fisher's model. *Evolution* 66(12):3815–3824.

212. Zampieri M, et al. (2017) Metabolic constraints on the evolution of antibiotic resistance. *Mol Syst Biol* 13(3):917.

213. Torres N, Antolín MC, Goicoechea N (2018) Arbuscular mycorrhizal symbiosis as a promising resource for improving berry quality in grapevines under changing environments. *Front Plant Sci* 9. doi:10.3389/fpls.2018.00897.

214. Olliff-Yang RL, Mesler MR (2018) The potential for phenological mismatch between a perennial herb and its ground-nesting bee pollinator. *AoB Plants* 10(4). doi:10.1093/aobpla/ply040.

215. Campbell EA, et al. (2001) Structural mechanism for rifampicin inhibition of bacterial RNA polymerase. *Cell* 104(6):901–912.

216. Kerr CH, Culham DE, Marom D, Wood JM (2014) Salinity-dependent impacts of *proQ*, *prc*, and *spr* deficiencies on *Escherichia coli* cell structure. *J Bacteriol* 196(6):1286–1296.

217. Seoane A, Sabbaj A, McMurry LM, Levy SB (1992) Multiple antibiotic susceptibility associated with inactivation of the *prc* gene. *J Bacteriol* 174(23):7844–7847.

218. Hanoulle X, et al. (2004) Structural analysis of *Escherichia coli* OpgG, a protein required for the biosynthesis of osmoregulated periplasmic glucans. *J Mol Biol* 342(1):195–205.

219. Spoering AL, Vulić M, Lewis K (2006) GlpD and PlsB participate in persister cell formation in *Escherichia coli*. *J Bacteriol* 188(14):5136–5144.

220. Basturea GN, Zundel MA, Deutscher MP (2011) Degradation of ribosomal RNA during starvation: comparison to quality control during steady-state growth and a role for RNase PH. *RNA* 17(2):338–345.

221. Agrawal P, Varada R, Sah S, Bhattacharyya S, Varshney U (2018) Species-specific interactions of Arr with RplK mediate stringent response in bacteria. *J Bacteriol* 200(6). doi:10.1128/JB.00722-17.

222. Manasherob R, Miller C, Kim K, Cohen SN (2012) Ribonuclease E modulation of the bacterial SOS response. *PLOS ONE* 7(6):e38426.

223. Adler M, Anjum M, Andersson DI, Sandegren L (2016) Combinations of mutations in *envZ, ftsI, mrdA, acrB* and *acrR* can cause high-level carbapenem resistance in *Escherichia coli*. *J Antimicrob Chemother* 71(5):1188–1198.

224. Schmidt O, et al. (2007) *prlF* and *yhaV* encode a new toxin-antitoxin system in *Escherichia coli*. *J Mol Biol* 372(4):894–905.

225. Nikaido H (2003) Molecular basis of bacterial outer membrane permeability revisited. *Microbiol Mol Biol Rev* 67(4):593–656.

226. Abouzeed YM, Baucheron S, Cloeckaert A (2008) *ramR* mutations involved in efflux-mediated multidrug resistance in *Salmonella enterica* Serovar Typhimurium. *Antimicrob Agents Chemother* 52(7):2428–2434.

227. Ling J, et al. (2012) Protein aggregation caused by aminoglycoside action is prevented by a hydrogen peroxide scavenger. *Mol Cell* 48(5):713–722.

228. Parry BR, Shain DH (2011) Manipulations of AMP metabolic genes increase growth rate and cold tolerance in *Escherichia coli*: Implications for psychrophilic evolution. *Mol Biol Evol* 28(7):2139–2145.

229. Baym M, et al. (2016) Spatiotemporal microbial evolution on antibiotic landscapes. *Science* 353(6304):1147–1151.

230. Fujita J, et al. (2017) Structural flexibility of an inhibitor overcomes drug resistance mutations in *Staphylococcus aureus ftsZ*. *ACS Chem Biol* 12(7):1947–1955.

231. Furin J, Cox H, Pai M (2019) Tuberculosis. *The Lancet*. doi:10.1016/S0140-6736(19)30308-3.

232. Lee DS, Lee S-J, Choe H-S (2018) Community-acquired urinary tract infection by *Escherichia coli* in the era of antibiotic resistance. *BioMed Res Int* 2018. doi:10.1155/2018/7656752.

233. Vestergaard M, Frees D, Ingmer H (2019) Antibiotic resistance and the MRSA problem. *Microbiol Spectr* 7(2). doi:10.1128/microbiolspec.GPP3-0057-2018.

234. Arhel N, Kirchhoff F (2010) Host proteins involved in HIV infection: New therapeutic targets. *Biochim Biophys Acta BBA - Mol Basis Dis* 1802(3):313–321.

235. Simonetti FR, Kearney MF (2015) Review: influence of ART on HIV genetics. *Curr Opin HIV AIDS* 10(1):49–54.

236. Chatterjee N, Bivona TG (2019) Polytherapy and targeted cancer drug resistance. *Trends Cancer* 5(3):170–182.

237. Sánchez-Gundín J, Fernández-Carballido AM, Martínez-Valdivieso L, Barreda-Hernández D, Torres-Suárez AI (2018) New trends in the therapeutic approach to metastatic colorectal cancer. *Int J Med Sci* 15(7):659–665.

238. Yeh P, Tschumi AI, Kishony R (2006) Functional classification of drugs by properties of their pairwise interactions. *Nat Genet* 38(4):489–494.

239. Ocampo PS, et al. (2014) Antagonism between bacteriostatic and bactericidal antibiotics is prevalent. *Antimicrob Agents Chemother* 58(8):4573–4582.

240. Acar JF (2000) Antibiotic synergy and antagonism. *Med Clin North Am* 84(6):1391–1406.

241. Yadav R, et al. (2017) Aminoglycoside concentrations required for synergy with carbapenems against *Pseudomonas aeruginosa* determined via mechanistic studies and modeling. *Antimicrob Agents Chemother* 61(12). doi:10.1128/AAC.00722-17.

242. Hu Y, et al. (2015) Combinations of β-lactam or aminoglycoside antibiotics with plectasin are synergistic against methicillin-sensitive and methicillin-resistant *Staphylococcus aureus*. *PLoS ONE* 10(2). doi:10.1371/journal.pone.0117664.

243. Kohanski MA, Dwyer DJ, Collins JJ (2010) How antibiotics kill bacteria: from targets to networks. *Nat Rev Microbiol* 8(6):423–435.

244. Liu Y, Li R, Xiao X, Wang Z (2018) Molecules that inhibit bacterial resistance enzymes. *Molecules* 24(1). doi:10.3390/molecules24010043.

245. Wittekind M, Schuch R (2016) Cell wall hydrolases and antibiotics: exploiting synergy to create efficacious new antimicrobial treatments. *Curr Opin Microbiol* 33:18–24.

246. Minato Y, et al. (2018) Mutual potentiation drives synergy between trimethoprim and sulfamethoxazole. *Nat Commun* 9. doi:10.1038/s41467-018-03447-x.

247. Sanders CC, Sanders WE, Goering RV (1982) *In vitro* antagonism of beta-lactam antibiotics by cefoxitin. *Antimicrob Agents Chemother* 21(6):968–975.

248. Weisblum B, Demohn V (1969) Erythromycin-inducible resistance in *Staphylococcus aureus*: survey of antibiotic classes involved. *J Bacteriol* 98(2):447–452.

249. Bollenbach T, Quan S, Chait R, Kishony R (2009) Non-optimal microbial response to antibiotics underlies suppressive drug interactions. *Cell* 139(4):707–718.

250. Eliopoulos GM, Eliopoulos CT (1988) Antibiotic combinations: should they be tested? *Clin Microbiol Rev* 1(2):139–156.

251. Kumar A, Safdar N, Kethireddy S, Chateau D (2010) A survival benefit of combination antibiotic therapy for serious infections associated with sepsis and septic shock is contingent only on the risk of death: A meta-analytic/meta-regression study. *Crit Care Med* 38(8):1651.

252. Figa R, et al. (2017) Periprosthetic joint infection by *Propionibacterium acnes*: Clinical differences between monomicrobial versus polymicrobial infection. *Anaerobe* 44:143–149.

253. Shah PM, et al. (2016) Do polymicrobial intra-abdominal infections have worse outcomes than monomicrobial intra-abdominal infections? *Surg Infect* 17(1):27–31.

254. Leisner JJ, Jørgensen NOG, Middelboe M (2016) Predation and selection for antibiotic resistance in natural environments. *Evol Appl* 9(3):427–434.

255. Fratini F, et al. (2017) A novel interpretation of the Fractional Inhibitory Concentration Index: The case *Origanum vulgare* L. and *Leptospermum scoparium* J. R. et G. Forst essential oils against *Staphylococcus aureus* strains. *Microbiol Res* 195:11–17.

256. Stein C, et al. (2015) Three dimensional checkerboard synergy analysis of colistin, meropenem, tigecycline against multidrug-resistant clinical *Klebsiella pneumonia* isolates. *PLoS ONE* 10(6). doi:10.1371/journal.pone.0126479.

257. Chase P, et al. (2016) An automated miniaturized method to perform and analyze antimicrobial drug synergy assays. *Assay Drug Dev Technol* 14(1):58–66.

258. Singh V, Bala M, Bhargava A, Kakran M, Bhatnagar R (2018) *In vitro* efficacy of 21 dual antimicrobial combinations comprising novel and currently recommended combinations for treatment of drug resistant gonorrhoea in future era. *PLoS ONE* 13(3). doi:10.1371/journal.pone.0193678.

259. Andersson DI, Hughes D (2010) Antibiotic resistance and its cost: is it possible to reverse resistance? *Nat Rev Microbiol* 8(4):260–271.

260. Lee AJ, et al. (2018) Robust, linear correlations between growth rates and β-lactam-mediated lysis rates. *Proc Natl Acad Sci U S A* 115(16):4069–4074.

261. Groot J, Cepress-Mclean SC, Robbins-Pianka A, Knight R, Gill RT (2017) Multiplex growth rate phenotyping of synthetic mutants in selection to engineer glucose and xylose co-utilization in *Escherichia coli*. *Biotechnol Bioeng* 114(4):885–893.

262. Hancock REW (1981) Aminoglycoside uptake and mode of action—with special reference to streptomycin and gentamicin. I. Antagonists and mutants. *J Antimicrob Chemother* 8(4):249–276.

263. Menninger JR (1995) Mechanism of inhibition of protein synthesis by macrolide and lincosamide antibiotics. *J Basic Clin Physiol Pharmacol* 6(3–4):229–250.

264. Greulich P, Doležal J, Scott M, Evans MR, Allen RJ (2017) Predicting the dynamics of bacterial growth inhibition by ribosome-targeting antibiotics. *Phys Biol* 14(6):065005.

265. Li B, Qiu Y, Shi H, Yin H (2016) The importance of lag time extension in determining bacterial resistance to antibiotics. *Analyst* 141(10):3059–3067.

266. Zampieri M, Zimmermann M, Claassen M, Sauer U (2017) Nontargeted metabolomics reveals the multilevel response to antibiotic perturbations. *Cell Rep* 19(6):1214–1228.

267. Vincent IM, Ehmann DE, Mills SD, Perros M, Barrett MP (2016) Untargeted metabolomics to ascertain antibiotic modes of action. *Antimicrob Agents Chemother* 60(4):2281–2291.

268. Freilich S, et al. (2011) Competitive and cooperative metabolic interactions in bacterial communities. *Nat Commun* 2:589.

269. Sanchez-Gorostiaga A, Bajić D, Osborne ML, Poyatos JF, Sanchez A (2018) High-order interactions dominate the functional landscape of microbial consortia. *bioRxiv*:333534.

270. Sy SKB, Zhuang L, Derendorf H (2016) Pharmacokinetics and pharmacodynamics in antibiotic dose optimization. *Expert Opin Drug Metab Toxicol* 12(1):93–114.

271. Davison HC, Woolhouse MEJ, Low JC (2000) What is antibiotic resistance and how can we measure it? *Trends Microbiol* 8(12):554–559.

272. Meredith HR, et al. (2018) Applying ecological resistance and resilience to dissect bacterial antibiotic responses. *Sci Adv* 4(12). doi:10.1126/sciadv.aau1873.

273. Berendonk TU, et al. (2015) Tackling antibiotic resistance: the environmental framework. *Nat Rev Microbiol* 13(5):310–317.

274. Lequette Y, Rollet E, Delangle A, Greenberg EP, Bohin J-P (2007) Linear osmoregulated periplasmic glucans are encoded by the *opgGH* locus of *Pseudomonas aeruginosa*. *Microbiology* 153(10):3255–3263.

275. Mah T-F, et al. (2003) A genetic basis for *Pseudomonas aeruginosa* biofilm antibiotic resistance. *Nature* 426(6964):306–310.

276. Sadovskaya I, et al. (2010) High-level antibiotic resistance in *Pseudomonas aeruginosa* biofilm: the *ndvB* gene is involved in the production of highly glycerol-phosphorylated beta-(1->3)-glucans, which bind aminoglycosides. *Glycobiology* 20(7):895–904.

277. Liu L, et al. (2010) Osmoregulated periplasmic glucans synthesis gene family of *Shigella flexneri*. *Arch Microbiol* 192(3):167–174.

278. Bhagwat AA, et al. (2009) Osmoregulated periplasmic glucans of *Salmonella enterica* serovar Typhimurium are required for optimal virulence in mice. *Microbiology* 155(1):229–237.

279. Adler M, Anjum M, Andersson DI, Sandegren L (2013) Influence of acquired β-lactamases on the evolution of spontaneous carbapenem resistance in *Escherichia coli*. *J Antimicrob Chemother* 68(1):51–59.

280. Michel J-B, Yeh PJ, Chait R, Moellering RC, Kishony R (2008) Drug interactions modulate the potential for evolution of resistance. *Proc Natl Acad Sci U S A* 105(39):14918–14923.

281. Yeh PJ, Hegreness MJ, Aiden AP, Kishony R (2009) Drug interactions and the evolution of antibiotic resistance. *Nat Rev Microbiol* 7(6):460–466.

282. Andersen JL, et al. (2015) Multidrug efflux pumps from *Enterobacteriaceae*, *Vibrio cholerae* and *Staphylococcus aureus* bacterial food pathogens. *Int J Environ Res Public Health* 12(2):1487–1547.

283. Roemhild R, Schulenburg H (2019) Evolutionary ecology meets the antibiotic crisis: Can we control pathogen adaptation through sequential therapy? *Evol Med Public Health* 2019(1):37–45.

284. Suzuki S, Horinouchi T, Furusawa C (2017) Acceleration and suppression of resistance development by antibiotic combinations. *BMC Genomics* 18. doi:10.1186/s12864-017-3718-2.

285. Lázár V, et al. (2013) Bacterial evolution of antibiotic hypersensitivity. *Mol Syst Biol* 9:700.

286. Teranishi H, et al. (2017) Clinical efficacy of cycling empirical antibiotic therapy for febrile neutropenia in pediatric cancer patients. *J Infect Chemother Off J Jpn Soc Chemother* 23(7):463–467.

287. Beardmore RE, Peña-Miller R, Gori F, Iredell J (2017) Antibiotic cycling and antibiotic mixing: which one best mitigates antibiotic resistance? *Mol Biol Evol* 34(4):802–817.

288. van Duijn PJ, et al. (2018) The effects of antibiotic cycling and mixing on antibiotic resistance in intensive care units: a cluster-randomised crossover trial. *Lancet Infect Dis* 18(4):401–409.

289. Bal AM, Kumar A, Gould IM (2010) Antibiotic heterogeneity: from concept to practice. *Ann N Y Acad Sci* 1213(1):81–91.

290. Perron GG, Kryazhimskiy S, Rice DP, Buckling A (2012) Multidrug therapy and evolution of antibiotic resistance: When order matters. *Appl Environ Microbiol* 78(17):6137–6142.

291. Goulart CP, et al. (2013) Designing antibiotic cycling strategies by determining and understanding local adaptive landscapes. *PLoS ONE* 8(2). doi:10.1371/journal.pone.0056040.

292. Nichol D, et al. (2015) Steering evolution with sequential therapy to prevent the emergence of bacterial antibiotic resistance. *PLoS Comput Biol* 11(9):e1004493.

293. Roemhild R, et al. (2018) Cellular hysteresis as a principle to maximize the efficacy of antibiotic therapy. *Proc Natl Acad Sci U S A* 115(39):9767–9772.

294. Stubbendieck RM, Vargas-Bautista C, Straight PD (2016) Bacterial communities: Interactions to scale. *Front Microbiol* 7. doi:10.3389/fmicb.2016.01234.

295. Vega NM, Gore J (2018) Simple organizing principles in microbial communities. *Curr Opin Microbiol* 45:195–202.

296. Burmølle M, et al. (2006) Enhanced biofilm formation and increased resistance to antimicrobial agents and bacterial invasion are caused by synergistic interactions in multispecies biofilms. *Appl Environ Microbiol* 72(6):3916.

297. Andersson DI, Hughes D (2014) Microbiological effects of sublethal levels of antibiotics. *Nat Rev Microbiol* 12(7):465–478.

298. Strugeon E, Tilloy V, Ploy M-C, Da Re S (2016) The stringent response promotes antibiotic resistance dissemination by regulating integron integrase expression in biofilms. *mBio* 7(4). doi:10.1128/mBio.00868-16.

299. Oz T, et al. (2014) Strength of selection pressure is an important parameter contributing to the complexity of antibiotic resistance evolution. *Mol Biol Evol* 31(9):2387–2401.

300. Andersson DI, Hughes D (2012) Evolution of antibiotic resistance at non-lethal drug concentrations. *Drug Resist Updat Rev Comment Antimicrob Anticancer Chemother* 15(3):162–172.

301. Ferroni A, et al. (2009) Effect of mutator *P. aeruginosa* on antibiotic resistance acquisition and respiratory function in cystic fibrosis. *Pediatr Pulmonol* 44(8):820–825.

302. Cabot G, et al. (2016) Evolution of *Pseudomonas aeruginosa* antimicrobial resistance and fitness under low and high mutation rates. *Antimicrob Agents Chemother* 60(3):1767–1778.

303. Ibacache-Quiroga C, Oliveros JC, Couce A, Blázquez J (2018) Parallel evolution of high-level aminoglycoside resistance in *Escherichia coli* under low and high mutation supply rates. *Front Microbiol* 9. doi:10.3389/fmicb.2018.00427.

304. Perron GG, Hall AR, Buckling A (2010) Hypermutability and compensatory adaptation in antibiotic-resistant bacteria. *Am Nat* 176(3):303–311.

305. Taddei F, et al. (1997) Role of mutator alleles in adaptive evolution. *Nature* 387(6634):700.

306. Luján AM, et al. (2011) Evolution and adaptation in *Pseudomonas aeruginosa* biofilms driven by mismatch repair system-deficient mutators. *PLoS ONE* 6(11). doi:10.1371/journal.pone.0027842.

307. Ishizawa Y, Ying B-W, Tsuru S, Yomo T (2015) Nutrient-dependent growth defects and mutability of mutators in *Escherichia coli*. *Genes Cells* 20(1):68–76.

308. Harrison F, Buckling A (2011) Wider access to genotypic space facilitates loss of cooperation in a bacterial mutator. *PLoS ONE* 6(2). doi:10.1371/journal.pone.0017254.

309. Racey D, Inglis RF, Harrison F, Oliver A, Buckling A (2010) The effect of elevated mutation rates on the evolution of cooperation and virulence of *Pseudomonas aeruginosa*. *Evolution* 64(2):515–521.

310. Bauer M, Graf IR, Ngampruetikorn V, Stephens GJ, Frey E (2017) Exploiting ecology in drug pulse sequences in favour of population reduction. *PLoS Comput Biol* 13(9). doi:10.1371/journal.pcbi.1005747.

311. Rico A, Zhao W, Gillissen F, Lürling M, Van den Brink PJ (2018) Effects of temperature, genetic variation and species competition on the sensitivity of algae populations to the antibiotic enrofloxacin. *Ecotoxicol Environ Saf* 148:228–236.

312. Nadell CD, Drescher K, Foster KR (2016) Spatial structure, cooperation and competition in biofilms. *Nat Rev Microbiol* 14(9):589–600.

313. Foster KR, Bell T (2012) Competition, not cooperation, dominates interactions among culturable microbial species. *Curr Biol CB* 22(19):1845–1850.

314. Gerardin Y, Springer M, Kishony R (2016) A competitive trade-off limits the selective advantage of increased antibiotic production. *Nat Microbiol* 1:16175.

315. Wright ES, Vetsigian KH (2016) Inhibitory interactions promote frequent bistability among competing bacteria. *Nat Commun* 7:11274.

316. Kosakowski J, Verma P, Sengupta S, Higgs PG (2018) The evolution of antibiotic production rate in a spatial model of bacterial competition. *PLoS ONE* 13(10). doi:10.1371/journal.pone.0205202.

317. Urem M, Świątek-Połatyńska MA, Rigali S, Wezel GP van (2016) Intertwining nutrient-sensory networks and the control of antibiotic production in *Streptomyces*. *Mol Microbiol* 102(2):183–195.

318. Liu G, Chater KF, Chandra G, Niu G, Tan H (2013) Molecular regulation of antibiotic biosynthesis in *Streptomyces*. *Microbiol Mol Biol Rev MMBR* 77(1):112–143.

319. Amano S, et al. (2010) Promomycin, a polyether promoting antibiotic production in *Streptomyces* spp. *J Antibiot (Tokyo)* 63(8):486–491.

320. van der Meij A, Worsley SF, Hutchings MI, van Wezel GP (2017) Chemical ecology of antibiotic production by actinomycetes. *FEMS Microbiol Rev* 41(3):392–416.

321. Rojo-Molinero E, Macià MD, Oliver A (2019) Social behavior of antibiotic resistant mutants within *Pseudomonas aeruginosa* biofilm communities. *Front Microbiol* 10. doi:10.3389/fmicb.2019.00570.

322. Vega NM, Gore J (2014) Collective antibiotic resistance: mechanisms and implications. *Curr Opin Microbiol* 21:28–34.

323. Brook I (2009) The role of beta-lactamase-producing-bacteria in mixed infections. *BMC Infect Dis* 9:202.

324. Dugatkin LA, Perlin M, Lucas JS, Atlas R (2005) Group-beneficial traits, frequency-dependent selection and genotypic diversity: an antibiotic resistance paradigm. *Proc R Soc B Biol Sci* 272(1558):79–83.

325. Marciano DC, Karkouti OY, Palzkill T (2007) A fitness cost associated with the antibiotic resistance enzyme SME-1 β-lactamase. *Genetics* 176(4):2381–2392.

326. Cordeiro NF, Chabalgoity JA, Yim L, Vignoli R (2014) Synthesis of metallo-β-lactamase VIM-2 is associated with a fitness reduction in *Salmonella enterica* serovar Typhimurium. *Antimicrob Agents Chemother* 58(11):6528–6535.

327. Fernández A, et al. (2012) Expression of OXA-Type and SFO-1 β-lactamases induces changes in peptidoglycan composition and affects bacterial fitness. *Antimicrob Agents Chemother* 56(4):1877–1884.

328. Orhan G, Bayram A, Zer Y, Balci I (2005) Synergy tests by E test and checkerboard methods of antimicrobial combinations against *Brucella melitensis*. *J Clin Microbiol* 43(1):140–143.

329. Frost I, et al. (2018) Cooperation, competition and antibiotic resistance in bacterial colonies. *ISME J* 12(6):1582.

330. Kashaf SS, Angione C, Lió P (2017) Making life difficult for *Clostridium difficile*: augmenting the pathogen's metabolic model with transcriptomic and codon usage data for better therapeutic target characterization. *BMC Syst Biol* 11. doi:10.1186/s12918-017-0395-3.

331. Berney M, Berney-Meyer L (2017) *Mycobacterium tuberculosis* in the face of host-imposed nutrient limitation. *Microbiol Spectr* 5(3). doi:10.1128/microbiolspec.TBTB2-0030-2016.

332. Nakamura MM, et al. (2006) Growth phase- and nutrient limitation-associated transcript abundance regulation in *Bordetella pertussis*. *Infect Immun* 74(10):5537–5548.

333. Fang FC, Frawley ER, Tapscott T, Vazquez-Torres A (2016) Bacterial stress responses during host infection. *Cell Host Microbe* 20(2):133–143.

334. Krismer B, et al. (2014) Nutrient limitation governs *Staphylococcus aureus* metabolism and niche adaptation in the human nose. *PLoS Pathog* 10(1). doi:10.1371/journal.ppat.1003862.

335. Shoaie S, et al. (2015) Quantifying diet-induced metabolic changes of the human gut microbiome. *Cell Metab* 22(2):320–331.

336. Sung J, et al. (2017) Global metabolic interaction network of the human gut microbiota for context-specific community-scale analysis. *Nat Commun* 8. doi:10.1038/ncomms15393.

337. Petschow B, et al. (2013) Probiotics, prebiotics, and the host microbiome: the science of translation. *Ann N Y Acad Sci* 1306(1):1–17.

338. Rivière A, Selak M, Lantin D, Leroy F, De Vuyst L (2016) Bifidobacteria and butyrate-producing colon bacteria: importance and strategies for their stimulation in the human gut. *Front Microbiol* 7:979.

339. Serrano-Villar S, et al. (2017) The effects of prebiotics on microbial dysbiosis, butyrate production and immunity in HIV-infected subjects. *Mucosal Immunol* 10(5):1279–1293.

340. Scaldaferri F, et al. (2013) Gut microbial flora, prebiotics, and probiotics in IBD: Their current usage and utility. *BioMed Res Int* 2013. doi:10.1155/2013/435268.

341. Rosier BT, Marsh PD, Mira A (2018) Resilience of the oral microbiota in health: Mechanisms that prevent dysbiosis. *J Dent Res* 97(4):371–380.

342. Rello J, et al. (2009) Severity of pneumococcal pneumonia associated with genomic bacterial load. *Chest* 136(3):832–840.

343. Darton T, et al. (2009) Severity of meningococcal disease associated with genomic bacterial load. *Clin Infect Dis* 48(5):587–594.

344. Werno AM, Anderson TP, Murdoch DR (2012) Association between pneumococcal load and disease severity in adults with pneumonia. *J Med Microbiol* 61(Pt 8):1129–1135.

345. Shapiro JA, Kaplan AR, Wuest WM (2019) From general to specific: Can *Pseudomonas* primary metabolism be exploited for narrow-spectrum antibiotics? *ChemBioChem* 20(1):34–39.

346. Gasparrini AJ, et al. (2016) Antibiotic perturbation of the preterm infant gut microbiome and resistome. *Gut Microbes* 7(5):443–449.

347. Raymond F, Déraspe M, Boissinot M, Bergeron MG, Corbeil J (2016) Partial recovery of microbiomes after antibiotic treatment. *Gut Microbes* 7(5):428–434.

348. Raymond F, et al. (2016) The initial state of the human gut microbiome determines its reshaping by antibiotics. *ISME J* 10(3):707–720.

349. Yoon MY, Yoon SS (2018) Disruption of the gut ecosystem by antibiotics. *Yonsei Med J* 59(1):4–12.

350. Carey DE, Zitomer DH, Hristova KR, Kappell AD, McNamara PJ (2016) Triclocarban influences antibiotic resistance and alters anaerobic digester microbial community structure. *Environ Sci Technol* 50(1):126–134.

351. Livanos AE, et al. (2016) Antibiotic-mediated gut microbiome perturbation accelerates development of type 1 diabetes in mice. *Nat Microbiol* 1(11):16140.

352. Monk JM, et al. (2013) Genome-scale metabolic reconstructions of multiple *Escherichia coli* strains highlight strain-specific adaptations to nutritional environments. *Proc Natl Acad Sci U S A* 110(50):20338–20343.

353. Zengler K, Zaramela LS (2018) The social network of microorganisms — how auxotrophies shape complex communities. *Nat Rev Microbiol* 16(6):383–390.

354. Kubicek-Sutherland JZ, et al. (2015) Host-dependent induction of transient antibiotic resistance: A prelude to treatment failure. *EBioMedicine* 2(9):1169–1178.

355. Mouton JW (2018) Soup with or without meatballs: Impact of nutritional factors on the MIC, kill-rates and growth-rates. *Eur J Pharm Sci* 125:23–27.

356. Onufrak NJ, Forrest A, Gonzalez D (2016) Pharmacokinetic and pharmacodynamic principles of anti-infective dosing. *Clin Ther* 38(9):1930–1947.

357. Veiga RP, Paiva J-A (2018) Pharmacokinetics–pharmacodynamics issues relevant for the clinical use of beta-lactam antibiotics in critically ill patients. *Crit Care* 22. doi:10.1186/s13054-018-2155-1.

358. Hoo GSR, Liew YX, Kwa AL-H (2017) Optimisation of antimicrobial dosing based on pharmacokinetic and pharmacodynamic principles. *Indian J Med Microbiol* 35(3):340.

359. Northfield TD, Ives AR (2013) Coevolution and the effects of climate change on interacting species. *PLOS Biol* 11(10):e1001685.

360. Tilman D (1999) The ecological consequences of changes in biodiversity: A search for general principles. *Ecology* 80(5):1455–1474.

361. Yachi S, Loreau M (1999) Biodiversity and ecosystem productivity in a fluctuating environment: The insurance hypothesis. *Proc Natl Acad Sci* 96(4):1463–1468.

362. Matias MG, Combe M, Barbera C, Mouquet N (2013) Ecological strategies shape the insurance potential of biodiversity. *Front Microbiol* 3. doi:10.3389/fmicb.2012.00432.

363. Awasthi A, Singh M, Soni SK, Singh R, Kalra A (2014) Biodiversity acts as insurance of productivity of bacterial communities under abiotic perturbations. *ISME J* 8(12):2445–2452.

364. Baho DL, Peter H, Tranvik LJ (2012) Resistance and resilience of microbial communities--temporal and spatial insurance against perturbations. *Environ Microbiol* 14(9):2283–2292.

365. Eisenhauer N, Scheu S, Jousset A (2012) Bacterial diversity stabilizes community productivity. *PLOS ONE* 7(3):e34517.

366. Boles BR, Thoendel M, Singh PK (2004) Self-generated diversity produces "insurance effects" in biofilm communities. *Proc Natl Acad Sci U S A* 101(47):16630–16635.

367. Leary DJ, Petchey OL (2009) Testing a biological mechanism of the insurance hypothesis in experimental aquatic communities. *J Anim Ecol* 78(6):1143–1151.

368. Corcoran AA, Boeing WJ (2012) Biodiversity increases the productivity and stability of phytoplankton communities. *PLOS ONE* 7(11):e49397.

369. Cavieres LA, Badano EI (2009) Do facilitative interactions increase species richness at the entire community level? *J Ecol* 97(6):1181–1191.

370. Tiunov AV, Scheu S (2005) Facilitative interactions rather than resource partitioning drive diversity-functioning relationships in laboratory fungal communities. *Ecol Lett* 8(6):618–625.